

2015-05-01

Fundamental Kinetic Studies of CO₂ and Steam Gasification

Gomez Quevedo, Ramon Arturo

Gomez Quevedo, R. A. (2015). Fundamental Kinetic Studies of CO₂ and Steam Gasification (Doctoral thesis, University of Calgary, Calgary, Canada). Retrieved from

<https://prism.ucalgary.ca>. doi:10.11575/PRISM/26248

<http://hdl.handle.net/11023/2227>

Downloaded from PRISM Repository, University of Calgary

UNIVERSITY OF CALGARY

Fundamental Kinetic Studies of CO₂ and Steam Gasification

by

Ramón Arturo Gómez Quevedo

A THESIS

SUBMITTED TO THE FACULTY OF GRADUATE STUDIES
IN PARTIAL FULFILMENT OF THE REQUIREMENTS FOR THE
DEGREE OF DOCTOR OF PHILOSOPHY

GRADUATE PROGRAM IN CHEMICAL AND PETROLEUM ENGINEERING

CALGARY, ALBERTA

APRIL, 2015

© Ramón Arturo Gómez Quevedo 2015

Abstract

Gasification is the thermochemical conversion of a carbon-based fuel into a combustible product gas (syngas) using a gasifying agent, such as steam, carbon dioxide (CO₂) or a combination of both. The application of this technology is limited, due to its slow reaction rate, making kinetics determination one of the most active research topics in this field. Different kinetic models have been proposed in the literature for the study of coal and biomass gasification, based on assumptions about their reaction mechanisms. Consequently, a thorough understanding of gasification mechanisms and the validity of these accepted assumptions is necessary to align theoretical studies and industrial results.

A maximum rate is typically observed when the experimental gasification rates are plotted against conversion. The scientific community considers this to be an inherent part of the reaction mechanism, associated specifically with char surface changes. It is proven here that the stated maximum rate is a consequence of the reaction gas concentration development. Moreover, the increase in time for which the sample is held in an inert atmosphere reduces the char mesopore area, thereby reducing the char reactivity. As a result of the non-existence of a maximum gasification rate associated with changes in the char surface, kinetic modeling can be simplified.

The active char surface area (based on its carbon content) and the amount of catalyst (related to the char alkali content) are the most important variables affecting char reactivity. A new semi-empirical equation correlating these two variables has been developed to estimate gasification rate constants of raw coal and their mixtures for a broad range of ash contents.

The selection of a kinetic model mathematically affects the estimation of the kinetic parameters, i.e. activation energy and frequency factor. Therefore, a validation tool for kinetic models is the comparison of their kinetic parameters with those estimated independent of a kinetic model. A new theoretical approach to estimate kinetic parameters independent of a kinetic model for batch experiments has been derived and evaluated for coal gasification. The method can be extended to any chemical reaction and is, therefore, a contribution to chemical reaction engineering fundamentals.

The assumption of no mass transfer limitations has been studied at temperatures lower than 900°C. It has been proven that steam gasification rates from most literature reports are limited by interparticle diffusion. A new experimental gasification procedure with negligible mass transfer limitations that do not induce a maximum rate has been developed, providing an alternative for more accurate kinetic studies.

Acknowledgements

I would like express my profound gratitude to my supervisor, Dr. Nader Mahinpey, for giving me the opportunity to work under his supervision within the Energy and Environment Research Group (EERG) at the University of Calgary. I wish to note that his continuous guidance, support, and tremendous patience helped me to develop my ideas as well as keep a balance between novelty and simplicity.

I would like to thank my supervisory committee members, Dr. Maen Husein and Dr. Alex De Visscher, for their constructive comments. I would also like to acknowledge Aqsha Aqsha and Rico Silberman, two members of the EERG.

The organization and facilities provided by the University of Calgary and the Department of Chemical and Petroleum Engineering were fundamental to conducting this research. The financial support of the Natural Sciences and Engineering Research Council (NSERC) of Canada is greatly appreciated.

There are very special individuals in my life and it would be almost impossible to mention all of them; however, I would like to dedicate this work to my parents who are my pillar of strength.

Table of Contents

Abstract.....	ii
Acknowledgements.....	iv
Table of Contents.....	v
List of Tables.....	ix
List of Figures and Illustrations.....	xi
List of Symbols, Abbreviations and Nomenclature.....	xv
CHAPTER ONE: INTRODUCTION.....	1
1.1 Overview.....	1
1.2 Literature review.....	5
1.2.1 Gasification technologies.....	7
1.2.2 Gasifying agents.....	9
1.2.3 Gasification reactions.....	10
1.2.4 Reactor types and configurations.....	11
1.2.4.1 Updraft and downdraft configuration.....	11
1.2.4.2 Feedstock distribution into the reactor.....	14
1.2.4.3 Solid by-product disposal.....	18
1.2.5 Variables affecting char reactivity.....	21
1.2.5.1 Reaction temperature.....	22
1.2.5.2 Total pressure and gasifying agent partial pressure.....	24
1.2.5.3 Pyrolysis and char surface area development.....	25
1.2.5.4 Mineral content and composition.....	28
1.2.6 Kinetic studies.....	30
1.2.6.1 CO ₂ gasification.....	31
1.2.6.2 Steam gasification.....	32
1.2.6.3 Assumptions and simplifications.....	33
1.2.6.4 Chemical reaction kinetic models.....	34
1.2.6.5 Langmuir-Hinshelwood kinetic models.....	37
1.3 Objectives.....	39
1.4 Thesis structure.....	41
1.5 References.....	44
CHAPTER TWO: DATA ANALYSIS AND EXPERIMENTS DESIGN.....	54
2.1 Gas-solid reaction progress.....	54
2.2 Implications of the variable transformation.....	55
2.2.1 Variable transformation.....	55
2.2.2 Collinearity.....	57
2.2.3 Heteroscedasticity.....	58
2.3 New data mining procedure.....	61
2.4 Kinetic model comparison.....	62
2.4.1 Coefficient of determination of normalized experimental data.....	64
2.4.2 Experiment design analysis.....	65
2.5 Summary.....	71
2.6 References.....	72

CHAPTER THREE: A COMPREHENSIVE EXPERIMENTAL PROCEDURE FOR CO ₂ COAL GASIFICATION: IS THERE REALLY A MAXIMUM REACTION RATE?	73
3.1 Presentation of the article	73
3.2 Abstract	74
3.3 Introduction	75
3.4 Experimental	77
3.4.1 Coal and char characterization	77
3.4.2 Experimental gasification procedures	78
3.4.2.1 Method 1: Direct gasification	79
3.4.2.2 Method 2: Non-isothermal pyrolysis plus gasification	79
3.4.2.3 Method 3: Non-isothermal and isothermal pyrolysis plus gasification	79
3.4.3 Gasification tests	80
3.4.3.1 Test 1: Non-isothermal pyrolysis plus gasification in two stages	80
3.4.3.2 Test 2: Different CO ₂ partial pressures	80
3.4.3.3 Test 3: Iterative switching of CO ₂ /N ₂ during isothermal gasification	81
3.5 Data and kinetic analysis	81
3.5.1 Data analysis	81
3.5.2 Kinetic model discussion	82
3.6 Results and discussion	83
3.6.1 Coal Properties	83
3.6.2 Comparison of the gasification methods (Method 1, Method 2 and Method 3)	84
3.6.3 Effect of gas switching: inducing maximum rate of reaction	87
3.6.3.1 Test 1: constant time after a gas switching perturbation	87
3.6.3.2 Test 2: the effect of the partial pressure in the time to reach a maximum reaction rate	90
3.6.3.3 Test 3: the maximum reaction rate does not occur at the start of the gasification	93
3.6.4 Effect of pyrolysis time	95
3.6.4.1 Reduction of mesopore area due to the pyrolysis time	96
3.6.4.2 Decrease in reaction rate due to the time of the pyrolysis	97
3.7 Conclusion	101
3.8 References	103
 CHAPTER FOUR: A NEW MODEL TO ESTIMATE CO ₂ GASIFICATION KINETICS BASED ONLY ON PARENT COAL CHARACTERIZATION PROPERTIES	 106
4.1 Presentation of the article	106
4.2 Abstract	107
4.3 Introduction	108
4.4 Data analysis and modeling	112
4.4.1 Data analysis	112
4.4.2 Kinetic model simplification	112
4.4.3 Model development	113
4.5 Results and discussion	117
4.5.1 Coal properties	117
4.5.2 Effect of the pore surface area on coal reactivity	118
4.5.3 Effect of the alkaline content on coal reactivity	123

4.5.4 New model evaluation	124
4.6 Conclusion	128
4.7 References.....	130

CHAPTER FIVE: A NEW METHOD TO CALCULATE KINETIC PARAMETERS

INDEPENDENT OF THE KINETIC MODEL: INSIGHTS ON CO₂ AND STEAM GASIFICATION.....

5.1 Presentation of the article	133
5.2 Abstract.....	134
5.3 Introduction.....	135
5.4 Experimental methods	137
5.4.1 CO ₂ gasification.....	137
5.4.2 Steam gasification	137
5.5 Kinetics analysis	138
5.5.1 Data analysis.....	138
5.5.2 Calculation of the activation energy from experimental data	139
5.5.3 Frequency factor approximation.....	142
5.6 Results and discussion	144
5.6.1 CO ₂ gasification kinetics from Alberta coals	144
5.6.2 CO ₂ gasification kinetics from coals with slag granules	149
5.6.3 CO ₂ gasification kinetics from char produced from Indian coal samples	153
5.6.4 CO ₂ gasification kinetics from coal plus catalyst (K ₂ CO ₃)	157
5.6.5 Steam gasification kinetics from char pyrolyzed at different pressures	161
5.7 Conclusion	165
5.8 References.....	167

CHAPTER SIX: KINETIC STUDY OF COAL STEAM AND CO₂ GASIFICATION: A NEW METHOD TO REDUCE INTERPARTICLE DIFFUSION

6.1 Presentation of the article	170
6.2 Abstract.....	171
6.3 Introduction.....	172
6.4 Experimental methods	174
6.4.1 Experimental setup	174
6.4.2 Coal characterization	174
6.4.3 Steam gasification	175
6.5 Kinetics analysis	178
6.5.1 Data analysis.....	178
6.5.2 Activation energy independent of the kinetic model.....	179
6.5.3 Chemical reaction kinetic models	179
6.6 Results and discussion	180
6.6.1 Coal properties.....	180
6.6.2 Effect of the bed sample thickness: TGA and crucible comparison	181
6.6.3 Effect of the sample size.....	183
6.6.4 Non-maximum reaction rate.....	184
6.6.5 Activation energy estimation and falsified kinetics	188
6.7 Conclusion	192
6.8 References.....	193

CHAPTER SEVEN: SYNTHESIS.....	196
7.1 Overview.....	196
7.2 Synthesis of the thesis.....	196
7.2.1 Real nature of the maximum gasification rate.....	198
7.2.2 Effect of the isothermal pyrolysis in the char reactivity.....	199
7.2.3 Variables affecting char reactivity.....	200
7.2.4 Estimation of kinetic parameters independent of the kinetic model	201
7.2.5 Reduction of interparticle diffusion in experimental studies	202
7.3 References.....	204
CHAPTER EIGHT: CONCLUSIONS AND RECOMMENDATIONS.....	207
8.1 Conclusions.....	207
8.2 Recommendations for future work	209
8.3 References.....	212
APPENDIX A: HEAT OF REACTION AT DIFFERENT TEMPERATURES.....	214
APPENDIX B: THEORETICAL MEANING OF E_A	216
APPENDIX C: ADDITIONAL TOPICS ABOUT CHAPTER FOUR.....	219
APPENDIX D: COPYRIGHT PERMISSIONS.....	226

List of Tables

Table 1.1 Properties of gasification reactor types. (Reprinted with permission from [40])	19
Table 1.2 Summary of slagging and non-slagging characteristics	20
Table 1.3 Summary of the effect of temperature on syngas production and gasification rate	24
Table 1.4 Summary of the effect of oxygen partial pressure and total gasification pressure. (Reprinted with permission from [63])	26
Table 2.1 Activation energy [kJ/mol] of CO ₂ gasification between 800°C to 900°C for 9 different coals and 5 chemical reaction kinetic models. (Reprinted with permission from [1]. Copyright 2013 American Chemical Society)	66
Table 2.2 Two-way ANOVA test with a 0.05 significance level for two factors: (1) coal type and (2) chemical reaction model.	67
Table 2.3 Binary differences of E _A averages [kJ/mol] for five different kinetic models, where subscripts refer to VM = 1, SCM = 2, ICM = 3, NDM = 4, RPM = 5.	69
Table 2.4 Binary differences of E _A averages [kJ/mol] for nine different coal samples, subscripts refer to Coal 1 = 1, Coal 2 = 2...Coal 7 = 7, Genesee 1 = 8, Genesee 2 = 9	70
Table 3.1 Comparison of TGA methods.....	78
Table 3.2 Comparison of TGA tests	82
Table 3.3 Proximate and Ultimate Analysis	84
Table 3.4 Dubinin-Radushkevich surface area (Micropore area using CO ₂ , m ² /g).....	84
Table 3.5 Mesopore and micropore surface area for chars from Genesee and coal 5, produced at 900°C with holding times of 5, 30 and 60 min	96
Table 4.1 Proximate and ultimate analyses and surface area (micropore area using CO ₂ at 273 K with the Dubinin-Radushkevich method)	118
Table 4.2 Ash composition and total specific molar alkaline content (equivalent- moles/g_coal). Mixtures 1 and 2 correspond to 82% and 38% Genesee coal (the balance is coal 6), respectively.....	119
Table 4.3 CO ₂ gasification results for 11 coal samples and two mixtures of coals. Mixtures 1 and 2 correspond to 82% and 38% Genesee coal (the balance is coal 6), respectively	120
Table 4.4 Parameter of regression r vs. f_2^* and parameter of regression t vs. f_2^*	128
Table 5.1 Analytic values of G(X) according to Eq. (5-11) and their respective logarithms for three reaction orders: 0.5, 1 and 2.	144

Table 5.2 Time (min) to reach three different conversions ($X_1 = 0.8$; $X_2 = 0.5$; $X_3 = 0.25$) for nine different coals. CO ₂ gasification at 800°C, 850°C and 900°C. Reported by Silbermann et al. [11].	146
Table 5.3 Activation energy [kJ/mole] based on Eq. (5-8) and the Arrhenius equation using five different kinetic models as reported by Silbermann et al. [11]. Temperature range from 1073 K to 1173 K.	148
Table 5.4 Intercept of Eq. (5-8) and frequency factor (min ⁻¹) based on Eq. (5-12) (fourth column) and the Arrhenius equation using five different kinetic models as reported by Silbermann et al. [11]. Temperature range from 1073 K to 1173 K.	149
Table 5.5 Activation energy and frequency factor calculated from Eqs. (5-8) and (5-12). Kinetic parameters reported data by Li et al. [7] using the Avrami-Erofeev (m=2) kinetic model. Temperature range from 1223 K to 1423 K.	150
Table 5.6 Activation energy and frequency factor calculated from Eqs. (5-8) and (5-12). Kinetic parameters reported data by Mandapati et al. [8] using the RPM.	157
Table 5.7 Activation energy and frequency factor calculated from Eqs. (8) and (12). Kinetic parameters reported data by Kopyscinski et al. [22] using the RPM and eRPM.	160
Table 5.8 Activation energy and frequency factor calculated from Eqs. (5-8) and (5-12). Kinetic parameters reported data by Feroso et al. [14] using the RPM. Temperature range from 1173 K to 1323 K.	164
Table 6.1 Proximate and ultimate analyses of two Central-West Canadian coals (dry basis). Surface micropore area using CO ₂ at 273 K with the Dubinin-Radushkevich method.	181
Table 6.2 Activation energy (kJ/mol) estimated independent of the kinetic model [23] at three different conversions and its respective coefficient of determination. Temperature range from 800°C to 900°C. Max. uncertainty: ± 7 kJ/mol	190
Table 6.3 Activation energy (kJ/mol) at three different conversions and its respective coefficient of determination using three kinetic models: VM, ICM and RPM. Temperature range from 800°C to 900°C. Max. uncertainty: ± 11 kJ/mol	191

List of Figures and Illustrations

Figure 1.1. Coal-fired electricity generation in Canadian provinces. (Used with permission from [3]).....	2
Figure 1.2 Coal rank classification in the United States based on carbon content and calorific value [7].	3
Figure 1.3 Possible plant configurations for different applications of gasification.....	8
Figure 1.4 Schematic of plasma gasification process by Zhang et al. (Reprinted with permission from [36])	12
Figure 1.5 Configuration of gasifiers according to direction of the feed streams: (a) updraft, (b) downdraft. Three sets of chemical reactions are presented as occurring in a gasifier: (1) combustion, (2) pyrolysis and (3) gasification.....	13
Figure 1.6 Fixed bed reactor configurations. (Reprinted with permission from [39])	15
Figure 1.7 Fluidized bed reactors used for gasification. (Reprinted with permission from [39]).....	16
Figure 2.1 CO ₂ gasification rate (r) vs. conversion (X) of coal 7 at 900°C: (a) data collection interval of 1 min and (b) data collection interval of 0.2 min.	59
Figure 2.2 CO ₂ gasification rate (r) vs. conversion (X) of Genesee coal at 900°C: (a) data collection interval of 1 min and (b) data collection interval of 0.2 min.	60
Figure 2.3 CO ₂ gasification rate (r) vs. conversion (X) at 900°C, with the proposed data mining procedure: (a) coal 7 and (b) Genesee coal.	63
Figure 2.4 Coefficient of determination for CO ₂ coal gasification at 850°C for 9 coals and 5 different chemical reaction models. (Reprinted with permission from [1]. Copyright 2013 American Chemical Society)	65
Figure 3.1 Comparison of the three CO ₂ coal gasification methods. Example for Genesee coal at 900°C	85
Figure 3.2 Comparison of the reaction rates for methods 1, 2 and 3 for CO ₂ Genesee coal gasification at 900°C	86
Figure 3.3 Comparison of the reactions rates for method 1, 2 and 3 for coal 5 coal gasification at 900°C	86
Figure 3.4 Test 1, the effect of the gas switching with the reaction rate vs. conversion for CO ₂ Genesee coal gasification. From 50% N ₂ / 50% CO ₂ to 100% CO ₂ at holding times of 0, 2, 4 and 8 min at 900°C.....	87

Figure 3.5 Test 1, the effect of the gas switching with the reaction rate vs. conversion for CO ₂ coal 5 gasification. From 50% N ₂ / 50% CO ₂ to 100% CO ₂ at holding times of 0, 2, 4 and 8 min at 900°C.....	88
Figure 3.6 Test 1, the effect of gas switching with the reaction rate vs. time for CO ₂ Genesee coal gasification. From 50% N ₂ / 50% CO ₂ to 100% CO ₂ at holding times of 0, 2, 4 and 8 min at 900°C	89
Figure 3.7 Test 1, the effect of gas switching with the reaction rate vs. time for coal 5 gasification. From 50% N ₂ / 50% CO ₂ to 100% CO ₂ at holding times of 0, 2, 4 and 8 min at 900°C	89
Figure 3.8 Test 2, the effect of partial pressure with the reaction rate vs. conversion when switching from N ₂ to 100% CO ₂ , 50% CO ₂ and 25% CO ₂ at 900°C at atmospheric pressure (88 kPa) for (a) Genesee coal and (b) coal 5	91
Figure 3.9 Test 2, the effect of partial pressure with the reaction rate vs. time when switching from N ₂ to 100% CO ₂ , 50% CO ₂ and 25% CO ₂ at 900°C at atmospheric pressure (88kPa) for (a) Genesee coal and (b) coal 5.....	92
Figure 3.10 Test3, the effect iterative switching with the maximum reaction rate vs. conversion	94
Figure 3.11 Test 3, the effect of iterative gas switching with the maximum reaction rate vs. time. From 0 to 100% CO ₂ and vice versa: CO ₂ Genesee coal and coal 5 gasification at 900°C.....	95
Figure 3.12 The effect of the holding time at 900°C during CO ₂ char gasification with reaction rate vs. conversion. Holding times: 5, 30 and 60 min for (a) Genesee char and (b) coal 5 char	98
Figure 3.13 Method 2 and 3 comparison. CO ₂ Genesee Char gasification compared with CO ₂ raw coal gasification at 900°C. (a) Genesee char (5 min) method 2 vs. Genesee coal method 3 (5 min), (b) Genesee char (60 min) method 2 vs. Genesee coal method 3 (60 min).....	99
Figure 3.14 Method 2 and 3 comparison. CO ₂ coal 5 Char gasification compared with CO ₂ raw coal gasification at 900°C. (a) Char 5 (5 min) method 2 vs. coal 5 method 3 (5 min), (b) Char 5 (60 min) method 2 vs. coal 5 method 3 (60 min)	100
Figure 4.1 Rate constant vs. coal-based micropore area (Dubinin-Radushkevich method) for deep mine coals (Coals 1 to 7).....	121
Figure 4.2 Rate constant vs. carbon-based micropore area (Dubinin-Radushkevich method) for deep mined coals (Coals 1 to 7)	122
Figure 4.3 Rate constant vs. carbon-based micropore area (Dubinin-Radushkevich method) for all coals presented in Table 4.2 at 850°C using direct gasification.....	122

Figure 4.4 Rate constant (min^{-1}) vs. alkaline content ‘Alk’ (equivalent-moles / g coal) for all coals presented in Table 4.2 at 850°C using direct gasification	124
Figure 4.5 Residence time (min at 80% conversion) vs. alkaline content ‘Alk’ (equivalent-moles / g coal) for all coals presented in Table 4.2 at 850°C using direct gasification	125
Figure 4.6 Activation energy vs. alkaline content ‘Alk’ (equivalent-moles / g coal) for direct CO ₂ gasification. Temperature range between 800°C and 900°C and using the ICM to obtain rate constant	126
Figure 4.7 Rate constant vs. f_2^* , according to the relationship stated in Eq. (4-8) for all coals presented in Table 4.2 at 850°C using direct gasification and the ICM to obtain rate constant	127
Figure 4.8 Residence time (for 80% conversion) vs. f_2^* , according to the relationship stated in Eq. (4-9) for all coals presented in Table 4.2 at 850°C using direct gasification	128
Figure 5.1 Logarithm of time vs. reciprocal of temperature. CO ₂ gasification between 800°C and 900°C: (a) Genesee coal and (b) Deep coal 7. Data from Silbermann et al. [11]	147
Figure 5.2 Logarithm of time vs. reciprocal of temperature. CO ₂ gasification between 950°C and 1150°C” (a) Coal/slag ratio of 1:0, (b) Coal/slag ratio of 1:1, (c) Coal/slag ratio of 1:2, (d) Coal/slag ratio of 1:3. Data from Li et al. [7].....	153
Figure 5.3 Logarithm of time vs. reciprocal of temperature. Char CO ₂ gasification: (a) Char A [937°C to 1026°C], (b) Char B [833°C to 917°C]; (c) Char C [934°C to 1021°C], (d) Char D [951°C to 1078°C]. Data from Mandapati et al. [8]	156
Figure 5.4 Logarithm of time vs. reciprocal of temperature. Coal CO ₂ gasification: (a) Gen-raw [700°C to 950°C], (b) Gen-ash-free plus 20% K ₂ CO ₃ [650°C to 750°C]; (c) Gen-ash-free [800°C to 900°C]. Data from Kopyscinski et al. [22]	159
Figure 5.5 Logarithm of time vs. reciprocal of temperature. Char steam gasification [30% vol H ₂ O – 70% vol N ₂] between 900°C and 1050°C: (a) DI-1, (b) DI-20; (c) HV-1, (d) HV-20. Data from Feroso et al. [14].....	163
Figure 6.1 (a) Schematic diagram of the experimental setup: TGA TherMax 500 coupled to a quartz reactor. (b) Schematic diagram of the “new” and “standard alumina” crucibles illustrating the sample thickness when filled with 10 mg coal sample.	176
Figure 6.2 Experimental Gasification Method. TGA TherMax 500, 12 mm internal diameter crucible, and 1.8 min ‘reactor volume/gas flow’ ratio.	177
Figure 6.3 Conversion vs. time for three experimental configurations during the CO ₂ gasification [10 mg sample] at 900°C: (a) Genesee coal and (b) Boundary Dam (BD) coal.	182

Figure 6.4 Effect of the weight sample during the gasification of Genesee coal at 900°C using a TherMax 500 TGA coupled to a quartz reactor and a 12mm quartz crucible: (a) steam gasification and (b) CO₂ gasification. 186

Figure 6.5 Effect of the weight sample during the gasification of Boundary Dam coal at 900°C using a TherMax 500 TGA coupled to a quartz reactor and a 12mm quartz crucible: (a) steam gasification and (b) CO₂ gasification. 187

Figure 6.6 BD and Genesee gasification rate vs. residence time at 900°C: (a) including gas mixing time and (b) excluding the time to replace gases. CO₂ and steam as gasifying agents. 189

List of Symbols, Abbreviations and Nomenclature

Symbols	Definition
a_k	Regression constant to obtain k_M from f_2^* ($\text{min}^{-1} \text{m}^{-2} \text{g}$)
a_t	First regression parameter to obtain t from f_2^* ($\text{min}^{-1} \text{m}^{-2} \text{g}$)
Alk	Specific molar alkaline content (mol g^{-1})
b	Correlation parameter in Arrhenius' exponential factor ($\text{mol g}^{-1} \text{K}^{-1}$)
c_t	Second regression constant to obtain residence time from f_2^* (g m^{-2})
E_A	Activation energy ($[\text{kJ mol}^{-1}]$)
$f_1(1 - X)$	Conversion function, instead of surface for gas-solid reaction ($\text{m}^2 \text{g}^{-1}$)
$f_2(\text{Alkali}, T)$	Alkali content (mol g^{-1}) and temperature (K) function, (dimensionless)
f_2^*	Product of f_1 and f_2 , ($\text{m}^2 \text{g}^{-1}$)
k	Rate constant for a first order reaction (min^{-1})
k_o	Frequency factor (min^{-1})
k_M	Rate constant (min^{-1})
m_a	Mass of ash (g)
m_o	Initial mass of char (g)
m_t	Mass of char at the particular time 't' (g)
r	Conversion rate (min^{-1})
R	Ideal gas law constant = $8.3144 \text{ (J mol}^{-1} \text{K}^{-1})$
S	Specific surface area ($\text{m}^2 \text{g}^{-1}$)
t	Time (min^{-1})
T	Temperature (K or $^{\circ}\text{C}$)
X	Conversion (dimensionless)
Greek Symbols	Definition
$\bar{\alpha}$	Change of activation energy due an alkali decrease (kJ /g)
α	Intercept of the logarithm of time (min) vs. reciprocal of temperature (K^{-1})
ψ	Char surface parameter of the random pore model (dimensionless)
Δ	Gradient of a determined variable

Abbreviations	Definition
ANOVA	Analysis of variance
BET	Branauer–Emmett–Teller method
DR	Dubinin–Radushkevich method
GC	Gas chromatography
EFR	Entrained flow reactor
FBR	Fluidized bed reactor
ICM	Integrated core model or power-law model
NDM	Normal distribution model
LH	Langmuir-Hinshelwood model
RPM	Random pore model
TGA	Thermogravimetric analysis
SCM	Shrinking core model
VM	Volumetric model
WGS	Water-gas shift reaction

Chapter One: Introduction

1.1 Overview

The volatility of oil prices has motivated research into coal and other carbon sources; however, the use of coal has been restricted worldwide due to environmental concerns. Conventional technologies, such as combustion, can only be justified when the feedstock contains very low mineral content. It is difficult to extract coal with minimum ash content and technologies to obtain ash-free coal, such as solvent extraction, are necessary [1]. Canada's western provinces have the biggest coal reserves and account for the major proportion of the produced coal in the country [2].

Coal is also one of the main contributors in the energy sector, especially in power generation. Fig. 1.1 shows coal consumption in proportion to electricity generated in Canada. As the figure illustrates, Alberta, Saskatchewan and Nova Scotia consume the largest amounts of coal in their electricity systems [3].

The depletion of conventional coal reservoirs has motivated the search and development of alternative processes to utilize coals with high ash contents. High-quality coal is not abundant, and it usually has different purity levels in the same ore. However, there has been increasing production of petroleum coke (petcoke) in Alberta, generated as a by-product of oil sands upgrading, which could be used as feedstock to replace natural gas in the oil sands extraction and upgrading [4]. There are several sources of non-conventional fuels, such as petcoke; and, the terminology used for coal has been extended to encompass all solid carbonaceous feedstock.

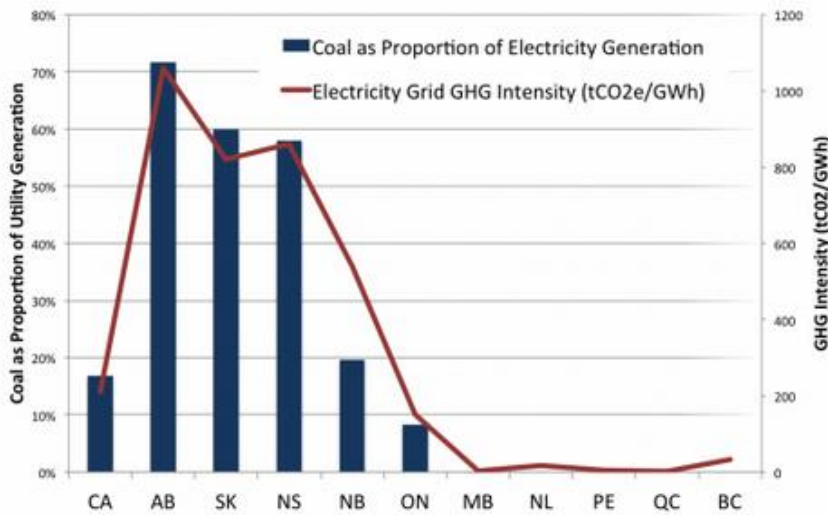


Figure 1.1. Coal-fired electricity generation in Canadian provinces. (Used with permission from [3]).

The term ‘rank’ is associated with the degree of change in physical and chemical properties from peat to anthracite, and the term ‘grade’ is associated with the content of carbon [5]. These two terms are often confused; and, in general, high-quality coals are commonly associated with high carbon and low mineral contents [6]. Low-rank coals exhibit a broad spectrum of properties directly associated with less maturity and usually higher inorganic matter [5, 7]. The coal rank is determined by carbon, moisture, volatile matter content and calorific value; and, the general rule is that high-rank coals are harder materials with less moisture and volatile matter and higher calorific values [7]. Fig. 1.2 shows a general classification of coals by rank in the United States [7], which can be more detailed using other rank-coal classifications [5]. Other solid fuels with high ash contents and similar or lower heat capacities are denominated low-grade fuels, such as biomass.

Current coal combustion technology was developed for high-grade coals; however, its extension to other feedstock has become very common. It is still the dominant process for thermal power generation. The utilization of low-grade feed stocks is possible using gasification instead of combustion, but there are challenges in its implementation at the industrial scale [8]. The most successful demonstration of gasification is in power generation with the use of the integrated gasification combined cycle (IGCC) for more than a decade.

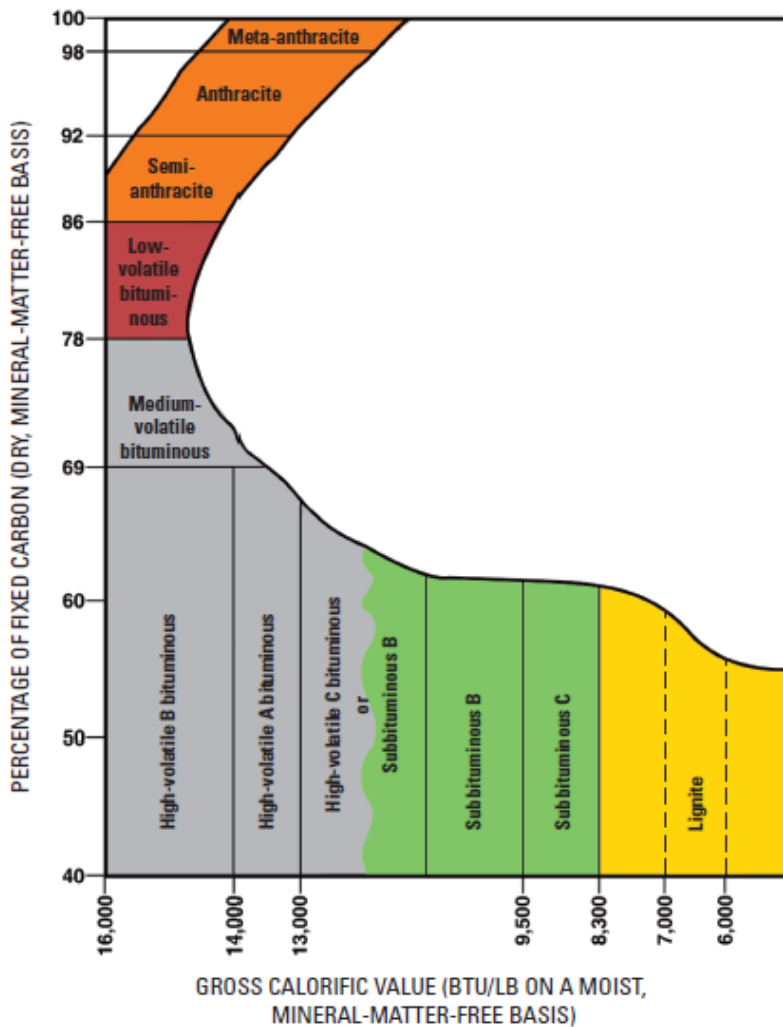


Figure 1.2 Coal rank classification in the United States based on carbon content and calorific value [7].

The established IGCC technology involves two major processes: coal gasification and combined cycle energy generation [9]; however, its feasibility is significantly impacted by the consumption of natural gas. Since coal and natural gas are the two major fossil fuels used in electricity generation, an increase in the consumption of one means a decrease in the consumption of the other. In the spring of 2012, natural gas prices dropped to historically low levels, which led to natural gas-fired generators being used over coal-fired generators [9]. In early 2013, coal regained market share after natural gas prices rose, which led natural gas-fired plants to lose their competitive advantage over time [10, 11]. Natural gas consumption also has two peaks each year: the first one is during the winter, when cold weather increases the demand for natural gas heating; and, the second peak is during the summer, where hot weather creates demand for air conditioning [12]. Significant uncertainty remains about the future prices of coal and natural gas [11]. Nonetheless, higher prices of coal give natural gas fired plants a competitive advantage and vice versa [11].

Gasification is an alternative for generating a clean fuel for heating purposes. It is an old process whose first industrial application was the production of syngas for lighting in 1792, with more than 1200 operation plants in the United States by the late 1920s [13]. Plasma gasification is useful in the treatment of municipal solid waste using, and it can be integrated with power generation using a combined cycle (IPGCC) [14, 15]. It also serves as an alternative for producing syngas, which is the feedstock for synthetic fuel manufacturing and hydrogen production for refinery and fuel upgrading [4, 16].

The main disadvantage is that theoretical studies are not aligned to the design of industrial reactors or to-scale processes since the reaction conditions are quite dissimilar between

laboratory and pilot plant. Even more complex is the diverse information presented in the literature with inconsistent criteria, which makes difficult to extrapolate results or correlate independent studies.

In summary, gasification is a thermochemical process that allows for the optimal use of non-conventional fuels and for better coal utilization. Industry's interest in gasification has been related to the prices of other fuels, which is why its technological development has not been consistent. In contrast, the scientific community has been more focused on theoretical research, particularly chemical reaction models with non-unique trends on the estimation of the kinetic parameters [17]. Therefore, there are gaps that must be filled to understand the differences between the results of kinetic studies conducted at laboratory scale and the performance of industrial gasifiers.

1.2 Literature review

Gasification is the thermochemical conversion of a carbon-based feedstock into a combustible product gas with the use of a gasifying agent, such as steam, carbon dioxide (CO_2) or their combination [18]. The main product gases, carbon monoxide (CO) and hydrogen (H_2), are used to produce heat and electricity or are converted into liquid hydrocarbons [19, 20]. Other by-products, such as methane (CH_4) and sulfur dioxide (SO_2), are generated from the rest of the components of the raw material reacting at high temperatures with oxygen or the gasification products. The non-reactive components, termed as ash, are not totally inert, since they can change their properties, due to solid-phase changes and partial oxidation or reduction.

Industrial gasification consists of three important processes [21-23]:

- Pyrolysis: This is a set of complex reactions that involves heating the solid fuel, usually up to 700°C, to produce char and release volatiles. Tars may also be produced when volatiles liquefy at low temperatures.
- Oxidation reactions: Char and volatiles are combusted with oxygen to produce the necessary gasifying agents (steam and CO₂) and CO. This is an exothermic process, where the released heat is used for reduction reactions.
- Reduction reactions (denominated gasification reactions): Char, tar and hydrocarbons are gasified with CO₂ and steam to produce synthetic gas (syngas), which mainly composed of CO, H₂ and CH₄. These reactions are endothermic, requiring the heat produced from the prior oxidation reactions. Steam promotes the steam reforming (endothermic) of char and tar, as well as water-gas shift reactions (exothermic) [24]. The reduction of H₂O in steam gasification is the most effective way of increasing H₂ production [25]. CO₂ promotes the Boudouard reaction (endothermic) to produce CO [26]. CO₂ may also be recirculated with oxygen (O₂) within oxy-fuel combustion/gasification [27].

Some limitations of incineration include harmful emissions of acidic gases and volatile organic compounds, as well as producing toxic wastes, such as dioxins, which contribute to air pollution [18]. Compared with incineration and combustion of the solid fuel, the use of syngas produces less solid waste and emits lower harmful gases into the environment [28]. Syngas combustion is an efficient and cleaner technology due to lower emissions of mono-nitrogen oxides (NO_x) and sulfur oxides (SO_x) and higher energy recovery [18, 29]. Gasification, on the other hand, allows the installation of small, low-cost, efficient reactors to reduce storage and transport costs. It allows the recovery of available energy from low-value materials, such as

biomass wastes and low-rank coals, reducing disposal costs and environmental concerns [29]. Gasification also provides an alternative for solid animal waste disposal through manure-fuel gasification [30].

1.2.1 Gasification technologies

There are various advantages to gasifying low-grade fuels over conventional processes and fossil fuels. Gasification processes can be applied to convert wastes to valuable forms of energy. These wastes range from any type of biomass and forestry residues to petroleum cokes. This helps the environment by preserving lands and providing an economic advantage in terms of saving storage costs, because gasification uses straw, agricultural waste and other products that cannot be economically processed with other technologies.

Gasification can be combined with power generation in integrated gasification combined cycle (IGCC) power plants to generate energy more efficiently and environmentally friendly. Large companies, like Siemens, GE, ConocoPhillips and Shell, have built IGCC facilities around the globe [9]. Fig. 1.3 shows a block flow diagram with the possible existing configurations for gasification plants. In IGCC plants, fuel is first converted to syngas in gasifiers; and, the syngas is then converted to electricity in a combined cycle power unit [31]. IGCC plants are designed with sulfur and CO₂ capture systems, in order to remove most of these harmful constituents from the produced gas. As shown in Fig. 1.3, one of the possible gasification routes is power generation using different feedstocks; however, chemical synthesis is also achievable with syngas through the use of the Fischer-Tropsch process [19, 20].

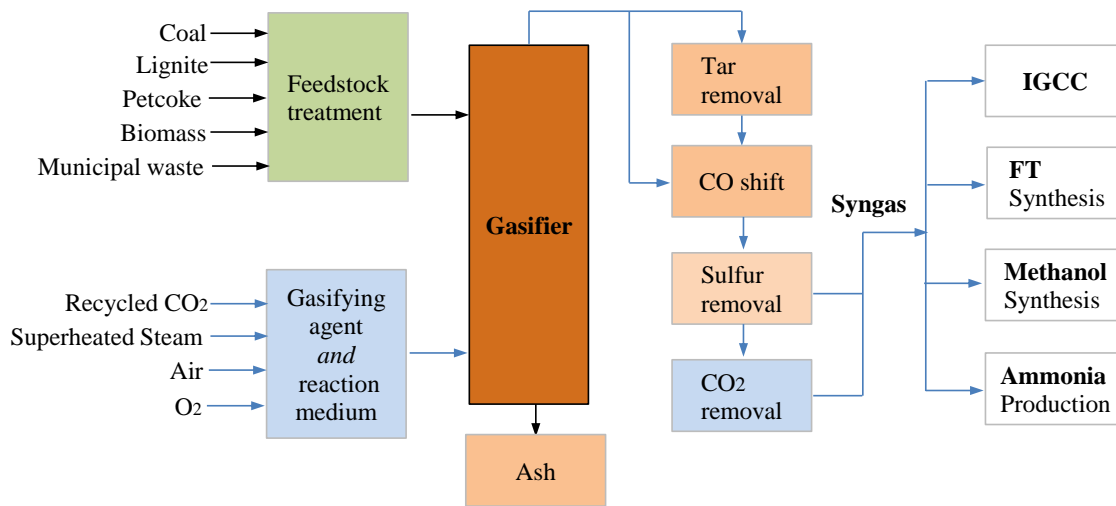


Figure 1.3 Possible plant configurations for different applications of gasification.

A general view of this technology implies the understanding of:

- Raw materials: Gasification is a technology that can be implemented with liquid feedstock; however, this provides no economic advantage. Solid fuels are the cheapest fuels, but their easy handling and upgrading can be achieved by transforming them into a gas stream. This thesis covers low-grade fuels, because they are the most abundant sources of carbon and their high mineral content allows them to be processed without the addition of a catalyst.
- Gasification process: There are two important elements that constitute the baseline for all possible configurations:
 - Reactor type: This is related to the way that the solid is held in the reaction chamber and to the direction of the gas flow with respect to the feed of the solid.
 - Heat transfer and heating sources: The main mechanism is radiation, since gasification is a set of endothermic gas-solid reactions occurring at temperatures above 500°C. For this reason, indirect heating is not efficient when the size of the

reactor increases. The most common gasifiers are directly heated by overheated steam and partial combustion of the feedstock.

- Syngas quality: Tar and other compounds must be removed to use the syngas (mainly CO and H₂). Without syngas cleaning, there are no environmental advantages to gasification with respect to direct combustion.
- Final application: As mentioned, IGCC is the best practical example of gasification implementation. There are other options, such as chemical synthesis, where the most important factor is the CO/H₂ ratio.

1.2.2 Gasifying agents

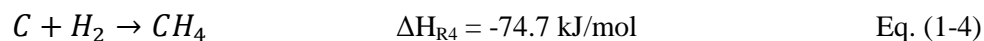
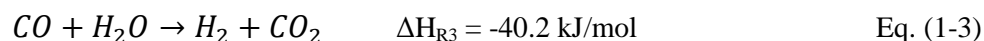
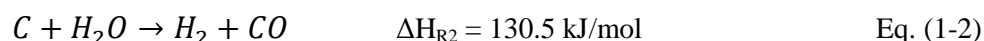
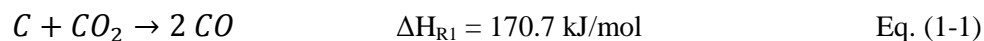
The gasifying agent is the gas that is required to perform gasification reactions. This gas reacts with chars, tars and gases to produce syngas. Some researchers have referred to air, oxygen, steam and CO₂ as gasifying agents. However, only steam and CO₂ are used in gasification reactions; and, O₂ is applied in the combustion step to provide the required energy for the endothermic reactions.

Steam and CO₂ have their own advantages in gasification. Steam promotes the steam reforming (endothermic) of char and tar, as well as the water-gas shift reaction (exothermic) [24]. The reduction of H₂O in steam gasification is the most effective way of increasing H₂ production [25]. CO₂ promotes the Boudouard reaction (endothermic) to produce CO [26]. CO₂ may also be combined with O₂ for oxy-fuel combustion, which is a better process than using air as an oxidant, due to less N₂ dilution [27].

A detailed explanation of the importance of each gasifying agent involved in the chemical reactions is provided in the following section.

1.2.3 Gasification reactions

The most important reactions considered for kinetic studies excluding combustion are presented in Eqs. (1-1) to (1-4) at standard conditions. The Boudouard reaction is the controlling step at low gasification temperatures during CO₂ gasification (lower than 1000°C) [32, 33].



Above 700°C the Boudouard reaction takes place, i.e. Eq. (1-1), and gasification starts. If the heating rate is higher than 200°C/min, there are no weight loss differences during the pyrolysis step, regardless of the sweeping gas used [34]. The idea, adopted by other authors, that introduces an isothermal step to separate pyrolysis from gasification is not the best solution, as pyrolysis is much faster than gasification and significantly affects char reactivity [32, 35].

CO₂ gasification and steam gasification, Eqs. (1-1) and (1-2), respectively, are endothermic reactions, which when combined improve the H₂ yield at higher temperatures. The water-gas shift reaction, Eq. (1-3), increases the H₂/CO ratio in the final mixture, but does not greatly impact the heating value of the syngas, since H₂ and CO combustion heats are almost identical on a molar basis. The variation of the heat of reaction at gasification conditions is smaller than 5 kJ/mol for all the reactions in Eqs. (1-1) to (1-4), with exception of the water-gas shift reaction,

Eq. (1-3), that changes from -40kJ/mol at standard conditions to -32kJ/mol at 900°C. The temperature dependence of the heat of reaction is presented in Appendix A.

Combustion is important, but under low air intake (or pure O₂ for oxy-fuel systems), the gasifier operates under reduction conditions. CO₂ is usually produced in situ by partial combustion of the char; however, it is not possible using an entrained flow reactor (EFR), since residence time in the order of a fraction of a second is not sufficient to ensure that the Boudouard reaction takes place. Usually, the reactor in industrial gasifiers can be ideally considered as three reactors connected in series to consider combustion, pyrolysis and gasification; however, the complexity increases when the sequence of these reactions is part of the model and when kinetics is considered instead of the reaching of equilibrium.

1.2.4 Reactor types and configurations

The sequence of reactions, gasifying agents and stream configurations determines the type of reactor. The first step is the explanation that the main difference between all reactor types is the sequence of reactions for solid and gas species in a gasifier. In general, the following steps for solid feed are present drying, pyrolysis, char gasification and ash melting (this is just part of some gasifier types). Fig. 1.4 shows a schematic of the plasma gasification process, which has the same elements that conventional gasification has plus the continuous melting of the ash [36].

1.2.4.1 Updraft and downdraft configuration

When the flow configuration is considered, the equivalents of updraft and downdraft gasifiers are co-current and counter-current reactors, respectively. The sequence of reactions presented in Fig. 1.4 is just one of many possible configurations, given the position of the

feedstock and gasifying agent inlets. Fig. 1.5 presents only the main set of gas-solid chemical reactions happening in a gasifier according to the stream configuration: combustion, pyrolysis and gasification. Drying and melting are not considered, since they do not affect the yield and composition of the syngas from a thermodynamic point of view.

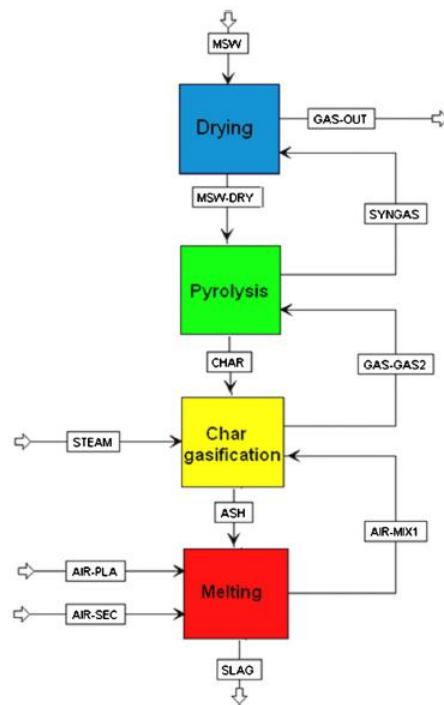


Figure 1.4 Schematic of plasma gasification process by Zhang et al. (Reprinted with permission from [36])

Fig. 1.5 illustrates that the order of the chemical reactions depends on the position of the gas or solid inlet. This has important consequences, such as:

- Tar formation is reduced using a downdraft reactor, since combustion follows pyrolysis [37]. This is impossible to achieve in an updraft reactor, and tar removal is required prior to the use of the gas products.

- Residence time is shorter in the downdraft reactor, since solids move faster due to gravity and drag force being aligned in the same direction. Lower carbon conversion is achieved in this configuration, compared with a similar size updraft reactor. This may be a problem if the solid product is not treated or if the reactor size is not increased. If the reactor is packed, its conversion can be analogous or higher using the updraft reactor; however, the heating value of the gas products is reduced compared to other configurations [38].

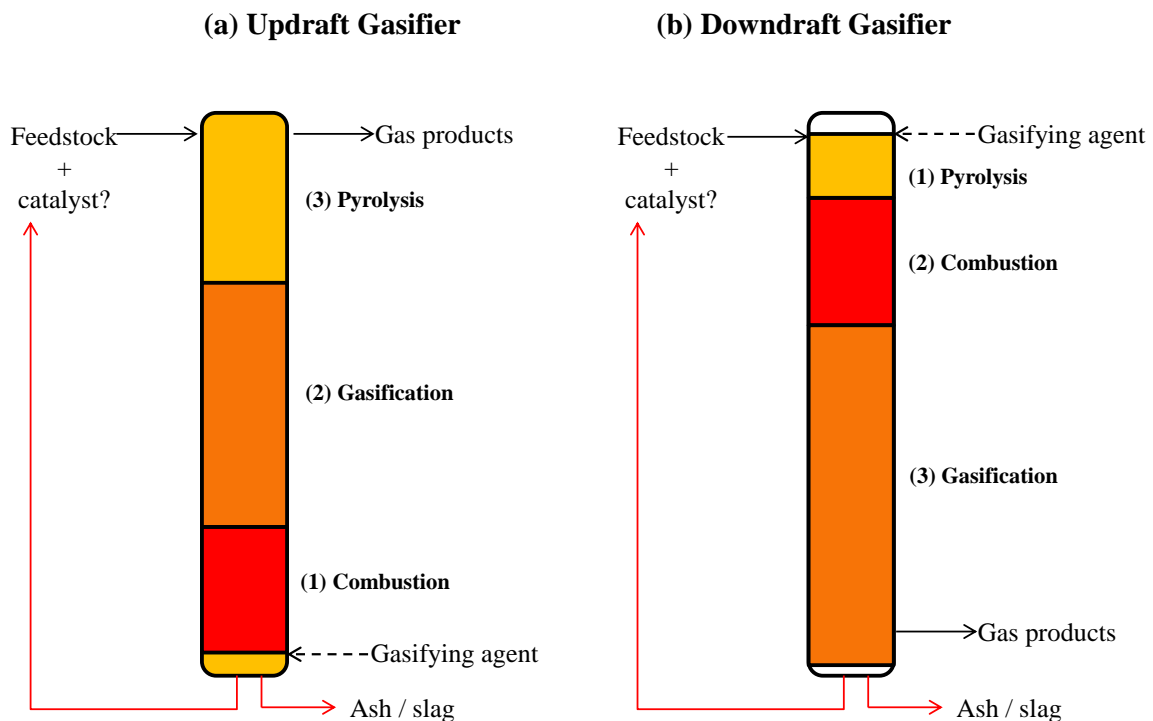


Figure 1.5 Configuration of gasifiers according to direction of the feed streams: (a) updraft, (b) downdraft. Three sets of chemical reactions are presented as occurring in a gasifier: (1) combustion, (2) pyrolysis and (3) gasification.

1.2.4.2 Feedstock distribution into the reactor

Fixed and fluidized bed reactors are the most common reactor types, but other types, such as the entrained flow reactor (EFR), have been widely used for gasification. The description of these reactors is accompanied by a comparison between the different reactor types and their most important operational variables.

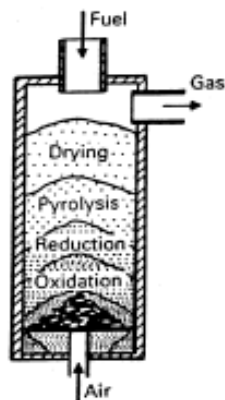
Fixed bed reactor:

The fixed bed reactor is sometimes called a moving bed, due to the slow motion of the solid with respect to the gas [37]. Fig. 1.6 illustrates the two possible configurations for this reactor type: updraft (co-current) and downdraft (counter-current) reactors [39]. As previously explained, the particular type of reactor is determined by the relative position of the intakes for the solid feedstock and gasifying agent.

The main differences between the two types of fixed bed reactors is the lower content of tar [37] and the reduction in the heating value of the product gas [38] when using the downdraft configuration. In addition, the downdraft configuration is less flexible than updraft reactors, which is related to the operational versatility for different feedstocks [37].

The most significant advantage of fixed bed reactors is their high conversion; however, they are usually limited to operation at low temperatures, i.e. below 1000°C [39].

**Counter-current
(Downdraft)**



**Co-current
(Updraft)**

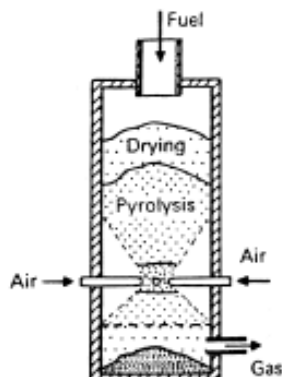


Figure 1.6 Fixed bed reactor configurations. (Reprinted with permission from [39])

Fluidized bed reactor:

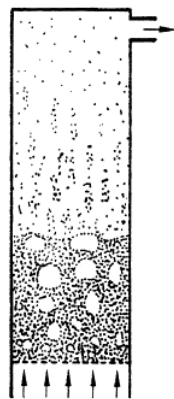
The fluidized bed reactor (FBR) has been extensively applied in coal gasification for several years [40]. However, its application is limited by low carbon conversion, as reported elsewhere [41]. This reactor type is continuously fed close to the bottom, and the gasifying agent flows in continuously from the bottom. The main advantage of the FBR is better distribution, thereby reducing heat and mass transfer limitations. On the other hand, this reactor type is equivalent to a combination between downdraft and updraft reactors, and the associated problem of the low tar cracking must be considered when using an FBR. A major disadvantage of this reactor type is that oxygen is trapped in bubbles, and combustion may take place in a fluidized regime, reducing the efficiency of the gasifier [37].

There are two common types of FBRs, as shown in Fig. 1.7: the bubbling fluidized bed, and the circulating fluidized bed reactor. The bubbling type consists of one single reaction chamber

and fluidization control may be a problem. In the circulating design, solids move in a cycle between the reactor vessel and a cyclone separator, where ash is removed and the remaining char and bed material return to the reaction vessel. In contrast to the bubbling design, the circulating fluidized bed has a very high gas velocity and can recycle very large amounts of solids; therefore, it is capable of handling large feed throughputs [40]. Bubbles do not exist in the circulating design; therefore, oxygen cannot be trapped, and efficiency does not decrease [37].

The operating temperature of fluidized bed gasifiers ranges from 800 to 1000°C, which prevents the buildup of ash. Therefore, these reactors have no limitations in processing feed with high ash content in this temperature range [37]. However, the potential of slagging at low temperatures is the main operational difficulty when using biomass, due to the lower melting point of its ash [39, 40]. The main consideration is how the ash is removed from this type of reactor, which has mostly been ignored in most of the reported literature proposing gasification studies with FBRs.

Bubbling bed



Circulating bed

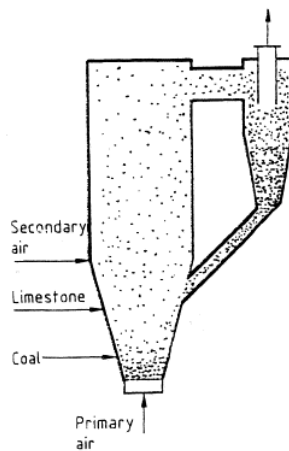


Figure 1.7 Fluidized bed reactors used for gasification. (Reprinted with permission from [39])

Entrained flow reactor (EFR):

Different authors have considered the use of an entrained flow reactor (EFR) in coal gasification [41, 42]. Gasification with an EFR has advantages, such as flexibility, low tar content of the gas product, and high char conversion. These benefits are the reasons why they are the most widely used type of gasifier, with over 75% of the 160 gasification projects in 2005 [43]. In entrained flow gasifiers, the feed powders (less than 75 μm) and gasifying agents both enter from the top of the gasifier. The speed of the gas through the reactor is very fast and enough to entrain all the feed particles.

As the EFR requires a very small particle size, grinding and achieving the appropriate feed size is critical and can sometimes be challenging. This reactor normally operates at temperatures between 1200°C and 1600°C and at pressures between 2MPa to 8 MPa [40, 43]. Due to the high operating temperature, the carbon conversion is higher [37]; however, there is restriction with respect to the material of construction. In this instance, it is vital to implement an effective cooling technique of the produced syngas, because the gas residence time in this reactor type is very short. A comparison of these three types of gasifiers is presented in Table 1.1, as reported by McKendry from the original Rampling work [40].

The heat transfer medium is usually ignored, but the energy required by the endothermic gasification reactions in all gasifiers is directly provided by the reaction gases, which is one reason the heating rate in industrial gasifiers is much faster than any laboratory kinetic study using indirect heating [41].

1.2.4.3 Solid by-product disposal

There are two operational types of flow gasifiers: slagging and non-slagging. In the slagging type, the operating temperature is above the melting temperature of the contained ash, and the molten ash flows down the wall of the gasifier and forms a solid slag layer. The slag layer protects the wall material from further corrosion. In the non-slagging type of flow gasifier, the operating temperature is below the melting temperature of the produced ash; therefore, no solid slag layer is formed. The non-slagging gasifier is more suitable for raw materials with lower ash content [41].

This classification of flow gasifiers is well known for EFRs, but it also extends to fixed bed reactors. Fixed and fluidized bed reactors do not operate at high temperatures, and just non-slagging reactors are considered. An exception is the plasma gasification reactor when fixed or fluidized plasma gasification is applied [14, 15]. This is also the best example of a slagging reactor, since plasma torches can easily melt any biomass or coal slag [44].

The selection of either a slagging or non-slagging reactor is not an easy task; however, it is important to distinguish whether there will be slag formation under specific conditions or not. This aspect is emphasized in the literature, as many authors mention the use of a catalyst and its regeneration; however, this is impossible under slagging conditions.

Table 1.1 Properties of gasification reactor types. (Reprinted with permission from [40])

Advantages	Disadvantages
Fixed / Moving Bed, Updraft	
<ul style="list-style-type: none"> ▪ Simple, inexpensive process ▪ Exit gas temperatures about 250°C ▪ Operates satisfactorily under pressure ▪ High carbon conversion efficiency ▪ Low dust level in gas ▪ High thermal efficiency 	<ul style="list-style-type: none"> ▪ Large tar production ▪ Potential channeling ▪ Potential bridging ▪ Small feed size ▪ Potential clinkering
Fixed / Moving Bed, Downdraft	
<ul style="list-style-type: none"> ▪ Simple process ▪ Only traces of tar in product gas 	<ul style="list-style-type: none"> ▪ Minimum feed size ▪ Limits to scaling up of capacity ▪ Limited ash content allowable in feed ▪ Potential for bridging and clinkering
Fluidized Bed	
<ul style="list-style-type: none"> ▪ Flexible feed rate and composition ▪ High-ash fuels acceptable ▪ Ability to pressurize ▪ High CH₄ in product gas ▪ High volumetric capacity ▪ Easy temperature control 	<ul style="list-style-type: none"> ▪ Operating temperature limited by ash clinkering ▪ High product gas temperature ▪ High tar and fines content in gas ▪ Possibility of high carbon in fly ash
Circulating Fluidized Bed	
<ul style="list-style-type: none"> ▪ Flexible process / up to 850°C operating temperature 	<ul style="list-style-type: none"> ▪ Corrosion and attrition problems ▪ Poor operational control using biomass
Double Fluidized Bed	
<ul style="list-style-type: none"> ▪ Oxygen not required ▪ High CH₄ due to low bed temperature ▪ Temperature limit in the oxidizer 	<ul style="list-style-type: none"> ▪ More tar due to lower bed temperature ▪ Difficult to operate under pressure
Entrained Bed	
<ul style="list-style-type: none"> ▪ Very low in tar and CO₂ ▪ Flexible to feedstock ▪ Exit gas temperature 	<ul style="list-style-type: none"> ▪ Low in CH₄ ▪ Extreme feedstock size reduction required ▪ Complex operational control ▪ Carbon loss with ash ▪ Ash slagging

A summary of slagging and non-slagging characteristics is presented in Table 1.2. The two most important parameters to predict slag formation are temperature and mineral composition,

because they determine the slag flow parameters, such as viscosity. In order to properly operate a slagging reactor, slag must remain in the liquid phase throughout the gasifier and be removed continuously at the bottom. The suggested slag viscosity from various sources varies from 8-15 Pa.s [19] to 1-10 Pa.s [45]. Low viscosity increases the slag velocity; therefore, the insulating layer that protects the wall gasifier may be lost [46]. On the other hand, the slag viscosity must not exceed 25 Pa.s [28, 46, 47] for successful slagging operation.

Table 1.2 Summary of slagging and non-slagging characteristics

Characteristics	
Slagging	<ul style="list-style-type: none"> ▪ Ash melts at a high temperature ▪ Slag protects the gasifier wall from corrosion ▪ Operating temperature is greater than ash melting temperature ▪ Slag temperature ~ 1300-1500°C
• Slag viscosity	<ul style="list-style-type: none"> ▪ Must be less than 25 Pa.s ▪ If too low, slag velocity increases and insulation may be lost ▪ If too high, slag may accumulate on the walls
• Ash composition	<ul style="list-style-type: none"> ▪ Alkali compounds, like sodium carbonate (Na_2CO_3), lower the melting point of silica ▪ Lime (CaO) also lowers the ash melting temperature ▪ Potassium, particularly potassium oxide (K_2O), may be lost through evaporation at high slagging temperature
Non-slagging	<ul style="list-style-type: none"> ▪ Reactor walls are kept free from slag ▪ Operating temperature is less than ash melting temperature ▪ Operates at 800-900°C

The composition of the ash greatly influences its melting temperature. Alkali metals and carbonates, such as sodium and potassium carbonates (Na_2CO_3 and K_2CO_3), are contained in the ash and react with other ash components (i.e. silica) to form low melting point silicates [48].

However, the literature indicates that silica or silicate compounds and not the alkali metals are responsible for lowering the ash melting temperature: for example, the ash melting behavior may be due to calcium silicate compounds and additives rich in quartz (a silicate mineral), which lower the melting temperature [19].

Potassium is beneficial in lowering the melting point of silica; however, it has disadvantages at certain slagging temperatures. As alkali compounds have high vapor pressures, they tend to suffer losses due to sublimation at extended gasifier temperatures [49, 50]. If the slagging temperature can be maintained below 1260°C, K₂O losses can be minimized to about 30% with the addition of rice straw ash [51]. A gasifying agent has been found to influence the melting point of Na₂CO₃. Steam is effective in lowering the melting temperature of Na₂CO₃ and, consequently, the formation temperature of liquid sodium disilicate [48, 52]. In a steam atmosphere, Na₂CO₃ melts at a lower temperature than its standard temperature of 851°C [52].

The selection of the right gasifier type is ultimately linked to the mineral composition of the feedstock; and, extrapolation from high-grade coal to low-grade coal is inconvenient. Moreover, slagging is usually ignored in kinetic modeling, and the assumption of constant alkali content may not be accurate at high temperatures.

1.2.5 Variables affecting char reactivity

Temperature and pressure are the controlled operation variables during gasification and are directly associated with the reactivity. The overall gasification process improves at a higher temperature, regardless of the gasifying agent used [24]. During pyrolysis, temperature and heating rate significantly influence char gasification reactivity more than pressure [53].

However, increasing these variables decreases the thermal efficiency of the process and can be economically unfeasible. Char surface area and total mineral content play important roles in the gasifier selection, since they are not constant properties. The transformation of the feedstock to char is a critical factor, with major differences of reported kinetic results and industrial gasifiers.

1.2.5.1 Reaction temperature

The choice of the reaction temperature to produce syngas can be viewed from two perspectives: (1) energy efficiency and (2) fuel utilization. If energy efficiency is the priority, a relatively low temperature and minimum oxygen input should be used [54]. However, an emphasis on fuel utilization may require a high temperature (about 1350°C) and a suitable excess air ratio (approximately 0.35) to produce desirable yields of H₂ and CO and to lower soot and tar yield [54]. The optimal temperature for gasification must be at a least 900°C to favor high carbon conversion and gas yield [21]. A wide range of temperatures is considered to determine the effect on produced syngas (as outlined below), and on the reaction rate, residence time and surface area.

At temperatures lower than 1000°C, CO decreased and H₂ increases [21, 55, 56]. This indicates that water-gas shift (WGS) reactions are more dominant than the Boudouard reaction [55]. For air-steam gasification, the H₂/CO ratio increases from 0.2 to 1 with increases in temperature, specifically from 750°C to 1150°C [26]. Steam enhances WGS and steam-reforming reactions [26, 57]. In contrast, the CO/CO₂ ratio decreases from 1.2 to 1.1 when the temperature is decreased from 1150°C to 750°C [26]. This justifies the balance between CO-producing (Boudouard, steam reforming) and CO-consuming (WGS) reactions [26].

The reaction rate is slower at low temperatures and takes a longer time to achieve high conversion [58]. Tar and volatile compounds that condense at low temperatures may also be produced, resulting in wall deposits and clogging of pipelines [24, 59].

At high temperatures ($> 1000^{\circ}\text{C}$), both CO and H_2 increase [54, 60, 61], due to enhanced Boudouard, steam-reforming and WGS reactions. CH_4 decreases due to its consumption in the steam-reforming reaction [54, 60, 61]. For air-steam gasification, the H_2/CO ratio increases from 0.6 to 1 when the temperature increases from 1000°C to 1200°C and remains constant at the higher temperature of 1350°C [55]. Tars decrease at high temperatures, due to thermal cracking and steam reforming [24]. Above 1000°C , cold gas efficiency is improved [59], and higher reaction rates and carbon conversion have been observed [22].

At very high temperatures ($1400\text{-}1500^{\circ}\text{C}$), both H_2 and CO decrease. At this temperature range, the reaction shifts to the combustion region from the gasification region [60]. Particles collapse and shrink, due to very high temperatures, which referred to as sintering [50]. A decrease in the produced syngas is obtained at very high temperature, as a result of the lower surface area, even at high residence times [61]. Table 1.3 presents a summary of the effects of temperature on syngas production, considering the corresponding reactions and reactivity.

Table 1.3 Summary of the effect of temperature on syngas production and gasification rate

Temperature	Characteristics
Low (<1000°C)	<ul style="list-style-type: none">- C decreases, H₂ increases; WGS reactions more dominant than Boudouard reactions- H₂/CO ratio increases for air-steam gasification, due to WGS and steam reforming reactions- CO/CO₂ ratio decreases, due to a balance between CO-producing and CO-consuming reactions- Slower reaction rate- Longer residence time to achieve high conversion- Tars may be produced
High (>1000°C)	<ul style="list-style-type: none">- CO and H₂ increases due to Boudouard, steam reforming and WGS reactions- CH₄ decreases due to steam reforming- H₂/CO ratio increases for air-steam gasification- Tars decreases due to thermal cracking and steam reforming- Improves cold gas efficiency (CGE)- Higher reaction rates and carbon conversion
Very high (~1500°C)	<ul style="list-style-type: none">- H₂ and CO decreases due to sintering- Reaction shifts to combustion from gasification region- Particles collapse and shrink- Lack of surface area

1.2.5.2 Total pressure and gasifying agent partial pressure

Several works have reported changes in the partial pressure of the gasifying agent by varying the proportion of gasifying agent with respect to an inert gas used as a carrier gas [21, 23, 25-27, 32, 33, 53-57]. The effects of total pressure [32, 57, 62, 63] have shown opposite relationships between thermodynamics and kinetics [63]. Since Boudouard and coal-steam reactions have a

net increase in gas molecules (Eqs. (1-1) and (1-2), respectively), increases in total pressure decrease the yield of gas products. For example, Fermoso et al. report that atmospheric gasification produces higher H₂ and CO yields with better cold gas efficiency and higher conversion than gasification at 15 atm [62].

Table 1.4 shows a summary of the oxygen partial pressure and total gasification pressure as presented by Wall et al. [63]. In general, it is accepted that the effect of the pressure is not significant compared with other variables, such as temperature and mineral composition; however, other technical problems related to slag formation are affected by total pressure. Some mineral components that melt at low temperatures are transformed in minerals with high melting points, such as mullite and sanidine. On the other hand, minerals with significant contents of iron reduce the melting point of the ash [64].

1.2.5.3 Pyrolysis and char surface area development

Usually the way that the char is produced is not considered during experimental kinetic studies [23-27, 33, 40, 44, 62, 65]. However, the experimental procedure can affect the char reactivity during gasification [35], because the most common gasification procedures follow the proximate analysis protocol using CO₂ or steam in the last step, instead of air or oxygen as indicated by the ASTM D5142 standard. The literature demonstrates a lack of understanding and accurate information about the relationship between pyrolysis and gasification; therefore, it is difficult to find a comparison of the results of chars produced with different methods as presented by Silbermann et al. [34].

Table 1.4 Summary of the effect of oxygen partial pressure and total gasification pressure.

(Reprinted with permission from [63])

Coal chemical/ physical	Effect of pressure on the process
Char combustion	Rate ↑ with increasing O ₂ partial pressure at a fixed total pressure
Char combustion	Rate first ↑ and then ↓ with increasing total pressure at a fixed O ₂
CO/CO ₂ ratio	Rate ↓ with increasing O ₂ partial pressure
Char temperature	↑ with increasing O ₂ partial pressure at a fixed total pressure
Char gasification	Rate ↑ with increasing reactant gas pressure
Pyrolysis volatile yield	↓ with increasing total pressure
Char reactivity	↓ with increasing pyrolysis pressure
Swelling property	First ↑, then ↓ with increasing pyrolysis pressure
Average char porosity	↑ with increasing total pyrolysis pressure
Initial char surface area	↓ with increasing total pyrolysis pressure
Heat transfer	No effect of total pressure (< 20 atm) on gas conductivity
Homogeneous reaction	Rate ↑ with increasing total pressure
Bulk diffusivity	↓ with increasing total pressure
Knudson diffusivity	No effect of total pressure

In 1994, Senneca et al. [67] provided an explanation for the reactivity differences of char produced with different holding times before the gasification and proposed a correlation between deactivation of the char surface and its exposure at high temperatures and pressures. The introduction of the thermal annealing concept to explain changes in the properties of char surfaces was very important; however, it is still incomplete, and no experimental tests to correlate surface area and reactivity reduction have been performed in further studies. Other authors have found that there is no agreement between experimental results and the expected activity of a specific char if the history from coal to char is omitted [32, 65].

If pyrolysis is considered as a part of the whole gasification, as shown in Fig. 1.5, its residence time in industrial gasifiers is necessarily lower than the residence time of gasification, due to the fact that pyrolysis is much faster than gasification, regardless of the gasifying agent. However, when pyrolysis and gasification are performed in different reactors or intentionally separated, the residence time of pyrolysis is increased, and the produced char is less reactive [65-67]. Unfortunately, recent works do not consider this important aspect of gasification, since the total time that the sample is held at high temperatures is not controlled and it is not negligible with respect to the total residence time. Therefore, kinetic studies do not model the exact behavior on an industrial scale.

Regardless of the solid feedstock (e.g. coal, biomass, petcoke), the controlled gasification variable associated with the pyrolysis step is the heating rate. It has been reported that the faster the heating rate, the more reactive the char [17, 58, 61], which is a well-known limitation of many experimental setups, such as thermogravimetric analyzers (TGA). To overcome this situation, some researchers have used a drop furnace reactor [53, 105], an entrained flow reactor (EFR) [58, 61] and other reactor setups [80] to produce the char, subsequently performing the char gasification in batch reactors with TGA or gas product analyses.

An unusual influence of the heating rate on the char surface was reported by Seo et al. [68], who showed that the pore surface area presents a maximum for a particular heating rate; however, it may be a consequence of heat transfer limitations. This phenomenon can be quantified using the Brunauer-Emmett-Teller (BET) method at different heating rates. It is important to note that control of the heating rate is only possible if gasification and pyrolysis

occur in different reactors, which is not an economical option, and there is no reason to reduce the heating rate.

The EFR has been used to produce char and minimize the changes on the char surface at the laboratory and bench scales [32, 33, 69]; however, their respective gasification kinetic studies were performed in a different reactor (high pressure TGA), holding the char at a high temperature before gasification. Complete kinetic studies of direct gasification (without separate pyrolysis from gasification) using an EFR have not been conducted, as this technology is only operational in power plants fuelled by coal (IGCC).

1.2.5.4 Mineral content and composition

The ranks and grades of coals and their difference are presented in Section 1.1. In different circumstances, coal characteristics overlap; and low-rank coals are considered as the same type of coal as low-grade coals. The reactivity of low-rank coals is higher than high-rank coals with similar ash contents [17, 70]; however, it also depends on the amount of alkali and alkaline earth metals.

It is interesting that reactivity is reduced when ash-free coal is gasified, which can be observed by comparing the gasification of the parent coal and its respective ash-free coal [71-74]. Different authors have presented alternative methods to obtain ash-free coal [1, 71]; however, it is important to determine whether it makes sense to remove the ash and, in a further step, add an alkali-based catalyst. For this reason, it is important to understand the effect of the mineral content as a catalyst and the advantage of low-grade coals in implementing gasification.

The total mineral content is determined using the ASTM D5142 standard and is equivalent to the ash content determined in the proximate analysis. This is a general classification, and it is useful in combustion; however, it is incomplete for gasification, since inorganic species act as a catalyst for the reaction itself. High ash content materials are definitely less desirable for combustion, but their gasification reactions are much faster than those of low-ash feedstock [17, 70]; therefore, co-feeding with low-grade coal or biomass is one alternative to improve the overall process [27].

The mineral composition determined by the ash analysis is usually performed using the ASTM D3682 standard, with ash obtained at 750°C. This is usually accurate for gasification at low temperatures; however, potassium can evaporate [72] or produce low melting point slag in the reaction temperature range [75]. Therefore, extrapolation of results at high temperatures must be analyzed in detail to avoid overestimation of the active mineral amounts. On the other hand, at low temperatures, the comparison of kinetic parameters is not easy if the reaction is not chemically controlled and free of thermodynamic limitations: for example, a comparison of activation energies (E_A) between CO₂ gasification [72] and steam gasification [74] using same ash-free coals yields unexpected and questionable results, such as $E_{A_CO_2} < E_{A_Steam}$.

There are different types of raw materials that can be used as feedstock for gasification, and their ash analysis is performed as described for coal. The most common ones are coal, biomass, and petcoke, which is a by-product of oil refinery operations that can be used as raw material for gasification if its low reactivity can be enhanced, thereby reducing problems related to its disposal and improving the energy balance in oil sands upgrading [28, 76]. Biomass is beneficial to the environment, because it is CO₂ neutral when using straw and other non-edible materials

[54]. Biomass has high reactivity, due to its high contents of volatiles and alkali compared with coal [41, 54, 77].

The key factor is the balance between the price of the raw material and the reactivity of the feedstock. The reactivity is directly related to the surface area and alkali content [78]. Alkali and alkaline earth metals undergo different catalytic activity to promote CO₂ gasification [34, 79, 80] and steam gasification [81, 82], with an effectiveness order of potassium (K) > sodium (Na) > calcium (Ca) > magnesium (Mg) [83]. Khalil et al. [84] reported a reduction in CH₄ formation when potassium carbonate (K₂CO₃) was added to the feedstock.

1.2.6 Kinetic studies

The aim of this section is provide an explanation of the differences between a single-step kinetic model and a multiple-step kinetic model, such as the Langmuir-Hinshelwood models. The reaction mechanism for gas-solid reactions indicates that multiple steps should be considered; however, an exact reaction sequence is implied or a reaction mechanism is assumed. For this reason, a simplified version is a single-step kinetic model if the reaction takes place in the temperature range where the reaction is chemically controlled [85].

The selection of a particular chemical reaction model depends on the trend presented by the experimental information; therefore, it is important to avoid inducing parallel effects of the experiment on the gasification itself. The number of references dealing with CO₂ gasification is significantly higher than steam gasification, due to the technological challenges when dealing with steam at high temperatures; however, there are no consistent criteria in the literature and results for the kinetic parameters vary among authors [17].

1.2.6.1 CO₂ gasification

Different studies related to CO₂ gasification have been reported TGA[27, 34, 35, 53, 65, 66, 69, 72, 73, 77, 82, 83, 85] or other methods to determine the progress of the reaction, such as gas analysis using gas chromatography [21, 29, 33, 56, 69, 84]. The main reason for using this technique is the continuous readings and more accurate information when data are recorded along the reaction progress [63]; however, one disadvantage is that selectivity of competitive reactions cannot be analyzed, just the global kinetics. Thus, it is enough to perform TGA experimentation, with its lower uncertainty, for CO₂ than with other product analysis techniques.

The most common kinetic methods are related to isothermal batch experiments, since just one experimental run is required to obtain the rate constant and reaction order for a particular combination of temperature and pressure [86]. Single-step models are an extension from coal combustion to gasification, with the same assumptions about the changes on the surface area with respect the grade of conversion [87, 88].

There is an overlap between pyrolysis and gasification, since the sample should be heated from ambient conditions to the reaction temperature; however, this overlap is not significant, and different experimental methods can be compared by changing the holding time after reaching the reaction temperature [34]. The experiment is often evaluated in two stages: (1) char production and (2) char gasification, for example, producing char in an EFR and performing kinetic studies with TGA [69]. An important flaw is that any thermal treatment at high temperature induces changes in the char surface area [65-67].

At the temperature range between 650°C and 750°C, the Boudouard reaction is thermodynamically limited [89], and a comparison of activation energies at different temperature ranges is not appropriate.

1.2.6.2 Steam gasification

The steam gasification rate is significantly slower than the combustion rate when using the same feedstock. Steam is highly corrosive at the reaction conditions [90, 91]; therefore, it is not possible to perform steam gasification using the conventional setup used for CO₂ gasification. Different authors have presented particular setups, i.e. batch reactors with analysis of the product gas [33, 88, 92, 93], TGA [82, 94] and flow reactors [26, 95]; however, experimental procedures are not standardized and they are similar to those used for CO₂ gasification.

Kinetic modeling of steam gasification is usually reported using single-step reaction models similar to those used for CO₂ gasification [34, 96, 97]. In the literature, intrinsic kinetic studies have revealed that the particle size and gas flow rate limit the overall reaction rate. In contrast, the amount of sample is usually disregarded, and there are studies that have used samples of less than 15 mg [34, 94, 96] and others with samples of more than 100 mg [33, 88, 92, 93], with no mention of the effects of the mass transfer.

Steam gasification is much faster than CO₂ gasification when compared under the same experimental conditions [33, 97, 98]. It is reported lower activation energy for steam with respect to the CO₂ gasifying agent [97, 98].

1.2.6.3 Assumptions and simplifications

A challenge in gasification research is that many of the assumptions in kinetic modeling have not been clearly mentioned, and the understanding of the implicit considerations of every single model is an onerous task. Three implicit assumptions must be reviewed in order to improve kinetic analysis:

Mass transfer limitation:

Below 1000°C, the chemical reaction is the controlling step; and, it is considered that mass transfer does not have a significant effect [33, 85]. This is an assumption that must be revised in this thesis, because it can affect results and is only related to intra-pore diffusion [86]. However, particle size information has been omitted, and chemical control is considered for experiments with samples of more than 1 g [27, 33]. Interparticle diffusion also plays an important role that cannot be overlooked [99] and is dependent on the internal geometrical configuration of the reactor. The related variables are not totally understood in the scientific community.

Char synthesis:

As mentioned in Section 1.2.5.3, the char synthesis path is usually ignored or at least not mentioned in technical reports or related literature. Most of the kinetic studies performed in an EFR have been designed to reduce the effect of a low heating rate [21, 26, 29, 55-57, 61, 69], with further analyses at low temperatures using TGA [61, 69].

Comparisons of different experimental works are difficult, since the way that char is produced is not well explained and not all elements are considered [17, 65]. The main assumption in most reported kinetic studies is that the pyrolysis step yields a unique char (using the same temperature, sweeping gas and heating rate). It is also assumed that char surface

characteristics are not affected by chemical treatments; for example, Kopyscinski et al. [72-74] presented three independent studies of ash-free coal without reporting the char surface area and its effect on char reactivity.

Existence of a maximum reaction rate:

It is implicitly accepted for almost all the references mentioned in this chapter that a maximum reaction rate at the beginning of the gasification is a consequence of changes on the char surface, with the exception of Silbermann et al. [34]. This assumption is emphasized when kinetic models are compared either for CO₂ or steam gasification to fit the experimental results [23, 27, 33, 53, 65, 69, 72, 88, 94, 96, 99-104].

These last two assumptions (char synthesis and maximum reaction rate) are implicit, and there is a lack of consensus in the scientific community on the differences of reported kinetic parameters [17]. The validity of these assumptions are presented in detail in Chapters 4 and 7.

1.2.6.4 Chemical reaction kinetic models

Single-step chemical reaction models are the simplest expressions that model the kinetic behavior of gas-solid reactions if adsorption and desorption are not considered or if they can be assumed as not limiting factors for the overall reaction. These reaction models can be considered as a good representation of the gas-solid reaction if the temperature range of the reaction takes place below 1000°C, whereby the chemical reaction is the controlling step and mass transfer does not have a significant effect [33, 85]. There is a theoretical explanation for these models and they are well clarified elsewhere [65, 96, 100]. The following points detail a brief presentation of the most common single-step chemical reaction kinetic models.

- The volumetric model (VM) is the simplest model that describes a gas-solid reaction. It considers that the reaction takes place uniformly within the volume of the particle. The volumetric model is given by:

$$\frac{dX}{dt} = k_{VM}(1 - X) \quad \text{Eq. (1-5)}$$

- The shrinking core model (SCM) assumes that the reaction occurs only on the surface area of a shrinking carbon core. The main assumption is that the reaction moves from the surface towards the interior of the particle. The model is described by:

$$\frac{dX}{dt} = k_{SCM}(1 - X)^{2/3} \quad \text{Eq. (1-6)}$$

- The integrated core model (ICM) considers a parameter n related to the reaction order: it can be interpreted as a form factor for different geometries of the particle, for spheres, $n=2/3$, cylinders, $n=1/2$, and flat plates, $n=0$.

$$\frac{dX}{dt} = k_{IM}(1 - X)^n \quad \text{Eq. (1-7)}$$

- The above models are unable to describe a maximum value of reaction rate. This is why different authors have considered the random pore model (RPM) as the best kinetic model [23, 27, 33, 53, 65, 69, 72, 88, 94, 99-104]. The RPM considers two competing effects of structural changes during the reaction. There is a growth of accessible pores in the initial state of gasification and the coalescence or overlapping of neighboring pores' surfaces, which reduces the area available for reaction [101, 102]. The overall reaction rate is given by:

$$\frac{dX}{dt} = k_{RPM}(1 - X)\sqrt{1 - \psi \ln(1 - X)} \quad \text{Eq. (1-8)}$$

where ψ represents a parameter that describes the internal structure of the non-converted char. The definition of ψ is given by:

$$\psi = \frac{4\pi L_0(1 - \varepsilon_0)}{S_0^2} \quad \text{Eq. (1-9)}$$

where S_0 is the pore surface area per volume, L_0 is the pore length per volume, ε_0 is the solid porosity, π is a mathematical constant (3.14159), and ψ is calculated using a reduced quantity, such as $t/t_{0.5}$ [90]:

$$\frac{t}{t_{0.5}} = \frac{\sqrt{1 - \psi \ln(1 - X)} - 1}{\sqrt{1 - \psi \ln(1 - X_{0.5})} - 1} \quad \text{Eq. (1-10)}$$

This method to estimate ψ is not representative if the data for r vs. X are not linear or show a maximum. A better approach is presented by Zou et al. [93] determining ψ with known experimental information when a maximum reaction rate is observed:

$$\psi = \sqrt{1 - \psi \ln(1 - X_m)} \quad \text{Eq. (1-11)}$$

In the particular case when the maximum is not observed, r_m is given at $X_m=0$, and the value of ψ in Eq. (1-11) is equal to 2.

The RPM has been widely accepted due to its nonlinear dependence on char surface, which can predict a maximum reaction rate as observed experimentally since Bhatia and Perlmutter proposed it in 1980 [101], with a further modification [102] for gas-solid reactions. Different modifications of the original model and their applications to fit experimental data have been reported: for example, some of the most recent works present extended [72] and adaptive [103] RPMs. Modeling improvement is commonly

attached to an increase in the number of the fitting parameters; however, this does not necessarily translate to a better understanding of the reaction mechanism.

- The normal distribution function (NDF) is able to describe the gasification rate, even if the maximum is at $X=0$ [96]. Parameters are estimated by using nonlinear regression instead of a determined conversion assumption, which makes this model easier to implement. The reaction rate can be expressed as a function of the intrinsic rate of reaction multiplied by a normal probability density:

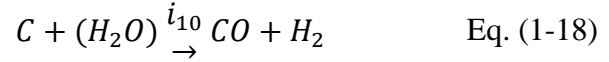
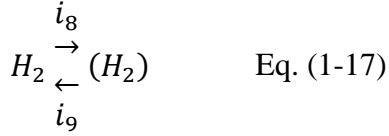
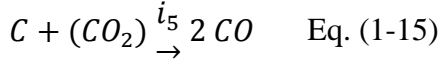
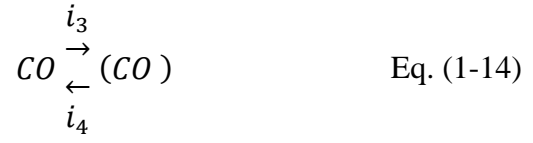
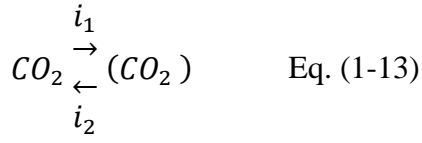
$$r = \frac{dX}{dt} = k_{NDF} \cdot \exp\left(\frac{-(X - X_m)^2}{\alpha}\right) \quad \text{Eq. (1-12)}$$

For all of the aforementioned models, the rate constant (k_{model}) is considered as a parameter at isothermal conditions. This parameter is a function of the reaction temperature (Arrhenius equation). In addition, the effect of the total pressure is included in this term, but it can also be an independent function if the total pressure is not constant along the reaction progress.

1.2.6.5 Langmuir-Hinshelwood kinetic models

Langmuir-Hinshelwood (LH) kinetic models were developed based on adsorption/desorption theories and are practical if there is competition between species. If the reaction temperature increases, the controlling step is intra-pore diffusion; therefore, an intrinsic kinetic model adjusted by adsorption/desorption (using an LH model) may fit better with the experimental results and permit the use of kinetic data extrapolation for higher temperatures, as proposed by Kajitani et al. [69] for CO₂ coal gasification.

Using a simplified version as proposed by Umemoto [104], the elementary reactions are:



The LH model (without considering the reduction in char area) for CO₂ gasification and steam gasification are expressed in Eq. (1-19) and Eq. (1-20), respectively:

$$r = \frac{k_{11}P_{CO_2}}{1 + k_{12}P_{CO_2} + k_{13}P_{CO}} \quad \text{Eq. (1-19)}$$

$$r = \frac{k_{21}P_{H_2O}}{1 + k_{22}P_{H_2O} + k_{23}P_{H_2}} \quad \text{Eq.(1-20)}$$

The complete expression, including the change on char surface, is obtained using two factors: one of them corresponds to an LH model, and the second term corresponds to the intrinsic kinetic model (without the rate constant). For example, when the RPM is considered, Eq. (1-21) shows a simplified model proposed by Kajitani et al. [69], obtained by the multiplication of Eqs. (1-19) and (1-8):

$$r = \frac{k_{11}P_{CO_2}}{1 + k_{12}P_{CO_2} + k_{13}P_{CO}} (1 - X) \sqrt{1 - \psi \ln(1 - X)} \quad \text{Eq. (1-21)}$$

Adsorption and desorption are less significant at high temperatures, since the heat of adsorption is at the same magnitude as the heat of condensation [86]; therefore, many of the advantages of using LH models at high temperature lack of theoretical support. These models present better fit, because they have more regression parameters; however, this does not necessarily offer a better explanation of the gasification mechanism.

Steam gasification occurs much faster than CO₂ gasification, but there is no comprehensive study in the literature that indicates the relative scale between both reactions. A few works have compared these two reactions under similar conditions (including the reaction gas flow rate) as presented by Ahmed and Gupta [33], Ren et al. [97] and Marquez et al. [98], showing that steam gasification rate is more than twice the CO₂ gasification rate.

1.3 Objectives

The main concern in gasification research is the determination of reliable kinetic information in order to formulate kinetic models that can be used in the design of industrial reactors. As a consequence, different assumptions for the modeling of the overall kinetics have been accepted in the scientific community as fact; unfortunately, some of these concepts are misinterpretations of the experimental procedure. Consequently, the main objective of this thesis is the provision of new findings related to the reaction mechanism and its kinetic modeling. Additionally, concepts on chemical reaction fundamentals must be developed to validate and compare different kinetic models.

The specific objectives of this thesis are:

- Evaluation of different TGA experimental procedures for CO₂ gasification to understand the effects of non-considered variables; e.g. isothermal pyrolysis, sample amount.
- Investigation of the effect of gas replacement to separate pyrolysis and gasification during experimental studies of gasification kinetics.
- Exploring the dependence of char reactivity relative to the char synthesis path.
- Investigation of the effect of the non-isothermal pyrolysis in char gasification reactivity.
- Investigation of the effect of the isothermal pyrolysis in char gasification reactivity.
- Linking of gasification and pyrolysis, determining if the process can be separated without introducing incorrect information and possible misinterpretation of the overall mechanism.
- Validation of assumptions about the general reaction mechanism of gasification with either CO₂ or steam as gasifying agents.
- Identification of the most important variables that affect the gasification conversion rate.
- Development of experimental procedures to improve the study of gasification kinetics for CO₂ and steam gasification.
- Evaluation of the effect of mass transfer during gasification studies and determination of whether they can be considered as intrinsic kinetic studies.
- Separation and explanation of the difference between interparticle and intraparticle diffusion effects.
- Evaluation of the accuracy of single-step chemical reaction kinetic models in the range where the reaction is chemically controlled.

- Determination of the parameters of the Arrhenius equation independent of the kinetic model.
- Validation of the accuracy of the chemical reaction models based on the consistency of the reaction mechanism and the kinetic parameters.
- Provision of fundamentals of chemical reaction engineering to validate consistency of kinetic models for any chemical reaction.

1.4 Thesis structure

This thesis contains eight chapters, organized sequentially in a paper-based structure. It is important to mention that each chapter from Chapters 2 to 6 introduces concepts and results that are fundamental elements or starting points of subsequent chapters.

- Chapter 1 deals with the introduction to this thesis, a literature review and objectives of the research. Definitions that are widely accepted in this field are described, without mentioning the new concepts that are presented in subsequent chapters.
- Chapter 2 illustrates a statistical analysis and transformation of variables required to use the experimental data in Chapters 3, 4 and 6. Some concepts not usually mentioned in journal papers relating to data processing for kinetic analysis are presented in detail, with special attention to heteroscedasticity and data point dispersion smoothing. It is demonstrated that the conventional approach of comparing kinetic models by the coefficient of determination may be inaccurate.
- Chapter 3 provides the definition of new terms associated with the experimental procedure, such as isothermal pyrolysis. Two important breakthroughs on gasification

related to the sequence of the experimental procedure are shown for the first time. The first one is the demonstration of the non-existence of a maximum reaction rate associated to changes on the char surface. The second breakthrough is an explanation of char reactivity reduction due to the reduction of the char pore surface area during isothermal pyrolysis. This chapter is focused on the first six objectives and is the starting point for the validation of old theories related to gasification.

- Chapter 4 shows the development of a new model to estimate gasification rate based on the properties of the parent coal. The model shows that the two most important gasification variables associated to the feedstock are micropore surface area and alkali content. A new approach is presented to cover a wider range of ash composition by showing that surface area based on carbon content (instead of coal content) best represents the involved active surface. The proposed model validates the estimated gasification rate of coal mixtures, without the assumption of a linear combination of the original species gasification rate.
- Chapter 5 introduces an alternative method for the estimation of the activation energy of any heterogeneous reaction independent of the kinetic model. This is presented to validate gasification kinetic models, since the existing kinetic models do not necessarily model the real gasification mechanism. The theoretically deduced equation goes beyond gasification and is, by itself, an important contribution to chemical reaction engineering fundamentals.
- Chapter 6 explains additional limitations to determine the intrinsic kinetics not detected in conventional experimental procedures. This chapter links the previous chapters and states the experimental procedure to perform steam gasification. It is the first

experimental study of steam gasification performed at the University of Calgary using thermogravimetric techniques.

- Chapter 7 is the synthesis of this thesis. This shows a summary of the new findings and presents the reasons of the thesis sequence and the connections between chapters.
- Chapter 8 presents the conclusions of this work and provides recommendations for future works within this field and for the general thermochemical conversion of solid feedstock.

The topics covered within the literature review, new findings and conclusions are the contributions of R. Arturo Gomez to a paper review done by Nader Mahinpey, Arturo Gomez and Aqsha Aqsha that will be submitted to *Chemical Engineering Science*.

1.5 References

- [1] Rivolta Hernandez M, Figueroa Murcia C, Gupta R, De Klerk A. Solvent–coal–mineral interaction during solvent extraction of coal. *Energy Fuels* 2012; 26 (11): 6834–6842.
- [2] Natural Resources Canada. <http://www.nrcan.gc.ca/energy/coal/4277>. (Last accessed on August 2014).
- [3] Thibault B. Electricity from coal: time to turn the page on Canada’s dirtiest source of power. Pembina Institute; 2012. <http://www.pembina.org/blog/634>. (Last accessed on July 2014).
- [4] Cousins A, Hughes RW, McCalden DJ, Lu DY, Anthony EJ. Waste classification of clag generated in a pilot-scale entrained-flow gasifier. *CSIRO-CanmetENERGY*; 2012 (4):37-44. www.coalcgp-journal.org. (Last accessed on August 2014).
- [5] Bielowicz B. A new technological classification of low-rank coal on the basis of Polish deposits. *Fuel* 2012; 96: 497–510.
- [6] O’Keefe JMK, Bechtel A, Christanis K, Dai S, DiMichele WA, Eble CF, Esterle JS, Mastalerz M, Raymond A, Valentim BV, Wagner NL, Ward CR, Hower JC. On the fundamental difference between coal rank and coal type. *Int J Coal Geol* 2013; 118: 58–87.
- [7] Stanley P. Schweinfurth. An introduction to coal quality. U.S. Geological Survey Professional Paper 1625–F.2009. <http://pubs.usgs.gov/pp/1625f/downloads/ChapterC.pdf>. (Last accessed on August 2014).
- [8] The national energy technology laboratory (NETL): gasification technologies: gasification markets and technologies- present and future. 2002. http://www.netl.doe.gov/File%20library/research/coal/energy%20systems/gasification/gasifipedia/Gasification_Technologies.pdf. (Last accessed on August 2014).
- [9] Hoffmann BS, Szklo A. Integrated gasification combined cycle and carbon capture: A risky option to mitigate CO₂ emissions of coal-fired power plants. *Appl Energy* 2011; 88: 3917-3929.

- [10] US Energy Information Administration. Year-to-date natural gas use for electric power generation is down from 2012. 2013. <http://www.eia.gov/todayinenergy/detail.cfm?id=10771>. (Last accessed on August 2014).
- [11] US Energy Information Administration. Future power market shares of coal, natural gas generators depend on relative fuel prices. 2013. <http://www.eia.gov/todayinenergy/detail.cfm?id=10951>. (Last accessed on August 2014).
- [12] US Energy Information Administration. Natural gas consumption has two peaks each year. 2011. <http://www.eia.gov/todayinenergy/detail.cfm?id=2050>. (Last accessed on August 2014).
- [13] Rezaiyan J, Cheremisinoff NP. Gasification Technologies, A premier for Engineer and Scientists. Boca Raton: CRC Press, Taylor & Francis Group; 2005.
- [14] Materazzi M, Lettieri P, Mazzei L, Taylor R, Chapman C. Tar evolution in a two stage fluid bed–plasma gasification process for waste valorization. Fuel Process Technol 2014; 128: 146–157.
- [15] Ruj B, Ghosh S. Technological aspects for thermal plasma treatment of municipal solid waste—A review. Fuel Process Technol 2014; 126: 298–308.
- [16] Dermot JR. A syngas network for reducing industrial carbon footprint and energy use. Appl Therm Eng 2013; 53: 299-304.
- [17] Di Blasi C. Combustion and gasification rates of lignocellulosic chars. Prog Energ Combust 2009; 35: 121–140.
- [18] Ma L, Zhu Y, Chen H, Ding Y. An environment friendly energy recovery technology: Municipal solid waste gasification. Third International Conference on Measuring Technology and Mechatronics Automation. 2011: 407-409.
- [19] Coda B, Cieplik MJ, de Wild P J, Kiel JH. Slagging behavior of wood ash under Entrained-flow gasification conditions. Energy Fuels 2007; 21: 3644-3652.

- [20] Bremaud M, Fongarland P, Anfray J, Jallais S, Schweich D, Khodakov AY. Influence of syngas composition on the transient behavior of a Fischer-Tropsch continuous slurry reactor. *Catal Today* 2005; 106: 137-142.
- [21] Zhao Y, Sun S, Tian H, Qian J, Su F, Ling F. Characteristics of rice husk gasification in an entrained flow reactor. *Bioresource Technol* 2009; 100: 6040-6044.
- [22] Qian F, Kong X, Cheng H, Du W, Zhong W. Development of a kinetic model for industrial entrained flow coal gasifiers. *Ind Eng Chem Res* 2013; 52: 1819-1828.
- [23] Feroso J, Arias B, Pevida C, Plaza MG, Rubiera F, Pis JJ. Kinetic models comparison for steam gasification of different nature fuel chars. *J Therm Anal Calorim* 2008; 91 (3): 779-786.
- [24] Hernandez JJ, Ballesteros R, Aranda G. Characterization of tars from biomass gasification: Effect of the operating conditions. *Energy* 2012; 50: 333-342.
- [25] Kim Y, Park J, Jung D, Miyawaki J, Yoon S, Mochida I. (2013). Low-temperature catalytic conversion of lignite: 1. Steam gasification using potassium carbonate supported on perovskite oxide. *J Ind Eng Chem* 20 (2014) 216–221.
- [26] Hernandez JJ, Aranda G, Barba J, Mendoza JM. Effect of steam content in the air-steam flow on biomass entrained flow gasification. *Fuel Process Technol* 2012; 99: 43-55.
- [27] Gil MV, Riaza J, Alvarez L, Pevida C, Pis JJ, Rubiera F. Kinetic models for the oxy-fuel combustion of coal and coal/biomass blend chars obtained in N₂ and CO₂ atmospheres. *Energy* 2012; 48: 510-518.
- [28] Duchesne MA, Ilyushechkin AY, Hughes RW, Lu DY, McCalden DJ, Macchi A, Anthony E J. Flow behavior of slags from coal and petroleum coke blends. *Fuel* 2012; 97: 321-328.
- [29] Hernandez JJ, Aranda-Almansa G, Bula A. Gasification of biomass wastes in an entrained flow gasifier: Effect of the particle size and the residence time. *Fuel Process Technol* 2012; 91: 681-692.

- [30] Pian CC. Regenerative gasification systems operating on farm-waste and bioenergy-crop feedstocks. 37th Intersociety Energy Conversion Engineering Conference 2002: 668-674.
- [31] Siemens Energy. Integrated gasification combined cycle. www.energy.siemens.com/hq/en/fossil-power-generation/power-plants/integrated-gasification-combined-cycle/integrated-gasification-combined-cycle.htm (Last accessed on August 2014).
- [32] Tremel A, Spliethoff H. Gasification kinetics during entrained flow gasification – Part II: Intrinsic char reaction rate and surface area development. *Fuel* 2013; 107: 653-661.
- [33] Ahmed II, Gupta AK. Kinetics of woodchips char gasification with steam and carbon dioxide. *Appl Energy* 2011; 88 (5): 1613-1619.
- [34] Silbermann R, Gomez A, Gates I, Mahinpey N, Kinetic studies of a novel CO₂ gasification method using coal from deep unmineable seams. *Ind Eng Chem Res* 2013; 52: 14787–14797.
- [35] Zhu W, Song W, Lin W. Catalytic gasification of char from co-pyrolysis of coal and biomass. *Fuel Process Technol* 2008; 89 (9): 890-896.
- [36] Zhang Q, Wu Y, Dor L, Yang W, Blasiak W. A thermodynamic analysis of solid waste gasification in the Plasma Gasification Melting process. *Appl Energy* 2013; 112: 405–413.
- [37] Ruiz J, Juarez M, Morales M, Munoz P, Mendivil M. Biomass gasification for electricity generation: Review of current technology barriers. *Renew Sust Energ Rev* 2013; 18: 174 - 183.
- [38] Kihedu JH, Yoshiie R, Nunome Y, Ueki Y, Naruse I. Counter-flow air gasification of woody biomass pellets in the auto-thermal packed bed reactor. *Fuel* 2014; 117: 1242–1247.
- [39] Warnecke R. Gasification of biomass: comparison of fixed bed and fluidized bed gasifier. *Biomass Bioenerg* 2000; 18: 489 - 497.
- [40] McKendry P. Energy production from biomass (part 3): gasification technologies. *Bioresource Technol* 2002; 83: 55 - 63.

- [41] Tremel A, Becherer D, Fendt S, Gaderer M, Spliethoff H. Performance of entrained flow and fluidised bed biomass gasifiers on different scales. *Energy Convers Manage* 2013; 69: 95 - 106.
- [42] Collot A. Matching gasification technologies to coal properties. *Int J Coal Geol* 2006; 65 (3): 191 - 212.
- [43] Minchener A. Coal gasification for advanced power generation. *Fuel* 2005; 84(17): 2222-2235.
- [44] Rutberg PhG, Bratsev AN, Kuznetsov VA, Popov VE, Ufimtsev AA, Shtengel SV. On efficiency of plasma gasification of wood residues. *Biomass Bioenerg* 2011; 35: 495 -504.
- [45] Wang B, Li X, Xu S, Paterson N, Dugwell D R, Kandiyoti R. Performance of Chinese coals under conditions simulating entrained-flow gasification. *Energy Fuels* 2005; 19 (5): 2006-2013.
- [46] Schrober HH, Streeter RC, Diehl EK. Flow properties of low-rank coal ash slags: Implications for slagging gasification. *Fuel* 1985; 64 (11): 1611-1617.
- [47] Kong L, Bai J, Bai Z, Guo Z, Li W. Effects of CaCO₃ on slag flow properties at high temperatures. *Fuel* 2012; 109: 76-85.
- [48] Kosminski A, Ross D P, Agnew JB. Influence of gas environment on reactions between sodium and silicon minerals during gasification of low-rank coal. *Fuel Process Technol* 2006; 87: 953-962.
- [49] Nzihou A, Stanmore B, Sharrock P. A review of catalysts for the gasification of biomass char, with some reference to coal. *Energy* 2013; 58: 305-317.
- [50] Jones JM, Darvell LI, Bridgeman TG, Pourkashanian M, Williams A. An investigation of the thermal and catalytic behaviour of potassium in biomass combustion. *Proceedings of the Combustion Institute* 2006; 31: 1955-1963.

- [51] Thy P, Jenkins B M, Lesher CE, Grundvig S. Compositional constraints on slag formation and potassium volatilization from rice straw blended wood fuel. *Fuel Process Technol* 2005; 87: 383-408.
- [52] Kosminski A, Ross DP, Agnew JB. Reactions between sodium and silica during gasification of a low-rank coal. *Fuel Process Technol* 2006; 87: 1037-1049.
- [53] Kajitani S, Hara S, Matsuda H. Gasification rate analysis of coal char with a pressurized drop tube furnace. *Fuel* 2001; 81: 539-546.
- [54] Qin K, Lin W, Jensen PA, Jensen AD. High-temperature entrained flow gasification of biomass. *Fuel* 2011; 93: 589-600.
- [55] Chhiti Y, Salvador S, Commandre J, Broust F, Couhert C. Wood bio-oil noncatalytic gasification: Influence of temperature, dilution by an alcohol and ash content. *Energy Fuels* 2011; 25: 345-351.
- [56] Zhao Y, Sun S, Zhou H, Sun R, Tian H, Luan J, Qian J. Experimental study on sawdust air gasification in an entrained-flow reactor. *Fuel Process Technol* 2012; 91: 910-914.
- [57] Senapati PK, Behera S. Experimental investigation on an entrained flow type biomass gasification system using coconut coir dust as powdery biomass feedstock. *Bioresource Technol* 2012; 117: 99-106.
- [58] Tremel A, Haselstenier T, Kunze C, Spliethoff H. Experimental investigation of high temperature and high pressure coal gasification. *Appl Energy* 2011; 92: 79-285.
- [59] Zhou J, Chen Q, Zhao H, Cao X, Mei Q, Luo Z, Cen K. Biomass-oxygen gasification in a high-temperature entrained-flow gasifier. *Biotechnol Adv* 2009; 27: 606-611.
- [60] Yoon SJ, Choi Y, Son Y, Lee S, Lee J. Gasification of biodiesel by-product with air or oxygen to make syngas. *Bioresource Technol* 2009; 101: 1227-1232.
- [61] Tremel A, Haselsteiner T, Nakonz M, Spliethoff H. Coal and char properties in high temperature entrained flow gasification. *Energy* 2012; 45: 176-182.

- [62] Fermoso J, Arias B, Gil MV, Plaza MG, Pevida C, Pis JJ, Rubiera F. Co-gasification of different rank coals with biomass and petroleum coke in a high-pressure reactor for H₂-rich gas production. *Bioresource Technol* 2010; 101: 3230–3235.
- [63] Wall TF, Liu G, Wu H, Roberts DG, Benfell KE, Gupta S, Lucas JA, Harris DJ. The effects of pressure on coal reactions during pulverised coal combustion and gasification. *Prog Energy Combust* 2002; 28: 405–433.
- [64] Jing N, Wang Q, Cheng L, Luo Z, Cen K, Zhang D. Effect of temperature and pressure on the mineralogical and fusion characteristics of Jincheng coal ash in simulated combustion and gasification environments. *Fuel* 2013; 104: 647–655.
- [65] Ochoa J, Cassanello M, Bonelli P, Cukierman A. CO₂ Gasification of Argentinean coal chars: A kinetic characterization. *Fuel Process Technol* 2001; 74(3): 161-176.
- [66] Senneca O, Russo P, Salatino P, Masi S. The relevance of thermal annealing to the evolution of coal char gasification reactivity. *Carbon* 1997; 35 (1): 141-151.
- [67] Senneca O, Cortese L. Thermal annealing of coal at high temperature and high pressure. Effects on fragmentation and on rate of combustion, gasification and oxy-combustion. *Fuel* 2014; 116: 221–228.
- [68] Seo D K, Park SS, Kim YT, Hwang J, Yu T. Study of coal pyrolysis by thermo-gravimetric analysis (TGA) and concentration measurements of the evolved species. *J Anal Appl Pyrol* 2011; 92(1): 209-216.
- [69] Kajitani S, Suzuki N, Ashizawa M, Hara S. CO₂ gasification rate analysis of coal char in entrained flow coal gasifier. *Fuel* 2006; 85 (2): 163-169.
- [70] Irfan M, Usman MR, Kusakabe K. Coal gasification in CO₂ atmosphere and its kinetics since 1948: A brief review. *Energy* 36 (2011) 12–40.
- [71] Kong Y, Kim J, Chun D, Lee S, Rhim Y, Lim J, Choi H, Kim S, Yoo J. Comparative studies on steam gasification of ash-free coals and their original raw coals. *Int J Hydrogen Energ* 2014; 39: 9212-9220.

- [72] Kopyscinski J, Habibi R, Mims ChA, Hill JM. K_2CO_3 -catalyzed CO_2 gasification of ash-free coal: Kinetic study. *Energy Fuels* 2013; 27: 4875–4883.
- [73] Kopyscinski J, Rahman M, Gupta R, Mims ChA, Hill JM. K_2CO_3 catalyzed CO_2 gasification of ash-free coal. Interactions of the catalyst with carbon in N_2 and CO_2 atmosphere. *Fuel* 2014; 117: 1181–1189.
- [74] Kopyscinski J, Lam J, Mims ChA, Hill JM. K_2CO_3 catalyzed steam gasification of ash-free coal. Studying the effect of temperature on carbon conversion and gas production rate using a drop-down reactor. *Fuel* 2014; 128: 210–219.
- [75] Tafur-Marinos JA, Ginepro M, Pastero L, Torazzo A, Paschetta E, Fabbri D, Zelano V. Comparison of inorganic constituents in bottom and fly residues from pelletised wood pyro-gasification. *Fuel* 2014; 119: 157–162.
- [76] Lee SH, Yoon SJ, Ra HW, Son Y, Hong JC, Lee JG. Gasification characteristics of coke and mixture with coal in an entrained-flow gasifier. *Energy* 2012; 35: 3239-3244.
- [77] Roll H, Hedden K. Entrained flow gasification of coarsely ground Chinese reed. *Chem Eng Process* 1994; 33: 353-361.
- [78] Hattingh BB, Everson RC, Neomagus H, Bunt JR. Assessing the catalytic effect of coal ash constituents on the CO_2 gasification rate of high ash, South African coal. *Fuel Process Technol* 2011; 92(10): 2048–2054.
- [79] Mitsuoka K, Hayashi S, Amano H, Kayahara K, Sasaoaka E, Uddin A. Gasification of woody biomass char with CO_2 : The catalytic effects of K and Ca species on char gasification reactivity. *Fuel Process Technol* 2011; 92: 26–31.
- [80] Umeki K, Moilanen A, Gómez-Barea A, Konttinen J. A model of biomass char gasification describing the change in catalytic activity of ash. *Chem Eng J* 2012; 207–208: 616–624.
- [81] Sharma A, Takanohashi T, Morishita K, Takarada T, Saito I. Low temperature catalytic steam gasification of HyperCoal to produce H_2 and synthesis gas. *Fuel* 2008; 87(4-5): 491–497.

- [82] Coetzee S, Neomagus HWJP, Bunt JR, Everson RC. Improved reactivity of large coal particles by K_2CO_3 addition during steam gasification. *Fuel Process Technol* 2013; 114: 75–80.
- [83] Huang Y, Yin X, Wu Ch, Wang C, Xie J, Zhou Z, Ma L, Li H. Effects of metal catalysts on CO_2 gasification reactivity of biomass char. *Biotechnol Adv* 2009; 27: 568–572.
- [84] Wang J, Jiang M, Yao Y, Zhang Y, Cao J. Steam gasification of coal char catalyzed by K_2CO_3 for enhanced production of hydrogen without formation of methane. *Fuel* 2009; 88 (9): 1572–1579.
- [85] Khalil R, Varhegyi G, Jaschke S, Gronli MG, Hustad J. CO_2 gasification of biomass chars: A kinetic study. *Energy Fuels* 2009; 23: 94–100.
- [86] Fogler HS. *Elements of Chemical Reaction Engineering. Diffusion and Reaction*. 4th ed. Boston: Pearson Education, Inc; 2006, p. 813-851.
- [87] Loewenberg DA, Levensis WA. Combustion behavior and kinetics of synthetic and coal-derived chars: Comparison of theory and experiment. *Combust Flame* 1991; 84: 47–65.
- [88] Su JL, Perlmutter DD. Effect of pore structure on char oxidation kinetics. *AIChE J* 1985; 31, 973–981.
- [89] Smith JM, Van Ness HC, Abbott MM. *Introduction to Chemical Engineering Thermodynamics*. 7th ed. New York: McGraw Hill; 2005.
- [90] Tomlinson L, Cory NJ. Hydrogen emission during the steam oxidation of ferritic steels: kinetics and mechanism. *Corros Sci* 1989; 29 (8): 939-965.
- [91] Marrone PA, Hong GT. Corrosion control methods in supercritical water oxidation and gasification processes. *J Supercritic Fluid* 2009; 51: 83–103.
- [92] Nipattummakul N, Ahmed I, Kerdsuwan S, Gupta AK. High temperature steam gasification of wastewater sludge. *Appl Energy* 2010; 87 (12): 3729-3734.
- [93] Umeki K, Namioka T, Yoshikawa K. The effect of steam on pyrolysis and char reactions behavior during rice straw gasification. *Fuel Process Technol* 2012; 94 (1): 53-60.

- [94] Feroso J, Gil MV, García S, Pevida C, Pis JJ, Rubiera F. Kinetic parameters and reactivity for the steam gasification of coal chars obtained under different pyrolysis temperatures and pressures. *Energy Fuels* 2011; 25: 3574–3580.
- [95] Detournay M, Hemati M, Andreux R. Biomass steam gasification in fluidized bed of inert or catalytic particles: Comparison between experimental results and thermodynamic equilibrium predictions. *Powder Technol* 2011; 208 (2): 558-567.
- [96] Zou JH, Zhou ZJ, Wang FC, Zhang W, Dai ZH, Liu HF, Yu ZH. Modeling reaction kinetics of petroleum coke gasification with CO₂. *Chem Eng Process* 2006; 46: 630–636.
- [97] Ren L, Yang J, Gao F, Yan J. Laboratory study on gasification reactivity of coals and petcoke in CO₂/steam at high temperatures. *Energy Fuels* 2013; 27: 5054–5068.
- [98] Marquez-Montesinos F, Cordero T, Rodríguez-Mirasol J, Rodríguez JJ. CO₂ and steam gasification of a grapefruit skin char. *Fuel* 2002; 81 (4): 423–429.
- [99] Mandapati, R.M., Daggupati, S., Mahajani, S.M., Aghalayam, P., Sapru, R.K., Sharma R.K. et al. Experiments and kinetic modeling for CO₂ gasification of Indian coal chars in the context of underground coal gasification. *Ind Eng Chem Res* 2012; 51: 15041–15052.
- [100] Malekshahian M, Hill J. Kinetic analysis of CO₂ gasification of petroleum coke at high pressure. *Energy Fuels* 2011; 25: 4043-4048.
- [101] Bhatia SK, Perlmutter D D. A random pore model for fluid–solid reactions: I. Isothermal and kinetic control. *AIChE J* 1980; 26 (3): 379–386.
- [102] Bhatia SK, Vartak BJ. Reaction of microporous solids: The discrete random pore model. *Carbon* 1996; 34 (11): 1383-1391.
- [103] Singer SL, Ghoniem AF. An adaptive random pore model for multimodal pore structure evolution with application to char gasification. *Energy Fuels* 2011; 25: 1423–1437.
- [104] Umemoto S, Kajitani S, Hara S. Modeling of coal char gasification in coexistence of CO₂ and H₂O considering sharing of active sites. *Fuel* 2013; 103: 14-21.

Chapter Two: Data analysis and experiments design

A better understanding of the experimental procedure is imperative, since many conclusions and assumptions related to the gasification mechanism are associated with the steps prior to the gasification. These steps are explained in following chapters; however, it is important to understand how the experimental information is transformed into the variables required for kinetic modeling.

This chapter explains why the experiments were conducted as they were in this research. There is also a description as to why the conventional approach of comparing coefficients of determination between kinetic models can be statistically inconsistent and why new tools for kinetic analysis needed to be developed.

The results discussed in this chapter led to an analytical method employed by Silbermann et al. [1], which was a study reporting kinetics of seven coal samples from deep core seams. R. Arturo Gomez's contribution to this paper relates to the data mining procedure, gasification experiments and kinetic modeling.

The main goal of this chapter is to provide a description of the processing method for the experimental kinetic information since this has not been explained in other publications.

2.1 Gas-solid reaction progress

Using Alberta coal samples, this chapter delineates the effects of the data collection interval and the consequences of the data transformation for kinetic purposes. Complete characterization of these coals is shown in Chapter 4 and methodology is extensive to any carbonaceous

feedstock; however, preliminary gasification experiments are required to define the method to process the experimental information. The experimental method was the direct CO₂ gasification [2] or method 1 [1], which has been widely mentioned in the following chapters.

2.2 Implications of the variable transformation

2.2.1 Variable transformation

The original variables recorded using thermogravimetric analyzer (TGA) are time (independent variable) and weight loss (dependent variable). It is important to mention that the main difference between TGA and gas chromatography (GC) analysis, with respect to the conversion of solids, is the interval of data acquisition; therefore, it is inaccurate to regard them as different reaction systems, when both are batch reactors.

This thesis is based on TGA experiments, since the interval of data collection can be reduced to a fraction of a second; however, gasification is not easy to perform with steam as the gasifying agent; therefore, a new experimental setup was constructed to carry out the experiments described and analyzed in Chapter 6. The data processing methodology can be extended to any heterogeneous chemical reaction, but a specific gasification method was selected for this part of the research.

For gas-solid kinetic studies, the reactor can be considered as a continuous system on the gas side, and the overall analysis should be as a semi-batch reactor [3]. This explanation appears obvious, but it is paramount given many implications, such as equilibrium, reverse reactions and bulk diffusion. For example, the Boudouard reaction cannot reverse above a temperature of 750°C with an excess of gasifying agent, if there are no mass transfer limitations, which can be

deduced by thermodynamic considerations and Le Chatelier's principle. For this reason, the gasifying agent was fed in excess in all the experiments. The minimum gas flow rate required to ensure that there was no bulk diffusion was determined by comparing the overall conversion rate at different flow rates. It was determined to be 1.8 times the reaction volume per minute.

The reaction progress is evaluated through the conversion, which is obtained at a particular time as follows:

$$X_t = \frac{m_0 - m_t}{m_0 - m_a} \quad \text{Eq. (2-1)}$$

where m_0 , m_a are the weight of the sample when the reaction starts and the remaining weight associated with the ash content, respectively.

When a molar balance of the solid is formulated in a batch reactor, the expression for the reaction rate in a homogeneous system is:

$$N_{A0} \frac{dX}{dt} = -r'_A V \quad \text{Eq. (2-2)}$$

where N_{A0} corresponds to the initial moles of reactant loaded in a reactor of volume V .

N_{A0} and V are constant; however, the concentration term is not used for heterogeneous systems; thus, many authors prefer to express the reaction rate as a conversion rate. For this reason, the chemical reaction models considered in this thesis present the reaction rate as a conversion rate:

$$\frac{dX}{dt} = -r_A \approx \frac{\Delta X}{\Delta t} \quad \text{Eq. (2-3)}$$

To study the effect of the data collection interval, Eq. (2-3) is used to calculate the CO₂ gasification rate at different intervals, as presented for coal 7 (a coal sample from a deep seam core) in Fig. 2.1. This coal was selected, since it shows the lower reactivity between all coals evaluated. It is also a good example for unreactive carbonaceous feedstock, such as petcoke. Comparison of Figs. 2.1a and 2.1b illustrates that data dispersion increases when data collection interval decreases, but important information at the beginning of the reaction is less reliable.

When coal reactivity increases, data dispersion is not affected significantly by the collection interval. This is presented in Fig. 2.2 for Genesee coal, which is a very reactive coal. An important consequence of increasing the data collection interval is that the initial information about the conversion rate is omitted. Figs. 2.1a and 2.2a show how the initial information is lost during the first 2 minutes of the gasification. In general, a higher data dispersion increases the uncertainty, which is a consequence of the data transformation and not the experimental conditions.

2.2.2 Collinearity

When more variables are introduced, the model becomes more sensitive to extreme values; and, in many cases, two or more variables are dependent on each other, which is one of the reasons why using polynomial regression improves the correlation coefficient. This situation is defined as collinearity; and, there are often nonlinear relationships among variables that affect the results. When more parameters are introduced, the model fits better; however, it does not explain the kinetic behavior (consider polynomial regression). This is well described in statistics and econometric literature [4, 5], and it is asserted that increasing regression parameters associated with new pseudo-variables (a different term including the original variable) will

improve the coefficient of determination, but will not guarantee a better prediction. This argument is introduced to explain why models, such as the random pore model (RPM), exhibit a better fit with conventional gasification procedures. This model is analyzed in the following chapters.

2.2.3 Heteroscedasticity

A common result for the Genesee coal and coal 7 presented in Figs. 2.1 and 2.2 is that all data points become closer as the conversion increases, which indicates that the transformation of variables generates a new data space with non-uniform variance [4]. This is induced heteroscedasticity, which is defined as the non-homogeneity of the variance. When the variable time disappears, the equidistant data collection interval changes, because the gasification rate decreases with conversion and more data points are present at higher conversion than at the beginning of the reaction. Analysis of heteroscedasticity is not common in kinetics, since it is complex and has been basically addressed in econometric studies. A good example of the effect of heteroscedasticity has been presented by Holger [7].

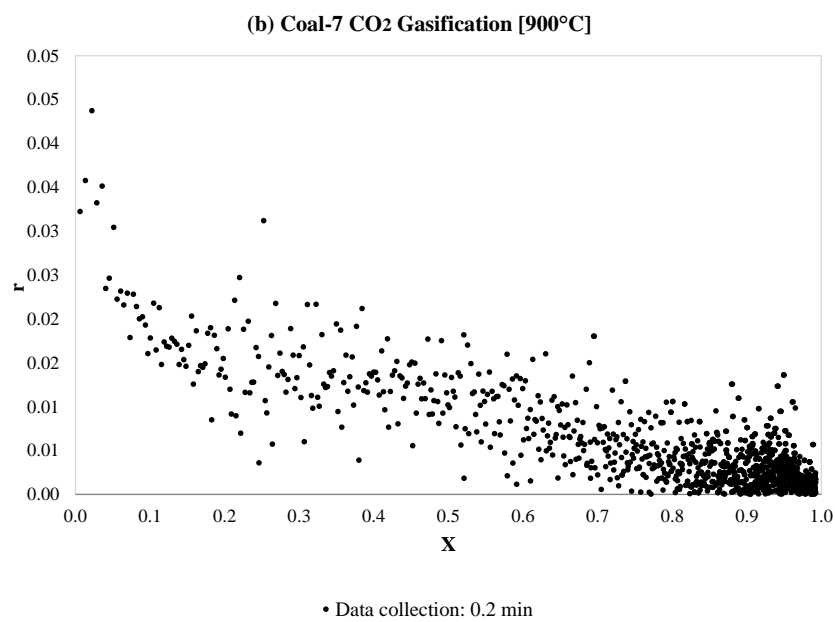
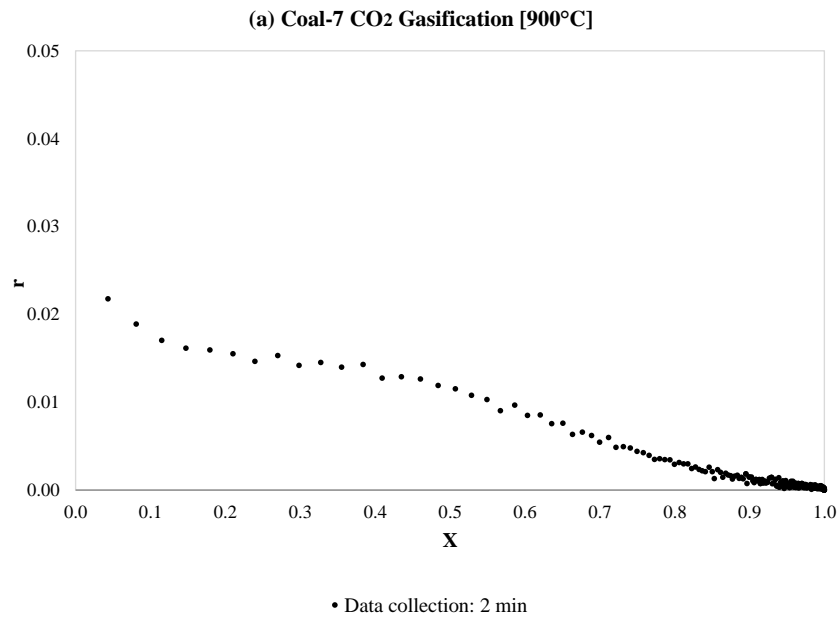


Figure 2.1 CO₂ gasification rate (r) vs. conversion (X) of coal 7 at 900°C: (a) data collection interval of 1 min and (b) data collection interval of 0.2 min.

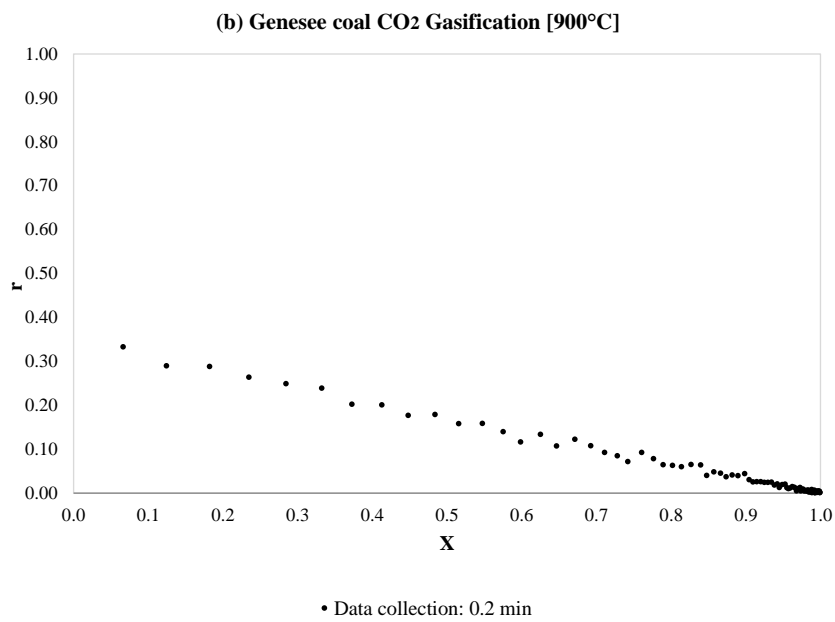
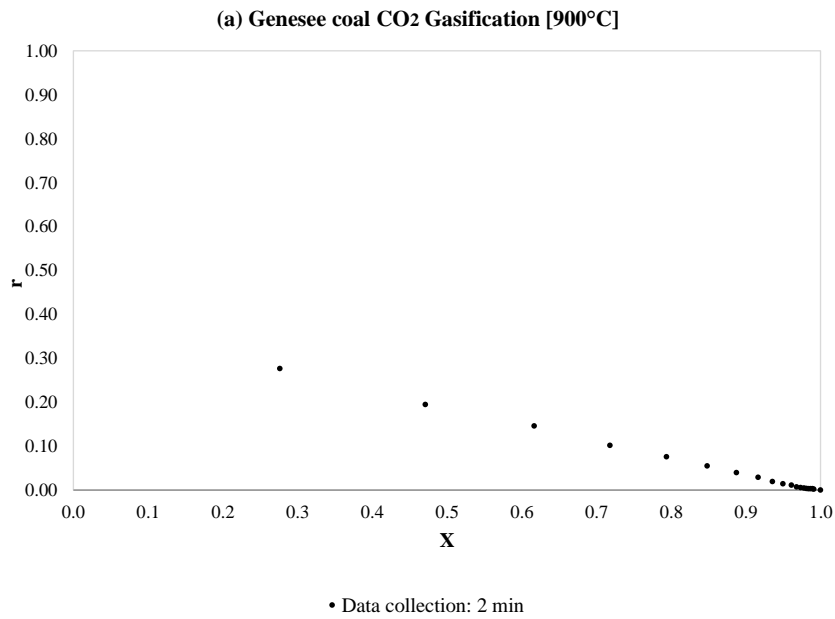


Figure 2.2 CO₂ gasification rate (r) vs. conversion (X) of Genesee coal at 900°C: (a) data collection interval of 1 min and (b) data collection interval of 0.2 min.

2.3 New data mining procedure

The only ways to deal with uniform variance and independent variables are to ensure that there are not inter-dependent variables and that data points in the new variable's space are equidistant.

A new procedure to process the experimental data has been developed, solving common limitations of traditional regression models with no imposed assumptions about homoscedasticity and non-collinearity among the variables. The ultimate goal of the developed method is the accurate comparison of conversion rates at different temperatures independent of the feedstock reactivity. The conversion rates can be calculated in a Microsoft EXCEL spreadsheet using the proposed procedure, instead of using the smoothing function of licensed software, as presented elsewhere [7, 8]. The procedure to reduce dispersion with uniform variance distribution consists of the following steps:

- Calculation of the conversion rate with Eq. (2-3): The best time increment for conversion and gasification rate calculations was found to be 12 s (0.2 min). This interval allows for the gathering of important information with respect to the maximum reaction rate and the most significant changes of the conversion rate at the beginning of the gasification.
- Uniform variance or homoscedasticity: From previously generated values, a new set of data points is selected using a uniform increment of conversion, i.e. the closest points to the desired conversion value with a data base search function.
- Reduction of data dispersion through the Central Limit Theorem: In small conversion intervals, the conversion rate is calculated as the average of the conversion rates between equidistant points from the selected point (to be smoothed). If there are no equidistant

points, the two closest points are selected, and linear interpolation is used instead of the average.

Results of the new procedure for coal 7 and Genesee coal are presented in Figs. 2.3a and 2.3b, respectively. When the conversion rate increased at a higher temperature or feed rate, the reaction of a more reactive feedstock, such as Genesee coal, can be considered as first order. The results of coal 7 and Genesee coal indicate that the intrinsic reaction mechanism differs for different coals, but can be associated with mass transfer limitations. It is essential to have a reliable procedure to obtain the conversion rate, which can then be accurately used in kinetic modeling. This is confirmed by comparisons of Fig. 2.1 with Fig. 2.3a and Fig. 2.2 with Fig. 2.3b.

2.4 Kinetic model comparison

The determination of the best model to fit experimental data requires the consideration of different variables, including the model itself. The next chapters do not discuss the validity of assumptions from the statistical point of view; however, an important first step in this thesis is proving that kinetic parameters calculated with different kinetic models can vary significantly. If two or more kinetic models accurately represent the reaction mechanism, their kinetic parameters should be the same or within the confidence interval of the specific parameter. For this reason, experimental design analysis was used to correlate the activation energy with coal type and the kinetic model from the data reported by Silbermann et al. [1].

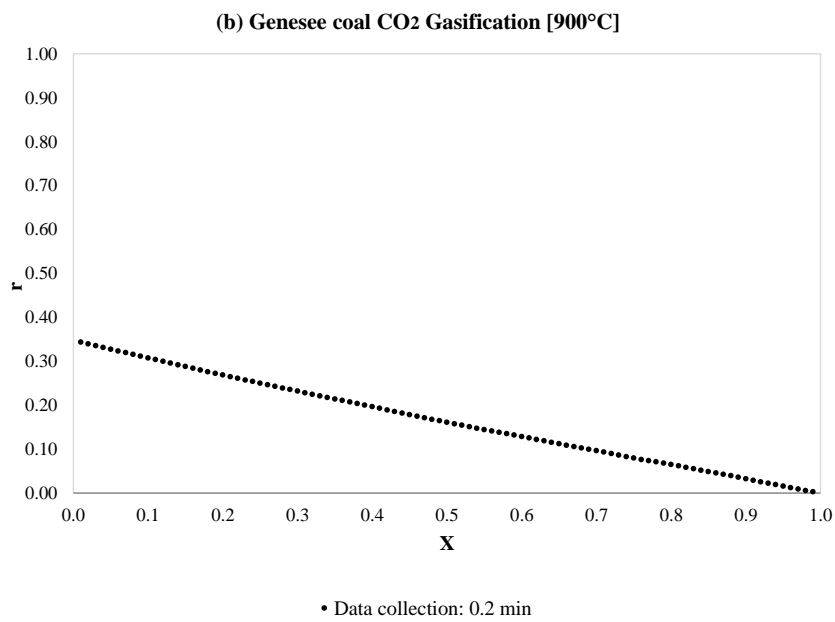
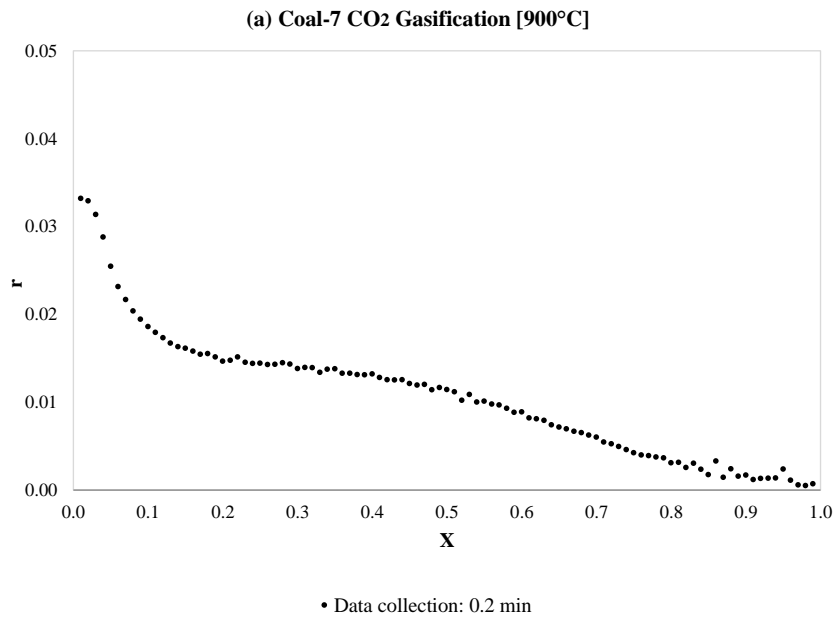


Figure 2.3 CO₂ gasification rate (r) vs. conversion (X) at 900°C, with the proposed data mining procedure: (a) coal 7 and (b) Genesee coal.

2.4.1 Coefficient of determination of normalized experimental data

Simpler models better fit the experimental data when (1) data mining and experimental procedures are developed to avoid a systematic error, such as in the case of transformation of variables (i.e. induced heteroscedasticity), and (2) there is no switch of the reaction gas [2]. Coefficients of determination for different kinetic models for CO₂ gasification of nine different coal samples are presented in Fig. 2.4, as reported by Silberman et al. [1]. The coefficients of determination are simpler tools for the consistent comparison of models, since the variance of all experiments (54 experiments – 9 coals at 3 temperatures with 2 repetitions) is almost uniform and is in the range of the uncertainty with respect to each model. Every experiment consisted of 200 data points uniformly distributed between 0 and 80% conversion. Fig. 2.4 illustrates that the integrated core (ICM) and normal distribution (NDM) models were the best models for all coal samples. However, a model with a higher determination coefficient does not necessarily represent the reaction mechanism of a particular feedstock during gasification.

This section presents a statistical analysis of whether the selection of a model fits the experimental data; however, an accurate representation of the reaction mechanism cannot be determined if kinetic parameters with a theoretical meaning cannot be correctly estimated. The results shown in Fig. 2.4 are different from those results reported in the literature since 1980, when Bhatia and Perlmutter proposed the random pore model (RPM) [9]. These atypical results were the starting point to prove the new findings presented in this thesis.

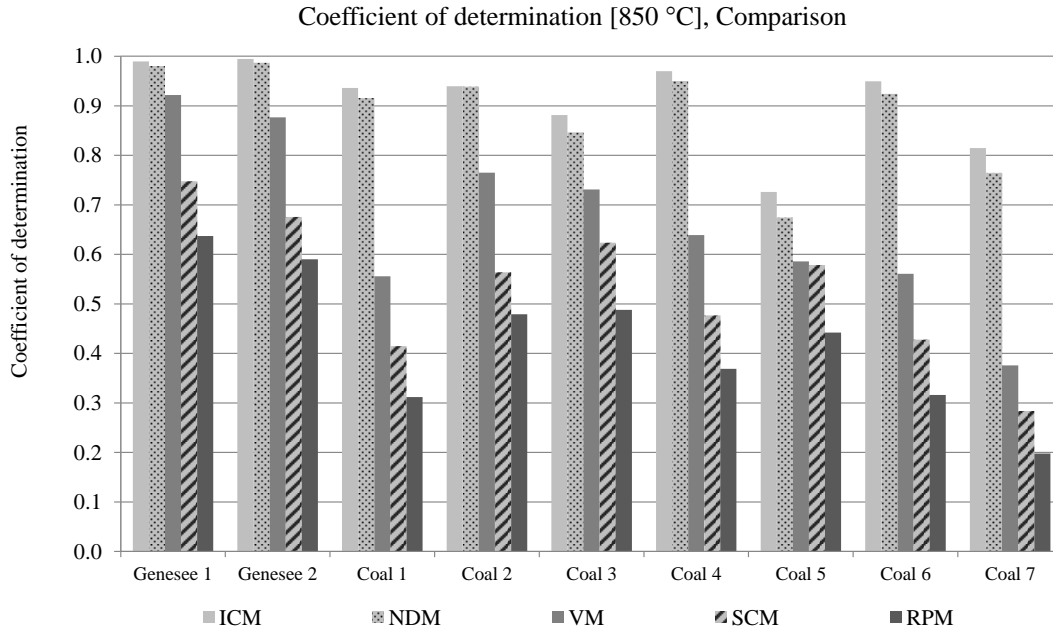


Figure 2.4 Coefficient of determination for CO₂ coal gasification at 850°C for 9 coals and 5 different chemical reaction models. (Reprinted with permission from [1]. Copyright 2013 American Chemical Society)

2.4.2 Experiment design analysis

A representative kinetic parameter and its correlation with two experimental factors are described in this section. In this case, the prediction of factors' significance is not necessary, because the relationship among variables in kinetics is well known [1-3, 6-9]. Originally, there were three factors to be considered, i.e. coal type, kinetic model and reaction conditions; however, only coal type and kinetic model have been considered in this section, because reaction conditions can be eliminated by working at atmospheric conditions in the same temperature range.

- Factor A: The five evaluated kinetic models were: (a) integrated core model (ICM); (b) normal distribution model (NDM); (c) volume model (VM); (d) shrinking core model (SCM); and (e) random pore model (RPM).
- Factor B: Type of coal, classified as two samples of surface mined coal (Genesee-1 and Genesee-2) and 7 coal samples of deep mined seams (termed as coal 1, coal 2, and so forth).

The kinetic parameter to be evaluated is the activation energy (E_A), since it should be a unique value if the reaction mechanism does not change in a particular temperature reaction range [3]. This is explained by the transition-state theory [10] and it has been one of the conditions assumed by other researchers [1, 7, 8] when they determined this parameter. Table 2.1 shows the E_A using direct gasification as reported by Silbermann et al. [1]. The reported E_A was obtained at three different temperatures, and each isothermal experiment was repeated twice. The maximum E_A uncertainty was ± 9 kJ/mol.

Table 2.1 Activation energy [kJ/mol] of CO₂ gasification between 800°C to 900°C for 9 different coals and 5 chemical reaction kinetic models. (Reprinted with permission from [1]. Copyright 2013 American Chemical Society)

Coal	VM	SCM	ICM	NM	RPM
Coal 1	124	119	139	137	117
Coal 2	139	128	164	169	126
Coal 3	209	209	208	216	211
Coal 4	162	153	209	205	151
Coal 5	203	205	193	200	140
Coal 6	186	186	209	211	187
Coal 7	205	209	230	233	212
BD	180	183	172	175	184
Genesee	191	187	193	195	187

Table 2.2 shows the result of the two-way analysis of variance (ANOVA) test, where differences among models and coals were discovered, which can be observed by verifying $F_{\text{factor}} > F_{\text{critical}}$. This corresponds with results presented in Figure, 2.4 since the performance of the different kinetic models were similar, regardless of the coal type, but the estimated E_A was different among models, as presented in Table 2.1.

Table 2.2 Two-way ANOVA test with a 0.05 significance level for two factors: (1) coal type and (2) chemical reaction model.

<i>SUMMARY</i>	<i>Count</i>	<i>Sum</i>	<i>Average</i>	<i>Variance</i>
Coal 1	5	636.64	127.33	101.65
Coal 2	5	724.61	144.92	411.51
Coal 3	5	1052.73	210.55	10.05
Coal 4	5	879.90	175.98	817.39
Coal 5	5	941.39	188.28	759.67
Coal 6	5	979.56	195.91	169.37
Coal 7	5	1089.02	217.80	168.57
BD	5	894.63	178.93	24.90
Genesee	5	953.19	190.64	12.18
Volume model	9	1599.31	177.70	907.58
Shrinking core model	9	1579.81	175.53	1170.40
Integrated core model	9	1716.28	190.70	790.65
Normal distr. F mod	9	1742.29	193.59	830.05
Random pore mode	9	1513.98	168.22	1280.04

ANOVA						
<i>Source of Variation</i>	<i>SS</i>	<i>df</i>	<i>MS</i>	<i>F</i>	<i>P-value</i>	<i>F crit</i>
r: Coal types	34036.90	8	4254.61	23.50	2.50E-11	2.24
c: Kinetic models	4108.28	4	1027.07	5.67	1.44E-03	2.67
Error	5792.91	32	181.03			
Total	43938.1	44				

To define differences between kinetic models, the Tukey procedure was applied [5] as follows:

- Define the numerical order of the models: VM = 1, SCM = 2, ICM = 3, NDM = 4, RPM = 5.
- Define the kinetic models as c , where $c = 5$, and the coal types as r , where $r = 9$. The Studentized range distribution, with c degrees of freedom in the numerator and $(c-1)(r-1) = 32$ in the denominator, is $q_u = 4.09$ (with 95% confidence, or $\alpha = 0.05$) [5].
- Estimate the critical range:

$$\text{Critical range} = q_u \sqrt{\frac{\text{MSE}}{r}} = 4.09 \sqrt{\frac{181.03}{9}} = 18.34 \frac{\text{kJ}}{\text{mol}} \quad \text{Eq. (2-4)}$$

- If the absolute difference between the E_A averages of two kinetic models, i.e. $\bar{x}_{model 1} - \bar{x}_{model 2}$, is smaller than the critical range, there is no evidence that the two models have different E_A values. On the other hand, both E_A values are different if their absolute difference is higher than the critical range; and, higher certainty of the test is obtained if the result is far from the critical range.

The Tukey procedure requires a comparison of all possible binary combinations. Table 2.3 shows the E_A differences of binary combinations among kinetic models, revealing that the models with similar coefficients of determination (R^2), according to Fig. 2.4, are not significantly different ($\bar{x}_3 - \bar{x}_4 = 2.89 \text{ kJ/mol} \ll \text{Critical range} = 18.34 \text{ kJ/mol}$). The RPM showed the greatest deviation, i.e. the smallest determination coefficient.

This test cannot provide information about which model fits better, but does verify that the E_A can differ significantly depending on the model used. A dependency of the E_A with respect to

the kinetic model is a contradiction of the Arrhenius equation. This is addressed in Chapter 5 and explanation about the theoretical limit of E_A for endothermic reactions is presented in Appendix B.

Table 2.3 Binary differences of E_A averages [kJ/mol] for five different kinetic models, where subscripts refer to VM = 1, SCM = 2, ICM = 3, NDM = 4, RPM = 5.

$\bar{x}_1 - \bar{x}_2$	$\bar{x}_1 - \bar{x}_3$	$\bar{x}_1 - \bar{x}_4$	$\bar{x}_1 - \bar{x}_5$	$\bar{x}_2 - \bar{x}_3$	$\bar{x}_2 - \bar{x}_4$	$\bar{x}_2 - \bar{x}_5$	$\bar{x}_3 - \bar{x}_4$	$\bar{x}_3 - \bar{x}_5$	$\bar{x}_4 - \bar{x}_5$
2.17	13.00	15.89	9.48	15.16	18.05	7.31	2.89	22.48	25.37

The Tukey test can be applied to the E_A differences due to coal type. The particular procedure is:

- Define the numerical order of coal types: Coal 1 = 1, Coal 2 = 2 ... Coal 7 = 7, Genesee 1 = 8, Genesee 2 = 9.
- Define the kinetic models as c, where c = 5, and the coal types as r, where r = 9. The Studentized range distribution, with r degrees of freedom in the numerator and (c-1)(r-1) = 32 in the denominator, is $q_u = 4.7$ (with 95% confidence or $\alpha = 0.05$) [5].
- Estimate the critical range:

$$\text{Critical range} = q_u \sqrt{\frac{\text{MSE}}{c}} = 4.7 \sqrt{\frac{181.03}{5}} = 28.28 \frac{\text{kJ}}{\text{mol}} \quad \text{Eq. (2-5)}$$

- If the absolute difference between E_A averages of two coal types, i.e. $\bar{y}_{coal 1} - \bar{y}_{coal 2}$, is smaller than the critical range, there is no evidence that the two coals have different E_A values. Table 2.4 shows the E_A differences between binary combinations revealing that

few coals have similar values for E_A . This depends on different variables, which is discussed in Chapter 4.

The ANOVA and Tukey tests applied to the estimated E_A values show that:

- Results obtained for the RPM are significantly different than those of the NDM and ICM; therefore, an in-depth study of the reaction mechanism is presented in Chapter 3.
- There is no difference between the two best models (according to R^2), i.e. ICM and NDM, as reported by Silbermann et al. [1].
- Differences among coals are consistent with the reactivity of the coal and with the ash content; therefore, this is further investigated in Chapter 4.

Table 2.4 Binary differences of E_A averages [kJ/mol] for nine different coal samples, subscripts refer to Coal 1 = 1, Coal 2 = 2...Coal 7 = 7, Genesee 1 = 8, Genesee 2 = 9

$\bar{y}_1 - \bar{y}_2$	$\bar{y}_1 - \bar{y}_3$	$\bar{y}_1 - \bar{y}_4$	$\bar{y}_1 - \bar{y}_5$	$\bar{y}_1 - \bar{y}_6$	$\bar{y}_1 - \bar{y}_7$	$\bar{y}_1 - \bar{y}_8$	$\bar{y}_1 - \bar{y}_9$	$\bar{y}_2 - \bar{y}_3$
17.59	83.22	48.65	60.95	68.58	90.48	51.60	63.31	65.62
$\bar{y}_2 - \bar{y}_4$	$\bar{y}_2 - \bar{y}_5$	$\bar{y}_2 - \bar{y}_6$	$\bar{y}_2 - \bar{y}_7$	$\bar{y}_2 - \bar{y}_8$	$\bar{y}_2 - \bar{y}_9$	$\bar{y}_3 - \bar{y}_4$	$\bar{y}_3 - \bar{y}_5$	$\bar{y}_3 - \bar{y}_6$
31.06	43.36	50.99	72.88	34.00	45.72	34.57	22.27	14.63
$\bar{y}_3 - \bar{y}_7$	$\bar{y}_3 - \bar{y}_8$	$\bar{y}_3 - \bar{y}_9$	$\bar{y}_4 - \bar{y}_5$	$\bar{y}_4 - \bar{y}_6$	$\bar{y}_4 - \bar{y}_7$	$\bar{y}_4 - \bar{y}_8$	$\bar{y}_4 - \bar{y}_9$	$\bar{y}_5 - \bar{y}_6$
7.26	31.62	19.91	12.30	19.93	41.83	2.95	14.66	7.63
$\bar{y}_5 - \bar{y}_7$	$\bar{y}_5 - \bar{y}_8$	$\bar{y}_5 - \bar{y}_9$	$\bar{y}_6 - \bar{y}_7$	$\bar{y}_6 - \bar{y}_8$	$\bar{y}_6 - \bar{y}_9$	$\bar{y}_7 - \bar{y}_8$	$\bar{y}_7 - \bar{y}_9$	$\bar{y}_8 - \bar{y}_9$
29.53	9.35	2.36	21.89	16.99	5.27	38.88	27.17	11.71

2.5 Summary

A new method to process the experimental information has been developed and introduces new data mining procedures to eliminate heteroscedasticity induced by the transformation of variables. This helps to analyze kinetic models in a more consistent way, since the coefficient of determination can be used as an effective comparison tool between kinetic models for the best fit with the experimental data. In addition, simpler models can be used, since there is a better match between the observations and the predictions without unnecessary assumptions. Chapter 3 discusses why common kinetic models do not predict the kinetic behavior using a different experimental procedure.

Changes in the E_A value, due to the coal type and kinetic model, are evidenced with the two-way ANOVA and Tukey tests. This approach is possible, due to small data dispersion and uniform variance, although it is impractical given the many feedstock combinations that can be used in gasification. The results of the statistical analysis of E_A are consistent with the reactivity of the different coals used. The most significant result is that the conventional way to estimate E_A depends on the kinetic model, which contradicts the Arrhenius equation. Therefore, a comprehensive explanation of the reaction mechanism of gasification is required, and kinetic parameters must be determined independent of the kinetic model selection.

2.6 References

- [1] Silbermann R, Gomez A, Gates I, Mahinpey N. Kinetic studies of a novel CO₂ gasification method using coal from deep unmineable seams. *Ind Eng Chem* 2013; 52 (42): 14787-14797.
- [2] Gomez A, Silbermann R, Mahinpey N. A comprehensive experimental procedure for CO₂ coal gasification: Is there really a maximum reaction rate?. *Appl Energy* 2014; 124: 73–81.
- [3] Fogler HS. *Elements of Chemical Reaction Engineering. Diffusion and Reaction.* 4th ed. Boston: Pearson Education, Inc; 2006.
- [4] Davidson R, MacKinnon JG. *Econometric theory and methods.* New York: Oxford University Press, 2004.
- [5] Levine DM, Ramsey PP, Smidt RK. *Applied Statistics for Engineers and Scientists.* 1st ed. Boston: Pearson Education, Inc; 2001.
- [6] Weiers RM. *Introduction to Business Statistics.* 4th ed. Belmont: Wadsworth Group; 2002.
- [7] Holger D. A consistent test for heteroscedasticity in nonparametric regression based on the kernel method. *J Stat Plan Infer* 2002; 103: 311–329.
- [8] Malekshahian M, Hill J. Kinetic analysis of CO₂ gasification of petroleum coke at high pressure. *Energy Fuels* 2011; 25: 4043-4048.
- [9] Kopyscinski J, Habibi R, Mims ChA, Hill JM. K₂CO₃-Catalyzed CO₂ Gasification of Ash-Free Coal: Kinetic Study. *Energy Fuels* 2013; 27: 4875–4883.
- [10] Smith JM. *Chemical Engineering Kinetics.* 3rd ed. New York: McGraw-Hill 1981.

Chapter Three: A comprehensive experimental procedure for CO₂ coal gasification: Is there really a maximum reaction rate?

3.1 Presentation of the article

The goal of this article is to present the effects of the experimental procedure on the interpretation of the reaction mechanism of a gas-solid chemical reaction to the scientific community. In recent decades, the existence of a maximum reaction rate when reaction rate is plotted against conversion has been the focus of kinetic studies using different kinetic models and assuming diverse theories related to changes on the solid surface. However, the time required to observe the amended maximum is independent of the feedstock for similar reaction conditions; therefore, the reason for the maximum is different. In this journal paper, it has been proven that the stated maximum is not a consequence of changes on the surface area, but that it is a result of changing an inert gas by the gasifying agent. Another important breakthrough is that the surface area is reduced during the isothermal pyrolysis. These two conclusions change the way the kinetic model has been conducted since the path used to produce the char significantly affects reactivity. Therefore, results are different between laboratory and industrial processes where pyrolysis and gasification are not separated.

The majority of this work has been undertaken by R. Arturo Gomez, including the design of experiments to compare the experimental methods and the main conclusions. Dr. Nader Mahinpey has supervised this work and refined some new terms used in gasification studies such as “isothermal pyrolysis”. Mr. Rico Silbermann performed the coal characterization and assisted in the analytical interpretation of results.

A Comprehensive Experimental Procedure for CO₂ Coal Gasification: Is There Really a Maximum Reaction Rate?

This article has been published in *Applied Energy* 124 (2014) 73–81. Reprinted with permission.

Arturo Gomez¹, Rico Silbermann¹, Nader Mahinpey¹

¹Chemical and Petroleum Engineering Department, University of Calgary, 2500 University Drive NW, Calgary, T2N 1N4, Canada

3.2 Abstract

A novel procedure to perform carbon dioxide (CO₂) gasification studies was tested with two different Alberta coals and compared to the most common procedures using thermogravimetric analysis (TGA). The designed experiments indicate that maximum reaction rates reported in the literature were probably a consequence of the increasing CO₂ concentration in the gas mixture when the inert gas was switched to CO₂. It has been proven that, independent of feedstocks, the time to observe this maximum reaction rate was constant, indicating the reported maximum reaction rate depends only on the gas dispersion when the gasifying agent is fed and not on the surface properties of the char.

In addition, the comparison of different experimental procedures shows the time that the char was exposed to an inert gas atmosphere prior to gasification, decreased the reactivity of the char. The reason is a reduction of the char mesopore area, which was induced when pyrolysis and

gasification were separated with an isothermal step using an inert gas. The random pore model is the most common model used to describe coal and biomass gasification in the literature, since it can predict a maximum reaction rate for a determined conversion. However, its usage may be inappropriate for gasification kinetics analysis, if the changing gas mixture effect and the char surface area reduction induced by the experimental procedure are not considered.

3.3 Introduction

The gasification of low-rank coals and biomass is a cleaner alternative than conventional combustion and a possible solution for utilizing the increasing amount of coke generated as a by-product of oil sands upgrading [1]. Earlier studies in this field isolated the kinetics of gasification from that of pyrolysis by first producing char and then proceeding with the char gasification [2-6], which does not apply to industrial gasifiers.

Studies of coal gasification have been performed using thermogravimetric analysis (TGA) and other gas product analysis techniques, by establishing an isothermal holding time with an inert gas before switching to carbon dioxide (CO₂). This procedure is used to separate the region where pyrolysis and gasification overlap [6-10]. An alternative procedure consists of immediately changing the inert gas used during pyrolysis with the gasifying agent when the reaction temperature is reached [10-14]. Previous studies have shown the differences in char conversion between these two methods are negligible [10].

Different kinetic models have been presented [7, 11, 15]; however, the random pore model presented by Bhatia and Perlmutter in 1980 [16-17], which explains the existence of a maximum rate of reaction as a consequence of pore area modification during gasification [7-14, 16-20], is

the most widely accepted. In a previous work, Silbermann et al. [15] proposed a new method to perform CO₂ gasification to minimize changes of the char surface area by increasing the heating rate and using CO₂ during the pyrolysis, where the maximum reaction rate is not observed. This procedure is a better representative of the gas behavior in an industrial gasifier, as there is no change of the reaction medium.

In this study, the gasification of two different Alberta coals was investigated through their reaction rates using a new procedure and a comparison with the most common methods used by other researchers is made [6-14]. For the common methods, it is reported for the first time how the reaction rate decreases significantly due to changes in the char surface area induced when an isothermal step is added to separate pyrolysis from gasification. The effects of temperature and heating rates, during pyrolysis, on char conversion and reactivity are well known [4, 19]; however, there are no previous studies that simultaneously correlate pyrolysis with gasification.

This work provides a novel alternative to perform gasification studies with a procedure more similar to an industrial scale process, thereby changing the way that kinetic analysis has been conducted in the last decades. A set of tests using a TGA and a horizontal reactor were designed to explore the effects of the changing gas mixture (nitrogen/CO₂) on the maximum reaction rate. Moreover, the effect of the length of isothermal pyrolysis time prior to gasification on the mesopore area, and thus, char reactivity are studied in detail.

3.4 Experimental

3.4.1 Coal and char characterization

An analysis of coal samples provided by the Saskatchewan Geological Survey of the Saskatchewan Ministry of the Economy was performed, and significant differences in the scale of their reaction rates during gasification with CO₂ were found [15]. The most reactive underground coal was selected for this study, which has been denominated as coal 5 (i.e., the 5th drilling core). Genesee coal, a surface mining coal that is mainly used as fuel for power generation, was also selected for this study, since it exhibits faster reactivity than the underground coals studied.

The coal samples were pre-dried, ground, dried again at 105°C and sieved; and, the fraction of particles smaller than 90 µm was used for characterization and the gasification study. The coal composition was determined using a Perkin Elmer CHNS/O 2400 elemental analyzer (ultimate analysis), and carbon characterization (proximate analysis) was performed at atmospheric pressure using a NETZSCH TG 209 Libra F1 analyzer (TGA). All characterization procedures were performed according to the ASTM D5142 standard for coal and coke.

Char was produced in a horizontal reactor with an internal diameter of 2.25cm and a length of 40cm and with a high heating rate of 200°C/min until reaching the reaction temperature of 900°C. An amount of 2.5 g of dry coal was placed in the reactor and then the system was kept at one of the three different holding times (i.e. 5, 30 or 60 min) before it was cooled down under 400°C in less than 20 seconds. During the whole process, an inert atmosphere was maintained at a flow rate of 240 mL/min to ensure a displacement of one and a half times the reactor volume per min (same as that in the TGA). The char was characterized using a Micrometrics model

ASAP 2020 analyzer to obtain the micropore area using CO₂ adsorption at 273K (Dubinin-Radushkevich micropore surface area), and mesopore area using N₂ adsorption at 77K and using the Branauer-Emmett-Teller method (BET surface area).

3.4.2 Experimental gasification procedures

The gasification experiments were performed in a NETZSCH TG 209 Libra analyzer. Three methods were performed using a sample weight of 10 mg (± 0.5 mg). The gas flow rate was 50 mL/min, and the partial pressure of CO₂ was modified by changing the proportions of CO₂ and nitrogen (N₂). The experimental gasification methods are summarized in the following subsections and in Table 3.1.

Table 3.1 Comparison of TGA methods

State	Characteristic	Method 1	Method 2	Method 3
General	Sample weight	10 \pm 0.5 mg	10 \pm 0.5 mg	10 \pm 0.5 mg
	Gas flow rate	50 ml/min	50 ml/min	50 ml/min
Start	Start temperature	25°C	25°C	25°C
	Isothermal time	5 min	5 min	5 min
	Gas	CO ₂	N ₂	N ₂
Heat up	25°C to 850°C	200°C/min	200°C/min	200°C/min
	850°C to 900°C	50°C/min	50°C/min	50°C/min
	Gas	CO ₂	N ₂	N ₂
At final temperature	Gas change after	no change	0 min	60 min
Isothermal gasification	Gas	CO ₂	CO ₂	CO ₂
Finish	Weight reading	constant	constant	constant

3.4.2.1 Method 1: Direct gasification

This is the new procedure proposed by Silbermann *et. al.* in 2013 [15]. It will be compared with the others previously used in the literature. The sample was kept at 25°C in a CO₂ atmosphere (sweeping gas) until its weight stabilized. The heating rate was 200K/min and analyzing the data of the gasification started when the sample reached the reaction temperature. Overheating was avoided by decreasing the high heating rate from 200K/min to 50k/min between 850 to 900°C. In this work, CO₂ gasification was analyzed at 900°C for all methods and tests.

3.4.2.2 Method 2: Non-isothermal pyrolysis plus gasification

The same conditions as the experiments with method 1 were used, but with N₂ as the sweeping gas instead of CO₂. When the sample reached 900°C, the gas was switched from N₂ to CO₂ immediately. Between 700°C and 900°C, the Boudouard reaction takes place, and the pyrolysis and gasification overlap; however, the order of magnitude of the pyrolysis rate is much higher than that of gasification [10].

3.4.2.3 Method 3: Non-isothermal and isothermal pyrolysis plus gasification

In this method, the sample was heated from 25°C to 900°C at 200K/min with N₂ as the sweeping gas. After reaching the reaction temperature, the sample was maintained isothermally with N₂ for one hour and then the gas was switched to CO₂. Usually the heating rate used is lower than 50K/min, which is the most common procedure employed to study gasification using the TGA technique [6-10]; however, the heating rate was maintained as high as possible. It was proven in a previous study that gasification using this method is significantly slower than method 1 [15]. It may not be correct to consider the reported kinetic data as intrinsic kinetics with this

procedure, since it is not representative of the gasification starting from the raw coal. All methods are described in Table 3.1.

3.4.3 Gasification tests

The aim of these tests was the determination of whether or not the observed maximum reaction rate was due to a mass transfer effect, gas dispersion, or an intrinsic property of the char surface. If the maximum is a consequence of the gas changing, the reaction time must be constant, as the volume of the reactor (TGA) and volumetric flow rate are constant. The basic idea is to induce a perturbation of the reaction system, at a pre-determined time after reaching the reaction temperature (gas switching), to detect a maximum reaction rate or an inflection point on the reaction rate.

3.4.3.1 Test 1: Non-isothermal pyrolysis plus gasification in two stages

The same heating rate as Method 1 (200K/min) with N₂ as the sweeping gas was used for Test 1. The gas was switched at 900°C from N₂ to an equimolar CO₂/N₂ mixture: 25 mL/min of CO₂ and 25 mL/min of N₂. The experiment was repeated with 4 different holding times [0, 2, 4 and 8 min], before switching to 100% CO₂.

3.4.3.2 Test 2: Different CO₂ partial pressures

Using the same procedure described in method 2, a constant gas volume (50 mL/min) with different CO₂/N₂ ratios was fed to the TGA. If the kinetic behavior can be explained by the random pore model, the maximum reaction rate should be observed at the same conversion for different partial pressures. If the hypothesis of a gas changing effect is true, the maximum reaction rate should be detected at a lower conversion, since a lower partial pressure yields a lower reaction rate.

3.4.3.3 Test 3: Iterative switching of CO₂/N₂ during isothermal gasification

The system started as described in method 1, and when the temperature reached 900°C the gases were switched to N₂. This process was repeated iteratively every 5 min from CO₂ to N₂ and vice versa.

This particular test was designed to explain what happens in the overlapping region of pyrolysis and gasification, which is between 700°C and 900°C when CO₂ is the reactive gas. If the observed maximum is an effect of the gas mixture, the time to observe a maximum after switching must be constant, which is contrary to the idea of the random pore model. All different tests are described in Table 3.2.

3.5 Data and kinetic analysis

3.5.1 Data analysis

Experimental data points were collected every 12 seconds; and, corrections were done to adjust for the buoyancy effect, using the information obtained from a blank run. For every single data point, the conversion is calculated using the following equation:

$$X = \frac{m_0 - m_t}{m_0 - m_a} \quad \text{Eq. (3-1)}$$

where m_0 is the sample mass when the system reaches the reaction temperature and when CO₂ is the reaction gas, m_t is the sample mass at a particular time (t) during the gasification step, and m_a is the mass of the ash based on the weight reading at 100% conversion.

The reaction rate, which is defined as the variation of the conversion during a period of time, is presented in the following equation:

$$r = \frac{\Delta X}{\Delta t} \quad \text{Eq. (3-2)}$$

To avoid non-homogeneity of the data variance, a uniform range of conversion points were selected using the same procedure for all tests.

Table 3.2 Comparison of TGA tests

State	Characteristic	Test 1	Test 2	Test 3
General	Sample weight	10 ± 0.5 mg	10 ± 0.5 mg	10 ± 0.5 mg
	Gas flow rate	50 ml/min	50 ml/min	50 ml/min
Start	Start temperature	25°C	25°C	25°C
	Isothermal time	5 min	5 min	5 min
	Gas	N ₂	N ₂	CO ₂
Heat up	25°C to 850°C	200°C /min	200°C /min	200°C /min
	850°C to 900°C	50°C /min	50°C /min	50°C /min
	Gas	N ₂	N ₂	CO ₂
Isothermal				
Gasification	Temperature [°C]	900	900	900
First switch	% CO ₂	50	100/50/25	0
	Holding [min]	2/4/8	To complete conversion	5
Second switch	% CO ₂	100	No switch	100
	Holding [min]	2/4/8		5
Switching iteration		No	No	Every 5 min
Finish	Weight reading	constant	constant	constant

3.5.2 Kinetic model discussion

Two models are explained in this study. The first one is the integrated core model (ICM), which was determined as the model that best fits the experimental data [15]:

$$\frac{dX}{dt} = k_{IM}(1 - X)^n \quad \text{Eq. (3-3)}$$

The second model is the random pore model (RPM) presented by Bhatia and Perlmutter [16]:

$$\frac{dX}{dt} = k_{RPM}(1 - X)\sqrt{1 - \psi \ln(1 - X)} \quad \text{Eq. (3-4)}$$

with the parameter ψ describing the internal structure of the non-converted char:

$$\psi = \frac{4\pi L_0(1 - \varepsilon_0)}{S_0^2} \quad \text{Eq. (3-5)}$$

where S_0 is the pore surface area per solid volume [m^2/m^3], L_0 is the pore length per solid volume [m/m^3], and ε_0 is the solid porosity.

Without mass transfer and gas dispersion effects, the change in total pore surface area can explain the existence of a maximum reaction rate for a particular conversion, as stated by the random pore model. If the maximum is a consequence of gas switching, it can be considered as a systematic error induced by the procedure to isolate pyrolysis from gasification. In this case, the ICM model fits better [15], and the modelling can be simplified.

3.6 Results and discussion

3.6.1 Coal Properties

Table 3.3 shows the properties of the two coals analyzed in this work; and, the D-R micropore surface area (Dubinin-Raduskevich method) is reported in Table 3.4, which was evaluated at 273K using CO_2 as the adsorbed gas. The BET (Branauer-Emmett-Teller method) surface areas for the coal samples were significantly smaller than micropore area; therefore, they are not presented here.

Table 3.3 Proximate and Ultimate Analysis

	Proximate Analysis			Ultimate Analysis			
	Volatiles	Fixed Carbon	Ash	C	H	N	S
	wt% _{dry}	wt% _{dry}	wt % _{dry}	wt% _{dry}	wt% _{d ry}	wt % _{dry}	wt % _{dry}
Coal 5	38.8	53.2	8.0	63.6	4.1	1.7	4.6
Genesee	31.2	41.8	27.0	50.9	3.4	1.4	1.7

Table 3.4 Dubinin-Radushkevich surface area (Micropore area using CO₂, m²/g)

Dubinin-Radushkevich	
	m ² /g
Coal 5	134.4
Genesee	130.1

3.6.2 Comparison of the gasification methods (Method 1, Method 2 and Method 3)

As described previously, three different experimental procedures were evaluated by comparing the reaction rate versus conversion. The original data was collected from the TGA. The information is presented in Fig. 3.1 for Genesee coal at 900°C. Similar results were obtained for coal 5.

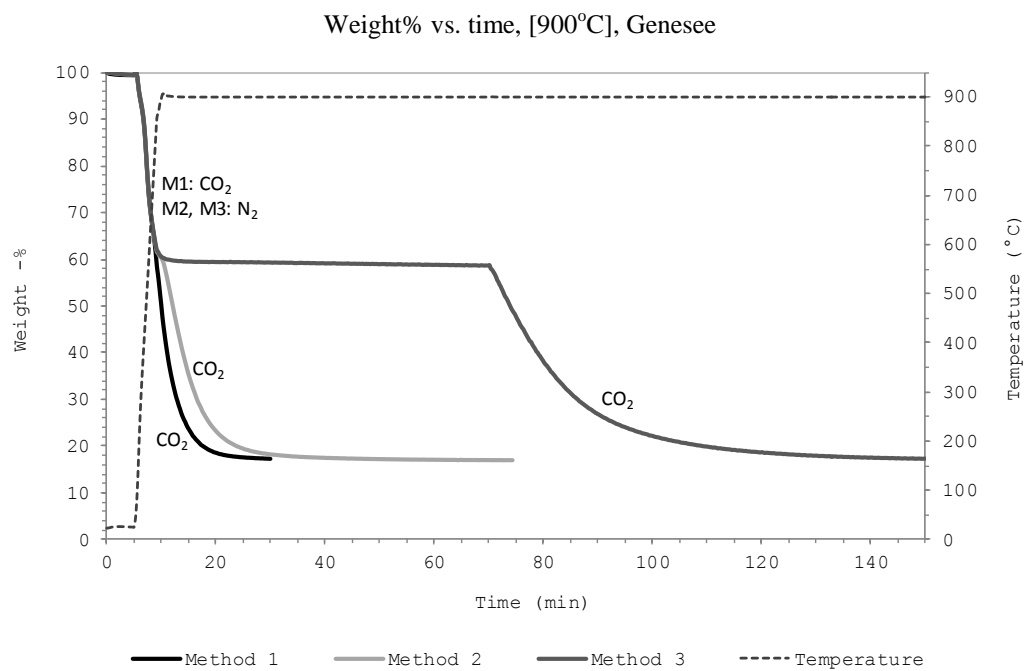


Figure 3.1 Comparison of the three CO₂ coal gasification methods. Example for Genesee coal at 900°C

Original data was used to obtain the reaction rate (r), using 50 data points for kinetic analysis. Figs. 3.2 and 3.3 show the reaction rate versus conversion (X) for Genesee coal and coal 5, respectively. In both cases, there was a maximum reaction rate when N₂ was switched to CO₂; however, it occurred at different conversions.

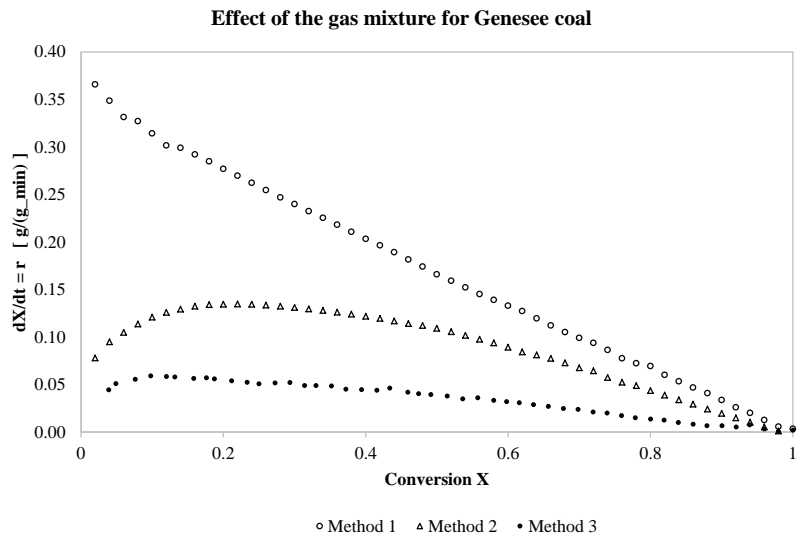


Figure 3.2 Comparison of the reaction rates for methods 1, 2 and 3 for CO₂ Genesee coal gasification at 900°C

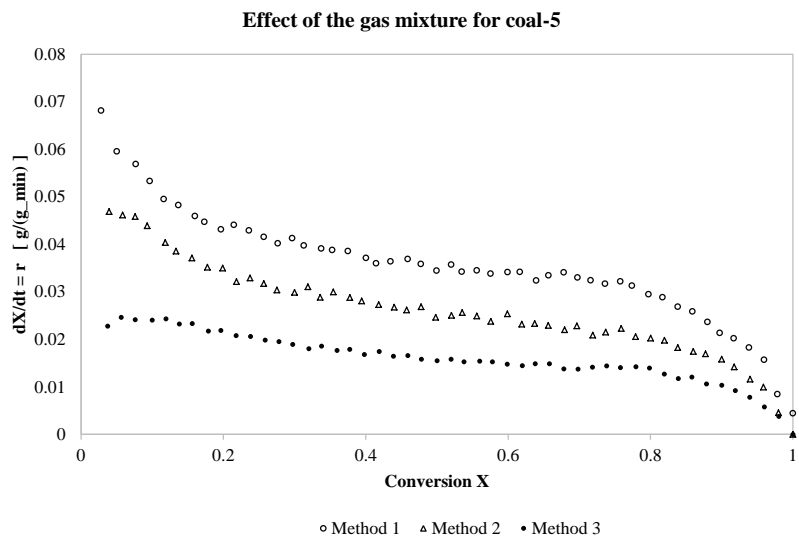


Figure 3.3 Comparison of the reactions rates for method 1, 2 and 3 for coal 5 coal gasification at 900°C

3.6.3 Effect of gas switching: inducing maximum rate of reaction

3.6.3.1 Test 1: constant time after a gas switching perturbation

Test 1 was developed to show the effect of the gas mixture. Starting with N₂ as the sweeping gas and switching to a mixture of CO₂ and N₂ (50% CO₂) when the temperature reached 900°C. The gas mixture was also replaced with 100% CO₂ after a fixed holding time. This experiment was repeated with different holding times (i.e. 0, 2, 4 and 8 min). The results are presented for Genesee coal and coal 5 in Figs. 3.4 and 3.5, respectively. The arrows in Figs. 3.4 and 3.5 indicate when a maximum reaction rate was detected.

It is important to mention that only the conversion and not the time at the maximum reaction rate was analyzed in previous studies [6-14]. However, the time definitely needs to be considered, as presented in this paper.

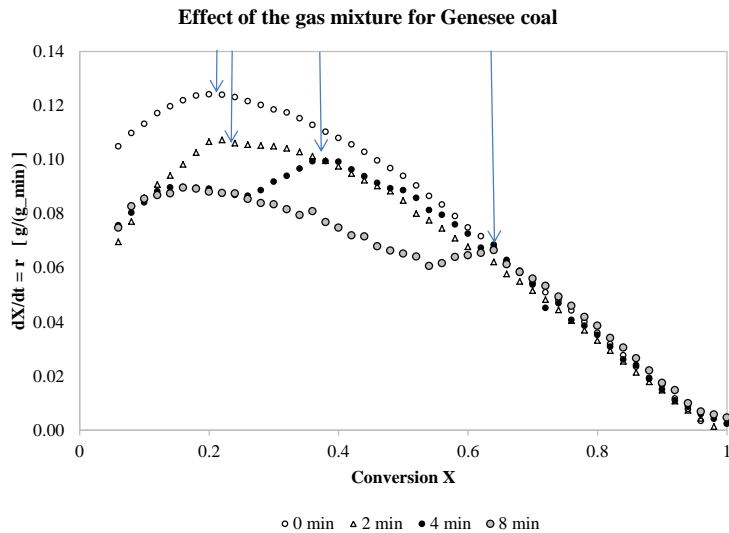


Figure 3.4 Test 1, the effect of the gas switching with the reaction rate vs. conversion for CO₂ Genesee coal gasification. From 50% N₂ / 50% CO₂ to 100% CO₂ at holding times of 0, 2, 4 and 8 min at 900°C

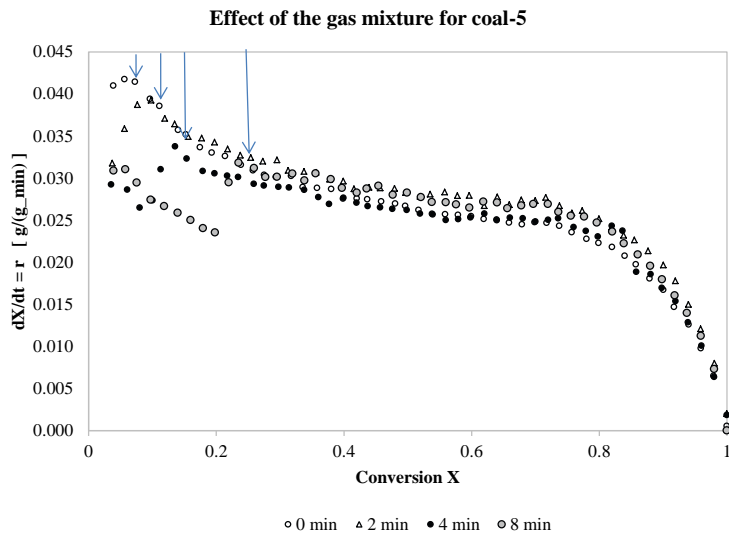


Figure 3.5 Test 1, the effect of the gas switching with the reaction rate vs. conversion for CO₂ coal 5 gasification. From 50% N₂ / 50% CO₂ to 100% CO₂ at holding times of 0, 2, 4 and 8 min at 900°C

Figs. 3.6 and 3.7 present the time when the maximum reaction rate was reached. In the case of holding times of 0 min there is just one maximum reaction rate corresponding to the CO₂ mole fraction of 0.5. The vertical lines mark the time when the perturbation is done and when the maximum reaction rate is observed. For the 2 min holding time, the first maximum reaction rate (in 50% CO₂) overlapped with the second one (in 100% CO₂), but only the second maximum reaction rate could be observed. The time to observe a maximum reaction rate when the gas was switched from 50% CO₂ to 100% CO₂ was 0.9 ± 0.1 min and independent of the type of coal and holding time when the gas change was done.

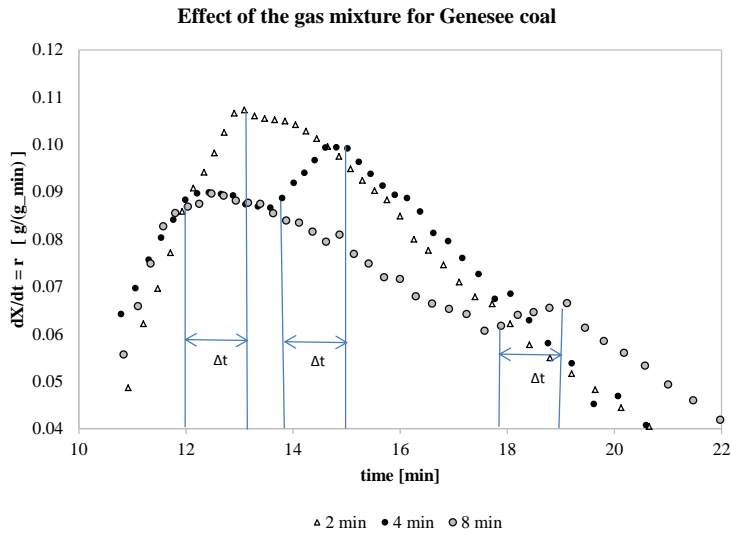


Figure 3.6 Test 1, the effect of gas switching with the reaction rate vs. time for CO₂ Genesee coal gasification. From 50% N₂ / 50% CO₂ to 100% CO₂ at holding times of 0, 2, 4 and 8 min at 900°C

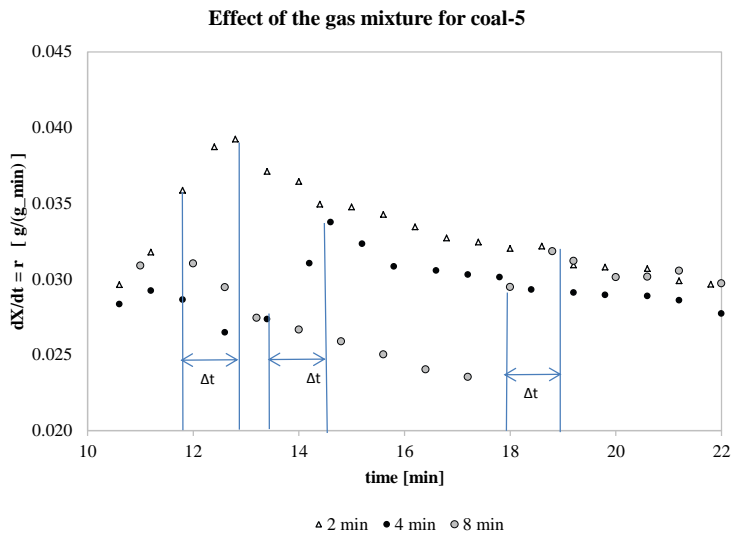


Figure 3.7 Test 1, the effect of gas switching with the reaction rate vs. time for coal 5 gasification. From 50% N₂ / 50% CO₂ to 100% CO₂ at holding times of 0, 2, 4 and 8 min at 900°C

It is important to mention that the difference in the magnitude of the reaction rates between Genesee coal and coal 5, which was almost 3:1 (Figs. 3.6 and 3.7), resulted in a lower conversion, when the maximum reaction rate was reached for coal 5 compared with Genesee coal (Figs. 3.4 and 3.5). This test proved that the conversion associated to the maximum reaction rate was affected by the gas mixture and also explains why more reactive coals exhibited a maximum reaction rate.

3.6.3.2 Test 2: the effect of the partial pressure in the time to reach a maximum reaction rate

Test 2 shows how the observed maximum reaction rate shifted to a lower conversion when the gasification was conducted with lower CO₂ partial pressure. If the reaction rate was too low, the maximum was negligibly visible, since it occurred at very low conversions. This result is contrary to the expected results based on the theory of surface structure changes described by the random pore model. Results for both coals are shown in Fig. 3.8 for the reaction rate vs. conversion and in Fig. 3.9 for reaction rate vs. time. The times from when N₂ was switched to CO₂ to the maximum reaction rate are presented in Fig. 3.9.

Results of test 2 show the time to reach the maximum reaction rate was constant and independent of the partial CO₂ pressure and the type of coal; it was 1.8 minutes for this particular setup (reactor and volumetric flow rate). This means that the time to reach a maximum is independent of the kinetics. As expected, this result confirms that the maximum reaction rate is a consequence of the changing gas mixture and depends on the reaction volume, i.e. a bigger reactor using the same gas flow rate will produce a maximum reaction rate when a higher conversion is reached. Other works present similar trends as those presented in Fig. 3.9, even showing that the maximum reaction rate was observed at the same time for both CO₂ and steam

gasification [21-23], confirming our findings. However, these other studies did not consider the effect of the gas mixture and modeled this behavior using the random pore model.

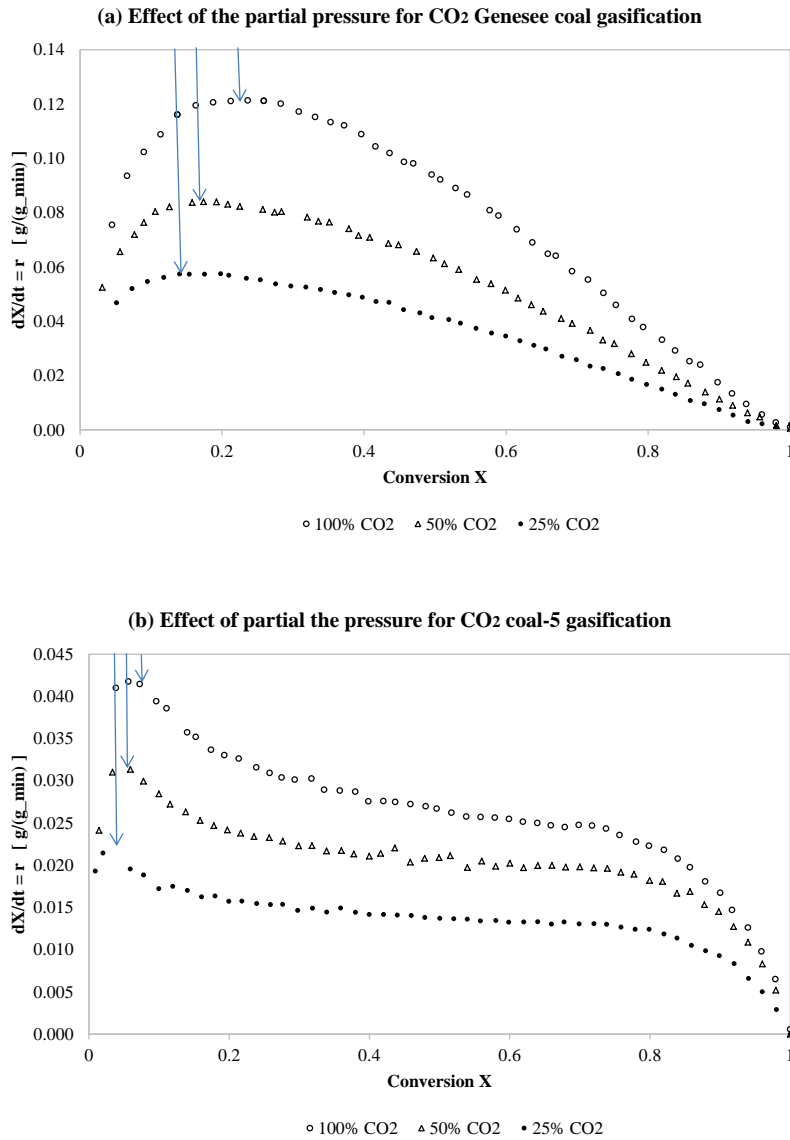


Figure 3.8 Test 2, the effect of partial pressure with the reaction rate vs. conversion when switching from N₂ to 100% CO₂, 50% CO₂ and 25% CO₂ at 900°C at atmospheric pressure (88 kPa) for (a) Genesee coal and (b) coal 5

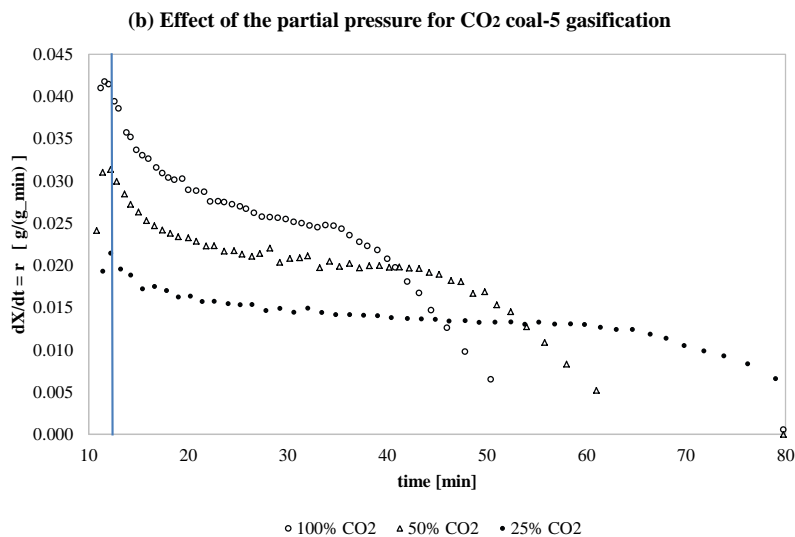
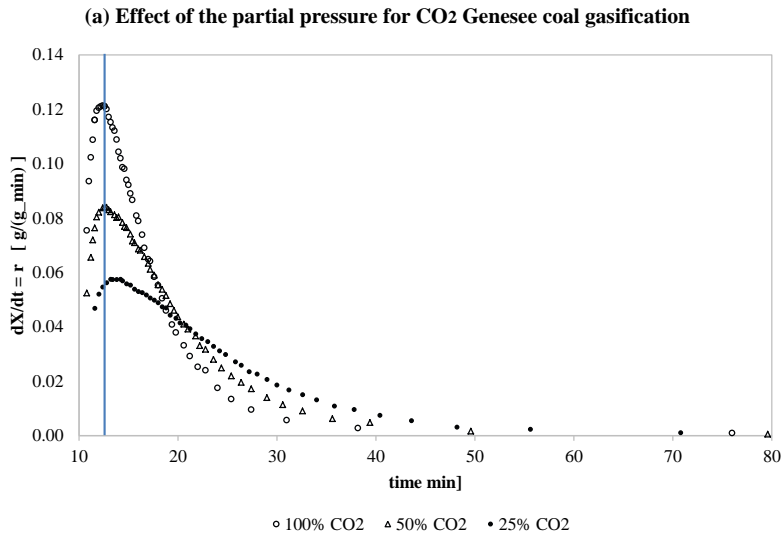


Figure 3.9 Test 2, the effect of partial pressure with the reaction rate vs. time when switching from N₂ to 100% CO₂, 50% CO₂ and 25% CO₂ at 900°C at atmospheric pressure (88kPa) for (a) Genesee coal and (b) coal 5

The result of test 2 is important, since the integrated core model fits it better; and, the kinetic modeling becomes simpler [15]. Another important result is the explanation of why highly reactive coals have been reported with a maximum reaction rate and those with low reactivity

have not reported a maximum reaction rate. This is also true for experiments conducted at lower temperatures. Since the time of changing gases is almost constant, the mixture effect influences the conversion when the maximum reaction rate is reached, which shifts to the left when the reaction rate decreases.

3.6.3.3 Test 3: the maximum reaction rate does not occur at the start of the gasification

Test 3 results are presented in Fig. 3.10 for Genesee coal and coal 5 for reaction rate vs. conversion. The purpose of this test was the evaluation of the mixing effect at different conversions, determining the time to observe a maximum after changing the gas from N_2 to CO_2 . Fig. 3.11 presents reaction rate vs. time for both coals Genesee and coal 5, showing in both cases the same time to reach a maximum since the gas is switched. It is important to mention that gasification started at the minute 10 for all experiments.

This test shows that the time to observe the maximum reaction rate was almost constant (between 1.8 and 2 min) and did not depend on a particular conversion or coal type. Similar value was obtained in test 2 for different partial CO_2 pressures, which suggests that the maximum reaction rate is a consequence of the gas dispersion into the reactor when the gas is switched. Since Genesee coal is more reactive than coal 5, it is possible just to record three maximums before the end of the gasification.

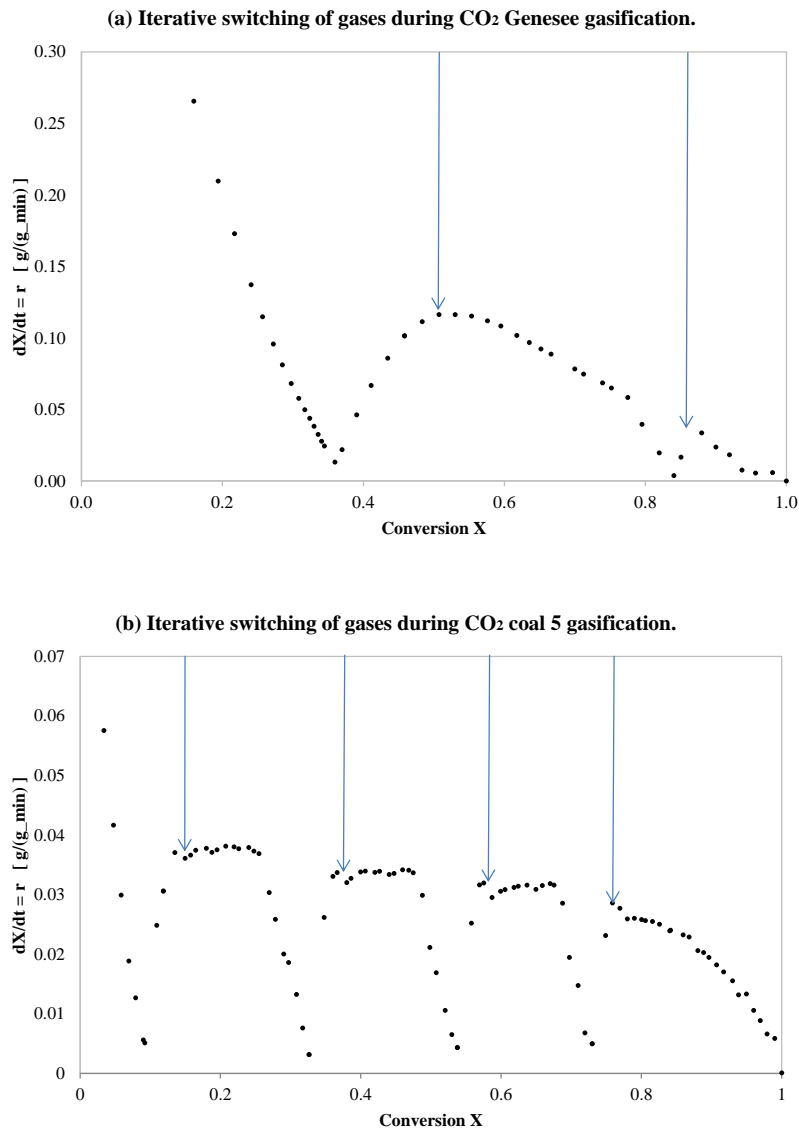


Figure 3.10 Test3, the effect iterative switching with the maximum reaction rate vs. conversion From 0 to 100% CO₂ and vice versa: CO₂ (a) Genesee coal and (b) coal 5 gasification at 900°C

Tests 1, 2 and 3 showed that the maximum reaction rates, using method 2 and 3, were influenced by the changing gas mixture. Method 1 (direct CO₂ gasification) avoided the induced gas dispersion effect that was present in other experimental procedures since there is no gas switching in this method. It is also important to mention that there was a small overlap of the

pyrolysis and gasification processes; however, it can be considered negligible, since the reaction rate of pyrolysis is much higher than that of gasification [10].

The effect of the gas mixture has not previously been associated with the maximum rate of reaction [10-14]. The direct CO₂ gasification is a novel procedure that is useful for kinetic analysis of gasification, since gasification with this method yields the highest reactivity and does not exhibit a maximum reaction rate as in the other experimental procedures.

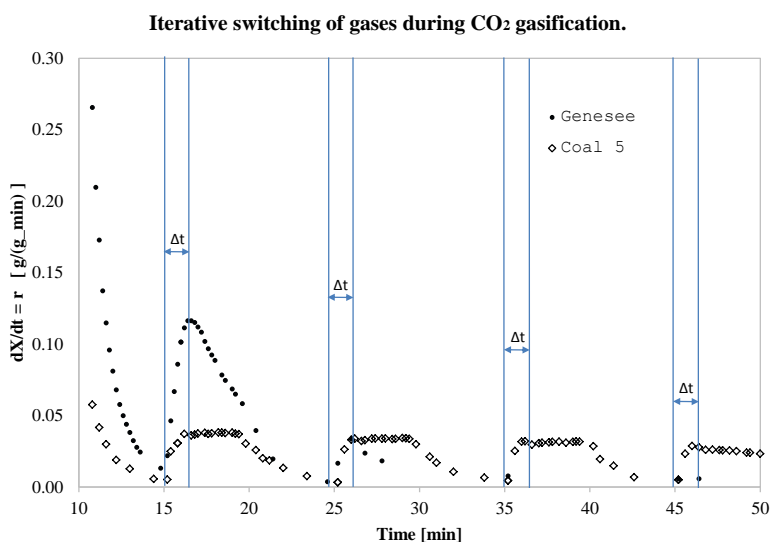


Figure 3.11 Test 3, the effect of iterative gas switching with the maximum reaction rate vs. time. From 0 to 100% CO₂ and vice versa: CO₂ Genesee coal and coal 5 gasification at 900°C

3.6.4 Effect of pyrolysis time

Method 1 (direct CO₂ gasification) produces faster reaction rates, followed by method 2 and method 3. Methods 2 and 3 were both influenced by the same gas mixture effects, but their reaction rates were significantly different, which may have been a consequence of changes in the char structure.

3.6.4.1 Reduction of mesopore area due to the pyrolysis time

Char from both coals was produced in a bench reactor simulating the TGA conditions. After reaching 900°C, the char was cooled down as fast as possible and subsequently characterized using BET and micropore area (CO₂ adsorption using the Dubinin-Raduskevich method). These results are presented in Table 3.5. The effects of cooling after char synthesis and heating during gasification were not considered in this study, due to experimental limitations.

Table 3.5 Mesopore and micropore surface area for chars from Genesee and coal 5, produced at 900°C with holding times of 5, 30 and 60 min

	<u>BET surface area [m²/g]</u>		
	Exposure time		
	5 min	30 min	60 min
Genesee char	93.6	19.8	12.9
Coal 5 char	2.8	1.1	0.7

BET surface area (N₂ adsorption at 77K)

	<u>D-R micropore area [m²/g]</u>		
	Exposure time		
	5 min	30 min	60 min
Genesee char	301.1	311.2	355.7
Coal 5 char	381.7	399.4	409.5

Dubinin-Radushkevich micropore surface area(CO₂ adsorption at 273K)

It was found that the variation in char micropore structure was less than 15%, for different isothermal pyrolysis time; however, mesopore area (BET surface area) decreased significantly when the isothermal pyrolysis time was increased. The variation proportion of the mesopore surface area was higher than that of the micropore area. Moreover, a reduction in reactivity was observed with a long pyrolysis time. This result is consistent with gasification experiments

starting from the raw coal, specifically the comparison of the reaction rates between methods 2 and 3.

3.6.4.2 Decrease in reaction rate due to the time of the pyrolysis

The chars obtained at the three holding times in a N₂ atmosphere and at 900°C were gasified using method 1 to avoid induced effects due to the gas mixture. The reaction rate results are presented for Genesee char and coal 5 char (char 5) in Fig. 3.12, showing that the reaction rate decreased when the char was maintained for a longer time at high temperature.

Ideally, gasification using method 3 is equivalent to producing char in the bench reactor using the same time during the isothermal pyrolysis and subsequently gasifying it using method 1. Fig. 3.13 presents a comparison between these two equivalent procedures for Genesee coal at holding times of 5 and 60 min. Fig. 3.14 illustrates the same comparison for coal 5.

Figs. 3.13 and 3.14 show that the effect of the holding time before gasification significantly influenced the reactivity of the char. It is important to mention that the TGA gasification of the char, produced in the horizontal reactor (TGA char gasification-method 1), has similar reactivity as the raw coal directly gasified in the TGA using the same isothermal holding times (TGA coal gasification-method 3). The only difference was the effect of the gas change at the beginning of the gasification. This indicates that the surface area of the char produced in the bench reactor represents almost the same surface area of the char produced in the TGA after the isothermal pyrolysis step.

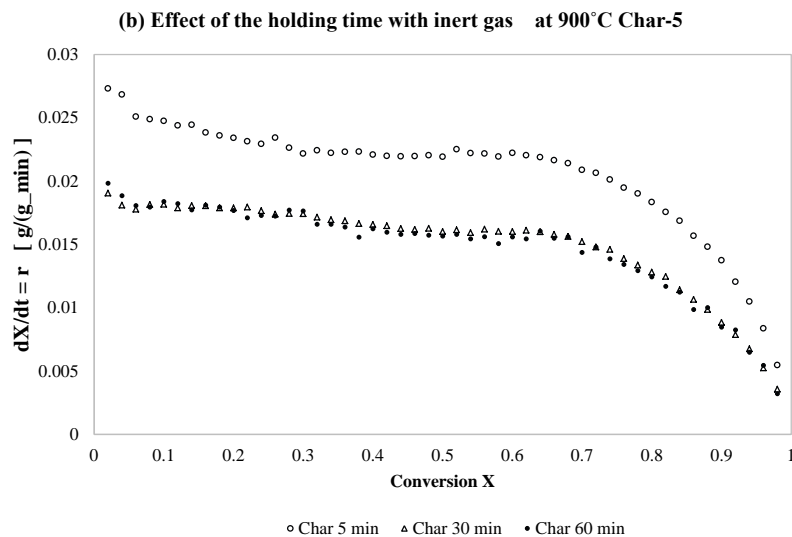
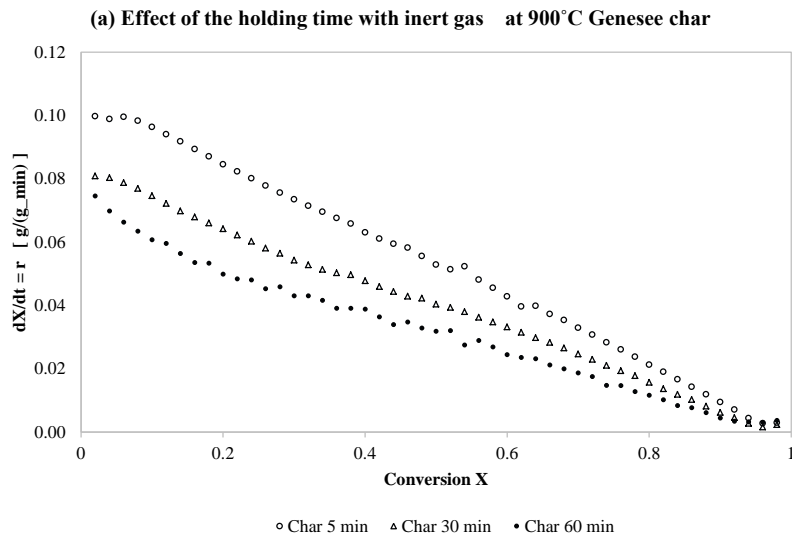


Figure 3.12 The effect of the holding time at 900°C during CO₂ char gasification with reaction rate vs. conversion. Holding times: 5, 30 and 60 min for (a) Genesee char and (b) coal 5 char

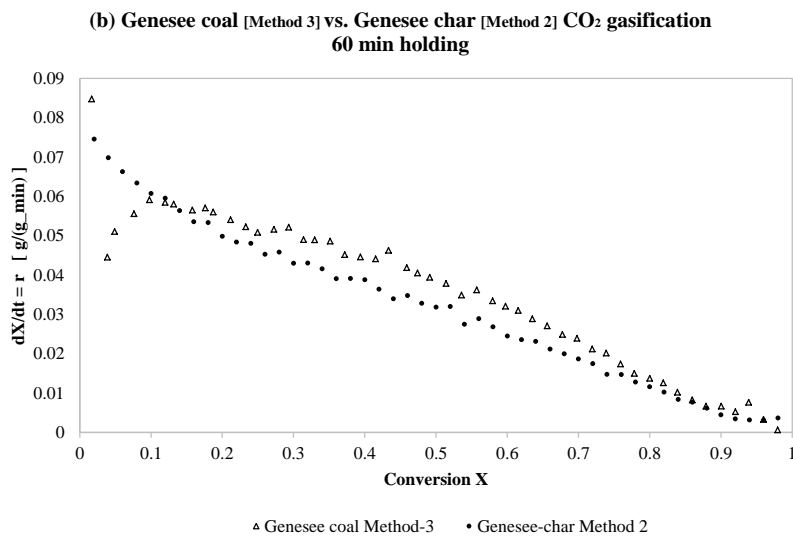
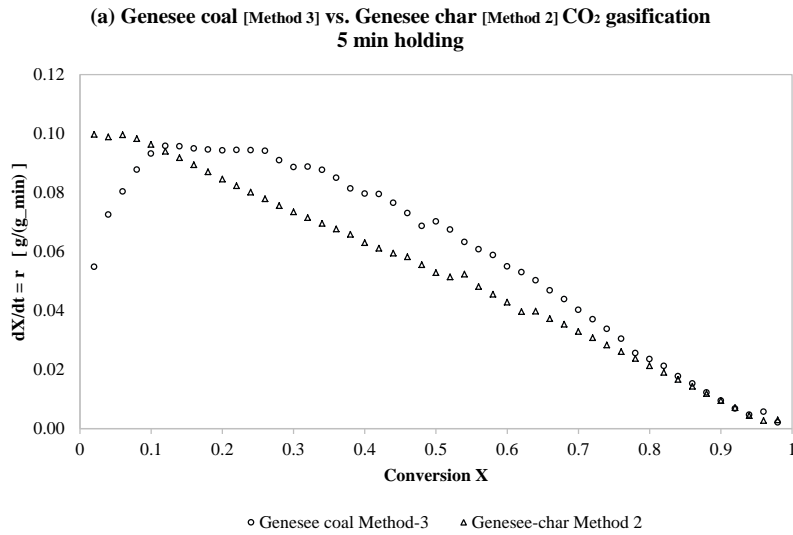


Figure 3.13 Method 2 and 3 comparison. CO₂ Genesee Char gasification compared with CO₂ raw coal gasification at 900°C. (a) Genesee char (5 min) method 2 vs. Genesee coal method 3 (5 min), (b) Genesee char (60 min) method 2 vs. Genesee coal method 3 (60 min)

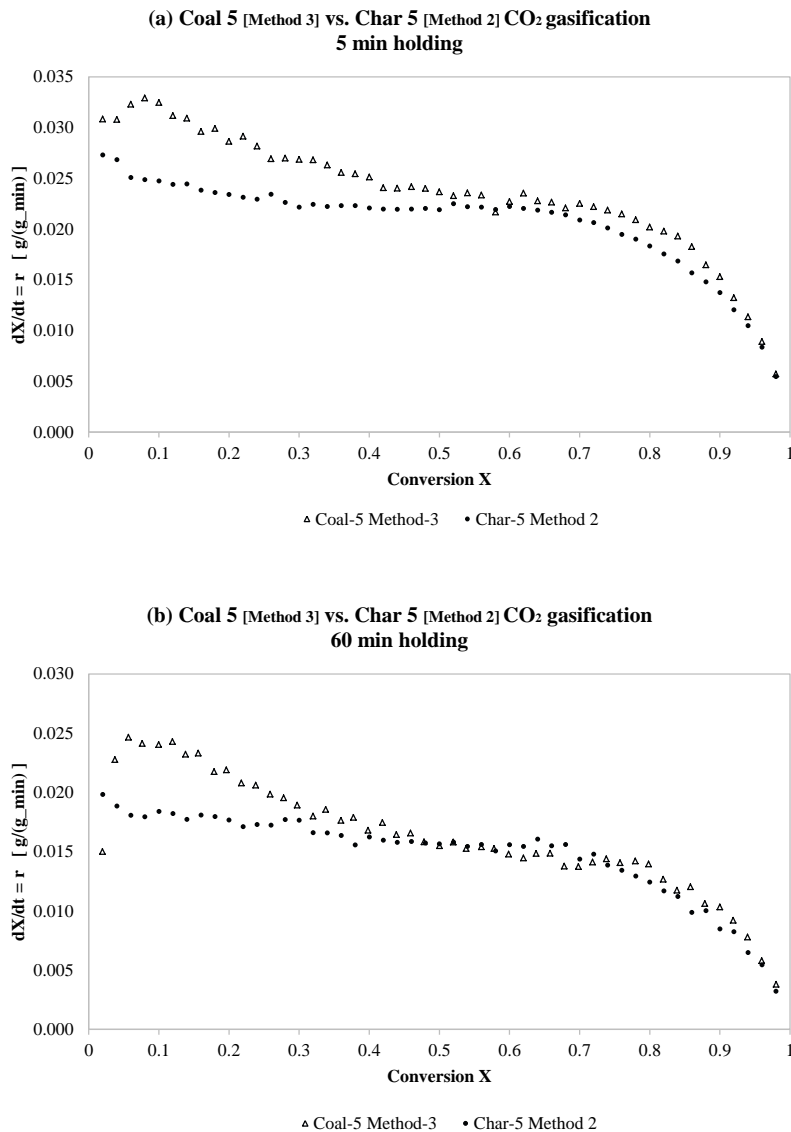


Figure 3.14 Method 2 and 3 comparison. CO₂ coal 5 Char gasification compared with CO₂ raw coal gasification at 900°C. (a) Char 5 (5 min) method 2 vs. coal 5 method 3 (5 min), (b) Char 5 (60 min) method 2 vs. coal 5 method 3 (60 min)

Another aspect is that the separation of pyrolysis and gasification has been conducted by holding the sample in an inert atmosphere for a fixed period of time, at 10 min [9], 30 min [7,

10], and more commonly 60 min or more [6, 8]. The isothermal pyrolysis affects the char surface area and thus, the kinetic analysis.

The different scales of reaction rates for the different methods can be explained by comparing the micropore and mesopore areas of the produced char at the reaction temperature and the changes that occur at different holding times before gasification (Table 3.5). The gasification results led to the conclusion that the BET and RD area characterization of the Genesee char and coal 5 char (produced in the bench reactor) represented the surface area of the char produced during the TGA raw coal gasification with an isothermal step prior to the CO₂ gasification.

3.7 Conclusion

A novel method to perform CO₂ gasification studies was compared to the most common procedures employed by other researchers [6, 14]. Conversion and reaction rate were calculated by the weight loss obtained using the thermogravimetric techniques. This method involves a higher heating rate and CO₂ at the start of the experimental procedure. In industrial applications, CO₂ is used as the sweeping gas instead of an inert gas; therefore, the proposed direct CO₂ gasification (method 1) and its kinetic analysis is more suitable for practical purposes.

Three different tests proved that the time to observe a maximum reaction rate, after changing the reaction gases, remained constant, thereby confirming the effect of the gas mixture on the gasification. This time was independent of the CO₂ partial pressure and coal reactivity. Conventional gasification procedures (method 2 and 3) are inducing a maximum rate of reaction

due to dispersion of the gases in the reaction chamber; which was particularly detected if the coal reactivity is high.

The nonexistence of a maximum rate of reaction changes the way that kinetic modeling is conducted for CO₂ gasification. Moreover, kinetic models that are simpler than the random pore model can be used. Also, the kinetic modeling of gasification using the random pore model should be reviewed, so that systematic errors can be avoided in the experimental procedure. The findings of this work illustrate the effects of changing the reaction medium; which is applicable for other feedstock and also different processes such as steam gasification.

The new experimental procedure results in a higher gasification reaction rate compared to those reported in the literature when an isothermal step (with an inert gas) is used to separate pyrolysis from gasification. Changes in the char surface are induced by experimental procedures with an isothermal pyrolysis step, decreasing the mesopore area and therefore the char reactivity.

3.8 References

- [1] Cousins A, Hughes RW, McCalden DJ, Lu DY, Anthony EJ. Waste classification of slag generated in a pilot-scale entrained-flow gasifier. CSIRO-CanmetENERGY 2012; 4:37-44. www.coalcgp-journal.org (Last accessed Nov 2014)
- [2] Hattingh BB, Everson RC, Neomagus H, Bunt JR. Assessing the catalytic effect of coal ash constituents on the CO₂ gasification rate of high ash, South African coal. Fuel Process Technol 2011; 92 (10): 2048-2054.
- [3] Gonzalo-Tirado C, Jiménez S, Ballester J. Kinetics of CO₂ gasification for coals of different ranks under oxy-combustion conditions. CSIC-University of Zaragoza. Combust Flame 2013; 160 (2): 411-416.
- [4] Umemoto S, Kajitani S, Hara S. Modeling of coal char gasification in coexistence of CO₂ and H₂O considering sharing of active sites. Fuel 2013; 103: 14-21.
- [5] Kajitani S, Suzuki N, Ashizawa M, Hara S. CO₂ gasification rate analysis of coal char in entrained flow coal gasifier. Fuel 2006; 85 (2): 163-169.
- [6] Ochoa J, Cassanello MC, Bonelli PR, Cukierman AL. CO₂ gasification of Argentinean coal chars: a kinetic characterization. Fuel Process Technol 2001; 74 (3): 161-176.
- [7] Malekshahian M, Hill J. Kinetic analysis of CO₂ gasification of petroleum coke at high pressure. Energy Fuels 2011; 25: 4043-4048.
- [8] Çakal G, Yücel H, Gürüz AG. Physical and chemical properties of selected Turkish lignites and their pyrolysis and gasification rates determined by thermogravimetric analysis. J Anal Appl Pyrol 2007; 80 (1): 262-268.
- [9] Beamish BB, Shaw KJ, Rodgers KA, Newman J. Thermo-gravimetric determination of the carbon dioxide reactivity of char from some New Zealand coals and its association with the inorganic geochemistry of the raw coal. Fuel Process Technol 1998; 53: 243-253.

- [10] Zhu W, Song W, Lin W. Catalytic gasification of char from co-pyrolysis of coal and biomass. *Fuel Process Technol* 2008; 89 (9): 890-896.
- [11] Zou JH, Zhou ZJ, Wang FC, Zhang W, Dai ZH, Liu HF, Yu ZH. Modeling reaction kinetics of petroleum coke gasification with CO₂. *Chem Eng Process* 2006; 46: 630–636.
- [12] Mani T, Mahinpey N, Murugan P. Reaction kinetics and mass transfer studies of biomass char gasification with CO₂. *Chem Eng Sci* 2011; 66 (1): 36-41.
- [13] Tremel A, Spliethoff H. Gasification kinetics during entrained flow gasification – Part II: Intrinsic char reaction rate and surface area development. *Fuel* 2013; 107: 653-661.
- [14] Kajitani S, Hara S, Matsuda H. Gasification rate analysis of coal char with a pressurized drop tube furnace. *Fuel* 2002; 81 (5): 539-546.
- [15] Silbermann R, Gomez A, Gates I, Mahinpey N. Kinetic studies of a novel CO₂ gasification method using coal from deep unmineable seams. *Ind Eng Chem Res* 2013; 52: 1487-14797.
- [16] Bhatia SK, Perlmutter DD. A random pore model for fluid–solid reactions: I. Isothermal and kinetic control. University of Pennsylvania. *AIChE J* 1980; 26 (3): 379–386.
- [17] Bhatia SK, Vartak BJ. Reaction of microporous solids: The discrete random pore model. *Carbon* 1996; 34 (11): 1383-1391.
- [18] Irfan M, Usman MR, Kusakabe K. Coal gasification in CO₂ atmosphere and its kinetics since 1948: A brief review. *Energy* 2011; 36: 12-40.
- [19] Tremel A, Haselsteiner T, Kunze C, Spliethoff H. Experimental investigation of high temperature and high pressure coal gasification. *Appl Energy* 2012; 92: 279-285.
- [20] Tremel A, Spliethoff H. Gasification kinetics during entrained flow gasification – Part III: Modelling and optimisation of entrained flow gasifiers. *Fuel* 2013; 107: 170-182.
- [21] Ahmed II, Gupta AK. Kinetics of woodchips char gasification with steam and carbon dioxide. *Appl Energy* 2011; 88 (5): 1613-1619.

[22] Nipattummakul N, Ahmed I, Kerdsuwan S, Gupta AK. High temperature steam gasification of wastewater sludge. *Appl Energy* 2010; 87 (12): 3729-3734.

[23] Prabowo B, Umeki K, Yan M, Nakamura MR, Castaldi MJ, Yoshikawa K. CO₂-steam mixture for direct and indirect gasification of rice straw in a downdraft gasifier: Laboratory-scale experiments and performance prediction. *Appl Energy* 2014; 113: 670–679.

Chapter Four: A new model to estimate CO₂ gasification kinetics based only on parent coal characterization properties

4.1 Presentation of the article

This article shows the correlation of the two most important variables in gasification, i.e. active char surface area and alkali content, which are estimated for catalytic CO₂ gasification. The motivation for this study was presented in Chapter 2 whereby statistics reveal that estimation of the activation energy is affected by feedstock properties. The effect of the surface area at different ash contents has not been reported and many authors consider the gasification rate of coal mixtures as the weighted average of the raw coal gasification rates; however, this a mixing rule that does not consider the catalytic nature of the alkali and alkaline earth metal. The proposed model, based on theoretical considerations, allows the estimation of the gasification rate of any feedstock on the basis of the raw material properties. This work is the continuation of the paper presented in the previous chapter, which shows an alternative method to perform CO₂ gasification without inducing a maximum gasification rate; a procedure that allows better correlation of the experimental data with simpler kinetic models.

The proposal, demonstration of the new semi-empirical equation, and required experiments at different temperatures to determine the activation energy (15 coal samples x 3 temperatures x 2 repetitions = 90 experiments) has been completed by R. Arturo Gomez. Dr. Nader Mahinpey has supervised this work and evaluated the validity of the proposed expression. Assumptions and additional analysis of the proposed model is presented in Appendix C.

A new model to estimate CO₂ coal gasification kinetics based only on parent coal characterization properties

This article has been published in Applied Energy 137 (2015) 126-133. Reprinted with permission.

Arturo Gomez¹, Nader Mahinpey¹

¹Chemical and Petroleum Engineering Department, University of Calgary, 2500 University Drive NW, Calgary, T2N 1N4, Canada

4.2 Abstract

A new mathematical model is proposed for the estimation of CO₂ gasification kinetics of different rank coals and ash contents. There are no previous reports on the determination of the conversion rate or even residence time of CO₂ or steam gasification based on coal characterization and for a wide range of ash content. This new approach can be used to infer the residence time and other parameters required for reactor design and operation optimization of newly mined coals or coal mixtures used as feedstock.

The coal micropore surface area and the alkaline content determined by the ash composition were proved to be the most significant variables influencing the gasification rate. These variables were correlated to formulate a semi-empirical expression based on the Arrhenius equation. An equation to infer residence time, independent of the kinetic model, is also presented.

The new equation is important in understanding the catalytic effect of the alkaline content in the temperature range where the chemical reaction is the controlling step. It can also be used as

the corresponding term of the chemical reaction in a gas-solid kinetic model when working at higher temperatures. This new approach is valid, if there is not loss of alkali and alkaline earth metals due to sublimation or melting, which results in a glassy slag structure. The proposed model has direct industrial application in simulation of gasifiers' performance with the knowledge of only coal characterization properties.

4.3 Introduction

Gasification is the thermochemical conversion of carbonaceous feedstock into carbon monoxide (CO), carbon dioxide (CO₂) and hydrogen (H₂). Other by-products are generated from the rest of the raw material's components reacting at a high temperature with gasification products. The non-reactive components are termed ash; however, they are not totally inert, since they can change their morphology due to solid-phase changes, partial oxidation or reduction, or even metal and oxide sublimation [1, 2].

Different models are used to represent the chemical reaction kinetics of CO₂ gasification as a particular case of gas-solid reactions. The simplest models are the volumetric model (VM), the shrinking core model (SCM), and the integrated core model (ICM), which are equivalent to a first, two third, and a general unknown reaction order on the solid phase, respectively [3-5]. The most widely used model is the random pore model (RPM), which was proposed by Bhatia and Perlmutter [6] to explain the existence of a maximum conversion rate usually observed experimentally. Other models with additional parameters can generate similar results than the RPM [7, 8]. It was proved that this maximum is a consequence of the experimental procedure when the inert gas is replaced by the reaction gas instead of associated changes on the char

surface area [9]. The ICM and the VM fit better to the experimental results than other models, if the experimental procedure is adjusted in order to avoid the gas switching [5, 9].

The heterogeneity among different feedstock is a challenge to implement gasification as an alternative process for coal and biomass utilization. Therefore, accurate and reliable gasification rate estimation is necessary to infer the performance of different reactors when the feedstock is changed. Information obtained from coal characterization, such as proximate and elemental analyses, has been widely studied, but there have been no results for the estimation of the kinetic behavior of coals, even with similar ash contents. Previous works in gasification have not mentioned the calculation of kinetic parameters based on parent coal properties, since consistent correlations had not been obtained; however, the effects of the most important variables, i.e., coal rank, temperature, pressure, ash composition and gasifying agents, have been reported [10].

A first attempt to estimate the reactivity of coals based on the physical and chemical properties of the coal was proposed by Adschiri et al. [11], who correlated porosity and micropore surface area with the initial carbon content of the parent coal. Other works have shown improvement in the gasification rate with an increase in ash content [12] and a general correlation for different rank coals using experimental kinetic parameters, such as the frequency factor and activation energy, without considering measurable properties of the raw material [13].

As coal reactivity is significantly affected by their ash content, alternative methodologies have been proposed to compare their gasification rates. For example, Ochoa et al. [14] presented master curves for different coals, which show the ratio between the conversion rate at a particular conversion and the conversion rate at 50% conversion. Reported results show that low-rank coals

exhibited higher reactivity than high-rank coals. This reactivity was associated with the alkaline content [15]. There have also been differences in the literature related to the activation energy even for the same rank coals [16, 17].

The most common chemical reaction kinetic models do not consider the effect of the ash composition [3, 4]; however, its catalytic nature has been mentioned as a variable affecting the activation energy [5]. The effects of alkali and alkaline earth metals as catalysts to enhance CO₂ gasification [18-20] have been widely discussed, with the order of effectiveness as potassium (K) > sodium (Na) > calcium (Ca) > iron (Fe) > magnesium (Mg) content [21]. Similar results have been presented for steam gasification [22, 23], plus a reduction in methane (CH₄) formation when potassium carbonate (K₂CO₃) was added to the feedstock [24]. Hatting et al. [25] showed that micropore surface area and mineral composition (determined by the ash analysis) were the most significant variables during CO₂ gasification, but did not present a model to estimate kinetic parameters.

Thermogravimetric analysis (TGA) studies have been conducted at low temperatures, where the chemical reaction was the controlling step and it was assumed that there were no slagging conditions but operating temperature for entrained flow reactors is higher than 1400 K [26]. For gas-solid reactions; adsorption, desorption, and surface reaction should be considered assuming a particular reaction mechanism [24], such as the Langmuir-Hinshelwood kinetic model [27]. However, many authors use a single step reaction model, when the chemical reaction is the controlling step [3-7, 9-11, 14, 17]. In addition, other attributes like pore diffusion and partial pressure resulted from the competition of gasifying agents to reach active surface sites must be taken into account [27]. Recent models assume that gasification rate of coal mixtures behaves as

a linear combination of the pure coal gasification rates [28]; however, this is not necessarily true for low rank-coals, because the effect of the catalyst amount on the activation energy should be considered in the Arrhenius equation [5, 23], which is a non-linear expression. It is a common practice in the laboratory set-up to have an isothermal stage prior to gasification to separate the pyrolysis from the gasification [3, 19]. This isothermal stage and its associated residence time will affect significantly the mesopore surface area, thereby influencing the gasification rate [9]. A new experimental procedure was proposed to eliminate the effects of the isothermal pyrolysis stage on the kinetics of gasification [5, 9]. These results were consistent with studies conducted using an entrained flow reactor [16, 28].

In this study, for the first time, a new mathematical model correlating simultaneously pore surface area and alkaline content, using the parent coal characterization, is proposed to estimate the CO₂ gasification rate in a broad range of ash contents and different morphologic properties of coals. This is possible due to a new approach using equivalent moles to standardize the combined activity of alkali and alkaline earth metals instead of describing qualitatively the effect the alkali content. The new equation is a semi-empirical expression based on the Arrhenius equation and it can be adapted to determine the residence time instead of the conversion rate, which is a procedure that is independent of an assumed kinetic model. Different coals and their mixtures were characterized and gasified with the new procedure evaluated by Gomez et al. [9], resulting in a good fit between the experimental data and the proposed model's results. The new model can be used to infer the gasification behavior of coal mixtures. This new approach provides an instrumental tool in process modeling and scaling up of gasification processes, when properties of feedstock vary or when feedstock is a blend of different coals.

4.4 Data analysis and modeling

4.4.1 Data analysis

Time and loss weight data were collected every 12 seconds. The conversion was calculated as:

$$X = \frac{m_o - m_t}{m_o - m_a} \quad \text{Eq. (4-1)}$$

where m_o is the mass of the sample when the system reaches the reaction temperature; m_t is the mass of the sample at a particular time, t ; and, m_a is the mass of the ash based on the weight reading at 100% conversion.

The gasification rate for a batch system usually is referred as the solid conversion rate [3-7, 9-11], defined as the variation of the conversion during a period of time and expressed as:

$$r = \frac{\Delta X}{\Delta t} \quad \text{Eq. (4-2)}$$

Details about data analysis and kinetic models can be found elsewhere [3-5].

4.4.2 Kinetic model simplification

Switching gases induces gas dispersion effects, resulting in a maximum conversion rate [9]. The random pore model (RPM) has been accepted as the best kinetic model, since it can predict a maximum conversion rate; however, the RPM does not represent the real behavior when these mixture effects are avoided. It was found that the integrated core model and normal distribution models provided better fits for experimental CO₂ gasification results [5]. For simplicity and because there is a theoretical explanation, the integrated core model was the kinetic model used

to obtain the rate constant from the experimental data. The integrated core model can be expressed as:

$$r = \frac{dX}{dt} = k_{IM}(1 - X)^n \quad \text{Eq. (4-3)}$$

where k_{IM} is the rate constant of this particular model.

Using direct gasification, the kinetic analysis is simplified, due to the corrections of the experimental procedure. The integrated core model (ICM) often tends to be similar to the volume model (VM), when the reaction order is close to one. The solution of the ordinary differential Eq. (4-3) gives:

$$\begin{cases} \frac{dX}{dt} = k(1 - X) = k e^{-kt} & \text{if } n = 1 \\ \frac{(1 - X)^{1-n} - 1}{n - 1} = kt & \text{if } n \neq 1 \end{cases} \quad \text{Eq. (4-4)}$$

It is observed a linear trend if the natural logarithm of time is plotted against temperature, or the reciprocal of temperature, as presented by Silbermann et al. [5]. This consideration is useful in determining a correlation independent of the kinetic model, in order to obtain the residence time for a determined conversion.

4.4.3 Model development

Some authors consider additive terms in the kinetic expression to consider different active sites for the catalytic and non-catalytic reactions as proposed by Kim et al. [29] based on the original work of Kitsuka et al. [30]. Under studied experimental conditions, the reaction is chemically controlled as reported in previous works [5, 9] and, therefore, a general chemical

reaction model based on a single overall reaction step has been used in this work [31]. The first assumption of this model is that the catalyst is homogeneously distributed on the char surface. This assumption holds true for the raw coal and coal impregnated with catalyst but not necessarily the case for coal-alkali dry mixtures. This general kinetic model is a function of two independent variables:

$$r = \frac{dX}{dt} = f_1(1 - X) \times f_2(T) \quad \text{Eq. (4-5)}$$

The first factor (f_1) depends on the total active surface, which is a function of conversion and is related to the initial total char pore surface. Usually, it is hard to correlate this surface area with the micropore and mesopore areas of the parent coal. However, when the char is produced during a short residence time using high heating rates and avoiding isothermal pyrolysis at high temperature, changes on the pore surface area of the char are minimized; and, this is proportional to the parent coal pore surface area [9] and can be expressed as:

$$f_1(X = 0) \sim S \left[\frac{\text{m}^2}{\text{g carbon}} \right] \quad \text{Eq. (4-6)}$$

The second assumption is that changes on the char pore surface due to devolatilization during pyrolysis are proportional to the raw coal pore surface area. This is particularly valid for coal, which is different from biomass due to the thermal decomposition of cellulose and hemicellulose.

It is clear that the ash composition must be included in one of the two terms in Eq. (4.5). Since alkali acts as a catalyst during CO_2 gasification, the activation energy is affected.

Therefore, the Arrhenius equation can be expressed as a new function, depending on temperature and a factor that groups the effect of the catalyst:

$$f_2(T, \text{alkali}) = k_0 e^{-\frac{E_a}{RT}} = k_0 e^{-\frac{(E_a + \frac{\bar{\alpha}}{\text{Alk}})}{RT}} \quad \text{Eq. (4-7)}$$

where E_a^* is the activation energy of the reactant saturated with catalyst, “Alk” is the specific molar alkali content [equivalent-moles/g coal], and “ $\bar{\alpha}$ ” is a proportionality constant. The third assumption of the model is that in Eq. (4-7) the activation energy is inversely proportional to the alkaline content. This assumption is consistent with the theory and experimental results [15, 16].

Considering the mentioned assumptions, Eqs. (4-6) and (4-7) can be rearranged for a representative conversion rate, avoiding the consideration of changes on the char surface during gasification. In the case of the integrated core model (IM), as with the most common chemical reaction kinetic models, the rate constant represents the gasification rate when the conversion is zero. In general, the initial conversion rate can be expressed as:

$$k_M \approx f_2^* = S \left[\frac{\text{m}^2}{\text{g carbon}} \right] \times \exp \left(\frac{-b}{\text{Alk} \left[\frac{\text{equivalent moles}}{\text{g coal}} \right] \times T[\text{K}]} \right) \quad \text{Eq. (4-8)}$$

where k_M is the rate constant [min^{-1}] for a particular kinetic model ‘M’; S is the initial surface area of the parent coal (based on carbon content) [$\text{m}^2/\text{g carbon}$]; “Alk” is the specific alkaline content [equivalent-moles/g coal]; and, “ b ” [$\text{g}_{\text{coal}} \text{K}/\text{alkaline equivalent moles}$] is a constant to fit experimental data, which incorporates the effect of the alkali content in the exponential factor of the Arrhenius equation. It is a dimensional parameter that is easy to obtain with nonlinear regression for a set of coal samples.

It is important to mention the sources of these variables. The carbon-based pore surface area corresponds to the total micropore area of coals, since the mesopore area is negligible compared with micropore area. It is usually obtained on a coal basis, but must be transformed to a carbon basis, which is accomplished by dividing the total pore surface area by the carbon percentage obtained from the elemental analysis [5].

The term corresponding to the alkaline content is obtained from the ash analysis, which is given as a mass percentage of the respective oxide, i.e., potassium oxide (K₂O), sodium oxide (Na₂O), magnesium oxide (MgO) and calcium oxide (CaO). This means that, for every gram of these compounds, the number of molecule equivalents (proportional to the number of bonds) is twice the mass fraction divided by the respective molecular weight. The specific alkaline content (Alk) is the sum of the K, Na, Mg and Ca contributions multiplied by the ash percentage, which is obtained from the proximate analysis.

The required time to reach a determined conversion (residence time) is a function of the second factor, f_2 , and depends on temperature and alkaline content. As mentioned, the graph of the natural logarithm of time plotted against the reciprocal of temperature (i.e., $\log(\text{time}[X])$ versus $1/T$) exhibits a linear trend independent of the kinetic model [5]; and, Eq. (4-8) can be reformulated to use time instead of the rate constant:

$$\ln(t_X) \approx f_2^* = S \left[\frac{\text{m}^2}{\text{g carbon}} \right] \times \exp \left(\frac{-b}{\text{Alk} \left[\frac{\text{equivalent moles}}{\text{g coal}} \right] \times T[\text{K}]} \right) \quad \text{Eq. (4-9)}$$

A comparison of correlation coefficients is presented in Section 4.5.4 as an examination of the results of Eqs. (4-8) and (4-9), using a conversion of 80% as the reference, since the

uncertainty of the gasification rate increases as the conversion become closer to 100%. This also allows the comparison with other works where conversion was 80% as the reference for obtaining the kinetic parameters [3-5].

4.5 Results and discussion

4.5.1 Coal properties

Table 4.1 summarizes the proximate and ultimate analyses and the micropore surface area using the Dubinin-Raduskevich method for 11 coals (not including the coal mixtures since they are considered as the linear combination of the original coals). The carbon-based micropore surface area is presented in the last column of Table 4.1 as the ratio between the coal-based micropore surface area and the carbon content obtained through the elemental analysis (column 4).

The ash composition is presented in Table 4.2. The information is shown as the mass percentage of the most common metal oxides, without considering morphologic characteristics. Unfortunately, it is impossible to measure the ash properties at the reaction temperature and in a CO₂ atmosphere with current technology. A model with this basic information has not been developed, since there is not an apparent trend when the conversion rate is correlated with different alkaline contents. The specific molar alkaline content is a measurement of the alkaline content and is shown in the last column of Table 4.2.

Table 4.1 Proximate and ultimate analyses and surface area (micropore area using CO₂ at 273 K with the Dubinin-Radushkevich method)

	Proximate Analysis			Ultimate Analysis				Micropore Surface Area	
	Volatiles	Fix Carbon	Ash	C	H	N	S	Dubinin-Radushkevich	
								Coal based	Carbon based
wt% _{dry}	wt% _{dry}	wt% _{dry}	wt% _{dry}	wt% _{dry}	wt% _{dry}	wt% _{dry}	wt% _{dry}	m ² /g _{Coal}	m ² /g _{Carbon}
Coal 1	24.4	19.0	56.6	22.6	2.0	<1	3.6	49	215
Coal 2	12.9	8.7	78.4	19.3	1.8	<1	4.2	50	260
Coal 3	39.5	54.1	6.4	64.8	4.3	1.6	5.0	134	206
Coal 4	23.6	32.9	43.5	40.0	2.6	1.1	2.3	82	204
Coal 5	39.0	53.5	7.5	63.6	4.1	1.7	4.6	135	212
Coal 6	36.9	55.2	7.9	61.7	3.9	1.2	5.3	124	201
Coal 7	43.2	47.5	9.3	60.8	4.1	<1	7.8	115	189
Genesee	32.3	43.0	24.7	50.9	3.4	1.4	1.7	130	256
Lausitzer KW	43.5	30.9	25.6	47.0	3.4	1.2	2.4	111	238
Lausitzer VE	54.1	39.2	6.7	61.7	4.5	1.4	1.5	151	244
MIBRAG	53.7	34.0	12.3	60.5	4.9	1.3	4.22	118	195

4.5.2 Effect of the pore surface area on coal reactivity

Gasification results are presented in Table 4.3, where the reported data correspond to the integrated core model's rate constant. The results for the two coal mixtures were the experimental data and not the weighted average values of the rate constants from the original constituents.

Table 4.2 Ash composition and total specific molar alkaline content (equivalent-moles/g_{coal}). Mixtures 1 and 2 correspond to 82% and 38% Genesee coal (the balance is coal 6), respectively

SAMPLE ID	% Ash	Ash composition [% ash based]											Alkaline content mol _{alk} /g _{coal}
		SiO ₂	Al ₂ O ₃	TiO ₂	Fe ₂ O ₃	CaO	MgO	Na ₂ O	K ₂ O	P ₂ O ₅	SO ₃	Undet.	
Coal 1	56.6	58.3	31.1	0.9	3.4	0.9	0.5	1.0	0.6	0.1	0.5	2.6	0.057
Coal 2	78.4	74.6	15.3	0.6	4.3	0.4	0.5	0.7	0.9	0.0	0.3	2.3	0.064
Coal 3	6.4	26.4	21.1	0.7	13.4	6.8	2.2	11.3	0.5	0.0	15.3	2.3	0.046
Coal 4	43.5	60.6	29.5	1.4	2.2	1.4	0.6	1.4	0.3	0.0	1.1	1.5	0.058
Coal 5	7.5	27.4	22.4	0.4	14.6	6.3	2.3	10.1	0.5	0.0	13.4	2.7	0.050
Coal 6	7.9	43.9	28.8	0.6	7.3	4.4	1.6	4.8	0.3	0.3	5.7	2.2	0.031
Coal 7	9.3	45.3	22.9	0.7	5.8	7.3	2.2	5.3	0.9	0.1	6.7	2.8	0.052
Genesee	24.7	37.3	39.2	0.6	6.9	3.3	1.1	5.0	0.4	0.2	3.4	2.6	0.084
Mixture 1	21.8	38.4	37.4	0.6	7.0	3.5	1.1	5.0	0.4	0.2	3.8	2.5	0.075
Mixture 2	14.4	41.3	32.8	0.6	7.2	4.0	1.4	4.9	0.4	0.3	4.8	2.3	0.052
Lausitzer KW	25.6	58.0	13.4	0.6	6.7	7.7	2.4	0.5	1.3	0.0	9.0	0.3	0.113
Lausitzer VE	6.7	17.0	5.5	0.2	20.0	25.7	9.3	0.3	0.2	0.0	19.9	1.9	0.094
MIBRAG	12.3	18.3	9.2	0.2	13.2	23.4	2.1	0.4	0.3	0.0	30.5	2.4	0.118

The new factor “ f_2^{*} ” proposed in Eqs. (8) and (9) was the product of the functional variables obtained from the parent coal characterization, which is presented in the last column of Table 4.3. Parameter “ b ” was obtained by nonlinear regression to fit the experimental data using the least squares method, with an optimal value equal to 226.7 g_{coal}K/equivalent moles at 850°C. This parameter covers coals in a wide range of ash content (*i.e.*, 6%-80%).

Table 4.3 CO₂ gasification results for 11 coal samples and two mixtures of coals. Mixtures 1 and 2 correspond to 82% and 38% Genesee coal (the balance is coal 6), respectively

SAMPLE ID	t [min] to reach X=0.8			k [g/g-min]			f ₂ [*]
	T= 800°C	T= 850°C	T= 900°C	T= 800°C	T= 850°C	T= 900°C	[m ² /g coal]
Coal 1	278.6	148.2	62.6	0.014	0.026	0.055	6.178
Coal 2	117.2	45.6	21.8	0.035	0.083	0.168	11.066
Coal 3	284.2	86.2	24.8	0.007	0.017	0.049	2.632
Coal 4	362.6	102.6	49	0.013	0.039	0.093	6.346
Coal 5	195.8	66.2	20.8	0.008	0.018	0.049	3.870
Coal 6	530.4	162.8	57.6	0.006	0.017	0.042	0.330
Coa 7	799.2	220.6	81.6	0.003	0.009	0.023	3.912
Genesee	29.8	13.2	5	0.066	0.146	0.345	23.443
Mixture 1	78.2	37.2	15.7	0.069	0.162	0.303	16.659
Mnixture 2	368	129.2	46.8	0.020	0.032	0.095	4.481
Lausitzer KW	11.1	5.1	2.8	0.152	0.371	0.660	39.875
Lausitzer VE	15.6	6.0	3.0	0.091	0.234	0.419	28.404
MIBRAG	5.3	2.9	1.6	0.226	0.392	0.741	35.163

The pore surface area has often been mentioned by different authors, but no trends have been found that explain the relationship between the reactivity and the total pore surface area [3, 4, 11], as presented in Fig. 4.1. The rate constant was obtained using the integrated core model. In this case, seven coals in a narrow range of total alkali contents have been compared.

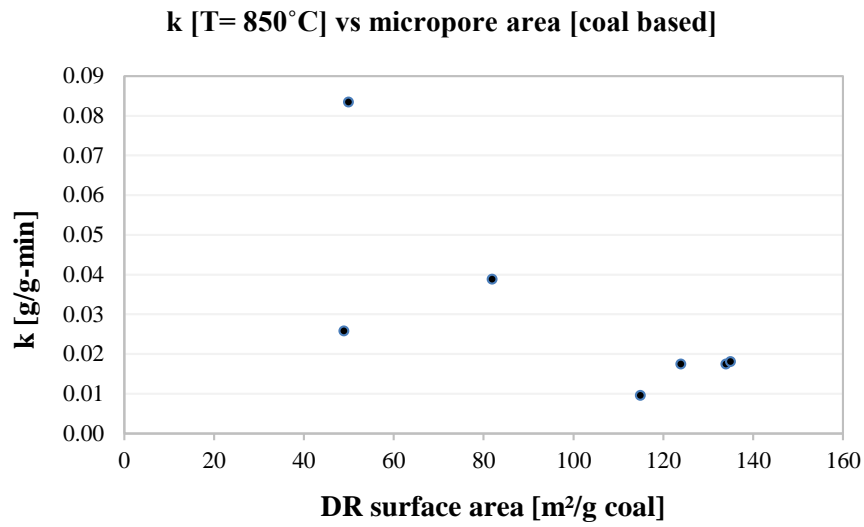


Figure 4.1 Rate constant vs. coal-based micropore area (Dubinin-Radushkevich method) for deep mine coals (Coals 1 to 7)

If the effect of the composition is isolated, it is possible to see a real trend using the methodology proposed by Silbermann et al. [5]. Fig. 4.2 shows the initial conversion rate (rate constant) versus the carbon-based micropore surface area using the same coals presented in Fig. 4.1. These coals exhibited the lowest alkaline content; therefore, the effect of the surface area was more dominant. When all of studied coals were compared, there were combined effects of the total surface area and catalytic activity of the alkali. This situation is presented in Fig. 4.3. Similar results at 850°C were obtained for the range of studied temperatures.

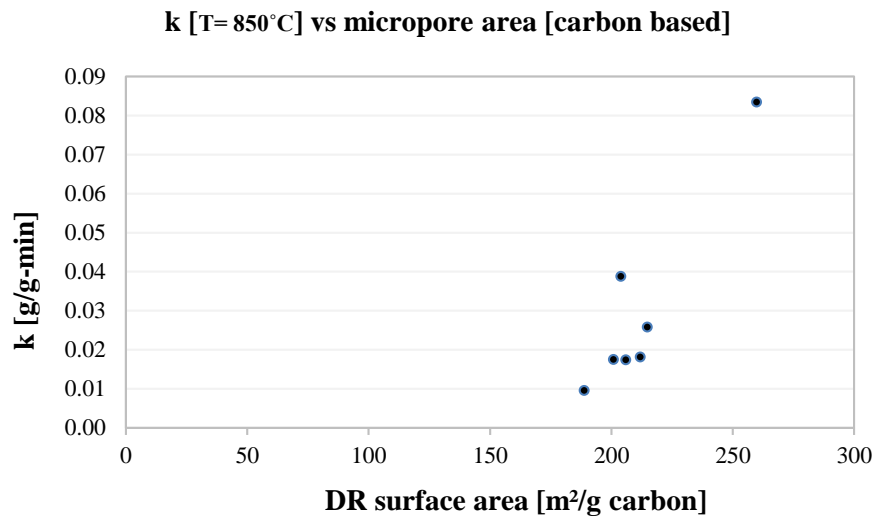


Figure 4.2 Rate constant vs. carbon-based micropore area (Dubinin-Radushkevich method) for deep mined coals (Coals 1 to 7)

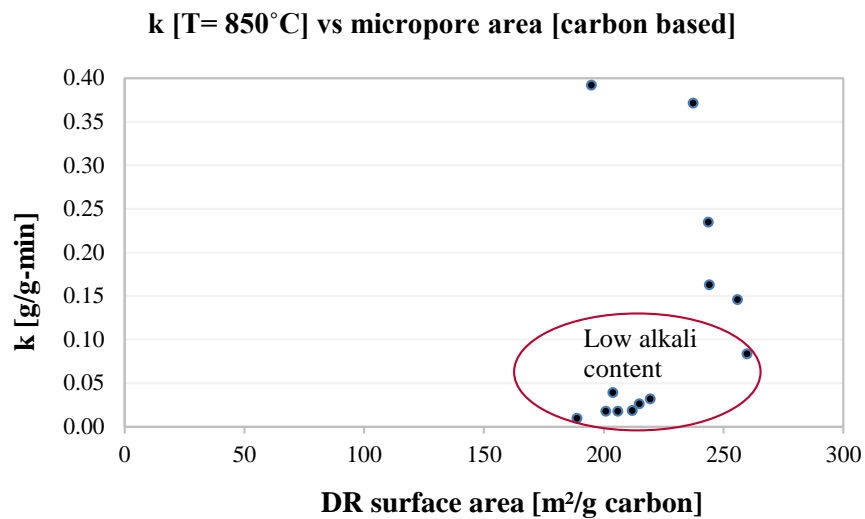


Figure 4.3 Rate constant vs. carbon-based micropore area (Dubinin-Radushkevich method) for all coals presented in Table 4.2 at 850°C using direct gasification

4.5.3 Effect of the alkaline content on coal reactivity

When the alkaline content is low, the CO₂ gasification rate depends mainly on the pore surface area. This pore surface area based on the carbon content is proportional to the char pore surface area; however, when the range of ash content is broad, the comparison and estimation of coal reactivity is not straightforward.

Other authors have used an alkaline index [25] and other variables to show the catalytic effect of alkaline metals; nevertheless, their results did not show a perceptible tendency when working with different ash contents. A more appropriate way to express alkaline content is the total equivalent moles of alkali per gram of carbon or specific molar alkaline content. This is a better approach to show the catalytic activity due to alkaline presence, assuming there is not loss of alkaline metal due to sublimation or melting to a glassy structure of the alkaline oxide. An alternative procedure to use the chemical reaction term at high temperatures is to perform the mineral composition analysis with ash produced at the gasification temperature, instead of 750°C as suggested by the ASTM D3682.

Results of the rate constant versus alkaline content are presented in Fig. 4.4, with a correlation coefficient greater than 0.9. The trend presented in Fig. 4.4 is especially important, since the ash content of the studied coal samples varied from 6.7% to 78.4% and exhibited significantly different gasification rates, despite some similar ash contents (i.e., coals 5 and 7). No apparent effect of the alkaline content was detected under a value of 0.004 equivalent-mole/g coal; as perhaps the catalytic effect was not significant compared with the total pore surface area. This signifies the fact that under certain value of alkali content, the inverse relationship between minerals and activation energy is not substantial.

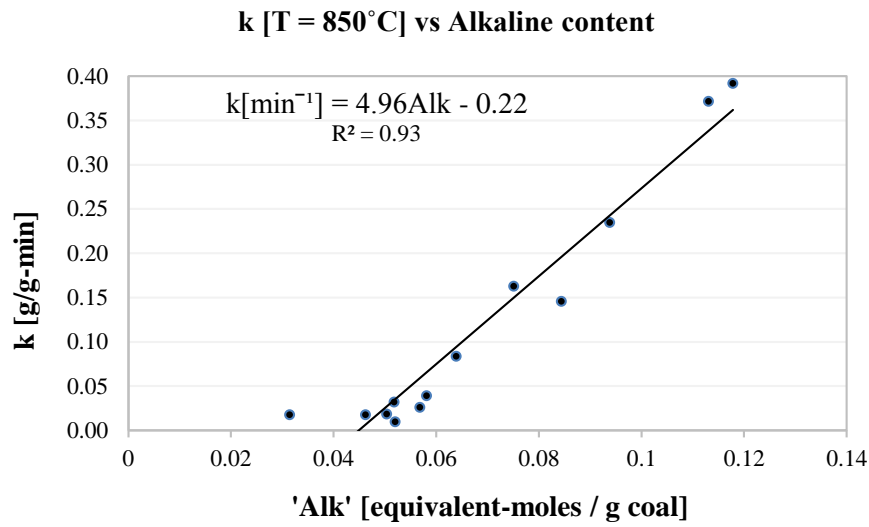


Figure 4.4 Rate constant (min^{-1}) vs. alkaline content 'Alk' (equivalent-moles / g coal) for all coals presented in Table 4.2 at 850°C using direct gasification

Fig. 4.5 shows the residence time for a conversion of 80% versus the alkaline content; where it is evident that there was a logarithmic trend for residence time, as analyzed in Eq. (4.4) and introduced by Silbermann et al. [5]. Different authors have used a conversion of 80% ($X = 0.8$) for kinetic analysis [3-5]; and, when reactivity was low, the relative uncertainty of the measurement was higher than 10% for conversions higher than 80%. The expression using the residence time instead of the conversion rate is independent of the kinetic model.

4.5.4 New model evaluation

The alkaline content affects activation energy [18-23], but its effect is not easily isolated from other variables. Fig. 4.6 presents the relationship between the apparent activation energy and the alkaline content for the integrated core model in the gasification temperature range. It is important to mention that the extrapolation to a zero alkaline content gives activation energy of

233 kJ/mol, keeping in mind that the reported activation energy for graphite is 270 kJ/mol [16]. Furthermore, when the equivalent molar alkaline content was greater than 0.06 equivalent-moles/g coal, the effect of alkali addition was negligible. The extrapolation indicates that the intercept was approximately 120 KJ/mol (when activation energy is plotted against the reciprocal of alkaline content), which is in accordance with the lowest reported value of activation energy of low-rank coals [16].

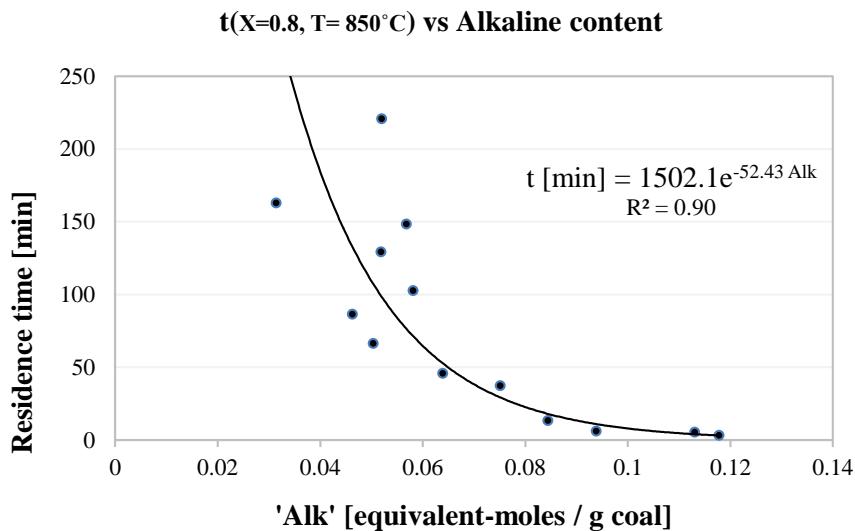


Figure 4.5 Residence time (min at 80% conversion) vs. alkaline content 'Alk' (equivalent-moles / g coal) for all coals presented in Table 4.2 at 850°C using direct gasification

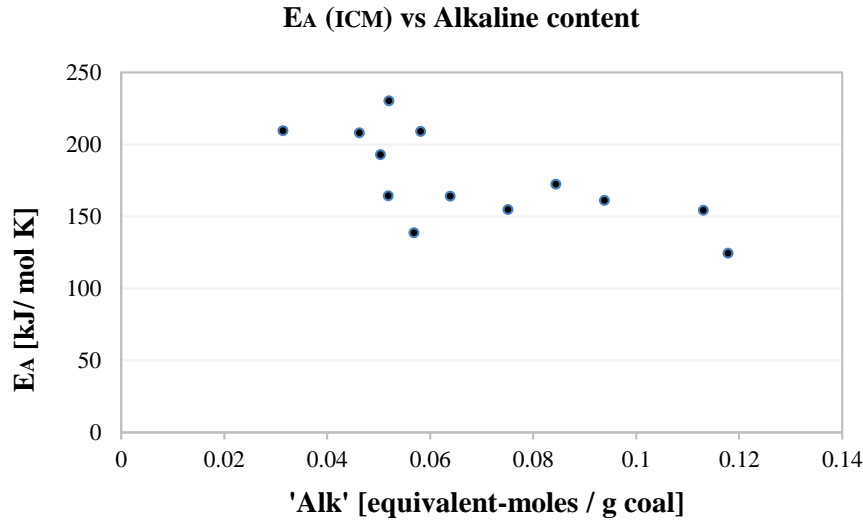


Figure 4.6 Activation energy vs. alkaline content ‘Alk’ (equivalent-moles / g coal) for direct CO₂ gasification. Temperature range between 800°C and 900°C and using the ICM to obtain rate constant

Figs. 4.7 and 4.8 show the relationship between rate constant and residence time ($X = 0.8$) at 850°C with the factor f_2^* , respectively; where f_2^* (m²/g coal) is the independent variable to calculate the rate constant and residence time using Eqs. (4-10) and (4-11), respectively:

$$k [\text{min}^{-1}] = a_k \times f_2^* \quad \text{Eq. (4-10)}$$

$$t[\text{min}] = a_t \times \exp(-c_t \times f_2^*) \quad \text{Eq. (4-11)}$$

where a_k , a_t and c_t are regression parameters.

The correlation coefficient in Fig. 4.7 and 4.8 were higher than the corresponding values presented in Figs. 4.4 and 4.5. The new expression models the cases at limit when both the total pore surface area and the ash composition are very low, since the conversion rate approaches zero ($r \rightarrow 0$) when $f_2^* \rightarrow 0$. When the alkaline content was low and ash content was high, there was

greater dispersion (i.e., f_2^* was between 2 and 6 m^2/g carbon), corresponding to the seven deep coals as presented in Fig. 4.8. As coal surface area and alkali content increases, the model fits more closely to experimental data.

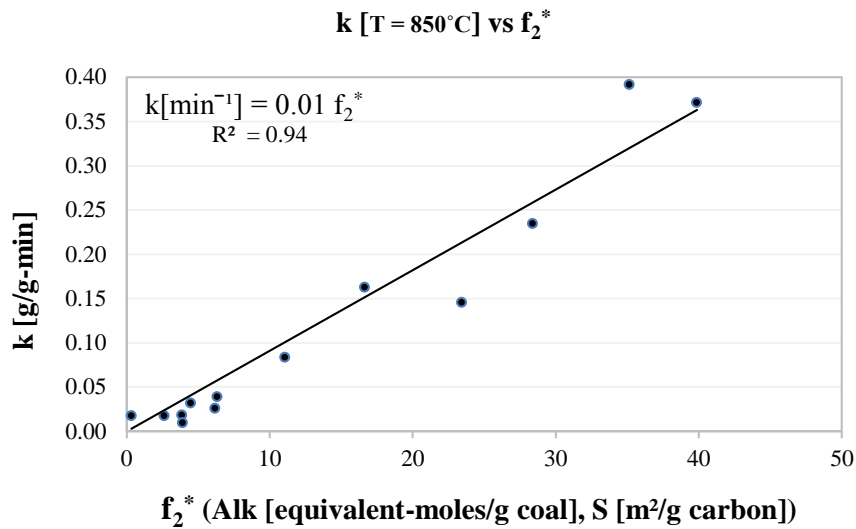


Figure 4.7 Rate constant vs. f_2^* , according to the relationship stated in Eq. (4-8) for all coals presented in Table 4.2 at 850°C using direct gasification and the ICM to obtain rate constant

Results of the regression parameters in the temperature range are presented in Table 4.4. When the temperature increased, the correlation coefficient improved for the rate constant regression and decreased for the residence time regression, which is consistent at low temperatures where the chemical reaction is the controlling step, since the conversion rate versus the conversion tends to be linear with a temperature increase.

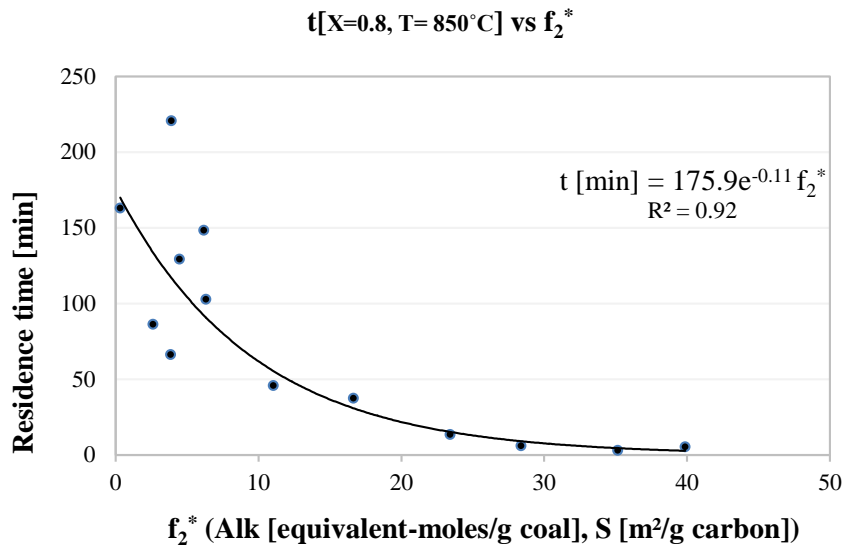


Figure 4.8 Residence time (for 80% conversion) vs. f_2^* , according to the relationship stated in Eq. (4-9) for all coals presented in Table 4.2 at 850°C using direct gasification

Table 4.4 Parameter of regression r vs. f_2^* and parameter of regression t vs. f_2^*

T [°C]	k		t [X=0.8]		
	a_k	R^2	a_t	c_t	R^2
	[$g_{\text{coal}} m^{-2} min^{-1}$]		[min^{-1}]	[$g_{\text{coal}} m^{-2}$]	
800	0.004	0.85	542.4	0.12	0.93
850	0.009	0.95	179.9	0.11	0.92
900	0.017	0.95	61.5	0.09	0.87

4.6 Conclusion

In this study, a new mathematical model has been developed to calculate the two most important variables during CO₂ gasification, *i.e.*, rate constant, and residence time. The model presented a good fit with the experimental data in a broad range of ash contents. It was developed as a semi-empirical model based on the Arrhenius equation, using characterization

variables of the parent coal to include the effect of both the surface area content (based on carbon) and the alkaline ash composition (equivalent alkali molecules per gram of coal).

The new approach includes the experimental method evaluated by Gomez et al. [9], thereby solving the associated gas dispersion effects to determine the residence time independent of the kinetic model. This new model proves the catalytic effect of alkali and alkali earth metals, showing for the first time a correlation for different rank coals in a broad range of ash compositions. It was shown that the method could quantify the behavior of coal mixtures, since it can estimate the rate constant and residence time of CO₂ gasification, depending on the weighted pore surface area and alkaline content expressed as equivalent moles of alkali per gram of coal.

The present study was conducted in the temperature range where the chemical reaction is the limiting step and considering a homogeneous distribution of the alkali on the char surface. The presented rate constant can be considered as the chemical reaction term in a general gas-solid model at higher temperatures if there is no loss of alkali during the gasification.

4.7 References

- [1] Li S, Whitty KJ. Physical phenomena of char–slag transition in pulverized coal gasification. *Fuel Process Technol* 2012; 95: 127–136.
- [2] Bunt JR, Waanders FB, Schobert H. Behaviour of selected major elements during fixed-bed gasification of South African bituminous coal. *J Anal Appl Pyrol* 2012; 93: 85–94.
- [3] Malekshahian M, Hill J. Kinetic analysis of CO₂ gasification of petroleum coke at high pressure. *Energy Fuels* 2011; 25: 4043-4048.
- [4] Zou JH, Zhou ZJ, Wang FC, Zhang W, Dai ZH, Liu HF, Yu ZH. Modeling reaction kinetics of petroleum coke gasification with CO₂. *Chem Eng Process* 2006; 46: 630–636.
- [5] Silbermann R, Gomez A, Gates I, Mahinpey N. Kinetic studies of a novel CO₂ gasification method using coal from deep unmineable seams. *Ind Eng Chem Res* 2013; 52 (42): 14787-14797.
- [6] Bhatia SK, Perlmutter DD. A random pore model for fluid–solid reactions: I. Isothermal and kinetic control. University of Pennsylvania. *AICHE J* 1980; 26 (3): 379–386.
- [7] Li P, Yu Q, Xie H, Qin Q, Wang K. CO₂ gasification rate analysis of Datong coal using slag granules as heat carrier for heat recovery from blast furnace slag by using a chemical reaction. *Energy Fuels* 2013; 27: 4810–4817.
- [8] Singer SL, Ghoniem AF. An adaptive random pore model for multimodal pore structure evolution with application to char gasification. *Energy Fuels* 2011; 25: 1423–1437.
- [9] Gomez A, Silbermann R, Mahinpey N. A Comprehensive experimental procedure for CO₂ coal gasification: Is there really a maximum reaction rate? *Appl Energy* 2014; 124: 73-81.
- [10] Irfan M, Usman MR, Kusakabe K. Coal gasification in CO₂ atmosphere and its kinetics since 1948: A brief review. *Energy* 2011; 36: 12–40.
- [11] Adschiri T, Shiraha T, Kojima T, Furusawa T. Prediction of CO₂ gasification rate of char in fluidized bed gasifier. *Fuel* 1986; 65(12): 1688–1693.

- [12] Milligan MS, Altwicker E. The catalytic gasification of carbon in incinerator fly ash. *Carbon* 1993; 31(6): 977–986.
- [13] Fu WB, Wang QH. A general relationship between the kinetic parameters for the gasification of coal chars with CO and coal type. *Fuel Process Technol* 2001; 72: 63–77.
- [14] Ochoa J, Cassanello MC, Bonelli PR, Cukierman AL. CO₂ gasification of Argentinean coal chars: A kinetic characterization. *Fuel Process Technol* 2001; 74(3): 161–176.
- [15] Beamish BB, Shaw KJ, Rodgers KA, Newman J. Thermo-gravimetric determination of the carbon dioxide reactivity of char from some New Zealand coals and its association with the inorganic geochemistry of the parent coal. *Fuel Process Technol* 1998; 53: 243–253.
- [16] Gonzalo-Tirado C, Jiménez S, Ballester J. Kinetics of CO₂ gasification for coals of different ranks under oxy-combustion conditions, CSIC-University of Zaragoza. *Combust Flame* 2013; 160(2): 411–416.
- [17] Lahijani P, Zainal ZA, Mohamed AR, Mohammadi M. CO₂ gasification reactivity of biomass char: Catalytic influence of alkali, alkaline earth and transition metal salts. *Bioresour Technol* 2013; 144: 288–295.
- [18] Mitsuoka K, Hayashi S, Amano H, Kayahara K, Sasaoaka E, Uddin A. Gasification of woody biomass char with CO₂: The catalytic effects of K and Ca species on char gasification reactivity. *Fuel Process Technol* 2011; 92: 26–31.
- [19] Zhu W, Song W, Lin W. Catalytic gasification of char from co-pyrolysis of coal and biomass. *Fuel Process Technol* 2008; 89(9): 890–896.
- [20] Umeki K, Moilanen A, Gómez-Barea A, Konttinen J. A model of biomass char gasification describing the change in catalytic activity of ash. *Chem Eng J* 2012; 207–208: 616–624.
- [21] Huang Y, Yin X, Wu Ch, Wang C, Xie J, Zhou Z, Ma L, Li H. Effects of metal catalysts on CO₂ gasification reactivity of biomass char. *Biotechnol Adv* 2009; 27: 568–572.

- [22] Sharma A, Takanohashi T, Morishita K, Takarada T, Saito I. Low temperature catalytic steam gasification of HyperCoal to produce H₂ and synthesis gas. *Fuel* 2008; 87(4-5): 491–497.
- [23] Coetzee S, Neomagus HWJP, Bunt JR, Everson RC. Improved reactivity of large coal particles by K₂CO₃ addition during steam gasification. *Fuel Process Technol* 2013; 114: 75–80.
- [24] Wang J, Jiang M, Yao Y, Zhang Y, Cao J. Steam gasification of coal char catalyzed by K₂CO₃ for enhanced production of hydrogen without formation of methane. *Fuel* 2009; 88(9): 1572–1579.
- [25] Hattingh BB, Everson RC, Neomagus H, Bunt JR. Assessing the catalytic effect of coal ash constituents on the CO₂ gasification rate of high ash, South African coal. *Fuel Process Technol* 2011; 92(10): 2048–2054.
- [26] Tremel A, Haselsteiner T, Kunze C, Spliethoff H. Experimental investigation of high temperature and high pressure coal gasification. *Appl Energy* 2012; 92: 279–285.
- [27] S. Umemoto, S. Kajitani, S. Hara, Modeling of coal char gasification in coexistence of CO₂ and H₂O considering sharing of active sites. *Fuel* 2013; 103: 14-21.
- [28] Monaghan RFD, Ghoniem AF. A dynamic reduced order model for simulating entrained flow gasifiers: Part I: Model development and description. *Fuel* 2012; 91(1): 61–80.
- [29] Kim HS, Kudo S, Tahara K, Hachiyama Y, Yang H, Norinaga K et al. Detailed kinetic analysis and modeling of steam gasification of char from Ca-loaded lignite. *Energy Fuels* 2013; 27: 6617–6631
- [30] Kitsuka T, Bayarsaikhan B, Sonoyama N, Hosokai S, Li CZ, Norinaga K, et al. Behavior of inherent metallic species as a crucial factor for kinetic of steam gasification of char from coal pyrolysis. *Energy Fuels* 2007; 21: 387–394.
- [31] Khalil R, Varhegyi G, Jaschke S, Gronli MG, Hustad J. CO₂ gasification of biomass chars: A kinetic study. *Energy Fuels* 2009; 23: 94–100.

Chapter Five: A new method to calculate kinetic parameters independent of the kinetic model: Insights on CO₂ and steam gasification

5.1 Presentation of the article

The estimation of the Arrhenius equation kinetic parameters, i.e. activation energy (E_A) and frequency factor (k_o), has been carried out since 1889 by correlating the logarithm of the rate constant ($\ln k$) with the reciprocal of temperature ($1/T$). This requires the determination of the rate constant from the experimental data; however, it is necessary to assume a kinetic model. It was presented in Chapter 2 that the estimation of the activation energy has a strong correlation with the selected kinetic model but E_A should be theoretically independent of the kinetic model if the reaction mechanism remains invariable. This article presents an alternative procedure to obtain the kinetic parameters independent of the kinetic model, which is based in a new equation deduced from the Arrhenius equation.

The main advantage of the new approach is that it provides a robust method to estimate the activation energy and the frequency factor range for any chemical reaction using isothermal batch experiments. For this reason, kinetic models can be evaluated by comparing their kinetic parameters' accuracy; therefore, assumptions about the reaction mechanism of gasification can be validated. This paper goes beyond gasification and can be applied to any chemical reaction, which contributes to the chemical reaction engineering fundamentals.

The theoretical deduction, modeling, and analysis of the study cases were done by R. Arturo Gomez. Dr. Nader Mahinpey has supervised this work and objectively contributed to extend the scope of this work for the kinetic analysis of any gas-solid reaction.

**A new method to calculate kinetic parameters independent of the kinetic model:
Insights on CO₂ and steam gasification**

This article has been published in Chemical Engineering Research and Design 95 (2015) 346-357.
Reprinted with permission.

Arturo Gomez¹, Nader Mahinpey¹

¹Chemical and Petroleum Engineering Department, University of Calgary, 2500 University Drive
NW, Calgary, T2N 1N4, Canada

5.2 Abstract

A new method to obtain the rate constant and activation energy independent of a kinetic model is proposed and evaluated for thermochemical conversion, specifically in the steam and CO₂ gasification of coal and biomass. Recent works on gas-solid reactions are based on single-step chemical reaction models that have been increasing in complexity through the use of more regression parameters to fit experimental data. These models fit better; however, sometimes their kinetic parameters are inconsistent, resulting in an incorrect interpretation of the reaction mechanism.

The proposed method, which does not require any assumed kinetic model, is useful in calculating the parameters of the Arrhenius equation using cumulative variables obtained from the experimental data, i.e. conversion and residence time. For this reason, the uncertainty is reduced compared to conventional methods. The new method could be used as a consistency test

between different kinetic models by comparing their kinetic parameters with those obtained with the proposed free-model method.

The procedure has been applied to our previous experimental work and other authors' information on CO₂ and steam gasification, verifying that the random pore model is not the best kinetic model to represent gasification and partial oxidation of coal and biomass. The new procedure can be used as a tool for chemical reaction engineering analysis in a broad range of thermochemical reactions under isothermal consideration.

5.3 Introduction

Gasification is one of the most promising thermochemical conversion technologies to use alternative fuels as feedstock, especially low-rank coals and biomass. Reviews have presented the most significant gasification variables [1-3]; however, the kinetics and analysis of its reaction mechanism are complex, since the reaction occurs at high temperatures and the solid characterization usually is performed at very low temperatures.

Kinetic information of partial oxidation and combustion has been reported, since the most common industrial gasifiers inject air to partially combust the fuel, providing the energy that the overall endothermic process requires. Moreover, experiments and modeling for partial oxidation [4, 5] have been extended for gasification modeling. Studies on gasification have been performed in carbon dioxide (CO₂) [6-11], steam atmospheres [12-14], or mixtures of both gasifying agents [15-19], since the Boudouard reaction, steam reforming and water-gas shifting are the main reactions. Analysis of the reported data in this field is complex, since there is not a criterion

consensus [2]; and, the modeling of a maximum reaction rate has been the focus of the research on gasification kinetics in recent years [7-12, 20-23].

Bhatia and Perlmutter (1980) proposed the random pore model (RPM) [20] with a further modification for gas-solid reactions [21]. This model has been widely accepted due to its nonlinear dependence on char surface, which can predict a maximum reaction rate as observed experimentally. Different modifications to the original model and their applications to fit experimental data have been reported; for example, some of the most recent works present extended and adaptive RPM [22, 23]. Modeling improvement is commonly attached to an increase in the number of the fitting parameters, which does not necessarily mean a direct relationship with the reaction mechanism.

Recently, Gomez et al. [24] demonstrated that the suggested maximum rate is a consequence of a change in the reaction medium, which is generated by an imposition of the experimental procedure, and proposed an alternative experimental method to avoid this effect. In independent studies [7, 19, 25-28], the time to observe a maximum rate was constant and independent of the char sample or gasifying agent, as proven by Gomez et al., despite many authors modeled this maximum [7, 19, 26]. For this reason, simpler expressions can be used to model gasification or other thermochemical reactions where the reaction is chemically controlled and thus one single overall step can be assumed. Therefore, it is important to validate the assumed kinetic model and its respective kinetic parameters (*i.e.*, rate constant and activation energy).

A new procedure is presented to obtain the rate constant and activation energy, based on a deduction from the Arrhenius equation and a general rate law, without transformation of

variables or assumption of a particular kinetic model. The aim of this work is the determination of kinetic parameters without restricting the analysis to a particular kinetic model. From reported data for CO₂ [7, 8, 11, 22] and steam gasification [14], the activation energy was calculated with the new approach and compared with the reported values, confirming previous findings [24] related to the convenience of using simpler models rather than the RPM for gasification. This new procedure can be used to determine the parameters of the Arrhenius equation for a set of isothermal experiments and can also be used as a tool for scaling industrial processes or testing the consistency of a particular kinetic model.

5.4 Experimental methods

5.4.1 CO₂ gasification

Original experimental information from Silbermann et al. related to CO₂ coal gasification was used to determine the activation energy and compare the obtained values with those reported for five different kinetic models [11]. The same procedure was applied to three other works using a nonlinear model [7] and to the RPM [8, 22]. They reported their results as the best fit among the compared kinetic models. It is important to mention that the main experimental difference between Silbermann et al. [11] and the other references is that its experimental procedure did not induce a maximum rate as a consequence of a gas change, as proven by Gomez et al. [24].

5.4.2 Steam gasification

Results for CO₂ and steam gasification follow the same trend, with a higher reactivity of the steam at lower temperatures. Kinetic modeling for steam gasification, using a single-step chemical reaction model, is similar to that of CO₂ gasification [19]. When CO₂ and steam are

mixed in different proportions, Langmuir-Hinshelwood (LH) models describe the competition for active sites considering the gas diffusion [18], but the chemical reaction contribution are assumed with a single-step kinetic model. Information presented by Fermoso et al. [14] was analyzed in the application of the proposed method to determine the activation energy and compare it with the reported values obtained using the RPM.

5.5 Kinetics analysis

5.5.1 Data analysis

Conversion and its associated reaction time were obtained from five independent studies; *i.e.* Li et al. [7], Mandapati et al. [8] and Silberman et al. [11], Fermoso et al. [14], Kopyscinski et al. [22]. Conversion is calculated from the weight at a particular time, which is the original information obtained by thermogravimetric analysis (TGA) or back calculating the information of the gas composition analysis. By definition, conversion is:

$$X = \frac{m_o - m_t}{m_o - m_a} \quad \text{Eq. (5-1)}$$

where m_o is the initial mass of the sample, m_t is the mass at a particular time, and m_a is the mass of the ash.

The conversion rate was not determined in this work, since the proposed method does not require it. This approach is especially useful, as many works have reported a maximum, which can affect the accuracy of the kinetic parameters. Considering the solid molar balance in a batch reactor, the conversion rate, r , is expressed as:

$$r = \frac{dX}{dt} \quad \text{Eq. (5-2)}$$

Regression parameters in all references were calculated with least square minimization and compared using the coefficient of determination (R^2). A complete description of the most common kinetic models can be found elsewhere [11]. In this work, linearized or linear regression of logarithm expressions were used to obtain these parameters. The activation energy was estimated through the correlation of data at different reaction temperatures in an alternative form of the Arrhenius equation.

5.5.2 Calculation of the activation energy from experimental data

A general rate law for gas-solid reactions can be represented as the product of two independent functions of the independent variables' temperature and conversion under isobaric considerations. Without considering the effect of the catalyst and mass transfer limitations, the conversion rate is given by:

$$r = \frac{dX}{dt} = k(T) f(X) \quad \text{Eq. (5-3)}$$

where k is the rate constant and $f(X)$ is a function of the solid surface and usually associated with the solid conversion.

The effect of temperature on the reaction rate is well described by the Arrhenius equation, which is given by:

$$k = k_0 e^{-\frac{E_A}{RT}} \quad \text{Eq. (5-4)}$$

where E_A is the activation energy (kJ/mol), k_o is the frequency factor (min^{-1}), R is the ideal gas law constant (kJ/mol K), and T is the absolute temperature (K).

Solving the first-order differential of Eq. (5-3), the product of time for the rate constant is a constant for a particular conversion:

$$\int_0^X \frac{dX}{f(X)} = G(X) = k_X(T) t_X(T) \quad \text{Eq. (5-5)}$$

where k_X and t_X are the rate constant (min^{-1}) and residence time (min) for a fixed conversion (X), and both are functions of the temperature.

From the general rate law and the Arrhenius equation, *i.e.* Eqs. (5-5) and (5-3), respectively, it is possible to state the following correlation of variables:

$$k_X(T) \sim \frac{1}{t_X(T)} \sim e^{-\frac{E_A}{RT}} \quad \text{Eq. (5-6)}$$

or in a logarithmic form:

$$\ln[t_X(T)] \sim -\ln[k_X(T)] \sim \frac{E_A}{RT} \quad \text{Eq. (5-7)}$$

The formal solution of Eq. (5-5) leads to:

$$\ln[t_X(T)] = \{\ln[G(X)] - \ln[k_o]\} + \frac{E_A}{RT} = \alpha + \frac{E_A}{RT} \quad \text{Eq. (5-8)}$$

where $\alpha = \ln[G(X)] - \ln[k_o]$ and is a constant for a particular conversion.

From Eq. (5-8), it is evident that the ratio of the activation energy and the ideal gas law constant (E_A/R) is the slope of the logarithm of time versus the reciprocal of temperature. By

definition, k is independent of the conversion in Eq. (5-3); thus, the plot $\ln(t)$ versus $1/T$ for different conversions should exhibit a linear trend and the same slope if the reaction mechanism follows the same path in the whole temperature range.

One of the limitations of kinetic analysis is the selection of the conversion to obtain the rate constant and other parameters involved in a particular model. Many authors use conversions lower than 100%, since uncertainty increases as the sample weight approaches zero. For this reason, the proposed method has just one way to obtain the activation energy, with a particular conversion representing the whole conversion range for practical purposes.

An alternative procedure to determine the activation energy without a kinetic model is using the initial reaction rate, which should be exactly the same rate constant for almost all kinetic models. To understand this, consider the simple power law kinetic model or integrated core model (ICM) as a particular case of Eq. (5-3):

$$r = \frac{dX}{dt} = k(1 - X)^n \rightarrow k = \left. \frac{dX}{dt} \right|_{X \rightarrow 0} \quad \text{Eq. (5-9)}$$

The main limitation of Eq. (5-9) is related to the accuracy of the initial reaction rate determination, when an inert gas is switched to a gasifying agent. Another limitation is that the calculation of the initial rate requires continuous reading of the weight variation (or small intervals of time), which can be difficult to achieve with techniques other than TGA (*i.e.* gas chromatography analysis). The most important application of Eq. (5-9) is for the consistency evaluation of a particular kinetic model, since the initial reaction rate should be close to the rate constant.

The uncertainty of the activation energy calculated as proposed in this study is smaller than the one reported by the independent studies considered as study cases, as there is uncertainty propagation of k with a kinetic model since this value is obtained from a regression for each isothermal experiment. Using the new approach, just one regression is necessary, instead of $m+1$ with the Arrhenius equation, *i.e.* one regression to obtain k (for m different temperatures) plus the Arrhenius equation. The maximum uncertainty for the activation energy estimated with the proposed method, considering three temperatures and two repetitions, is ± 13.5 kJ/mol with a coefficient of determination higher than 0.99. It is important to mention that residence time is a cumulative function and increases monotonically with conversion, thereby improving accuracy by increasing conversion.

5.5.3 Frequency factor approximation

As mentioned in the analysis of Eq. (5-9), the rate constant should be equal to the initial reaction rate when the conversion is close to zero. In fact, the rate constant is the most difficult parameter to be determined, since the experimental procedure affects the initial rate and the partial pressure of the gasifying agent is often not constant during the first instant of the reaction [24].

A similar expression to Eq. (5-8) was presented by De Micco et al. [29], but there was no reference about the frequency factor estimation independent of the kinetic model. From Eq. (5-8), the intercept at constant conversion (α) is a term including conversion and the rate constant at infinite temperature. It is expressed in the following equation:

$$\ln[k_o] = \ln[G(X)] - \alpha \quad \text{Eq. (5-10)}$$

where $G(X) = \int_0^X \frac{dX}{f(X)}$ is a function for a particular conversion, k_o (min^{-1}) is the rate constant at infinite temperature or frequency factor, and α (min^{-1}) is the intercept of Eq. (5-8). Function $G(X)$ is unknown; however, it is possible to infer the magnitude order between α and $G(X)$. For example, for an n -order reaction model (ICM), this function is given by:

$$G(X)_{n \text{ order}} = \begin{cases} \ln\left(\frac{1}{1-X}\right) & \text{if } n = 1 \\ \frac{(1-X)^{1-n} - 1}{n-1} & \text{if } n \neq 1 \end{cases} \quad \text{Eq. (5-11)}$$

Table 5.1 shows the values of $G(X)$ and its logarithm at different conversion based on Eq. (5-11). The respective values at 80% and 50% conversion are highlighted; illustrating that logarithm of $G(X)$ is negative below 50% conversion and positive above 80% conversion regardless of the reaction order. The frequency factor for steam and CO_2 gasification is in the range of $1 \times 10^4 \text{ min}^{-1}$ to $1 \times 10^{10} \text{ min}^{-1}$ between 700°C and 900°C [2, 3, 11, 14], where the reaction is chemically controlled. The logarithm of k_o (min^{-1}) in the mentioned range is between 9.2 and 23. For a conversion range between 0.5 and 0.8, the absolute value of the function $G(X)$ is much smaller than α ; therefore, the following expression can be considered for CO_2 and steam gasification:

$$\ln[k_o] = \ln[G(X)] - \alpha \approx -\alpha \quad 0.5 \leq X \leq 0.8, T \gg 700^\circ\text{C} \quad \text{Eq. (5-11)}$$

A simple way to determine k_o is the use of the average of α for 2 different conversions, if the absolute difference between both intercepts is lower than 1 min^{-1} . Although this is not the exact value, it does give a very good idea about the magnitude order of the frequency factor; and considering 50% and 80% conversion provides the upper and lower limits of the frequency

factor. For other reactions, the same analysis applies with special attention to the selected temperature range.

Table 5.1 Analytic values of G(X) according to Eq. (5-11) and their respective logarithms for three reaction orders: 0.5, 1 and 2.

X	G(X) at the indicated reaction order			ln[G(X)]		
	0.5	1	2	0.5	1	2
0.00	0.00	0.00	0.00	-6.91	-6.91	-6.91
0.01	0.01	0.01	0.01	-4.60	-4.60	-4.60
0.05	0.05	0.05	0.05	-2.98	-2.97	-2.94
0.10	0.10	0.11	0.11	-2.28	-2.25	-2.20
0.20	0.21	0.22	0.25	-1.56	-1.50	-1.39
0.30	0.33	0.36	0.43	-1.12	-1.03	-0.85
0.40	0.45	0.51	0.67	-0.80	-0.67	-0.41
0.50	0.59	0.69	1.00	-0.53	-0.37	0.00
0.60	0.74	0.92	1.50	-0.31	-0.09	0.41
0.70	0.90	1.20	2.33	-0.10	0.19	0.85
0.80	1.11	1.61	4.00	0.10	0.48	1.39
0.90	1.37	2.30	9.00	0.31	0.83	2.20
0.95	1.55	3.00	19.00	0.44	1.10	2.94
0.99	1.80	4.61	99.00	0.59	1.53	4.60
1.00	1.94	6.91	999.00	0.66	1.93	6.91

5.6 Results and discussion

5.6.1 CO₂ gasification kinetics from Alberta coals

The original data reported by Silbermann et al. [11] were time and weight loss; and, the activation energy and other kinetic parameters (depending on the kinetic model) were obtained at an 80% conversion. Conversions and the associated times for nine different coal samples (seven deep coals and two surface mined coals) are presented in Table 5.2.

From Eq. (5-8), the logarithm of time versus the reciprocal of temperature was plotted in Fig. 5.1 for two of the nine coals presented by Silbermann et al. [11]. It is worth noting that all nine coals exhibited the same trends; however, for practical reasons, just the coals with the fastest (Genesee) and the slowest (coal 7) reactivity are shown in Fig. 5.1. The slopes of the logarithm of time versus the reciprocal of temperature plots followed a linear trend and varied slightly with conversion.

Complete information of the activation energy for all nine coals is shown in Table 5.3. The activation energies obtained by regression of the Arrhenius equation for the first four models (ICM, VM, SCM and NDM) were close to the activation energy calculated from Eq. (5-8) (absolute deviation was smaller than 20 kJ/mol). Using the proposed method as the reference value, the deviation of the RPM was the highest among all five models. For example for coal 5, the activation energy estimated with the RPM (140 kJ/mol) is lower than the other models and the free-model approach (higher than 200kJ/mol); it is evident that the RPM did not represent the reaction mechanism of coal 5.

The ICM yielded the most accurate results among all models, and a similar result was reported [11] through the analysis of the coefficient of determination. The reasons were the lack of a maximum reaction rate and a logarithmic correlation that better fit the experimental data. It was shown that the RPM underestimated the activation energy; therefore, there is no reason to consider such a complex model in direct gasification, *i.e.* no gases switching.

Table 5.2 Time (min) to reach three different conversions ($X_1 = 0.8$; $X_2 = 0.5$; $X_3 = 0.25$) for nine different coals. CO₂ gasification at 800°C, 850°C and 900°C. Reported by Silbermann et al. [11]

T[°C]	Residence time (min) at different temperature (°C)								
	X=0.8			X=0.5			X=0.25		
	800	850	900	800	850	900	800	850	900
Genesee 1	29.8	13.2	5	11.4	5.2	2.1	4.2	1.9	0.85
Genesee 2	49.6	19.8	7.4	17.2	6.8	2.8	6	2.4	1.15
Coal 5	195.8	66.2	20.8	96.2	34.6	11.6	35.6	14	5.1
Coal 2	117.2	45.6	21.8	28.6	10.8	5.5	7.2	3	1.8
Coal 3	284.2	86.2	24.8	126.6	34.9	12.4	45.6	15.3	5.2
Coal 4	362.6	102.6	49	181.6	52.2	19.4	60.4	18.4	7.1
Coal 6	530.4	162.6	57.6	92.6	26.6	11.4	24.6	7.5	3.5
Coal 1	278.6	148.2	62.6	74	39.8	16.4	19.4	10	4.3
Coal 7	799.2	220	80.1	352	88.6	32.6	117.6	32.4	13.6

A comparison of the reference activation energies from 50% and 80% conversions, as obtained from Eq. (5-8), indicated that they were similar, given that the average relative uncertainty was $\pm 7.3\%$. The maximum difference between coals is expressed as:

$$\text{Maximum} \left[\frac{|E_{A,X=0.8} - E_{A,X=0.5}|}{E_{A,X=0.8}} \right] = 5.2\%, \text{ for coal 5}$$

The same comparison between 25% and 80% conversions yielded a higher difference 17% for coal 2, which had the highest ash content of all coal samples. Moreover, the activation energy was smaller at the lower conversion for all cases: $E_{A,X=0.8} \geq E_{A,X=0.25}$ (columns 2-4 and 8-10 of Table 5.2, respectively). This may be attributed to part of the alkali being inactivated or lost during the gasification, or intraparticle diffusion when char to ash ratio is decreasing. This analysis is important since one of the conditions for intrinsic kinetic modeling is the assumption that the catalyst remains active.

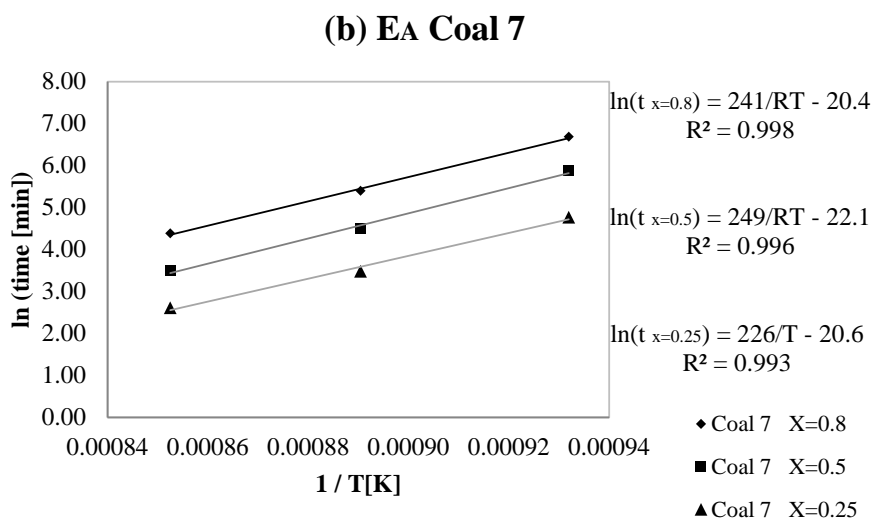
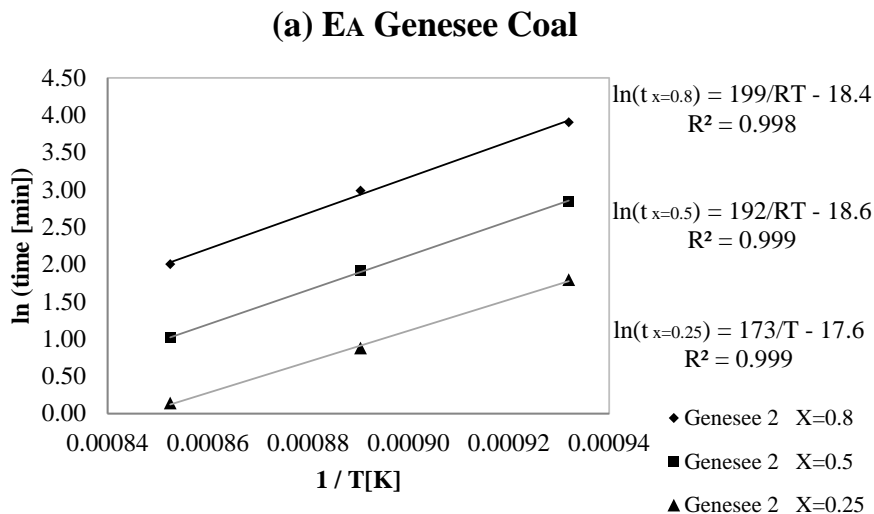


Figure 5.1 Logarithm of time vs. reciprocal of temperature. CO₂ gasification between 800°C and 900°C: (a) Genesee coal and (b) Deep coal 7. Data from Silbermann et al. [11]

Another possible reason to be considered when reactivity decreases during long time exposition at high temperature is thermal annealing [30]; however, the coals exposed to a longer gasification time (coals 7, 6 and 4) show similar activation energy between 50% and 80% conversion (within the uncertainty). If the reaction follows the same mechanism in the whole

conversion range, the activation energy calculated at different conversions should be almost the same. This analysis can be useful to understanding the mechanism path of any gas-solid reaction.

Table 5.3 Activation energy [kJ/mole] based on Eq. (5-8) and the Arrhenius equation using five different kinetic models as reported by Silbermann et al. [11]. Temperature range from 1073 K to 1173 K.

	E_A (kJ/mol) from Eq. (5-8)			E_A (kJ/mol) for each kinetic model at $X=0.8$				
	X=0.8	X=0.5	X=0.25	VM	SCM	IM	NDM	RPM
Genesee 1	186	177	167	180	183	172	175	184
Genesee 2	199	192	173	191	187	193	195	187
Coal 1	156	157	157	124	119	139	137	117
Coal 2	176	173	146	139	128	164	169	126
Coal 3	255	243	227	209	209	208	216	211
Coal 4	210	220	205	162	153	209	205	151
Coal 5	234	221	203	203	205	193	200	140
Coal 6	232	234	224	186	186	209	211	187
Coal 7	241	249	226	205	209	230	233	212

The Arrhenius frequency factor calculated using Eq. (5-12) is presented in the 5th column of Table 5.4 and it was taken as the reference for comparison with the frequency factors obtained from the original data for the five different models. The ICM had the closest value to the reference; and, the RPM underestimated the frequency factor and, in some cases such as the coal 5, had a very different value when comparing their relative magnitude orders. This indicates that the calculation of k_o using Eq. (5-12) is in good agreement with the experimental results and gives a clear indication about the magnitude order of the frequency factor.

Table 5.4 Intercept of Eq. (5-8) and frequency factor (min^{-1}) based on Eq. (5-12) (fourth column) and the Arrhenius equation using five different kinetic models as reported by Silbermann et al. [11]. Temperature range from 1073 K to 1173 K.

	α (min^{-1}) Eq. (5-8)			k_0 Eq. (5-12)	k_0 (min^{-1}) at 80% for each kinetic model				
	X=0.8	X=0.5	X=0.25		VM	SCM	ICM	NDM	RPM
Genesee 1	-17.5	-17.3	-17.3	3.6E+07	3.6E+07	3.7E+07	1.6E+07	1.9E+07	3.5E+07
Genesee 2	-18.4	-18.6	-17.6	1.1E+08	7.7E+07	4.3E+07	1.1E+08	1.2E+08	3.5E+07
Coal 5	-21.0	-20.2	-19.2	8.7E+08	7.0E+07	7.5E+07	1.8E+07	3.7E+07	7.1E+04
Coal 2	-15.0	-16.1	-14.4	5.6E+06	1.7E+05	4.0E+04	3.4E+06	4.6E+06	2.7E+04
Coal 3	-22.9	-22.5	-21.6	7.1E+09	1.1E+08	1.0E+08	8.5E+07	1.8E+08	1.0E+08
Coal 4	-17.7	-21.1	-21.1	2.7E+08	9.6E+05	3.1E+05	1.9E+08	9.6E+07	1.9E+05
Coal 6	-19.8	-20.1	-19.8	4.7E+08	6.8E+06	5.9E+06	9.1E+07	8.9E+07	5.7E+06
Coal 1	-11.8	-13.3	-14.6	2.7E+05	1.3E+04	6.6E+03	7.7E+04	5.4E+04	4.3E+03
Coal 7	-20.4	-22.1	-20.6	1.7E+09	3.2E+07	4.0E+07	4.3E+08	5.2E+08	4.8E+07

5.6.2 CO_2 gasification kinetics from coals with slag granules

The conversion and time at different temperatures for CO_2 gasification of four different coal/slag ratios (1:0, 1:1, 1:2, 1:3), as reported by Li et al. [7], were correlated using Eq. (5-8). Fig. 2 shows the plots of the logarithm of time versus the reciprocal of temperature for two different sets of conversion data points. The experimental procedure performed in the original study switched gases after reaching the reaction temperature. The temperature range from 1223 K to 1423 K was the same for all four different coal/slag samples.

Table 5.5 shows the reference activation energies and frequency factors obtained using Eqs. (5-8) and (5-12), respectively, for 80% and 50% conversions. The same parameters were reported using a nonlinear kinetic model, i.e. the Avrami-Erofeev ($m=2$) model [7], as presented in columns 4 and 7 of Table 5.5, respectively. The reported activation energies were very close to the reference values obtained at 80% conversion for the four different coal/slag ratios, which

is consistent with the way that the rate constant is usually calculated for a representative conversion interval (considering data points until conversion equal or higher than 80%).

Table 5.5 Activation energy and frequency factor calculated from Eqs. (5-8) and (5-12). Kinetic parameters reported data by Li et al. [7] using the Avrami-Erofeev (m=2) kinetic model. Temperature range from 1223 K to 1423 K.

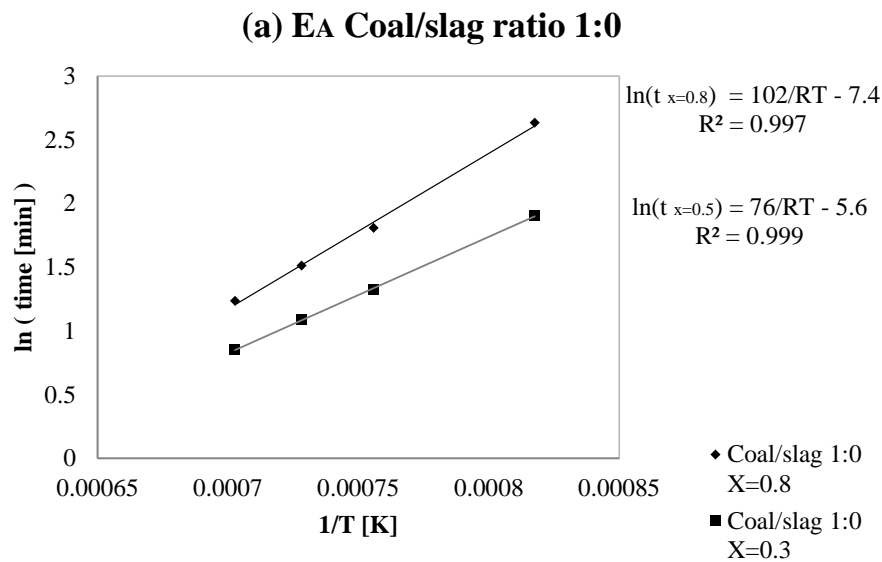
	E_A (kJ/mol)			k_0 (min ⁻¹)		
	Eq. (5-8)		<i>A-E model</i>	Eq. (5-12)		<i>A-E model</i>
	X=0.8	X=0.5		X=0.8	X=0.5	
Coal/slag ratio 1:0	102	76	112	1612	265	4806
Coal/slag ratio 1:1	91	71	94	1033	244	1625
Coal/slag ratio 1:2	84	77	87	662	501	965
Coal/slag ratio 1:3	56	53	53	61	58	52

The linear trend presented in Fig. 5.2 indicates that the reaction mechanism did not change in the studied temperature range. In all cases, the activation energies at 50% conversion were lower than those at 80% conversion. When the coal/slag ratio was 1:3, both values were almost the same, probably due to the slag acting as a catalyst, which can be associated with the alkali content. Results from this particular case led to the same conclusions as those obtained from the Silbermann et al. [11] data in the previous section, i.e. the loss of catalyst as the gasification progresses. In this particular case, thermal annealing [30] might not very well explain why the activation energy estimated at different conversions remains practically constant with excess amount of catalyst.

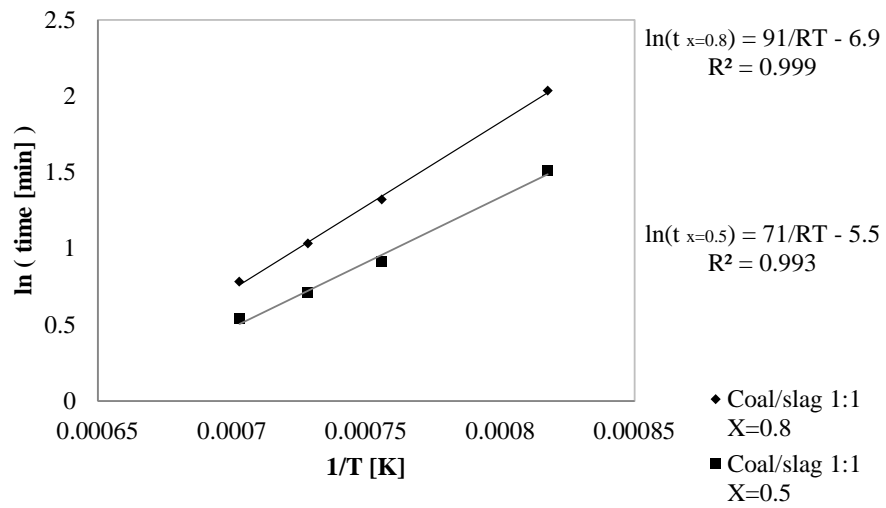
There was definitely no coherent trend with the frequency factor, which can be attributed to the existence of a maximum rate in the reported data detected at 1.5 min after the gases are

switched [7]. For the highest temperature (1423 K), the total residence time to achieve an 80% conversion was 3.4 min for the less reactive sample (coal/slag ratio of 1:0), indicating that the time to replace the gases significantly affected the reading of the conversion rate in a considerable portion of the conversion range. The selected kinetic model overestimated the frequency factor, but was in reasonable agreement for the activation energy.

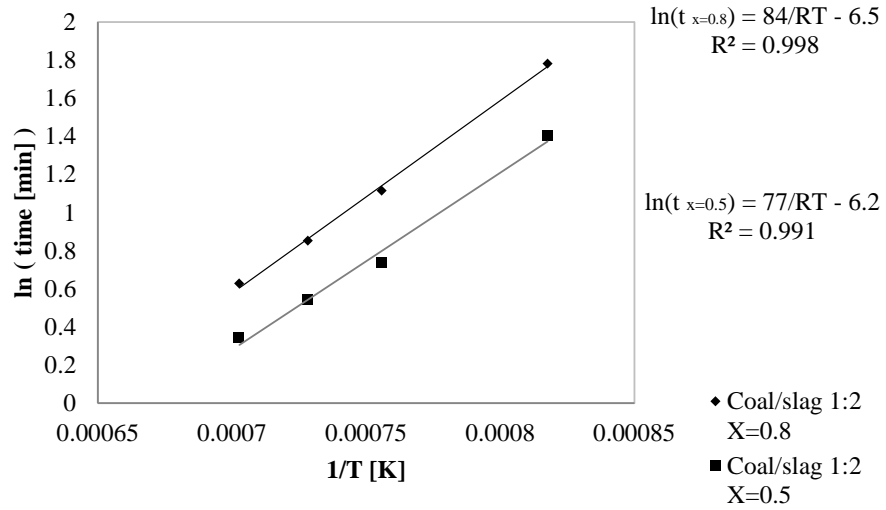
Using the proposed approach, it is possible to conclude that the initial part of the gasification affects the results. This effect is more pronounced as the conversion rate increases; therefore, at higher reaction temperatures or greater catalyst contents, the parameters calculated from a kinetic model could be significantly different with respect to the free-model calculations.



(b) EA Coal/slag ratio 1:1



(c) EA Coal/slag ratio 1:2



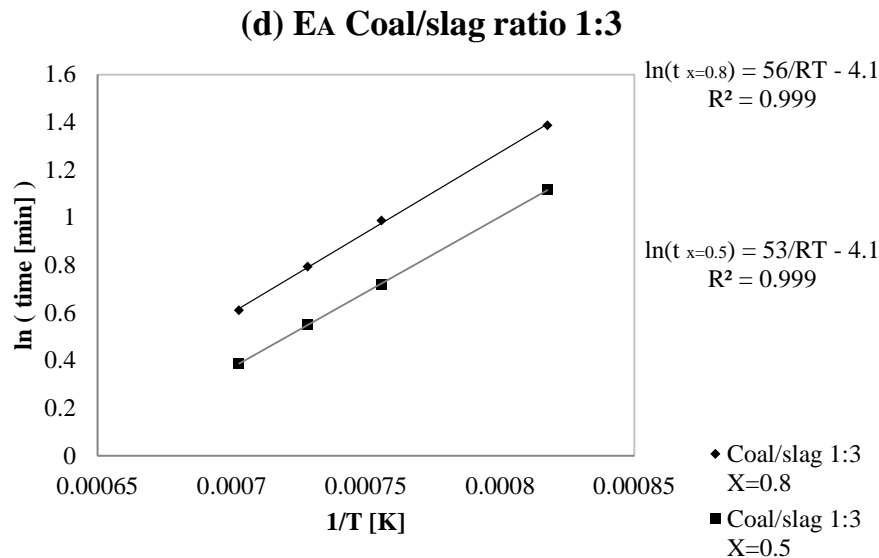


Figure 5.2 Logarithm of time vs. reciprocal of temperature. CO₂ gasification between 950°C and 1150°C” (a) Coal/slag ratio of 1:0, (b) Coal/slag ratio of 1:1, (c) Coal/slag ratio of 1:2, (d) Coal/slag ratio of 1:3. Data from Li et al. [7]

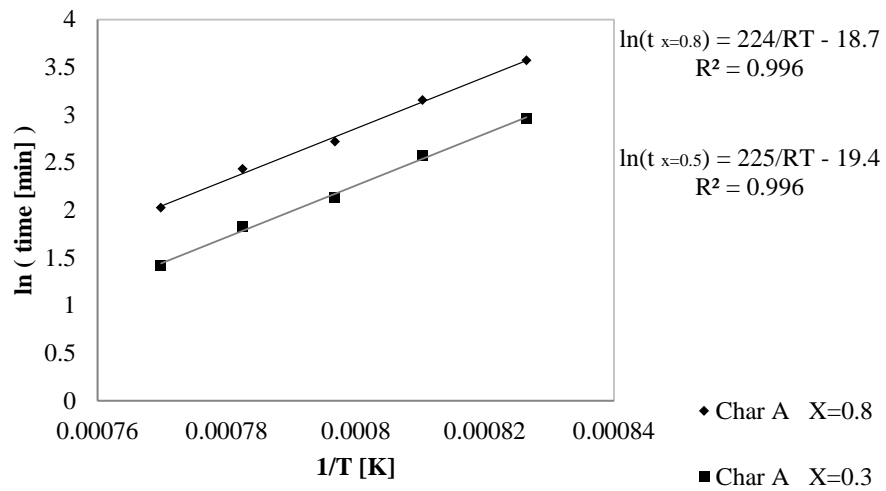
5.6.3 CO₂ gasification kinetics from char produced from Indian coal samples

Data reported by Mandapati et al. [8] for CO₂ gasification of chars produced from four Indian coals (chars A, B, C, and D) were correlated using Eq. (5-8). Fig. 5.3 shows the plots of the logarithm of time versus the reciprocal of temperature for two different sets of conversion data points. Similar to the previous case, the experimental procedure involved a change of the reaction gas at the reaction temperature. The temperature range of the reported experiment was different between samples; however, it was significantly higher than the range where the reaction is thermodynamically limited. A linear trend for all four chars could be observed with a coefficient of determination higher than 0.99.

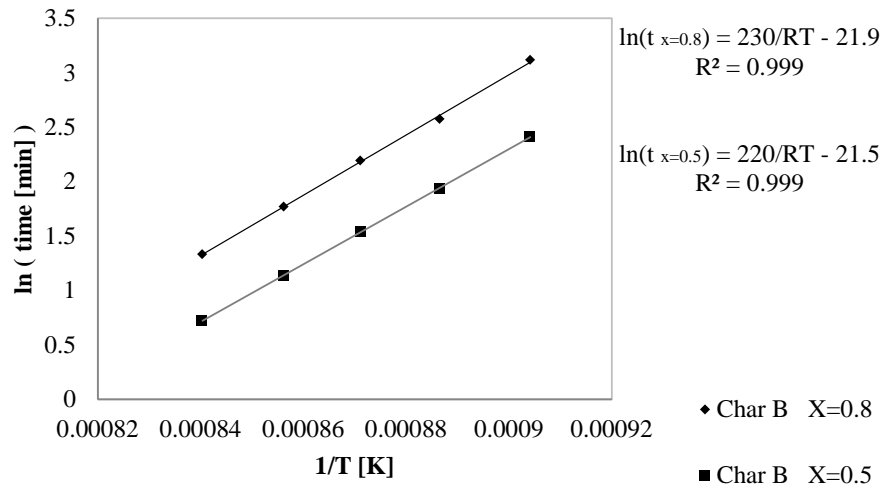
Kinetic parameters are presented in Table 5.6, comparing the reference results obtained from Eqs. (5-8) and (5-12) for 80% and 50% conversions with the same reported parameters using the RPM model (columns 5 and 8, respectively). The reported activation energy values were in good agreement with the reference values proposed in this study. There was no significant difference between the reference activation energies calculated at 80% and 50% conversions, indicating that there was no loss of catalyst in these experiments and negligible mass transfer effects, which is consistent with the experimental procedure to reduce bed diffusion [8].

The time to observe a maximum rate after switching the gasifying agent was not reported; however, this time did not significantly affect the kinetics, since the time to achieve an 80% conversion for the less reactive char was almost three times higher than the previous study case (11.1 min for char D at 1351 K). The previous statement was verified, when parameter ψ (which should be higher than 2 if there really was a maximum rate [11]) of the RPM was checked in the original work: $\psi_A = 3.74$, $\psi_B = 3.19$, $\psi_C = 0.91$ and $\psi_D = 0.15$. This suggests that the model was considered nonlinear, but that the contribution of the nonlinear term was insignificant and just improved the determination coefficient of the regression.

(a) EA Char A



(b) EA Char B



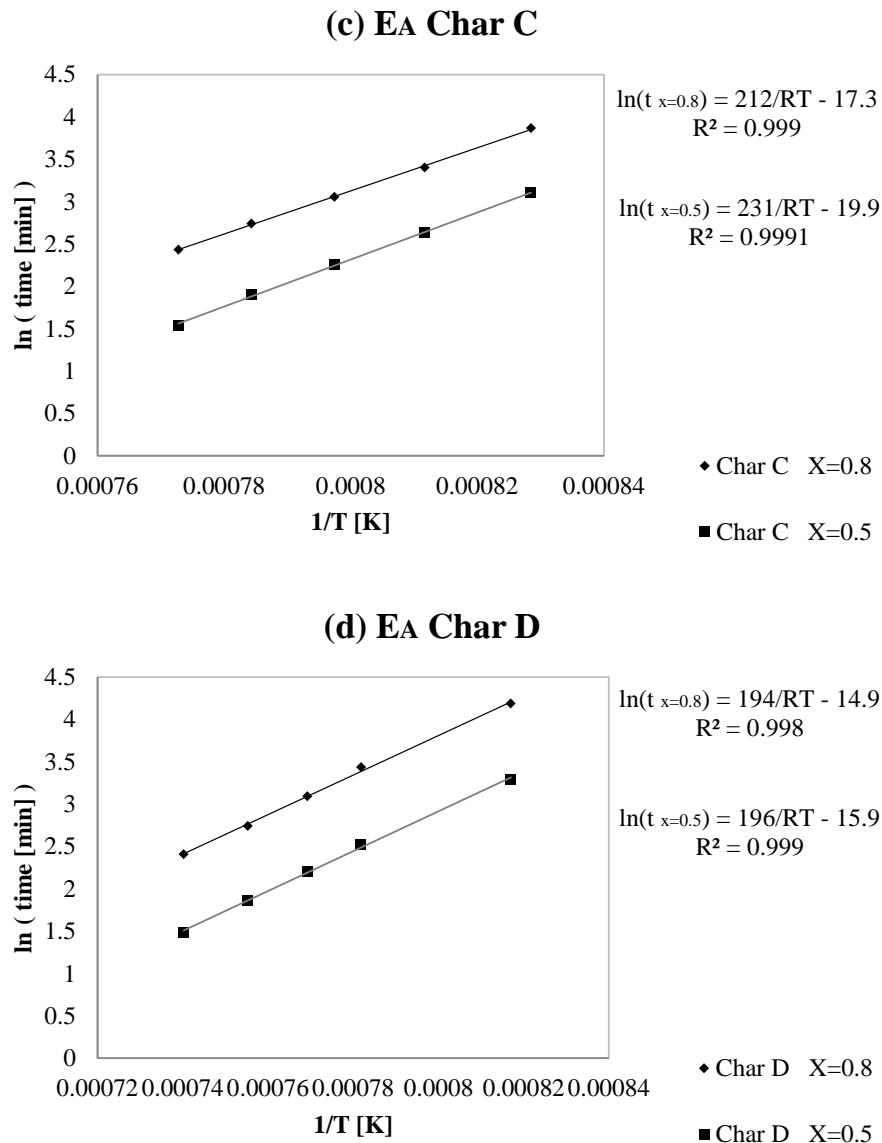


Figure 5.3 Logarithm of time vs. reciprocal of temperature. Char CO₂ gasification: (a) Char A [937°C to 1026°C], (b) Char B [833°C to 917°C]; (c) Char C [934°C to 1021°C], (d) Char D [951°C to 1078°C]. Data from Mandapati et al. [8]

The reported frequency factors were different with respect to the ones estimated from the free-model method, but with a similar magnitude order. Thus, the RPM with a ψ parameter close to 2 worked well and provided reasonable kinetic parameters, because those first minutes of the

gasification (gas replacement into the reactor) that induced a maximum reaction rate were just a small part of the total residence time. If the experimental procedure was changed to avoid this situation, simpler models would give better correlations [11, 24].

Table 5.6 Activation energy and frequency factor calculated from Eqs. (5-8) and (5-12). Kinetic parameters reported data by Mandapati et al. [8] using the RPM.

	Temperature range (K)	E_A (kJ/mol)			k_o (min ⁻¹)		
		Eq. (5-8)		RPM	Eq. (5-12)		RPM
		X=0.8	X=0.5		X=0.8	X=0.5	
Char A	1210-1299	224	225	229	1.4E+08	2.7E+08	4.2E+09
Char B	1106-1190	230	220	213	3.4E+09	2.2E+09	1.1E+08
Char C	1207-1294	212	231	215	3.1E+07	4.4E+08	1.3E+08
Char D	1224-1351	194	196	193	2.9E+06	8.3E+06	1.8E+07

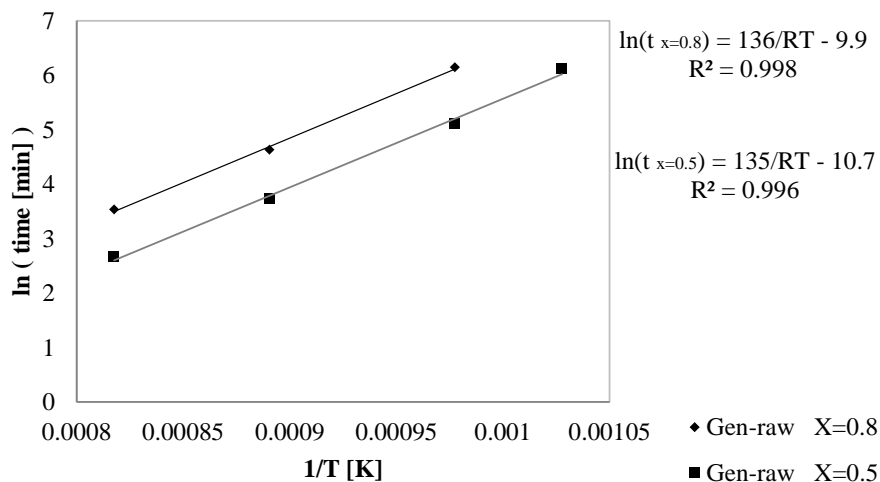
5.6.4 CO₂ gasification kinetics from coal plus catalyst (K₂CO₃)

A recent study presenting the gasification of raw coal, ash-free coal, and ash-free coal plus catalyst (catalytic CO₂ gasification) was presented by Kopyscinski et al. [22]. The authors also presented a variation of the RPM called the extended random pore model (eRPM). Fig. 5.4 shows the plots of the logarithm of time versus the reciprocal of temperature for different sets of conversion data points.

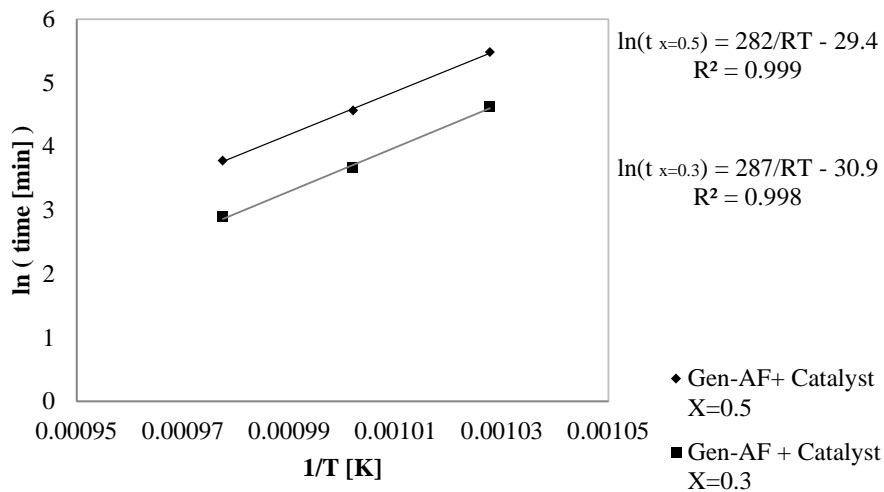
Linear trends could be observed, but the reported activation energies were quite different to the references obtained from Eq. (5-8). For the ash-free coal, an increase in temperature increased the activation energy, as presented in Fig. 4C; and, the reported data underestimated the real activation energy that could not be considered constant in the temperature range. With no

alkali in the coal composition, the reactivity significantly decreased, and temperature must be increased for a practical constant reading of activation energy.

(a) EA Gen-raw



(b) EA Gen-AF + 20% K₂CO₃



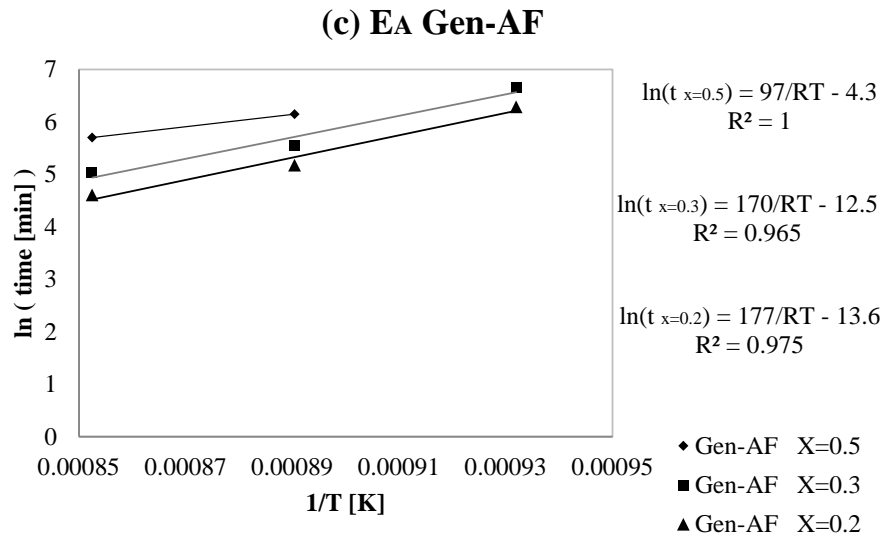


Figure 5.4 Logarithm of time vs. reciprocal of temperature. Coal CO₂ gasification: (a) Gen-raw [700°C to 950°C], (b) Gen-ash-free plus 20% K₂CO₃ [650°C to 750°C]; (c) Gen-ash-free [800°C to 900°C]. Data from Kopyscinski et al. [22]

Complete information on the kinetic parameters obtained by the proposed method and the reported parameters from the RPM (ash-free coal) and eRPM (raw coal and ash-free plus catalyst) are presented in Table 5.7, including the temperature ranges and the reference temperature to calculate the rate constant. The activation energies for the proposed method and those reported for the three samples were similar. Even the activation energy values between the RPM and the eRPM were almost identical for the same coal type [22]. The reason is similar to the study case of Mandapati et al. [8] and related to the parameters of the RPM. Kopyscinski et al. [22] reported the values of the parameter ψ for the RPM as $\psi_{\text{Gen}} = 0$, $\psi_{\text{Gen-ash-free}} = 0.45$ and $\psi_{\text{Gen-ash-free+catalyst}} = 0.0$ and those of the eRPM as $\psi_{\text{Gen}} = 4.3$ and $\psi_{\text{Gen-ash-free+catalyst}} = 64$.

If parameter ψ was close to 2, the nonlinear part did not significantly affect the reaction rate. A large change of this parameter from the RPM to its modified version (eRPM) was mainly a consequence of an increase in the regression parameters. If the experimental procedure is performed without changing the gases, there will not be a maximum rate; and, the modeling can be reduced to a first-order reaction model.

Table 5.7 Activation energy and frequency factor calculated from Eqs. (8) and (12). Kinetic parameters reported data by Kopyscinski et al. [22] using the RPM and eRPM.

	Temperature range (K)	E_A (kJ/mol)			k_{Tref} (min^{-1})			Ref. temperature (K)
		Eq. (5-8)		RPM	Eq. (5-4)		eRPM	
		X=0.8	X=0.5		X=0.8	X=0.5		
Gen-raw	1023-1223	136	135	131	2.2E-03	5.5E-03	7.5E-04	1023
Gen-AF 20wt% K_2CO_3	923-1023	282	287	264	4.2E-03	1.0E-02	1.1E-04	973

	Temperature range (K)	E_A (kJ/mol)			k_{Tref} (min^{-1})			Ref. temperature (K)
		Eq. (5-8)		RPM	Eq. (5-4)		RPM	
		X=0.3	X=0.2		X=0.3	X=0.2		
Gen-AF	1073-1173	170	177	124	1.4E-03	2.0E-03	6.5E-04	1073

A strange result was reported for the catalytic gasification of ash-free coal, since the activation energy was higher than the ones presented for the gasification of the ash-free and raw coals. Different explanations were given by Kopyscinski et al. [22]; however, there is an important fact that it was not considered: at the temperature range from 650°C to 750°C, Boudouard reaction is thermodynamically limited, and a comparison of activation energies at different temperature ranges is not appropriate. If the experiments for this coal type are

performed at the same temperature range as the others, *i.e.* between 800°C and 900°C, a different result would probably be observed (*i.e.* lower activation energy) and the assumption of similar reaction mechanisms would make more sense.

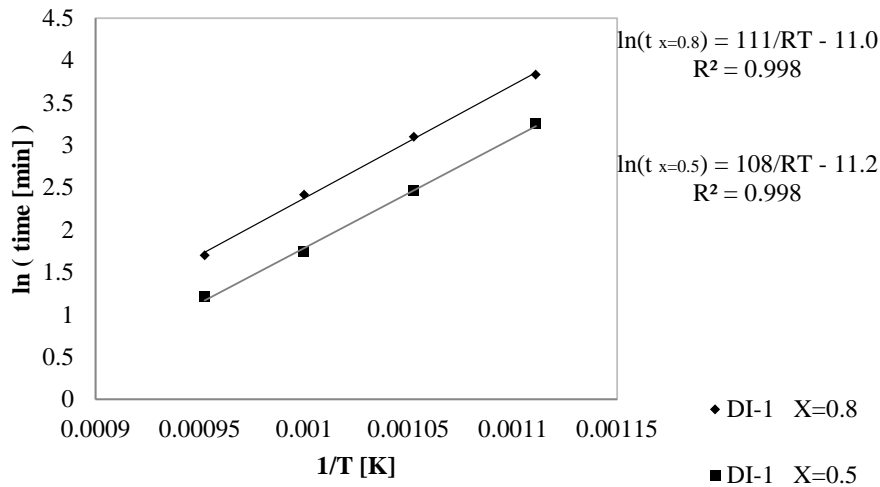
Rate constants were presented instead of frequency factors, since Kopyscinski et al. [22] reported them for different reference temperatures. The results were inconsistent for the ash-free coal plus catalyst compared with the other coal types: for example, using the eRPM at 1000 K as reference temperature, $k_{\text{Gen-raw}}$ was greater than $k_{\text{Gen-ash-free+catalyst}}$; however, the fastest coal at this temperature was the one with catalyst. This is a contradiction when Eq. (5-9) is considered (using the eRPM when the conversion is zero) and can be explained by the activation energy being obtained from a different temperature range where the reaction mechanism was different (Boudouard reactions just advance after 700°C).

5.6.5 Steam gasification kinetics from char pyrolyzed at different pressures

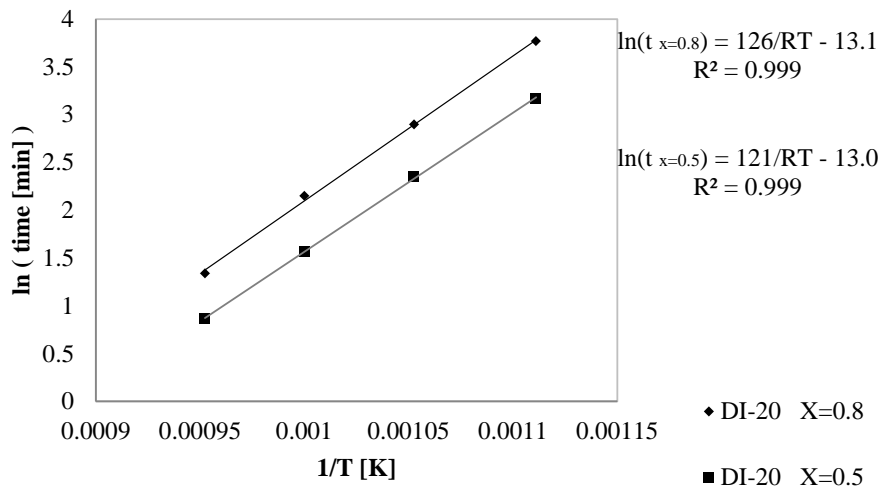
The last experimental study analyzed in this work corresponds to steam gasification using data reported by Fermoso et al. [14] for four char samples (D1-1, D1-20, HI-1, HI-20), which were prepared from two different raw coals (DI, HV) and two different operation pressures during the pyrolysis (1 atm and 20 atm) at 1000°C. Fig. 5.5 shows the plots of the logarithm of time versus the reciprocal of temperature for two different sets of conversion data points. The experimental procedure involved the change of the reaction gas at the reaction temperature. The temperature range of the reported experiment was between 1173 K and 1323 K for all the experiments.

The RPM was selected by Fermoso et al. [14] as the best kinetic model to fit the experimental data. The reported activation energies and frequency factors are presented in Table 5.8. These reference kinetic parameters were determined using Eqs. (5-8) and (5-10) for 80% and 50% conversions, respectively. Comparisons of the frequency factors and activation energies indicate that the reported data were overestimated, and the differences were significant.

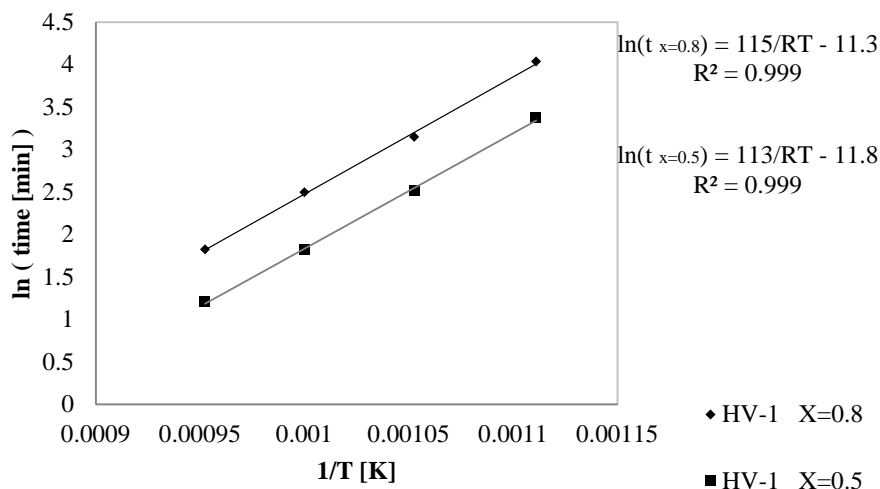
(a) EA Steam Gasification DI-1



(b) EA Steam Gasification DI-20



(c) EA Steam Gasification HV-1



(d) EA Steam Gasification HV-20

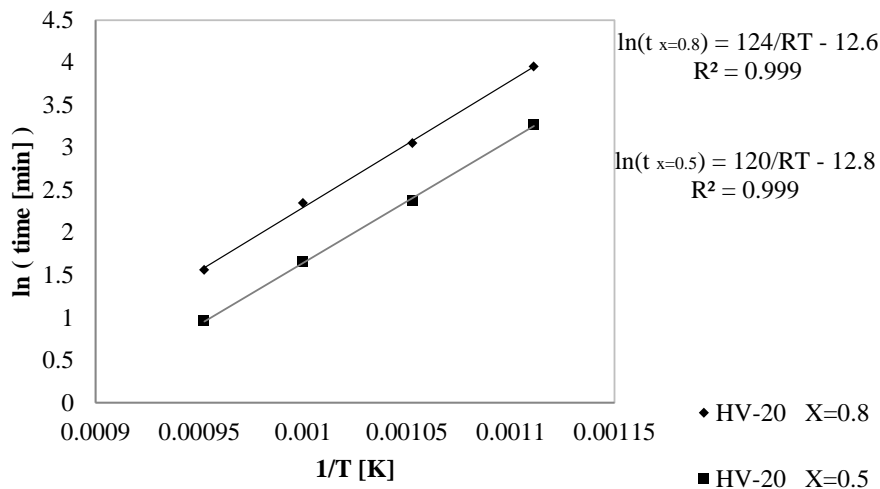


Figure 5.5 Logarithm of time vs. reciprocal of temperature. Char steam gasification [30% vol H₂O – 70% vol N₂] between 900°C and 1050°C: (a) DI-1, (b) DI-20; (c) HV-1, (d) HV-20. Data from Feroso et al. [14]

Activation energy must be considered carefully, since the reported data for steam gasification is close to 200 kJ/mol, which is an average value for CO₂ gasification at the same temperature range [2, 3, 11]. Analyzing other authors' works [2, 16] in similar temperature ranges, the

activation energies of steam gasification were significantly smaller than those of CO₂ gasification, which is in good agreement with the results of the proposed method. This can be attributed to the selection of the RPM as the best kinetic model, due to the gas switching performed during the experimental procedure.

There was no reported information about the time when the maximum rate was observed, but it is usually between one and two minutes with TGA [24]. The time to reach an 80% conversion at the highest temperature for all char samples was between 4 and 8 min. A similar reasoning to the previous study cases can be presented for the analysis of the value of parameter ψ in the original reference. This maximum significantly affected the determination of the reaction rate and it is the reason why kinetic parameters cannot be calculated with this model for the particular reaction conditions.

Table 5.8 Activation energy and frequency factor calculated from Eqs. (5-8) and (5-12). Kinetic parameters reported data by Fermoso et al. [14] using the RPM. Temperature range from 1173 K to 1323 K

	E_A (kJ/mol)			k_o (min ⁻¹)		
	Eq. (5-8)		RPM	Eq. (5-12)		RPM
	X=0.8	X=0.5		X=0.8	X=0.5	
DI-1	111	108	178	5.9E+04	7.1E+04	1.6E+06
DI-20	126	121	200	4.8E+05	4.3E+05	1.6E+07
HV-1	115	113	183	8.4E+04	1.3E+05	2.5E+06
HV-20	124	120	195	3.0E+05	3.7E+05	7.8E+06

Comparisons of the reference activation energies and rate constants at 50% and 80% conversions indicate that they were practically the same. This was a consequence of the higher reactivity of the char with steam than with CO₂: a faster reaction rate increased the accuracy of the proposed method. On the other hand, an increase in reactivity by increasing the temperature or adding catalyst decreased the accuracy of the RPM in determining the parameters of the Arrhenius equation, which is applicable if the experimental procedure induces a maximum reaction rate. If there is no maximum rate, there is no need for the RPM or other complex kinetic models.

5.7 Conclusion

A new method to obtain the parameters of the Arrhenius equation, *i.e.* activation energy and frequency factor, independent of the kinetic model has been presented and evaluated for five independent experimental studies. The plots of the logarithm of residence time, $\ln(\text{time})$, for a particular conversion versus the reciprocal of temperature, $1/T$, followed a linear trend in the same way as an Arrhenius plot with a better coefficient of determination.

The slope of $\ln(\text{time})$ versus $1/T$ yields the ratio of the activation energy to the ideal gas law constant (E_A/R). The advantage of this method is that just one regression is required, rather than the $m+1$ (m is the number of experimental temperatures) needed when a kinetic model is used. The uncertainty of the method is smaller, and it is less sensitive to any particular variation of the reaction rate, *e.g.* when a maximum rate is induced due to the switching of the gases during steam and CO₂ gasification kinetic studies.

Activation energies and frequency factors calculated with the proposed method with Eqs. (5-8) and (5-12), respectively, produced consistent results. Their accuracy increased at high temperature ranges. These values can be used to test one single overall step kinetic models, which is a tool to scale-up industrial processes or validate assumptions about the reaction mechanism. Similar activation energies in two different range intervals indicated that the reaction mechanism was the same. Comparison of the estimated activation energy at different conversions (but the same range temperature) lets to prove assumptions about the constant amount of active catalyst and mass transfer limitations during the reaction progress.

Analyses of reported literature can be adjusted and kinetic parameters can be correctly compared, as was presented for five gasification experimental works: four CO₂ gasification studies and one steam gasification investigation. In particular, the random pore model did not estimate accurately the kinetic parameters of gasification, confirming the incidence of the reaction medium change generated by the experimental procedure.

5.8 References

- [1] Hobbs ML, Radulovic PT, Smoot LD. Combustion and gasification of coals in fixed-beds. *Prog Energ Combust* 1993; 19: 505–586.
- [2] Di Blasi C. Combustion and gasification rates of lignocellulosic chars. *Prog Energ Combust* 2009; 35: 121–140.
- [3] Irfan M, Usman MR, Kusakabe K. Coal gasification in CO₂ atmosphere and its kinetics since 1948: A brief review. *Energy* 2011; 36: 12–40.
- [4] Su JL, Perlmutter DD. Effect of pore structure on char oxidation kinetics. *AIChE J* 1985; 31: 973–981.
- [5] Loewenberg DA, Levensis WA. Combustion behavior and kinetics of synthetic and coal-derived chars: Comparison of theory and experiment. *Combust Flame* 1991 84: 47–65.
- [6] Wang L, Sandquist J, Varhegyi G, Matas Güell B. CO₂ gasification of chars prepared from wood and forest residue: A kinetic study. *Energy Fuels* 27 (2013) 6098–6107.
- [7] Li P, Yu Q, Xie H, Qin Q, Wang K. CO₂ gasification rate analysis of Datong coal using slag granules as heat carrier for heat recovery from blast furnace slag by using a chemical reaction. *Energy Fuels* 2013; 27: 4810–4817.
- [8] Mandapati RM, Daggupati S, Mahajani SM, Aghalayam P, Sapru RK, Sharma RK et al. Experiments and kinetic modeling for CO₂ gasification of Indian coal chars in the context of underground coal gasification. *Ind Eng Chem Res* 2012; 51:15041–15052.
- [9] Jeong HJ, Park SS, Hwang J. Co-gasification of coal–biomass blended char with CO₂ at temperatures of 900–1100°C. *Fuel* 2014 116: 465–470.
- [10] Duman G, Uddin MA, Yanik J. The effect of char properties on gasification reactivity. *Fuel Process Technol* 2014; 118: 75–81.

- [11] Silbermann R, Gomez A, Gates I, Mahinpey N. Kinetic studies of a novel CO₂ gasification method using coal from deep unmineable seams. *Ind Eng Chem Res* 2013; 52: 14787–14797.
- [12] Lin L, Strand M. Online Investigation of steam gasification kinetics of biomass chars up to high temperatures. *Energy Fuels* 2014; 28:607–613.
- [13] Kim HS, Kudo Sh, Tahara K, Hachiyama Y, Yang H, Norinaga K et al. Detailed kinetic analysis and modeling of steam gasification of char from Ca-loaded lignite. *Energy Fuels* 2013; 27: 6617–6631.
- [14] Feroso J, Gil MV, García S, Pevida C, Pis JJ, Rubiera F. Kinetic parameters and reactivity for the steam gasification of coal chars obtained under different pyrolysis temperatures and pressures. *Energy Fuels* 2011; 25: 3574–3580.
- [15] Zhang R, Wang QH, Luo ZY, Fang MX, Cen KF. Coal char gasification in the mixture of H₂O, CO₂, H₂, and CO under pressured conditions. *Energy Fuels* 2014; 28: 832–839.
- [16] Ren L, Yang J, Gao F, Yan J. Laboratory study on gasification reactivity of coals and petcoke in CO₂/steam at high temperatures. *Energy Fuels* 2013; 27: 5054–5068.
- [17] Guizani C, Escudero Sanz FJ, Salvador S. The gasification reactivity of high-heating-rate chars in single and mixed atmospheres of H₂O and CO₂. *Fuel* 2013; 108: 812–823.
- [18] Umemoto S, Kajitani S, Hara S. Modeling of coal char gasification in coexistence of CO₂ and H₂O considering sharing of active sites. *Fuel* 2013; 103: 14–21.
- [19] Ahmed II, Gupta AK. Kinetics of woodchips char gasification with steam and carbon dioxide. *Appl Energy* 2011; 88: 1613–1619.
- [20] Bhatia SK, Perlmutter DD. A random pore model for fluid–solid reactions: I. Isothermal and kinetic control. *AIChE J* 1980; 26: 379–386.
- [21] Bhatia SK, Vartak BJ. Reaction of microporous solids: The discrete random pore model. *Carbon* 1996; 34: 1383–1391.

- [22] Kopyscinski J, Habibi R, Mims ChA, Hill JM. K_2CO_3 -catalyzed CO_2 gasification of ash-free coal: kinetic study. *Energy Fuels* 2013; 27: 4875–4883.
- [23] Singer SL, Ghoniem AF. An adaptive random pore model for multimodal pore structure evolution with application to char gasification. *Energy Fuels* 2011; 25: 1423–1437.
- [24] Gomez A, Silbermann R, Mahinpey N. A comprehensive experimental procedure for CO_2 coal gasification: Is there really a maximum reaction rate? *Appl Energy* 2014; 124: 73–81.
- [25] Woodruff RB, Weimer AW. A novel technique for measuring the kinetics of high-temperature gasification of biomass char with steam. *Fuel* 2013; 103: 749–757.
- [26] Popa T, Fan M, Argyle MD, Slimane RB, Bell DA, Towler BF. Catalytic gasification of a Powder River Basin coal. *Fuel* (2013) 103: 161–170.
- [27] Nipattummakul N, Ahmed I, Kerdsuwan S, Gupta AK. High temperature steam gasification of wastewater sludge. *Appl Energy* 2010; 87: 3729–3734.
- [28] Prabowo B, Umeki K, Yan M, Nakamura MR, Castaldi MJ, Yoshikawa K. CO_2 -steam mixture for direct and indirect gasification of rice straw in a downdraft gasifier: laboratory-scale experiments and performance prediction. *Appl Energy* 2014; 113: 670–679.
- [29] De Micco G, Nasjleti A, Bohe AE. Kinetics of the gasification of a Rio Turbio coal under different pyrolysis temperatures. *Fuel* 2012; 95: 537-543.
- [30] Senneca O, Russo P, Salatino P, Masi S. The relevance of thermal annealing to the evolution of coal char gasification reactivity. *Carbon* 1997; 35: 141-151.

Chapter Six: Kinetic study of coal steam and CO₂ gasification: A new method to reduce interparticle diffusion

6.1 Presentation of the article

The present article is the first experimental work using thermogravimetric analysis (TGA) on steam gasification performed in the University of Calgary. Most of the gasification kinetic studies have been conducted using CO₂ gasification since operation conditions and tracking of the reaction progress are not easy tasks when the gasifying agent is steam. A new quartz reactor and wider crucible were used to present the effect of the interparticle diffusion during CO₂ and steam gasification, with very positive results of the in-house setup compared with commercial TGAs.

It is demonstrated that at low temperatures where the chemical reaction is supposed to be the controlling step, there is interparticle diffusion dependent upon geometrical parameters of the reaction system that is usually omitted in the literature. This work applies concepts and findings presented in Chapters 3-5 to develop a new method to perform steam and/or CO₂ gasification with negligible mass transfer effects and without inducing a maximum gasification rate.

The design of the new quartz crucible, development of the experimental procedure, and all experiments were done by R. Arturo Gomez. Dr. Nader Mahinpey has supervised this work and helped to re-define mass transfer concepts. The authors would like to acknowledge Mr. Rico Silbermann for helping to configure the home-built TGA setup.

**Kinetic study of coal steam and CO₂ gasification:
A new method to reduce interparticle diffusion**

This article has been published in Fuel 148 (2015) 160-167. Reprinted with permission.

Arturo Gomez¹, Nader Mahinpey¹

¹Chemical and Petroleum Engineering Department, University of Calgary, 2500 University Drive NW, Calgary, T2N 1N4, Canada

6.2 Abstract

The effect of coal bed thickness was studied and compared between steam and CO₂ gasification. Despite using small amounts of coal sample, both gasifying agents' kinetics, i.e., steam and CO₂, proved to be affected by bulk and interparticle diffusion. Comparison between the gasifying agents indicates that mass transfer effects are minimized when the raw material layer and particle size are smaller than 0.14 mm and 90 μm, respectively.

In addition to mass transfer limitations, studies have confirmed that the reported maximum reaction rate is a consequence of the gas switching between inert and reaction gas during steam gasification; therefore, the time to replace the reaction medium cannot be considered as part of the kinetic analysis or taken into account in the kinetic model that represents the reaction mechanism. Nevertheless, it is not appropriate to use steam alone during pyrolysis and gasification in kinetic studies, since these two reactions overlap in the same temperature reaction range. An alternative method to overcoming these restrictions is proposed in this study.

The present study demonstrates a consistent method to perform gasification in the chemically controlled temperature range between 750°C and 900°C. In addition, the apparent activation energy is estimated independent of the kinetic model.

6.3 Introduction

Gasification is defined as the thermochemical conversion of a rich carbon feedstock into syngas, thus providing advantages in the undertaking of pre-combustion conditioning compared to conventional processes such as combustion. Steam gasification of coal and biomass increases the hydrogen to carbon monoxide ratio (H_2/CO) of the produced syngas [1]; therefore, it is suitable for power generation when carbon capture is an option [2-4] or as a source of reactants for further chemical transformation [5]. Steam gasification yields a much slower chemical reaction than combustion using the same feedstock and because steam is highly corrosive at the reaction conditions [6, 7], it is not possible to perform steam gasification using the conventional setup used for CO_2 gasification. Different authors present particular setups, *i.e.* batch reactors with product gas product analysis [8-10], TGA [11, 12] and flow reactors [1, 13]; however, experimental procedures are not standardized and they are similar to those used for CO_2 gasification.

Kinetic modeling of steam gasification is usually reported using single-step reaction models [14, 15] similar to those used for CO_2 gasification [16]. The most common kinetic model is the random pore model (RPM) proposed by Bhatia and Perlmutter [17]. This model can predict a maximum reaction rate; however, this is a consequence of the reaction medium change [18]. In the literature, intrinsic kinetic studies reveal that particle size and gas flow rate limit the overall

reaction rate, considering 90 μm as a safe particle size to reduce intrapore diffusion [15, 18]. There are studies in the literature that do not consider relationship of sample weight and existence of mass transfer effect, such as [11, 14, 15] whom authors have used less than 15mg and [8-10, 19] whom authors chose more than 100mg as sample size. However, amount of sample, reactor configuration and crucible are significant in kinetic analysis, since the sample thickness affects the reaction rate due to interparticle diffusion [20].

Activation energy of steam gasification ($E_{A \text{ steam}}$) is reported as significantly smaller than the activation energy of the CO_2 gasification ($E_{A \text{ CO}_2}$) in the same temperature range [21, 22], but the experimental procedure affects E_A results, and its calculation depends on the kinetic model since the rate constant is obtained from a linear regression when a single-step chemical reaction model is considered. This leads to some unexpected results such as similar E_A values for steam and CO_2 gasification [23]. An alternative E_A can be calculated without assuming a kinetic model [24, 25]; therefore, providing a more accurate value of the estimated E_A .

A new method to perform steam and CO_2 gasification with negligible bulk and interparticle diffusion effects is presented in this work. Different setup configurations are compared to determine if coal bed thickness is the most important variable associated with interparticle diffusion, instead of the sample amount which depends on the setup configuration. The activation energy of steam gasification calculated with an independent kinetic model approach with the proposed experimental method is consistently smaller than the activation energy of CO_2 gasification. This study helps to explain the difference between laboratory studies and pilot results using reactors with better fuel distribution. It also demonstrates that activation energy of

steam gasification may be underestimated in the literature [20, 21] as a consequence of the mass transfer limitations with small thicknesses of the coal bed layer.

6.4 Experimental methods

6.4.1 Experimental setup

A TGA TherMax 500 coupled with a home-built quartz reactor was used to perform atmospheric gasification in steam and CO₂ atmosphere. The schematic of the experimental setup is presented in Fig. 6.1a. The time interval to replace 98% of the inert gas with the reaction gas into the quartz reactor with 10 mg coal sample was 0.8 min, which was preliminary determined by estimation of the gases residence-time distribution with a step tracer experiment [18]. The volumetric flow rate of the gases was 1.8 times the reactor volume per minute to avoid bulk diffusion as presented elsewhere [15, 18]. A quartz crucible with a 12 mm internal diameter and external conical shape allows support of a layer of coal smaller than 1mm with a stable weight reading. A graphical comparison between this crucible and the conventional alumina crucible is illustrated in Fig. 6.1b. In contrast, the time interval to replace all gases using a NETZSCH TG 209 Libra F1 analyzer (TGA) was 1.8 min, with the same ratio of gas flow rate to reactor volume [18].

6.4.2 Coal characterization

Two Central-Western Canadian coals, Genesee coal (mined in Alberta) and Boundary Dam coal (mined in Saskatchewan), were analyzed in this study. Coal samples with particle size smaller than 90 μm were prepared as presented elsewhere [15, 18] to insure intrapore diffusion does not control the coal gasification rate. The coal sample was composed of 70% of particles

between 75 and 90 μm , and 30% smaller than 75 μm . The elemental composition was determined using a Perkin Elmer CHNS/O 2400 elemental analyzer (ultimate analysis). The proximate analysis was performed at atmospheric pressure using a NETZSCH TG 209 Libra F1 analyzer (TGA) according to the ASTM D5142 standard for coal and coke. The coal micro-pore surface area was determined using a Micrometrics model ASAP 2020 analyzer by CO_2 adsorption at 273K (Dubinin-Radushkevich method).

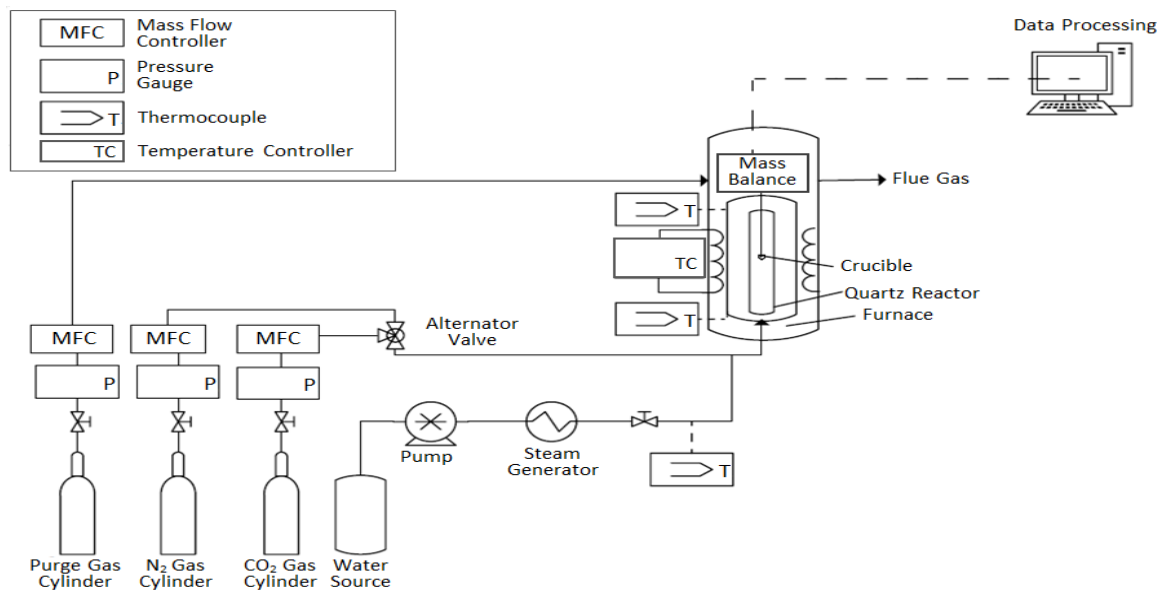
6.4.3 Steam gasification

Silbermann *et al* [15] suggested that direct gasification using CO_2 is the best method to carry out their experiments, since it shows a higher reaction rate [18]. Unfortunately, direct gasification (using same reaction gas during pyrolysis and gasification) cannot be applied when steam is the gasifying agent, since gasification overlaps with pyrolysis in the same temperature range due to the steam gasification rate being much higher than CO_2 [19, 21, 22] and the overall reaction is not thermodynamically limited by the Boudouard reaction below 700°C [26]. Other methods that separate pyrolysis and gasification reduce char reactivity due to the reduction of the initial char mesopore area during the isothermal pyrolysis [18].

Another method consists of changing an inert gas by the gasifying agent; which is the most common experimental procedure presented by other authors to study steam gasification [8-12, 19]. The beginning of the gasification is often considered when the reaction system reaches the reaction temperature if there is no isothermal pyrolysis step, the exact time at which the gases are simultaneously changed. The main disadvantage of this method is that a maximum gasification rate is observed at the same time after switching the inert gas for the gasifying agent [8, 18, 19,

21]. Thus, the starting point of the gasification should be reconsidered to avoid misinterpretations about the reaction mechanism [18]. As a consequence, this work presents an alternative method to overcome the main limitations of most common gasification experimental procedures.

(a) Schematic diagram of the experimental setup



(b) Schematic diagram of crucibles comparison

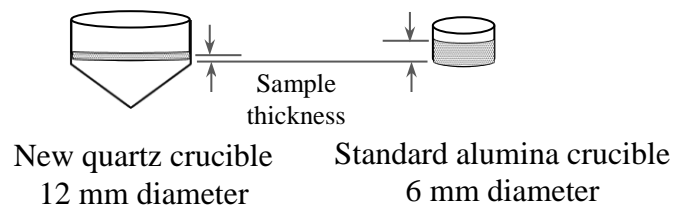


Figure 6.1 (a) Schematic diagram of the experimental setup: TGA TherMax 500 coupled to a quartz reactor. (b) Schematic diagram of the “new” and “standard alumina” crucibles illustrating the sample thickness when filled with 10 mg coal sample.

Using the new experimental setup, the proposed method to perform gasification either with steam or CO₂ as gasifying agents consisted of: (1) keeping the sample at an ambient temperature in a N₂ atmosphere until its weight became stable; (2) heating up the sample at 100°C/min (limitation of the new experimental setup); (3) decreasing the heating rate from 100°C/min to 20°C/min, when the temperature reaches 10°C below the reaction temperature, to avoid overheating; and (4) replacing N₂ with steam or CO₂ at the reaction temperature. The gasification was considered to start after the inert gas was completely replaced into the reaction chamber to avoid the incorrect interpretation of a maximum gasification rate [18]. The temperature range used in this study was between 800°C and 900°C where the Boudouard reaction was not thermodynamically limited and the chemical reaction was the controlling step [19]. The completed procedure is explained in Fig. 6.2 for a particular gasification temperature.

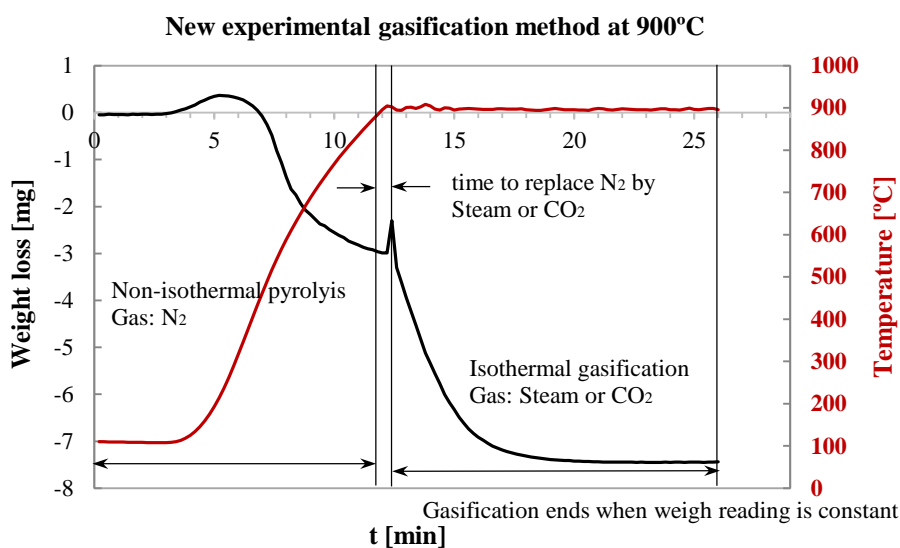


Figure 6.2 Experimental Gasification Method. TGA TherMax 500, 12 mm internal diameter crucible, and 1.8 min ‘reactor volume/gas flow’ ratio.

6.5 Kinetics analysis

6.5.1 Data analysis

Conversion can be obtained directly from the original weight loss vs. time or back calculating the carbon conversion from the gas product analysis vs. time. In this study, the weight loss and its associated time using TGA will be considered instead of the gas product analysis to ensure certainty when these two variables are continuously recorded.

To compare the effect of the interparticle diffusion, conversion vs. time will be compared for different setups. By definition conversion is:

$$X = \frac{m_o - m_t}{m_o - m_a} \quad \text{Eq. (6-1)}$$

where m_o is the initial mass of char or the mass at the beginning of the gasification; m_t is the mass at a particular time; and, m_a is the mass of the ash.

For the particular gas-solid reaction system, considered as a semi-batch reactor, the gasification rate can be obtained by the molar balance of the solid and expressed as:

$$r = \frac{dX}{dt} \quad \text{Eq. (6-2)}$$

The plot of conversion rate vs. conversion illustrates its mathematical form. This can be used to assume a chemical reaction kinetic model, if a consistent trend is observed and if there is no evidence of mass transfer limitations.

6.5.2 Activation energy independent of the kinetic model

As presented elsewhere [24, 25], there is a simpler way to obtain the Arrhenius equation parameters for a particular conversion using the original information, *i.e.*, reaction time and temperature. The slope of the logarithm of residence time vs. reciprocal of the absolute temperature yields the activation energy divided by the ideal gas law constant ‘ E_A/R ’. This procedure determines the accuracy of the most common chemical reaction kinetic models used in gasification at temperatures below 1000°C by comparing the precision of the activation energy estimation with respect to the free model calculation.

6.5.3 Chemical reaction kinetic models

Different models represent the chemical reaction kinetics of either steam or CO₂ gasification. For practical purposes three kinetic models will be discussed. These are known as single-step gas-solid kinetic models, which have received more attention in recent years and are described elsewhere [14, 15].

The first model is the volumetric model (VM) or first order reaction:

$$\frac{dX}{dt} = k_{VM}(1 - X) \quad \text{Eq. (6-3)}$$

The second model is the integrated core model (ICM), which represents the best fit for experimental data, if there is no gas switching during the experimental procedure [15]:

$$\frac{dX}{dt} = k_{IM}(1 - X)^n \quad \text{Eq. (6-4)}$$

The last model is the random pore model (RPM), which was presented for the first time by Bhatia and Perlmutter [17]. This model gained popularity due to its capacity to reproduce a maximum reaction rate. It is expressed by:

$$\frac{dX}{dt} = k_{RPM}(1 - X)\sqrt{1 - \psi \ln(1 - X)} \quad \text{Eq. (6-5)}$$

with ψ as a parameter associated with the internal surface structure of the non-converted char, and ideally expressed by:

$$\psi = \frac{4\pi L_o(1 - \varepsilon_o)}{S_o^2} \quad \text{Eq. (6-6)}$$

where S_o is the pore surface area per solid volume [m^2/m^3], L_o is the pore length per solid volume [m/m^3], and ε_o is the solid porosity. Mathematically, $\psi = 2$ if there is not a maximum rate after the beginning of the gasification [14, 15]; however, this restriction is not considered in many papers reporting the RPM as the best model to fit the experimental data [11, 19, 20].

6.6 Results and discussion

6.6.1 Coal properties

Results of the proximate and ultimate analysis for both Boundary Dam (BD) and Genesee coal are presented in Table 6.1. As illustrated in the table, both coals are similar in their elemental composition but contain different ash contents. High ash content is usually associated with a fast reaction rate during gasification, especially if the alkali and alkaline earth metal content is significant [12].

6.6.2 Effect of the bed sample thickness: TGA and crucible comparison

The comparison of different setups using CO₂ is necessary since it is not possible to use steam as the gasifying agent in the NETZSCH TG 209 Libra F1 analyzer (TGA), which was the system used in our previous work [18]. Steam gasification is much faster than CO₂ gasification [18, 20, 21]; therefore, diffusional effects detected during CO₂ gasification affect steam gasification at lower temperatures. Fig. 6.3 illustrates conversion vs. time at 900°C for CO₂ gasification of Genesee and Boundary Dam coals. Three different experimental configurations are presented, i.e. (1) NETZSCH TGA using the manufacturer recommendation of a 6mm diameter alumina crucible, (2) TherMax 500 TGA coupled with a quartz reactor and a 6mm crucible, and (3) TherMax 500 TGA coupled with a quartz reactor and a new crucible design of 12mm diameter.

Table 6.1 Proximate and ultimate analyses of two Central-West Canadian coals (dry basis). Surface micropore area using CO₂ at 273 K with the Dubinin-Radushkevich method.

	Proximate Analysis			Ultimate Analysis				Surface Area	
	Volatiles wt %	Fix Carbon wt %	Ash wt %	C wt %	H wt %	N wt %	S wt %	Dubinin-Radushkevich	
								Coal based m ² /g _{Coal}	Carbon based m ² /g _{Carbon}
Boundary Dam	35.8	46.9	17.3	58.0	3.4	1.8	1.0	156	269
Genesee	31.2	41.8	27	50.9	3.4	1.4	1.7	130	256

Changing the crucible shape and diameter can change the reaction mechanism, as presented in Fig. 6.3, which indicates that diffusional effects are significant above 900°C for both coals.

For this reason it is not possible to refer to intrinsic kinetics due to the fact that the reaction is mass transfer limited using the NETZSCH TGA. The main difference between both coals is their ash content and micropore surface areas; however, when comparing the micropore surface area based on carbon content they are similar, as presented in Table 6.1.

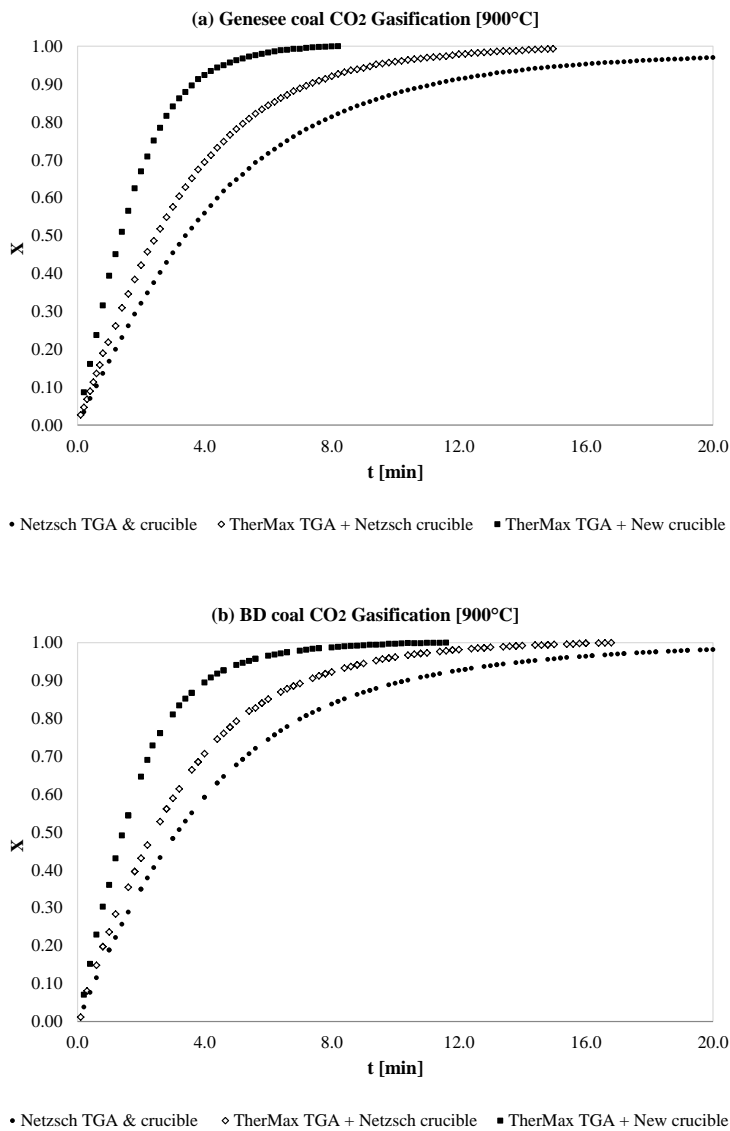


Figure 6.3 Conversion vs. time for three experimental configurations during the CO₂ gasification [10 mg sample] at 900°C: (a) Genesee coal and (b) Boundary Dam (BD) coal.

It is important to note that reactivity of both coals is similar and the residence time to achieve a determined conversion is in the same range. The difference between the TherMax 500 TGA and the NETZSCH TGA could be associated with the design of the crucible (which cannot be placed in a commercial TGA due to its diameter). Similar conclusions were presented for Mandapati *et al.* [20], demonstrating that interparticle diffusion through the coal bed is very important and comparison of literature is difficult because the total sample bed thickness is a significant factor. The bulk density of Genesee and Boundary Dam coals are 0.65 and 0.81 g/cm³, respectively, which would explain why diffusional effects are different for the same sample weight between both coals. These results indicate that bulk and interparticle diffusion, associated to the TGA design and sample thickness respectively, limit the overall reaction rate.

6.6.3 Effect of the sample size

It was found that the new experimental setup (TherMax 500 coupled with a quartz reactor) using a crucible with a larger diameter and a conical shape is appropriate for a stable weight reading using a small amount of sample with negligible bulk diffusion, as presented previously for the comparison of the new setup against a commercial TGA. However, interparticle diffusion is important and it should be kept to a minimum [20]. In order to determine the effect of the interparticle diffusion, a set of gasification experiments changing the weight sample was performed for both steam and CO₂ gasification in the temperature range between 800°C and 900°C.

Because mass transfer effects dominate at high temperatures [27], a reaction at 900°C was selected to determine the minimum weight, where it is assumed that mass transfer does not

control the overall reaction rate [28]. Of significance, 100% steam is used as a gasifying agent which is why the reaction is much faster compared with CO₂ gasification. Figs. 6.4 and 6.5 show conversion vs. time at 900°C for Genesee and Boundary coal gasification, respectively, using (a) steam and (b) CO₂ as gasifying agents. For steam gasification, Figs. 6.4a and 6.5a, illustrate that bed diffusion using a 12mm crucible is negligible (below 10mg for both coals). It is not possible to eliminate mass transfer effects of gasification using 5 mg at 900°C but the overall kinetics can be calculated using 10 mg, which is much faster than using other experimental configurations for both coals as presented in Fig. 6.3. At lower temperature ranges (*i.e.*, 800 and 850), there is no significant difference between 5mg and 10 mg samples.

Findings suggest that interparticle diffusion is negligible if the thickness of the sample layer is smaller than 0.14mm (10 mg sample of the coal with the lowest bulk density). Since most of the coal particles are in the range between 75 and 90 μm, a coal bi-layer distribution does not pose significant interparticle diffusion. This diffusional effect is important when the thermochemical reaction is over 900°C and the raw material has a lower bulk density such as biomass. Therefore, combined intraparticle and interparticle diffusion can affect the overall reaction rate and the assumption that the reaction is chemically controlled might be unsound.

6.6.4 Non-maximum reaction rate

In a previous study [18], it was stated that the commonly reported maximum reaction rate is a consequence of the gases switching. For CO₂ gasification, an alternative experimental procedure was presented [15] and an alternative procedure is proposed in this work either for steam or CO₂ coal gasification. There are recent works on steam gasification that attempt to explain the stated

maximum using the random pore model to correlate gasification experimental data [11, 14, 19, 20]. To extend previous findings in a general way for gasification or for any chemical reaction where the reaction medium is replaced, the conversion rate vs. residence time is presented in Fig. 6.6 for Genesee and Boundary Dam coals using CO₂ and steam as gasifying agents.

Fig. 6.6a show that the time it takes to reach a maximum is independent of the gasifying agent and coal type for a constant gas flow rate. This is related to a dispersion phenomenon and is not associated with changes on the char surface during gasification [18]. Constant time to observe a maximum is presented in other works using different experimental setups [8, 19, 21]. To overcome this phenomenon, this work proposes a procedure which considers as the initial time of the gasification 0.8 of a minute after switching the inert gas for the gasifying agent (Fig. 6.6b). It is important to clarify that this time interval depends on the reactor geometry, reactor volume, and the gas flow rate.

The new method is equivalent to the direct gasification when CO₂ is the gasifying agent, which can be appreciated by comparing the initial conversion rate for Genesee coal in this study (Fig. 6.6b) and the initial conversion rate at the same conditions reported by Silbermann et al. (Method 1 on Fig. 3 of the cited reference) [15]. This confirms that there are not combined effects between pyrolysis and CO₂ gasification.

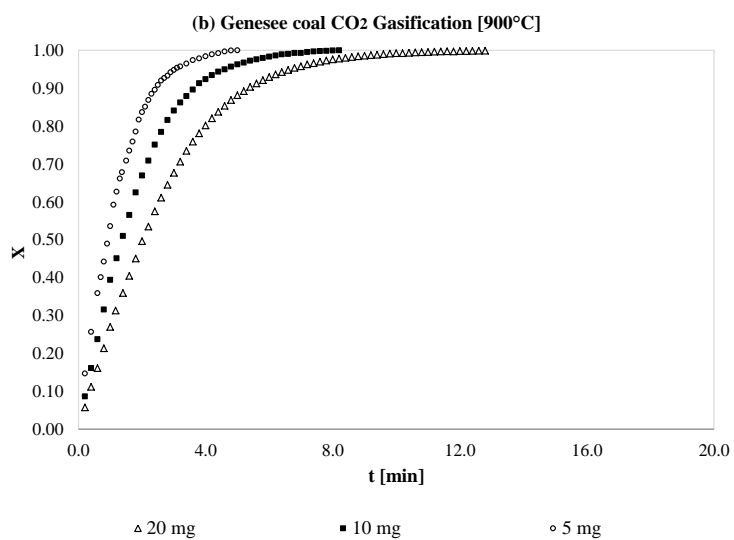
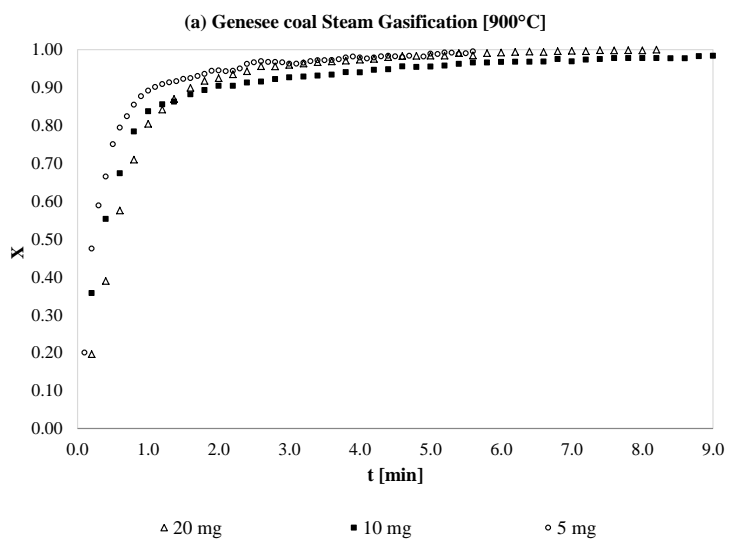


Figure 6.4 Effect of the weight sample during the gasification of Genesee coal at 900°C using a TherMax 500 TGA coupled to a quartz reactor and a 12mm quartz crucible: (a) steam gasification and (b) CO₂ gasification.

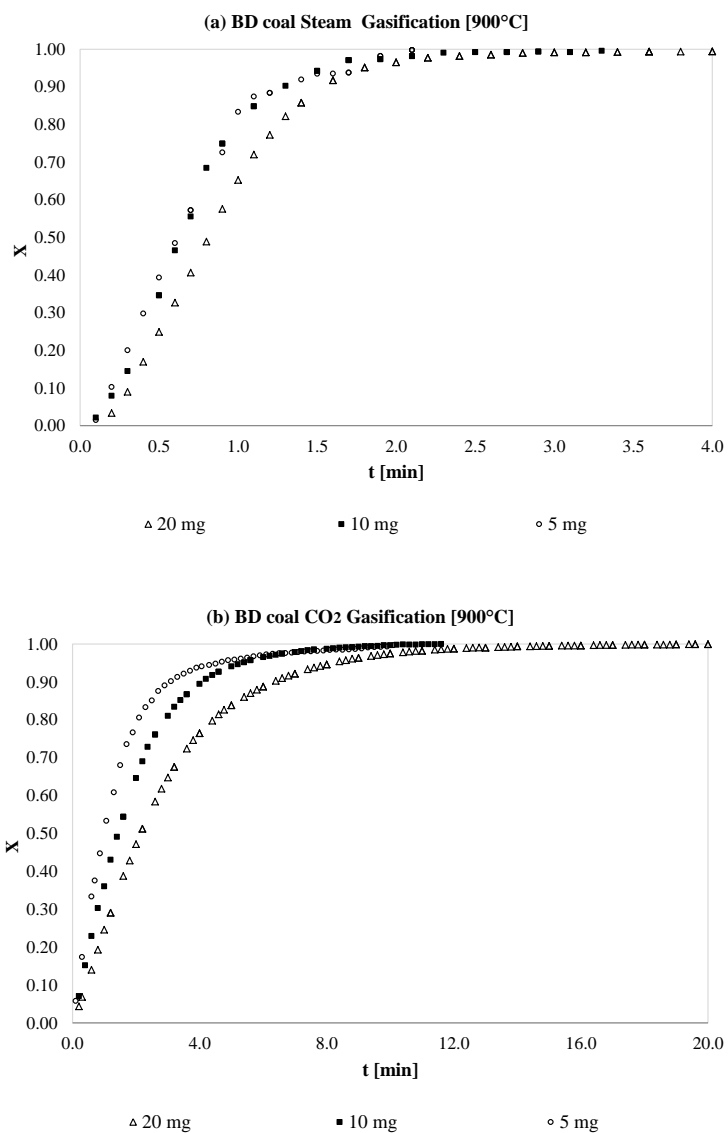


Figure 6.5 Effect of the weight sample during the gasification of Boundary Dam coal at 900°C using a TherMax 500 TGA coupled to a quartz reactor and a 12mm quartz crucible: (a) steam gasification and (b) CO₂ gasification.

6.6.5 Activation energy estimation and falsified kinetics

The effect of interparticle diffusion on kinetic parameters has not been reported in literature relating to steam gasification. Using a free-model approach [24, 25] at three different temperatures, the activation energy is obtained independent of the kinetic model for different coal samples, i.e. 20mg, 10mg and 5 mg; results are represented in Table 3 at 25%, 50%, and 80% conversion.

The activation energy of steam gasification ($E_{A-Stream}$) for these two coals ranges between 80 and 130 kJ/mol, and it is smaller than the activation energy of CO₂ gasification (E_{A-CO_2}). However, $E_{A-Stream}$ is not half of E_{A-CO_2} as it is reported elsewhere [21, 22]. The maximum uncertainty is ± 7 kJ/mol which is reflected in the coefficient of determination higher than 0.99 in almost all cases. Analyzing activation energy at different conversions, it is evident that the thickness of the sample has greater impact on steam gasification than CO₂ gasification because gasification with steam is much faster than using CO₂ as a gasifying agent (Table 6.2). Genesee coal shows higher activation energy than Boundary Dam coal for both steam and CO₂, which could be associated with the alkaline and alkali earth metal content [12, 29].

The activation energy calculated at a lower conversion is smaller than at a higher conversion, especially when the amount of sample is higher. The most important consideration of the activation energy at different conversions is related to the reaction mechanism, because theoretically E_A should be constant and independent of the conversion [24, 25]. Considering a single-step chemical reaction, an increase in the activation energy when conversion increases could be associated with a change in the reaction mechanism due to: (1) reduction or deactivation of the catalyst (alkali) and (2) intraparticle diffusion (gas diffusion through the ash)

[25]. Changes of activation energy at different conversions are similar between steam and CO₂ with 5 or 10 mg samples (they are within the range of the experimental error), which indicates that intrapore diffusion does not affect the overall reaction rate significantly.

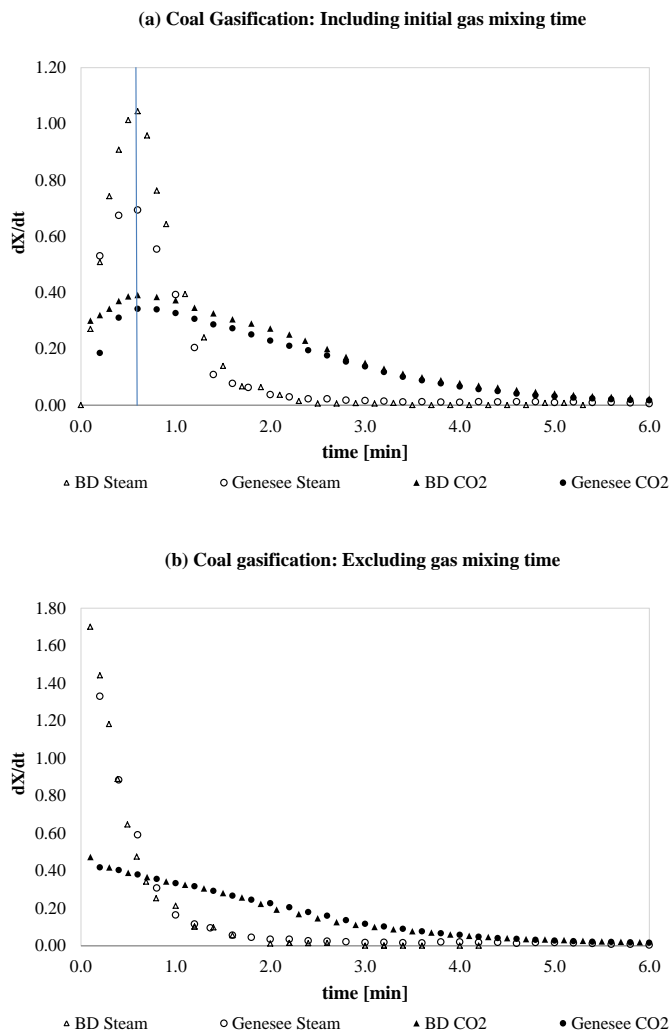


Figure 6.6 BD and Genesee gasification rate vs. residence time at 900°C: (a) including gas mixing time and (b) excluding the time to replace gases. CO₂ and steam as gasifying agents.

Table 6.2 Activation energy (kJ/mol) estimated independent of the kinetic model [23] at three different conversions and its respective coefficient of determination. Temperature range from 800°C to 900°C. Max. uncertainty: ± 7 kJ/mol

Coal	Sample (mg)	E _A [kJ/mol] Steam Gasification						E _A [kJ/mol] CO ₂ Gasification					
		<u>X=0.25</u>		<u>X=0.5</u>		<u>X=0.8</u>		<u>X=0.25</u>		<u>X=0.5</u>		<u>X=0.8</u>	
		E _A	R ²	E _A	R ²	E _A	R ²	E _A	R ²	E _A	R ²	E _A	R ²
BD	20	83	0.99	82	0.99	93	0.99	113	0.95	131	0.97	141	0.99
BD	10	109	0.99	101	0.99	109	1.00	112	1.00	120	1.00	134	1.00
BD	5	110	1.00	103	0.99	105	0.98	120	0.99	113	1.00	118	0.99
Genesee	20	103	1.00	103	1.00	125	1.00	140	1.00	155	1.00	171	1.00
Genesee	10	111	1.00	112	1.00	129	1.00	145	0.99	157	0.99	169	0.99
Genesee	5	132	0.99	141	1.00	144	1.00	162	1.00	170	1.00	185	1.00

The kinetic models discussed in this work include the volumetric model (VM), integrated core model (ICM) and the random pore model (RPM). These models were applied to the experimental information from 0% to 80% conversion to obtain rate constant. The Arrhenius equation was used to calculate the activation energy by correlating the logarithm of rate constant vs. reciprocal of temperature. Results are presented in Table 6.3. The maximum uncertainty was ± 11 kJ/mol; with a lower coefficient of determination compared with the method independent of the kinetic model.

It might be misleading to conclude that a particular kinetic model underestimates or overestimates the activation energy for CO₂ gasification. For steam gasification the three kinetic models analyzed underestimated the activation energy; the situation was exacerbated when the sample amount was increased. These results indicate as to why the activation energy should be calculated independent of the kinetic model, which additionally provides information relating to the reaction mechanism.

Table 6.3 Activation energy (kJ/mol) at three different conversions and its respective coefficient of determination using three kinetic models: VM, ICM and RPM. Temperature range from 800°C to 900°C. Max. uncertainty: ± 11 kJ/mol

Coal	Sample (mg)	EA [kJ/mol] Steam Gasification						EA [kJ/mol] CO ₂ Gasification					
		<u>V M</u>		<u>I C M</u>		<u>R P M</u>		<u>V M</u>		<u>I C M</u>		<u>R P M</u>	
		E _A	R ²	E _A	R ²	E _A	R ²	E _A	R ²	E _A	R ²	E _A	R ²
BD	20	82	0.99	71	0.97	84	0.99	126	0.98	117	0.98	129	0.98
BD	10	99	1.00	84	1.00	101	1.00	121	1.00	112	1.00	123	1.00
BD	5	99	0.94	98	0.96	93	0.91	117	1.00	116	1.00	116	1.00
Genesee	20	98	1.00	88	1.00	98	1.00	165	1.00	157	0.99	168	1.00
Genesee	10	123	0.99	127	0.92	123	1.00	157	0.99	148	0.98	159	0.99
Genesee	5	120	1.00	102	0.99	124	1.00	177	1.00	169	1.00	178	1.00

Overall, a decrease in the sample amount increases the value of activation energy either for steam or CO₂ gasification, which is denominated falsified kinetics [27]. Other alternatives such as the effectiveness factor can be used to determine if the reaction is mass transfer limited; however, it requires the assumption of the kinetic model which is useful for intraparticle diffusion but complex to model interparticle diffusion, which is not a single particle with a uniform shape. A challenge for kinetic analysis is that the bed thickness is limited by the experimental configuration, as presented in section 4.2. Another restriction is that decreasing of the sample size increases the uncertainty and inaccuracy of the reading. In view of these flaws, the 10 mg sample used in the experimental setup is an ideal sample amount with a small incidence of interparticle diffusion and virtually no other diffusional effects for both steam and CO₂ gasification.

6.7 Conclusion

A new method to perform steam gasification with lower incidence of interparticle and intraparticle diffusion was presented. Interparticle diffusion is not significant with a raw material bed thickness of less than 0.14mm; consequently, the reaction is not mass transfer limited in the temperature range between 800°C and 900°C.

It was presented that findings about the non-existence of a maximum CO₂ gasification rate are extensive to steam gasification. This is important as some of the most accepted kinetic models were developed to predict the stated maximum; therefore, a different approach in kinetic modeling should be implemented for future studies.

Changes of the activation energy at different conversions, estimated independent of the kinetic model, suggest that if the reaction mechanism is the same along the reaction progress; particularly in an increase of the activation energy at higher conversions, could evidence either mass transfer limitations or catalyst deactivation. This procedure is useful to validate the accuracy of different kinetic models and determine if the reaction is not mass transfer limited.

For the atmospheric steam gasification of coal at temperatures higher than 900°C the reaction is mass transfer limited. At this point, interparticle and intraparticle diffusion control the overall reaction, and, thus, single step kinetic models are not appropriate for estimating kinetic parameters. If mass transfer is negligible, the activation energy of steam gasification is about 30 kJ/mol lower than that of CO₂ gasification.

6.8 References

- [1] Hernández J, Aranda G, Barba J, Mendoza JM. Effect of steam content in the air–steam flow on biomass entrained flow gasification. *Fuel Process Technol* 2012; 99: 43-55.
- [2] Ratafia-Brown J, Manfredo L, Hoffmann J, Ramezan M. Major environmental aspects of gasification-based power generation technologies. U.S. Department of Energy, Office of Fossil Energy, National Energy Technology Laboratory, 2002. <http://www.netl.doe.gov/File%20Library/Research/Coal/energy%20systems/gasification/pubs/final-env.pdf> [cited 13.11.14]
- [3] Kunze C, Riedl K, Spliethoff H . Structured exergy analysis of an integrated gasification combined cycle (IGCC) plant with carbon capture. *Energy* 2011; 36: 1480-1487.
- [4] Giuffrida A, Romano MC, Lozza G. Thermodynamic analysis of air-blown gasification for IGCC applications plant with carbon capture. *Appl Energy* 2011; 88: 3949–3958.
- [5] Dermot JR. A syngas network for reducing industrial carbon footprint and energy use. *Appl Therm Eng* 2013; 53: 299-304.
- [6] Tomlinson L, Cory NJ. Hydrogen emission during the steam oxidation of ferritic steels: kinetics and mechanism. *Corros Sci*, 1989; 29 (8): 939-965.
- [7] Marrone PA, Hong GT. Corrosion control methods in supercritical water oxidation and gasification processes. *J Supercritic Fluid* 2009; 51: 83–103.
- [8] Nipattummakul N, Ahmed I, Kerdsuwan S, Gupta AK. High temperature steam gasification of wastewater sludge. *Appl Energy* 2010; 87 (12): 3729-3734.
- [9] Wang J, Jiang M, Yao Y, Zhang Y, Cao J. Steam gasification of coal char catalyzed by K_2CO_3 for enhanced production of hydrogen without formation of methane. *Fuel* 2009; 88 (9): 1572–1579.
- [10] Umeki K, Namioka T, Yoshikawa K. The effect of steam on pyrolysis and char reactions behavior during rice straw gasification. *Fuel Process Technol* 2012; 94 (1): 53-60.

- [11] Feroso J, Gil MV, García S, Pevida C, Pis JJ, Rubiera F. Kinetic parameters and reactivity for the steam gasification of coal chars obtained under different pyrolysis temperatures and pressures. *Energy Fuels* 2011; 25: 3574–3580.
- [12] Coetzee S, Neomagus HWJP, Bunt JR, Everson RC. Improved reactivity of large coal particles by K_2CO_3 addition during steam gasification. *Fuel Process Technol* 2013; 114: 75-80.
- [13] Detournay M, Hemati M, Andreux R. Biomass steam gasification in fluidized bed of inert or catalytic particles: Comparison between experimental results and thermodynamic equilibrium predictions. *Powder Technol* 2011; 208 (2): 558-567.
- [14] Zou JH, Zhou ZJ, Wang FC, Zhang W, Dai ZH, Liu HF, Yu ZH. Modeling reaction kinetics of petroleum coke gasification with CO_2 . *Chem Eng Process* 2006; 46: 630–636.
- [15] Silbermann R, Gomez A, Gates I, Mahinpey N. Kinetic studies of a novel CO_2 gasification method using coal from deep unmineable seams. *Ind Eng Chem Res* 2013; 52 (42): 14787-14797.
- [16] Bhatia SK, Perlmutter DD. A random pore model for fluid–solid reactions: I. Isothermal and kinetic control. University of Pennsylvania. *AIChE J* 1980; 26 (3): 379–386.
- [17] Irfan M, Usman MR, Kusakabe K. Coal gasification in CO_2 atmosphere and its kinetics since 1948: A brief review, *Energy* 36 (2011) 12–40.
- [18] Gomez A, Silbermann R, Mahinpey N. A comprehensive experimental procedure for CO_2 coal gasification: Is there really a maximum reaction rate?. *Appl Energy* 2014; 124: 73–81.
- [19] Ahmed II, Gupta AK. Kinetics of woodchips char gasification with steam and carbon dioxide. *Appl Energy* 2011; 88 (5): 1613-1619.
- [20] Mandapati RM, Daggupati S, Mahajani SM, Aghalayam P, Sapru RK, Sharma RK, Ganesh A. Experiments and kinetic modeling for CO_2 gasification of Indian coal chars in the context of underground coal gasification. *Ind Eng Chem Res.* 2012; 51: 15041–15052.

- [21] Ren L, Yang J, Gao F, Yan J. Laboratory study on gasification reactivity of coals and petcoke in CO₂/steam at high temperatures. *Energy Fuels* 2013; 27: 5054–5068.
- [22] Marquez-Montesinos F, Cordero T, Rodríguez-Mirasol J, Rodríguez JJ. CO₂ and steam gasification of a grapefruit skin char. *Fuel* 2002; 81 (4): 423–429.
- [23] Huo W, Zhou Z, Wang F, Wang Y, Yu G. Experimental study of pore diffusion effect on char gasification with CO₂ and steam. *Fuel* 2014; 131: 59–65.
- [24] De Micco G, Nasjleti A, Bohe AE. Kinetics of the gasification of a Rio Turbio coal under different pyrolysis temperatures. *Fuel* 2012; 95: 537-543.
- [25] Gomez A, Mahinpey N. A new method to calculate kinetic parameters independent of the kinetic model: Insights on CO₂ and steam gasification. *Chem Eng Res Des* 2015; 95: 346-357.
- [26] Renganathan T, Yadav MV, Pushpavanam S, Voolapalli RK, Cho YS. CO₂ utilization for gasification of carbonaceous feedstocks: A thermodynamic analysis . *Chem Eng Sci* 2012; 83: 159–170.
- [27] Fogler HS. *Elements of Chemical Reaction Engineering. Diffusion and Reaction.* 4th ed. Boston: Pearson Education, Inc; 2006, p. 813-851.
- [28] Tremel A, Haselstenier T, Kunze C, Spliethoff H. Experimental investigation of high temperature and high pressure coal gasification. *Appl Energy* 2011; 92: 79-285.
- [29] Gomez A, Mahinpey N. A new model to estimate CO₂ coal gasification kinetics based only on parent coal characterization properties. *Appl Energy* 2015; 137: 126-133.

Chapter Seven: Synthesis

7.1 Overview

A comprehensive review of recent research trends and accepted theories in the field of gasification and thermochemical conversion was discussed in Chapter 2. Chapters 3-6 are based on four journal papers and present findings that are required for research conclusions. This chapter (Chapter 7) provides an explanation of the relationships between these chapters and also the reason why sequential order is required to present gasification kinetics.

7.2 Synthesis of the thesis

The main goal of this work was the derivation of new elements related to gasification kinetics with a minimum amount of assumptions. A previous study using a new experimental procedure [1] showed unexpected results with respect to previous gasification kinetics literature and may have explained why reported kinetic parameters do not exhibit uniform trends [2].

Chapter 2 demonstrates a set of statistical proofs of the correlation between the estimation of kinetic parameters and the selection of a particular kinetic model. This is a critical flaw in kinetic analysis since kinetic parameters should be theoretically independent of the kinetic model. Moreover, authors commonly propose kinetic models with a higher number of fitting parameters with a better coefficient of correlation (R^2) [3, 4], but are not necessarily related to the reaction mechanism. Therefore, proving that the activation energy (E_A) for a single-reaction step is affected by the kinetic model is equivalent to stating that the best kinetic model cannot be the

one with highest R^2 . This is critical if its E_A is significantly different from the real activation energy.

There were four questions that this research sought to answer in order to attain a greater understanding of gasification:

- (1) How does the experimental procedure bias the interpretation of the reaction mechanism?
- (2) What are the most significant variables affecting the gasification rate, regardless of the feedstock?
- (3) What is the real E_A if the result is biased by a particular kinetic model?
- (4) Are all assumptions correct about existence/absence of mass transfer limitations at low temperatures?

The answer to the first question probably explains why different authors who use the same procedure but a different setup can report different results, as discussed in Chapter 3. Chapter 4 attempts to resolve question 2 and provides the elements to estimate the CO_2 gasification kinetics of coal for a broad range of ash contents. Answering the third question is not related to the gasification itself and is addressed with a new approach on chemical reaction engineering fundamentals, as presented in Chapter 5.

The chemical control of the overall reaction is the main assumption at low gasification temperatures; therefore, the circumstances under which mass transfer affects gasification at temperatures below 1000°C is addressed in Chapter 6.

7.2.1 Real nature of the maximum gasification rate

Bhatia and Perlmutter [5] explained that the maximum rate observed when the gasification rate is plotted against conversion is associated with changes of the char surface. However, there is a contradiction with their theory, because the conversion to achieve a maximum gasification rate is not constant: conversion decreases when the reaction temperature [3, 6-9] or partial pressure [10] decreases.

Different attempts to explain this situation have been reported in the literature; one example is the non-uniform pore distribution condition [4]. As presented in Chapter 3, one should note that the time it takes to observe a maximum gasification rate is constant independent of the partial pressure [10], reaction temperature [11], gasifying agent [10], steam to fuel ratio [12] and addition of catalyst [13].

The existence of a maximum rate has been proven to be associated with the dispersion of the gases into the reactor, i.e. when the inert gas is replaced by the reaction gas [14]. The experimental methods were based on the perturbation of a reaction system considered in steady state. This reveals that the time to observe a maximum rate is constant and related to the reactor volume and volumetric flow rate. Three different tests were designed to prove this for CO₂ [14] and steam coal gasification [15]; and, in general, it can be extended to any gas-solid reaction.

This is a breakthrough in gasification, since the amended maximum rate has been considered as an inherent part of the reaction mechanism; therefore, the understanding of the gasification mechanism provides elements to improve kinetic analysis in future studies for all researchers.

This explains why kinetic studies in continuous reactors do not show a maximum rate, which can be attributed to the non-separation between pyrolysis and gasification.

The most important conclusion is that kinetics modeling becomes simplified and classic kinetic models, such as power-law and first-order kinetic models, can be used to fit experimental results more precisely than complex models [1, 14].

7.2.2 Effect of the isothermal pyrolysis in the char reactivity

Another important finding in gasification, as presented in Chapter 3, is the decrease of char mesopore surface area during isothermal pyrolysis [14], which is more significant when the reaction temperature increases. This is associated with the non-existence of a maximum gasification rate, since isothermal pyrolysis is introduced as an additional step to separate pyrolysis and gasification during experimentation. Ordinarily, the extension of the isothermal pyrolysis is not considered as a variable affecting char reactivity, which accounts for differences between laboratory studies and industrial gasifiers.

Some authors show different reactivities of chars exposed to different isothermal pyrolysis; however, the explanation has been linked to thermal annealing [16-17], even if there is no temperature gradient. The char surface area increases during non-isothermal pyrolysis [18] and reduces during isothermal pyrolysis [14], which explains the reactivity differences among chars synthesized from the same raw material under different experimental conditions.

A new experimental procedure was proposed [1] that minimizes the effects of the experimental procedure in gasification kinetics studies [14]. This particular method has

demonstrated that direct gasification is sufficient to evaluate CO₂ gasification; however, it cannot be extended to steam gasification [15].

7.2.3 Variables affecting char reactivity

The most important variables affecting gasification were determined and correlated using a reliable experimental procedure to perform CO₂ gasification, such as direct gasification, with a new semi-empirical equation based on the Arrhenius equation. This is explained in Chapter 4.

The char pore surface area has been identified as one of the most important variables affecting gasification rate [14]; however, consistent trends between reactivity and micropore surface area at different ash contents have not been reported. Another limitation is the indirect measurement of char mesopore and micropore surface areas, since Brunauer-Emmett-Teller (BET) and Dubinin-Radushkevich (DR) characterizations are carried out at 77 K and 273 K, respectively. The char micropore surface area can be associated with its respective parent coal and a consistent trend between gasification rate and micropore area can be observed at different ash contents, if the micropore surface area is based on carbon content instead of coal content [19].

The alkali content most affects the coal reactivity during gasification. Due to the catalytic nature of alkali and alkaline earth metals, the gasification rate of different feedstock mixtures cannot be considered as the linear contribution of the raw species gasification rates [19], as normally reported in literature [20, 21]. The concept of alkali content equivalents to measure all alkali oxides activity has been introduced, and the catalytic effect of the alkali can be quantified in a broad range of ash contents and for different feedstocks.

This confirms the co-existence of catalytic and non-catalytic gasification reactions. Consideration should be given as to whether it makes sense to remove the ash and, in a further step, to add a catalyst, as usually proposed in ash-free coal gasification studies [3].

7.2.4 Estimation of kinetic parameters independent of the kinetic model

After demonstrating different aspects of the gasification reaction mechanism, the question remains as to which kinetic model should be used to estimate kinetic parameters and to accurately model gasification kinetics. In kinetic studies, as in many other applications, the experimental information is fitted to a particular equation by least squares regression, and the model with a higher coefficient of determination (R^2) is considered the best.

As presented in Chapter 2, the estimation of kinetic parameters, such as E_A and frequency factor, is correlated with the kinetic model; however, in theory, kinetic parameter estimation should be independent of the kinetic model. The conventional approach to the estimation of E_A requires the previous determination of the rate constant at different reaction temperatures; and this involves the selection of a kinetic model to fit isothermal experimental data [1, 3, 8, 9, 11, 20]. However, the assumption is that the particular kinetic model correctly represents the reaction mechanism. Therefore, it is important to estimate the kinetic parameters independent of the kinetic model, but using the same experimental information used for kinetic modeling.

A new theoretical deduction to estimate E_A and frequency factor, independent of the kinetic model, is presented in Chapter 5 [22]. This is based on a molar balance for a batch reactor and the Arrhenius equation. Additional assumptions to the ones considered in kinetic studies, such as single-step overall reaction with the chemical reaction as the controlling step, are not required.

This is an important contribution to the chemical reaction engineering fundamentals, since it can be extended to any batch reaction experiment. Validation of a set of kinetic models can be done by comparing their kinetic parameters with those calculated from the free-model approach.

7.2.5 Reduction of interparticle diffusion in experimental studies

Many researchers have considered the main assumption that the chemical reaction is the controlling step in kinetic studies using a single-step kinetic model by working at temperatures lower than 1000°C [1-3, 10-12, 18]. These studies have been carried out in that way, because in theory there are no associated mass transfer effects, regardless of the amount of sample, i.e. 10 mg or less [1, 3, 14, 20], 11mg to 100 mg [9, 11, 17, 18], and more than 1g [10, 12]. Most of these investigations considered intrinsic kinetics if the particle size was below 90µm [1, 9]; however, even at low temperatures and small particle sizes, there is interparticle diffusion [8, 15].

Chapter 6 presents a set of experiments that compared a commercial thermogravimetric analyzer (TGA) with a home-built TGA. These experiments demonstrated that the sample amount affected the gasification rate. It was proven that the most important variable associated with the interparticle diffusion is the thickness of the feedstock sample [8, 15], which depends on the geometry of the crucible or sample holder [15].

Steam gasification is faster than CO₂ gasification; thus, mass transfer effects are more important at the same temperature. Application of the method presented in Chapter 5 in the determination of the E_A independent of the kinetic model revealed that the reported E_A of steam gasification was significantly smaller than the one calculated if interparticle diffusion was

minimized [15]. This is denominated falsified kinetics [23] and indicated that the assumption of intrinsic kinetics is not possible for steam gasification, even at low reaction temperatures, using conventional methods. A new experimental procedure, with negligible interparticle diffusion and without inducing a maximum gasification rate in CO₂ and/or steam gasification is proposed, incorporating all the findings presented in this thesis.

7.3 References

- [1] Silbermann R, Gomez A, Gates I, Mahinpey N, Kinetic studies of a novel CO₂ gasification method using coal from deep unmineable seams. *Ind Eng Chem Res* 2013; 52: 14787–14797.
- [2] Di Blasi C. Combustion and gasification rates of lignocellulosic chars. *Prog Energ Combust Sci* 2009; 35: 121–140.
- [3] Kopyscinski J, Habibi R, Mims ChA, Hill JM. K₂CO₃-catalyzed CO₂ gasification of ash-free coal: Kinetic study. *Energy Fuels* 2013; 27: 4875–4883.
- [4] Singer SL, Ghoniem AF. An adaptive random pore model for multimodal pore structure evolution with Application to Char Gasification. *Energy Fuels* 2011; 25: 1423–1437.
- [5] Bhatia SK, Perlmutter D D. A random pore model for fluid–solid reactions: I. Isothermal and kinetic control. *University of Pennsylvania AIChE J* 1980; 26 (3): 379–386.
- [6] Irfan M, Usman MR, Kusakabe K. Coal gasification in CO₂ atmosphere and its kinetics since 1948: A brief review. *Energy* 36 (2011) 12–40.
- [7] Umeki K, Moilanen A, Gómez-Barea A, Konttinen J. A model of biomass char gasification describing the change in catalytic activity of ash. *Chem Eng J* 2012; 207–208: 616–624.
- [8] Mandapati, R.M., Daggupati, S., Mahajani, S.M., Aghalayam, P., Sapru, R.K., Sharma R.K. et al. Experiments and kinetic modeling for CO₂ gasification of Indian coal chars in the context of underground coal gasification. *Ind Eng Chem Res* 2012; 51: 15041–15052.
- [9] Malekshahian M, Hill J. Kinetic analysis of CO₂ gasification of petroleum coke at high pressure. *Energy Fuels* 2011; 25: 4043-4048.
- [10] Ahmed II, Gupta AK. Kinetics of woodchips char gasification with steam and carbon dioxide. *Appl Energy* 2011; 88 (5): 1613-1619.
- [11] Ren L, Yang J, Gao F, Yan J. Laboratory study on gasification reactivity of coals and petcoke in CO₂/steam at high temperatures. *Energy Fuels* 2013; 27: 5054–5068.

- [12] Nipattummakul N, Ahmed I, Kerdsuwan S, Gupta AK. High temperature steam gasification of wastewater sludge. *Appl Energy* 2010; 87 (12): 3729-3734.
- [13] Wang J, Jiang M, Yao Y, Zhang Y, Cao J. Steam gasification of coal char catalyzed by K_2CO_3 for enhanced production of hydrogen without formation of methane. *Fuel* 2009; 88 (9): 1572–1579.
- [14] Gomez A, Silbermann R, Mahinpey N. A comprehensive experimental procedure for CO_2 coal gasification: Is there really a maximum reaction rate? *Appl Energy* 2014; 124: 73-81.
- [15] Gomez A, Mahinpey N. Kinetic study of coal steam and CO_2 gasification: A new method to reduce interparticle diffusion. *Fuel* 2015; 148: 160-167.
- [16] Senneca O, Russo P, Salatino P, Masi S. The relevance of thermal annealing to the evolution of coal char gasification reactivity. *Carbon* 1997; 35 (1): 141-151.
- [17] Senneca O, Cortese L. Thermal annealing of coal at high temperature and high pressure. Effects on fragmentation and on rate of combustion, gasification and oxy-combustion. *Fuel* 2014; 116: 221–228.
- [18] Tremel A, Haselstenier T, Kunze C, Spliethoff H. Experimental investigation of high temperature and high pressure coal gasification. *Appl Energy* 2011; 92: 79-285.
- [19] Gomez A, Mahinpey N. A new model to estimate CO_2 coal gasification kinetics based only on parent coal characterization properties. *Appl Energy* 2015; 137: 126-133.
- [20] Feroso J, Arias B, Pevida C, Plaza MG, Rubiera F, Pis JJ. Kinetic models comparison for steam gasification of different nature fuel chars. *J Therm Anal Calorim* 2008; 91 (3): 779-786.
- [21] Gil MV, Rianza J, Alvarez L, Pevida C, Pis JJ, Rubiera F. Kinetic models for the oxy-fuel combustion of coal and coal/biomass blend chars obtained in N_2 and CO_2 atmospheres. *Energy* 2012; 48: 510-518.

[22] Gomez A, Mahinpey N. A new method to calculate kinetic parameters independent of the kinetic model: Insights on CO₂ and steam gasification. Chem Eng Res Des 2015; 95: 346-357.

[23] Fogler HS. Elements of Chemical Reaction Engineering. Diffusion and Reaction. 4th ed. Boston: Pearson Education, Inc; 2006, p. 813-851.

Chapter Eight: Conclusions and recommendations

8.1 Conclusions

The correct interpretation and modeling of the gasification mechanism cannot be achieved without incorporating new concepts, experimental techniques and fundamentals in chemical reaction engineering. This research has resulted in new findings related to the gasification reaction mechanism and the interpretation of kinetic results.

The maximum gasification rate observed when the conversion rate is plotted against conversion is not a consequence of changes of the char surface during the gasification itself as proposed by Bhatia and Perlmutter in 1980 [1]. This notion has been widely accepted by researchers in the gasification and combustion field. It has been proven that the maximum rate is a consequence of different gasifying agent partial pressures during the stabilization time after the inert gas is replaced with the reaction gas [2]. This becomes evident when the conversion rate is plotted against the residence time, showing a constant time to achieve a maximum rate, if the experimental setup is the same.

An increase in the time that the char is held at the reaction temperature with an inert gas (isothermal pyrolysis) decreases the gasification rate [2]. This indicates the importance of the thermal history of the char and explains the differences between laboratory and industrial gasifiers kinetics [2, 3]. This reduction of the char reactivity was reported to be associated with thermal annealing [3]; however, a better explanation of the decreased reactivity can be associated with the reduction of the mesopore surface area [2]. Pyrolysis and gasification cannot be separated without inducing changes on the char surface or creating a false maximum gasification

rate; therefore, pyrolysis should be as fast as possible in order to simulate industrial conditions and increase char reactivity.

The char micropore surface area and the catalyst content are the two most important variables affecting the gasification rate. In CO₂ coal gasification, the characterization properties of the parent coal, i.e. coal micropore surface area and alkali content, can be assumed as proportional to the total char surface area and catalyst content, respectively [4]. A new semi-empirical equation based on the Arrhenius equation correlates these two variables to estimate the rate constant in a broad range of ash contents with a coefficient of determination (R^2) higher than 0.97 [4]. The new equation can be used to estimate the rate constant of feedstock mixtures considering the catalytic nature of alkali and alkaline earth metal instead of the weighted average of the raw components rate constants, as commonly presented by other researchers [5, 6].

It has been proven that the selection of a kinetic model affects the estimation of the kinetic parameters using the Arrhenius equation in its conventional form (first the evaluation of k and then correlation of the logarithm of k vs. the reciprocal of the temperature). However, in theory, these parameters should be independent of the kinetic model.

A new method to calculate the kinetic parameters (activation energy and frequency factor) independent of the kinetic model was developed [7]. The comparison of the kinetic parameters obtained from a particular kinetic model with those calculated from the free-model approach is a validation tool to determine whether or not the kinetic model represents the reaction mechanism of a particular reaction. This method was developed to compare the accuracy of different gasification kinetic models, but it can be used in any chemical reaction.

The main assumption during kinetic studies at low temperatures (below 1000°C) is that the chemical reaction is the controlling step [8, 9]; however, experiments with small particle size (90 µm) and small sample amounts (10 mg) exhibited interparticle diffusion limitations, due to the thickness of the sample [10]. It was proven that the reported activation energy of steam gasification is usually underestimated [10], which is associated with mass transfer limitations, specifically interparticle diffusion. This can be considered as false kinetics [11], showing that the consideration of intrinsic kinetics of steam gasification in previous studies is not possible.

A new procedure denominated direct gasification can be used for CO₂ gasification overcoming the limitations of conventional experimental procedures in kinetic studies; i.e. a false maximum gasification rate and reduction of the mesopore surface area. However, this method cannot be applied for steam gasification, since pyrolysis and gasification overlap when steam is the gasifying agent. Another experimental protocol for conducting either steam or CO₂ gasification with negligible mass transfer limitations was developed (Chapter 6).

8.2 Recommendations for future work

There are many research groups around the world studying gasification depending on a particular need. For example, in Canada, the efficient use of coal, biomass, and petroleum coke (petcoke) offers the opportunity to research new technologies.

The new findings presented in this research provide elements to improve kinetic analysis, since the most used kinetic model – the random pore model – cannot be considered as an accurate representation of the gasification mechanism. The error incurred by the separation of pyrolysis and gasification affects most of the experimental works reported in the literature.

Therefore, it is advisable to encourage other researchers to conduct experiments using same protocols, even standardizing the experimental procedure at the laboratory scale.

The conclusions related to the experimental procedure of gasification in this research can be extended to combustion and other gas-solid reactions with gas switching and where isothermal steps have been introduced. Kinetic parameter comparison between kinetic models can be used in different chemical reactions, helping to avoid misinterpretation of the experimental results due autocorrelation of the variables. The new method to determine kinetic parameters, independent of the kinetic model, is an important contribution to the chemical reaction engineering fundamentals and will be invaluable in kinetic modeling evaluation of previous studies and in future works.

As mentioned, the assumptions supporting the most common kinetic models have been demonstrated to be invalid. It is sufficient to consider simple and conventional kinetic models for simulations and to predict changes of reactivity due to changes on the feedstock as proposed by Silbermann et al. [8] and Gomez et al. [2]. It is necessary to determine whether or not Langmuir-Hinshelwood (LH) expressions provide accurate solutions, since they need the correspondent term for surface chemical reaction discussed in this thesis. Even complex models such as LH can be misinterpreted, if an incorrect assumption is made for the chemical reaction term. An example of this misinterpretation is illustrated in Eq. (1-21), as reported elsewhere [12, 13].

In this research, CO₂ and steam gasification processes were investigated independently; however, the combination of both gasifying agents and the reversibility of the Boudouard reaction at low temperatures should be studied with the same experimental setup, but with a

better gas analysis system. As proposed by Umemoto et al. [13], the competition between active sites and the effect of the mass transfer must be addressed.

While kinetics can now be studied with simpler kinetic models, challenges remain, such as the determination of the real CO, CO₂ and H₂O concentrations at the char surface due to the water-gas shift reaction. Small sample amounts help to reduce mass transfer effects, but increase data dispersion, which will make it almost impossible to determine gas concentrations in real time. This is one reason why gas chromatography was not used in this study. However, for parallel reactions, the weight loss is insufficient, and at least two more reaction products should be tracked.

Efforts in catalytic gasification by eliminating the ash and subsequently adding a specific catalyst should be reconsidered. The ash-free feedstock (especially coal) is a great alternative for combustion, but it is not logical to reduce the feedstock surface area and remove the catalyst in an acid leaching process for further addition of a more expensive catalyst. Reuse of the ash is a promising alternative; therefore, studies in non-conventional reactor configurations will help to increase raw feedstock gasification efficiency.

8.3 References

- [1] Bhatia SK, Perlmutter D D. A random pore model for fluid–solid reactions: I. Isothermal and kinetic control. University of Pennsylvania AIChE J 1980; 26 (3): 379–386.
- [2] Gomez A, Silbermann R, Mahinpey N. A comprehensive experimental procedure for CO₂ coal gasification: Is there really a maximum reaction rate? Appl Energy 2014; 124: 73-81.
- [3] Senneca O, Russo P, Salatino P, Masi S. The relevance of thermal annealing to The evolution of coal char gasification reactivity. Carbon 1997; 35 (1): 141-151.
- [4] Gomez A, Mahinpey N. A new model to estimate CO₂ coal gasification kinetics based only on parent coal characterization properties. Appl Energy 2015; 137: 126-133.
- [5] Feroso J, Arias B, Pevida C, Plaza MG, Rubiera F, Pis JJ. Kinetic models momparison for steam gasification of different nature fuel chars. J Therm Anal Calorim 2008; 91 (3): 779-786.
- [6] Gil MV, Riaza J, Alvarez L, Pevida C, Pis JJ, Rubiera F. Kinetic models for the oxy-fuel combustion of coal and coal/biomass blend chars obtained in N₂ and CO₂ atmospheres. Energy 2012; 48: 510-518.
- [7] Gomez A, Mahinpey N. A new method to calculate kinetic parameters independent of the kinetic model: Insights on CO₂ and steam gasification. Chem Eng Res Des 2015; 95: 346-357.
- [8] Silbermann R, Gomez A, Gates I, Mahinpey N, Kinetic studies of a novel CO₂ gasification method using coal from deep unmineable seams. Ind Eng Chem Res 2013; 52: 14787–14797.
- [9] Ahmed II, Gupta AK. Kinetics of woodchips char gasification with steam and carbon dioxide. Appl Energy 2011; 88 (5): 1613-1619.
- [10] Gomez A, Mahinpey N. Kinetic study of coal steam and CO₂ gasification: A new method to reduce interparticle diffusion. Fuel 2015; 148: 160-167.
- [11] Fogler HS. Elements of Chemical Reaction Engineering. Diffusion and Reaction. 4th ed. Boston: Pearson Education, Inc; 2006, p. 813-851.

[12] Kajitani S, Suzuki N, Ashizawa M, Hara S. CO₂ gasification rate analysis of coal char in entrained flow coal gasifier. *Fuel* 2006; 85 (2): 163-169.

[13] Umemoto S, Kajitani S, Hara S. Modeling of coal char gasification in coexistence of CO₂ and H₂O considering sharing of active sites. *Fuel* 2013; 103: 14-21.

Appendix A: Heat of reaction at different temperatures

The estimation of the heat of reaction at different temperatures (ΔH_T^o) is a thermodynamic calculation based on the stoichiometry of a particular reaction [1]. The steps and equations to determine ΔH_T^o are as follows:

- Consider a generic expression for heat capacity regardless of the pure component phase:

$$C_p = A + B T + C T^2 + D T^{-2} \quad (\text{A-1})$$

where A, B, C and D are experimental constants for a pure component.

- The standard heat of reaction is defined as:

$$\Delta H_T^o = \sum_i v_i H_i^o \quad (\text{A-2})$$

where v_i and H_i^o are the stoichiometric coefficients (positive for products and negative for reactants) and the enthalpy of the component i at temperature T in its standard state.

- At the standard-state pressure (1 bar) , the standard enthalpies are functions of temperature:

$$dH_i^o = C_{p,i}^o dT \quad (\text{A-3})$$

- Combining Eqs. (A-1) to (A-3) is obtained:

$$\Delta H_T^o = \Delta H_0^o + R \int_{T_0}^T \frac{\Delta C_P^o}{R} \quad (\text{A-4})$$

$$\int_{T_0}^T \frac{\Delta C_P^o}{R} = \Delta A T_0 (\tau - 1) + \frac{\Delta B}{2} T_0^2 (\tau^2 - 1) + \frac{\Delta C}{3} T_0^3 (\tau^3 - 1) + \frac{\Delta D}{T_0} \frac{(\tau - 1)}{\tau} \quad (\text{A-5})$$

where $\tau = T/T_0$ and ΔH_0^o is the heat of reaction at the reference temperature reference. The heat capacity coefficients of the mixture are given by the analogous form of Eq. (A-2), e.g.

$$\Delta A = \sum_i v_i A_i.$$

The heat of the chemical reactions described in Chapter 1 (Section 1.2.3) in the temperature range considered in this research is presented in columns 2 to 4 of Table A.1. The standard heat of reaction (at 25°C) is presented in the first column of the same table.

Table A.1 Heats of reaction at different temperatures for the main reactions involve in gasification

	Heats of reaction [kJ/mol]			
	25°C	700°C	800°C	900°C
R ₁ : Boudouard reaction	170.7	169.3	168.5	167.6
R ₂ : Steam reforming	130.5	135.4	135.5	135.6
R ₃ : Water-gas shift	-40.2	-33.9	-32.9	-32.0
R ₄ : Methanation	-74.7	-78.9	-78.0	-76.8

A.1. References

- [1] Smith JM, Van Ness HC, Abbott MM. Introduction to Chemical Engineering Thermodynamics. 7th ed. New York: McGraw-Hill; 2005.

Appendix B: Theoretical meaning of E_A

Different theories present the relationship between activation energy (E_A) and heat of reaction (ΔH_T^0) considering kinetic molecular theory [1, 2]. A similar result can be obtained from thermodynamic considerations with the transition-state theory. This is particular useful to state limits for E_A of elementary reactions. This method consists of the following steps [2]:

- Consider the general endothermic chemical reaction:



- The previous irreversible reaction may be considered as two elementary sequential reactions:



where $(AB)^*$ corresponds to the activated form of the components A and B(or transition-state form).

- The first reaction is in equilibrium, reason why the concentration of the intermedium component is given by:

$$C_{(AB)^*} = K^* C_A C_B \quad (\text{B-4})$$

where K^* is the equilibrium constant for the formation of $(AB)^*$

- The rate of formation of C is controlled by the formation of the intermedium component since the second reaction is non-reversible. Therefore, the expression for the second elementary reaction is:

$$r_C = -r_A = k^* C_{(AB)^*} = k^* \times K^* \times C_A \times C_B \quad (\text{B-5})$$

where k is the rate constant of reaction (B-3).

- The evaluation of the equilibrium constant at different temperature is explained by the Van't Hoff equation [3]:

$$\frac{d \ln K}{dT} = \frac{\Delta H_T^0}{R T^2} \quad (\text{B-6})$$

where R is the ideal gas constant.

- The integration of Eq. (B-6) for the equilibrium constant of reaction (B-2) is:

$$K^* = \alpha e^{\frac{-\Delta H^*}{RT}} \quad (\text{B-7})$$

where α is the integration constant.

- Finally, Eq. (B-5) becomes:

$$r_C = k^* \alpha e^{\frac{-\Delta H^*}{RT}} C_A C_B = k C_A C_B \quad (\text{B-8})$$

with

$$k = k_0 e^{\frac{-\Delta H^*}{RT}} \quad (\text{B-9})$$

where $k_0 = k^* \alpha$

Eq. (B-9) is in the same form than the Arrhenius equation; therefore the E_A is related to the energy to reach a transition state. The theoretical deduction is not useful to determine the real value of E_A ; however, for endothermic elementary reactions shows the minimum value of E_A ,

which should be higher than the heat of reaction at the reaction temperature. This illustrated in Fig. B.1

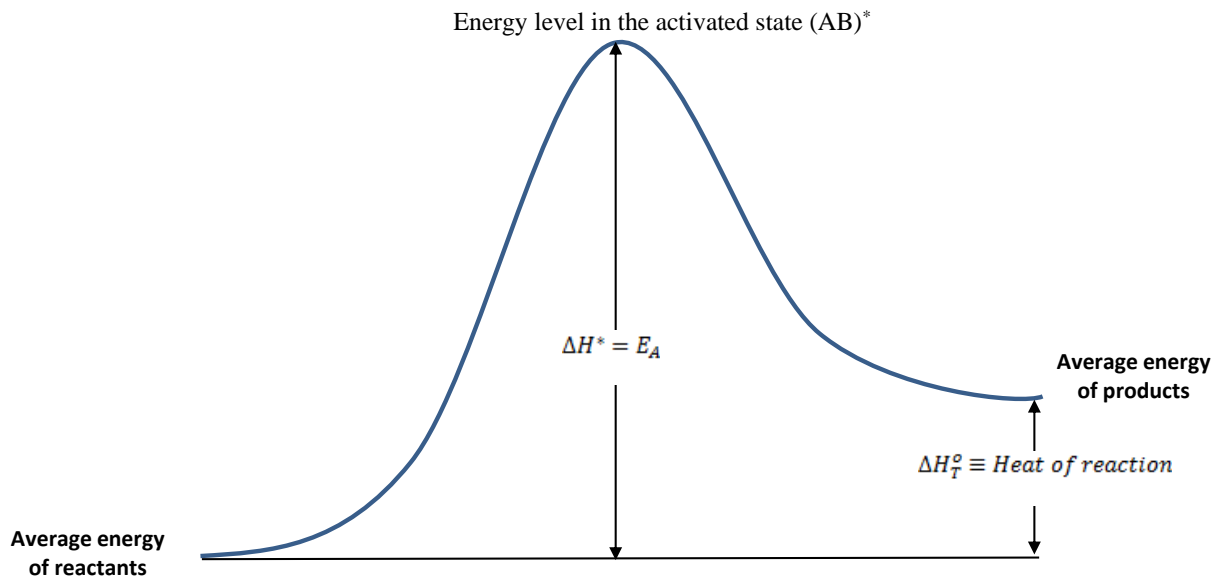


Figure B.1 CO₂ gasification rate (r) vs. conversion (X) of Genesee coal at 900°C: (a) data collection interval of 1 min and (b) data collection interval of 0.2 min.

B.1. References

- [1] Fogler HS. Elements of Chemical Reaction Engineering. Diffusion and Reaction. 4th ed. Boston: Pearson Education, Inc; 2006.
- [2] Smith JM. Chemical Engineering Kinetics. 3rd ed. New York: McGraw-Hill 1981.
- [3] Smith JM, Van Ness HC, Abbott MM. Introduction to Chemical Engineering Thermodynamics. 7th ed. New York: McGraw-Hill; 2005.

Appendix C: Additional topics about Chapter Four

The semi-empirical equations presented in Chapter 4 are the result of combining a general rate law and the Arrhenius equation to incorporate measurable properties of the solid feedstock, such as initial char surface area and total amount of catalyst. Eqs. (4-8) and (4-9) are the simplified version of the model presented in a previous work [1] with implicit assumptions that will be clearly stated in this section.

C.1. Detailed model development for rate constant estimation

- The overall rate of gasification is the sum of two terms corresponding to the catalytic (c) and non-catalytic (nc) gasification. The most difficult part to quantify is the active sites involved in each reaction, and the competition of gasifying agents for the active sites [2, 3]. The simplest expression for the overall gasification rate for one gasifying agent is:

$$r = r_c + r_{nc} \quad (C-1)$$

- Non-catalytic gasification rate is negligible with respect to the catalytic gasification rate (assumption 1).
- The overall reaction can be considered as a series of sequential elementary reactions (assumption 2). The general rate law, which is the product of independent variables, represents the rate of reaction for the controlling step [3, 4]. For CO_2 gasification, the reaction rate is as follows:

$$r = f_1(\text{Solid surface}) \times f_2(\text{Temperature}) \times f_3(C_{\text{CO}_2}) \quad (C-2)$$

- To study the solid reaction mechanism, experiments in a semi batch reactor (batch for the solid side and continuous for the gases stream) are carried out at constant partial pressure. The total char surface area is proportional to the total char weight (assumption 3); therefore, the previous equation can be reduced to:

$$r = \frac{dX}{dt} = f_1(1 - X) \times f_2(T) \times f_3 = f_1(1 - X) \times f'_2(T) \quad (C-3)$$

where $f'_2(T) = f_2(T) \times [f_3(C_{CO_2})]_{constant}$

This expression is similar to Eq. (4-5) presented in page 115.

- For a single-step kinetic model, the rate constant is equal to the initial gasification rate. At the beginning of the gasification, the initial surface area is generated during pyrolysis, which can be estimated by the characterization of the char that is synthesized at a particular reaction temperature. Assuming the char surface area is proportional to the initial surface area of the parent feedstock (assumption 4), the following expression is valid to estimate rate constant:

$$f_1(X = 0) \sim S \left[\frac{m^2}{g \text{ carbon}} \right] \quad (C-4)$$

- At isothermal conditions, the second term of Eq. (B-3) is equivalent to the rate constant (k):

$$f'_2(T|_{constant}) = k_T \quad (C-5)$$

- Based on the transition-state theory [3] and by considering the activation energy (E_A) as inversely proportional to the content of alkali (assumption 5), E_A can be expressed as:

$$E_A = E_A^* + \frac{\bar{\alpha}}{\text{Alk}} \quad (\text{C-6})$$

where E_A^* is the activation energy of the reactant saturated with catalyst, Alk is the specific molar alkali content [equivalent-moles/g coal], and $\bar{\alpha}$ is a proportionality constant. This assumption is consistent with the theory and experimental results [5, 6].

- Combining Eqs. (B-5) and (B-6) with the Arrhenius equation:

$$f'_2(T, \text{alkali}) = k_o e^{-\frac{(E_A^* + \frac{\bar{\alpha}}{\text{Alk}})}{RT}} \quad (\text{C-7})$$

- This can be written as:

$$f'_2(T, \text{alkali}) = k_o e^{-\frac{(E_A^* + \frac{\bar{\alpha}}{\text{Alk}})}{RT}} = k_o e^{-\frac{E_A^*}{RT}} e^{-\frac{\bar{\alpha}}{RT}} = k'_o e^{-\frac{b}{\text{Alk} T}} \quad (\text{C-8})$$

where k'_o [min^{-1}] is equivalent to the rate constant within a small temperature interval; “ b ” [$\text{g}_{\text{coal}} \text{K}/\text{alkaline equivalent moles}$] is a constant to fit the experimental data, which incorporates the effect of the alkali content in the exponential factor of the Arrhenius equation.

- Substituting Eqs (C-4) and (C-8) into Eq. (C-3), thus:

$$k_M = a_k S \left[\frac{\text{m}^2}{\text{g carbon}} \right] \times \exp \left(\frac{-b}{\text{Alk} \left[\frac{\text{equivalent moles}}{\text{g coal}} \right] \times T[\text{K}]} \right) = a_k f_2^* \quad (\text{C-9})$$

where k_M is the rate constant [min^{-1}] for a particular kinetic model (M); S [$\text{m}^2/\text{g carbon}$] is the initial surface area of the parent coal (based on carbon content); Alk [equivalent-

moles/g coal] is the specific alkaline content; and b [$\text{g}_{\text{coal}} \text{K}/\text{alkaline equivalent moles}$] and a_k [$\text{g}_{\text{coal}} \text{m}^{-2} \text{min}^{-1}$] are regression parameters.

C.2. Model extension

- The main limitation of Eq. (C-9) is the temperature effect on the parameter a_k since it was considered as a constant for isothermal experiments, but it changes with temperature as presented in Table 4.4.
- Figure C.1 shows a_k by considering it as a linear relationship between the logarithm of a_k and the reciprocal of temperature (similar to the Arrhenius equation).

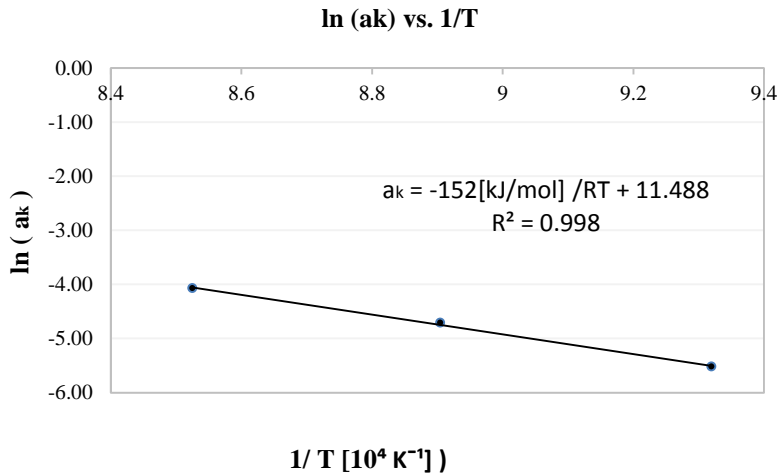


Figure C.1 Temperature dependency of the parameter a_k

- For endothermic elementary reactions (or sequence of elementary reactions) $E_A^* \geq \Delta H_0^o$ (Appendix B) and due to the assumption that catalytic gasification is dominant (assumption 1), the following relationship can be stated:

$$\frac{\bar{\alpha}}{\text{Alk}} \leq E_A^* \rightarrow e^{-\frac{\bar{\alpha}}{RT}} \gg e^{-\frac{E_A^*}{RT}} \quad (\text{C-10})$$

This means the term that contains the alkali content is sensitive to the reaction temperature changes more than the other terms. However, the parameter a_k cannot be considered as a constant. E_A^* and $\bar{\alpha}$ can be predicted by considering the following theoretical restrictions of E_A and some experimental observations:

- $E_A^* = \Delta H_{900^\circ C}^0 = 168 \text{ kJ/mol}$ (Appendix A) which is the minimum value of E_A possible for CO_2 gasification at 900°C .

- The low alkali content was found to be approx. 0.003 equivalent-moles/g_coal (Figure 4.6).

- The maximum value of E_A for CO_2 gasification (when the solid feedstock is graphite) is approx. 270 kJ/mol [6]. The right value for $\bar{\alpha}$ when $168 \text{ kJ/mol} \leq E_A \leq 270 \text{ kJ/mol}$ and

$$Alk \geq 0.003 \text{ kJ} \cdot \frac{\text{equivalent-moles}}{\text{g coal}} \text{ is } 2.6 \text{ kJ} \cdot \text{equivalent} - \text{moles/mol} \cdot \text{g coal}.$$

This case is illustrated in Fig. C.2, showing that for high alkali content (Fig 4.2) or more than 0.08 equivalent-moles/g_coal, Eq. (B-10) makes sense.

- Eq. (B-9) can be generalized without many fitting parameters, just using E_A^* and $\bar{\alpha}$ values that have been previously presented:

$$k_M = c \times f_2^* = c \times S \left[\frac{\text{m}^2}{\text{g carbon}} \right] \times \exp \left(\frac{E_A^* + \frac{\bar{\alpha}}{Alk}}{Alk \left[\frac{\text{equivalent moles}}{\text{g coal}} \right] \times T[\text{K}]} \right) \quad (\text{C-11})$$

where c is a fitting parameter and can be obtained by a simple linear regression as presented in Fig. C.3. Note that f_2^* in Eqs. (C-9) and (C-11) is different. An evaluation of result differences between Eqs. (C-11) and (C-9) is possible by comparing Figs. C.3 and 4.7 respectively. The extended model with one regression parameter (Fig. C.3) yields

higher coefficient of determination than the simplified model with two regression parameters (Fig. 4.7).

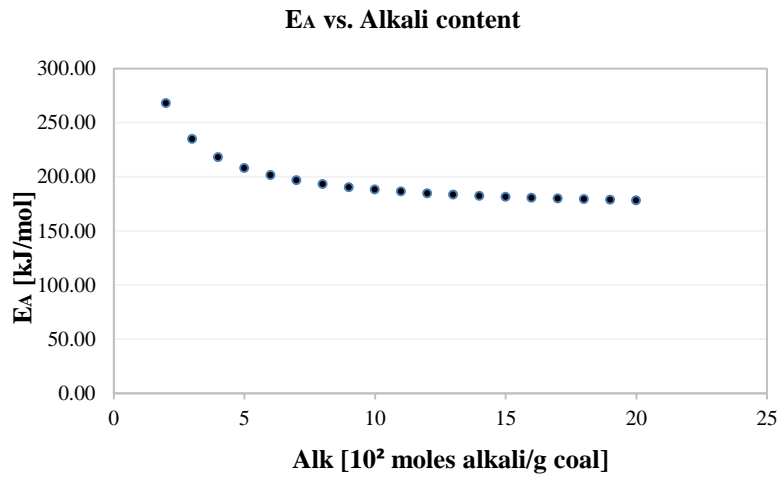


Figure C.2 E_A for the CO_2 catalytic gasification of coal assuming the heat of Boudouard reaction as the lower limit and the activation energy of graphite gasification as the upper limit.

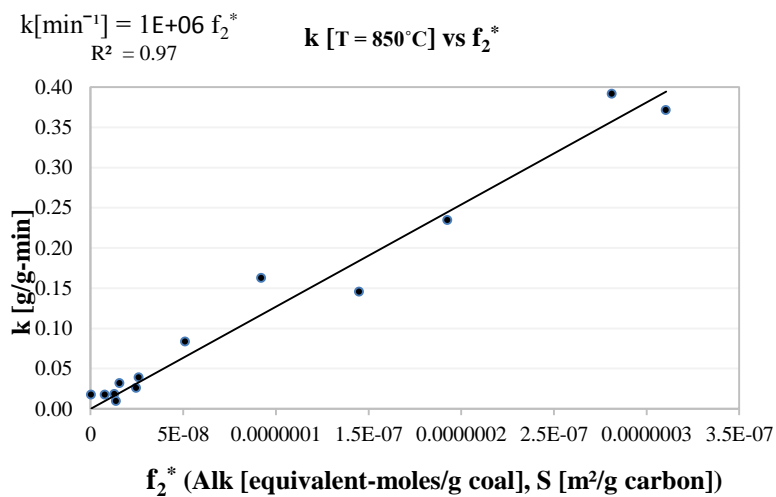


Figure C.3 Rate constant vs. f_2^* , as stated in Eq. (C-11) for all coals presented in Table 4.2 at 850°C using direct gasification and the ICM to obtain rate constant

C.3. References

- [1] Gomez A, Mahinpey N. A new method to calculate kinetic parameters independent of the kinetic model: Insights on CO₂ and steam gasification. *Chem Eng Res Des* 2015; 95: 346-357.
- [2] Kajitani S, Suzuki N, Ashizawa M, Hara S. CO₂ gasification rate analysis of coal char in entrained flow coal gasifier. *Fuel* 2006; 85 (2): 163-169.
- [3] Umemoto S, Kajitani S, Hara S. Modeling of coal char gasification in coexistence of CO₂ and H₂O considering sharing of active sites. *Fuel* 2013; 103: 14-21.
- [3] Smith JM. *Chemical Engineering Kinetics*. 3rd ed. New York: McGraw-Hill 1981.
- [4] Fogler HS. *Elements of Chemical Reaction Engineering. Diffusion and Reaction*. 4th ed. Boston: Pearson Education, Inc; 2006.
- [5] Beamish BB, Shaw KJ, Rodgers KA, Newman J. Thermo-gravimetric determination of the carbon dioxide reactivity of char from some New Zealand coals and its association with the inorganic geochemistry of the parent coal. *Fuel Processing Technology* 1998; 53: 243–253.
- [6] Gonzalo-Tirado C, Jiménez S, Ballester J. Kinetics of CO₂ gasification for coals of different ranks under oxy-combustion conditions, CSIC-University of Zaragoza. *Combustion and Flame* 2013; 160(2): 411–416.

Appendix D: Copyright permissions

D.1. Figure 1.1

From: Kirk Heuser
Sent: Thursday, March 5, 2015 2:51 PM
To: Ramon Arturo Gomez Quevedo
Subject: Re: Copyright permission

Arturo,

Yes, you can use the information. The report is in the public domain, the only thing we ask is you reference the Pembina Institute.

Good luck with your thesis!

Kirk Heuser
Communications Lead | Pembina Institute

>Sender: Arturo Gomez

>Good afternoon Kirk,

>

> I am PhD student at the university of Calgary and within my thesis I used one of Pembina's publications as a reference. Particularly I want to add a graph (The first one) to the literature review of my thesis (Chapter 1) from the following article: <http://www.pembina.org/blog/634>
>I sent this email to a permission letter to include the graph of the amended article in my thesis.

>

>I really appreciate your answer to this email,

>

>Kind regards,

>

>Ramon Arturo Gomez

>Department of Chemical and Petroleum Engineering

D.2. Figure 1.2

Supplier	Elsevier Limited The Boulevard, Langford Lane Kidlington, Oxford, OX5 1GB, UK
Registered Company Number	1982084
Customer name	Arturo Gomez
License number	3617771237465
License date	Apr 28, 2015
Licensed content publisher	Elsevier
Licensed content publication	Applied Energy
Licensed content title	A thermodynamic analysis of solid waste gasification in the Plasma Gasification Melting process
Licensed content author	None
Licensed content date	December 2013
Licensed content volume number	112
Licensed content issue number	n/a
Number of pages	9
Start Page	405
End Page	413
Type of Use	reuse in a thesis/dissertation
Portion	figures/tables/illustrations
Number of figures/tables/illustrations	1
Format	both print and electronic
Are you the author of this Elsevier article?	No
Will you be translating?	No
Original figure numbers	Fig. 2
Title of your thesis/dissertation	Fundamental kinetic studies of CO ₂ and steam gasification
Expected completion date	Apr 2015
Estimated size (number of pages)	228
Elsevier VAT number	GB 494 6272 12

D.3. Figures 1.6 and 1.7

Supplier	Elsevier Limited The Boulevard, Langford Lane Kidlington, Oxford, OX5 1GB, UK
Registered Company Number	1982084
Customer name	Arturo Gomez
License number	3617780324665
License date	Apr 28, 2015
Licensed content publisher	Elsevier
Licensed content publication	Biomass and Bioenergy
Licensed content title	Gasification of biomass: comparison of fixed bed and fluidized bed gasifier
Licensed content author	Ragnar Warnecke
Licensed content date	1 June 2000
Licensed content volume number	18
Licensed content issue number	6
Number of pages	9
Start Page	489
End Page	497
Type of Use	reuse in a thesis/dissertation
Portion	figures/tables/illustrations
Intended publisher of new work	other
Number of figures/tables/illustrations	2
Format	both print and electronic
Are you the author of this Elsevier article?	No
Will you be translating?	No
Original figure numbers	Figs. 1 and 2
Title of your thesis/dissertation	Fundamental kinetic studies of CO ₂ and steam gasification
Expected completion date	Apr 2015
Estimated size (number of pages)	228
Elsevier VAT number	GB 494 6272 12

D.4 Table 1.1

Supplier	Elsevier Limited The Boulevard, Langford Lane Kidlington, Oxford, OX5 1GB, UK
Registered Company Number	1982084
Customer name	Arturo Gomez
License number	3584880217304
License date	Mar 09, 2015
Licensed content publisher	Elsevier
Licensed content publication	Bioresource Technology
Licensed content title	Energy production from biomass (part 3): gasification technologies
Licensed content author	Peter McKendry
Licensed content date	May 2002
Licensed content volume number	83
Licensed content issue number	1
Number of pages	9
Start Page	55
End Page	63
Type of Use	reuse in a thesis/dissertation
Intended publisher of new work	other
Portion	figures/tables/illustrations
Number of figures/tables/illustrations	1
Format	both print and electronic
Are you the author of this Elsevier article?	No
Will you be translating?	No
Original figure numbers	Table 1
Title of your thesis/dissertation	Comprehensive kinetic study of CO ₂ and steam gasification: New findings and fundamentals
Expected completion date	Apr 2015
Estimated size (number of pages)	225
Elsevier VAT number	GB 494 6272 12

D.5. Table 1.4

Supplier	Elsevier Limited The Boulevard,Langford Lane Kidlington,Oxford,OX5 1GB,UK
Registered Company Number	1982084
Customer name	Arturo Gomez
License number	3617781278454
License date	Apr 28, 2015
Licensed content publisher	Elsevier
Licensed content publication	Progress in Energy and Combustion Science
Licensed content title	The effects of pressure on coal reactions during pulverised coal combustion and gasification
Licensed content author	Terry F Wall,Gui-su Liu,Hong-wei Wu,Daniel G Roberts,Kathy E Benfell,Sushil Gupta,John A Lucas,David J Harris
Licensed content date	2002
Licensed content volume number	28
Licensed content issue number	5
Number of pages	29
Start Page	405
End Page	433
Type of Use	reuse in a thesis/dissertation
Intended publisher of new work	other
Portion	figures/tables/illustrations
Number of figures/tables/illustrations	1
Format	both print and electronic
Are you the author of this Elsevier article?	No
Will you be translating?	No
Original figure numbers	Table 5
Title of your thesis/dissertation	Fundamental kinetic studies of CO ₂ and steam gasification
Expected completion date	Apr 2015
Estimated size (number of pages)	228
Elsevier VAT number	GB 494 6272 12

D.6. Figure 2.4 and Table 2.1



RightsLink®

Home

Account Info

Help



ACS Publications
Most Trusted. Most Cited. Most Read.

Title: Kinetic Studies of a Novel CO₂ Gasification Method Using Coal from Deep Unmineable Seams
Author: Rico Silbermann, Arturo Gomez, Ian Gates, et al
Publication: Industrial & Engineering Chemistry Research
Publisher: American Chemical Society
Date: Oct 1, 2013

Logged in as:
Arturo Gomez
Account #:
3000895259

LOGOUT

Copyright © 2013, American Chemical Society

PERMISSION/LICENSE IS GRANTED FOR YOUR ORDER AT NO CHARGE

This type of permission/license, instead of the standard Terms & Conditions, is sent to you because no fee is being charged for your order. Please note the following:

- Permission is granted for your request in both print and electronic formats, and translations.
- If figures and/or tables were requested, they may be adapted or used in part.
- Please print this page for your records and send a copy of it to your publisher/graduate school.
- Appropriate credit for the requested material should be given as follows: "Reprinted (adapted) with permission from (COMPLETE REFERENCE CITATION). Copyright (YEAR) American Chemical Society." Insert appropriate information in place of the capitalized words.
- One-time permission is granted only for the use specified in your request. No additional uses are granted (such as derivative works or other editions). For any other uses, please submit a new request.

If credit is given to another source for the material you requested, permission must be obtained from that source.

D.7. Chapter 3

Supplier	Elsevier Limited The Boulevard, Langford Lane Kidlington, Oxford, OX5 1GB, UK
Registered Company Number	1982084
Customer name	Arturo Gomez
License number	3617790420095
License date	Apr 28, 2015
Licensed content publisher	Elsevier
Licensed content publication	Applied Energy
Licensed content title	A comprehensive experimental procedure for CO ₂ coal gasification: Is there really a maximum reaction rate?
Licensed content author	Arturo Gomez, Rico Silbermann, Nader Mahinpey
Licensed content date	1 July 2014
Licensed content volume number	124
Licensed content issue number	n/a
Number of pages	9
Start Page	73
End Page	81
Type of Use	reuse in a thesis/dissertation
Portion	full article
Format	both print and electronic
Are you the author of this Elsevier article?	Yes
Will you be translating?	No
Title of your thesis/dissertation	Fundamental kinetic studies of CO ₂ and steam gasification
Expected completion date	Apr 2015
Estimated size (number of pages)	228
Elsevier VAT number	GB 494 6272 12

D.8. Chapter 4

Supplier	Elsevier Limited The Boulevard, Langford Lane Kidlington, Oxford, OX5 1GB, UK
Registered Company Number	1982084
Customer name	Arturo Gomez
License number	3617790738834
License date	Apr 28, 2015
Licensed content publisher	Elsevier
Licensed content publication	Applied Energy
Licensed content title	Fundamental kinetic studies of CO2 and steam gasification
Licensed content author	None
Licensed content date	1 January 2015
Licensed content volume number	137
Licensed content issue number	n/a
Number of pages	8
Start Page	126
End Page	133
Type of Use	reuse in a thesis/dissertation
Portion	full article
Format	both print and electronic
Are you the author of this Elsevier article?	Yes
Will you be translating?	No
Title of your thesis/dissertation	Fundamental kinetic studies of CO2 and steam gasification
Expected completion date	Apr 2015
Estimated size (number of pages)	228
Elsevier VAT number	GB 494 6272 12

D.9. Chapter 5

Supplier	Elsevier Limited The Boulevard, Langford Lane Kidlington, Oxford, OX5 1GB, UK
Registered Company Number	1982084
Customer name	Arturo Gomez
License number	3617790946923
License date	Apr 28, 2015
Licensed content publisher	Elsevier
Licensed content publication	Chemical Engineering Research and Design
Licensed content title	A new method to calculate kinetic parameters independent of the kinetic model: Insights on CO ₂ and steam gasification
Licensed content author	None
Licensed content date	March 2015
Licensed content volume number	95
Licensed content issue number	n/a
Number of pages	12
Start Page	346
End Page	357
Type of Use	reuse in a thesis/dissertation
Intended publisher of new work	other
Portion	full article
Format	both print and electronic
Are you the author of this Elsevier article?	Yes
Will you be translating?	No
Title of your thesis/dissertation	Fundamental kinetic studies of CO ₂ and steam gasification
Expected completion date	Apr 2015
Estimated size (number of pages)	228
Elsevier VAT number	GB 494 6272 12

D.10. Chapter 6

Supplier	Elsevier Limited The Boulevard, Langford Lane Kidlington, Oxford, OX5 1GB, UK
Registered Company Number	1982084
Customer name	Arturo Gomez
License number	3617791201293
License date	Apr 28, 2015
Licensed content publisher	Elsevier
Licensed content publication	Fuel
Licensed content title	Kinetic study of coal steam and CO ₂ gasification: A new method to reduce interparticle diffusion
Licensed content author	None
Licensed content date	15 May 2015
Licensed content volume number	148
Licensed content issue number	n/a
Number of pages	8
Start Page	160
End Page	167
Type of Use	reuse in a thesis/dissertation
Intended publisher of new work	other
Portion	full article
Format	both print and electronic
Are you the author of this Elsevier article?	Yes
Will you be translating?	No
Title of your thesis/dissertation	Fundamental kinetic studies of CO ₂ and steam gasification
Expected completion date	Apr 2015
Estimated size (number of pages)	228
Elsevier VAT number	GB 494 6272 12